

ORTHONORMAL BASES FOR ADAPTIVE FILTERING

PROEFSCHRIFT

ter verkrijging van de graad van doctor aan de
Technische Universiteit Eindhoven, op gezag van
de Rector Magnificus, prof.dr. M. Rem, voor
een commissie aangewezen door het College van
Dekanen in het openbaar te verdedigen op

maandag 12 mei 1997 om 16.00 uur

door

HARM JAN WILLEM BELT

geboren te 's Hertogenbosch

Dit proefschrift is goedgekeurd
door de promotoren:

prof.Dr.-Ing. H.J. Butterweck
prof.dr.ir. W.M.G. van Bokhoven

en de copromotor:

dr.ir. A.C. den Brinker

CIP-DATA LIBRARY TECHNISCHE UNIVERSITEIT EINDHOVEN

Belt, Harm J.W.

Orthonormal bases for adaptive filtering / by Harm J.W. Belt. -
Eindhoven : Technische Universiteit Eindhoven, 1997.

Proefschrift. - ISBN 90-386-0290-1

NUGI 832

Trefw.: adaptieve filters / orthogonale reeksen.

Subject headings: adaptive filters / IIR filters / least squares approximations.

Voorwoord

Met het schrijven van dit voorwoord sluit ik nu een periode af bij de vakgroep signaalverwerking die voor mij veel heeft betekend en bovendien, daar ben ik zeker van, ook in de toekomst veel zal blijven betekenen. Ik ben de afgelopen vier jaar, met betrekking tot het voltooien van dit proefschrift, bijgestaan door een aantal mensen die ik daarvoor zeer dankbaar ben.

Als eerste dr. Bert den Brinker, die mijn dagelijkse begeleiding voor zijn rekening heeft genomen. Ik ben hem uitermate dankbaar voor zijn betrokkenheid en voor het altijd direct bereid zijn tot het voeren van discussie. De vele gesprekken die ik met hem heb gehad zijn voor mij enorm leerzaam geweest. Een bijzonder woord van dank gaat uit naar mijn eerste promotor, prof. Hans Jürgen Butterweck, voor de vele interessante discussies en voor het zorgvuldig plaatsen van kritische noten bij mijn proefschrift.

Dat ik de afgelopen vier jaar op een prettige manier mijn werk heb kunnen doen heb ik voor een groot deel te danken aan de overige leden van de signaalverwerkingsgroep, te weten Martin Bastiaans, Jean Ritzerfeld, Harrie van Meer, Gérard Verkroost, Tiny Verhoeven, en bovendien mijn kamergenoten Mark Smidt en Arno van Leest.

Vervolgens wil ik prof. Wim van Bokhoven, prof. Okko Bosgra en dr. Anton Stoorvogel bedanken voor hun constructieve opmerkingen na het kritisch proeflezen van het manuscript.

Special thanks goes to dr. Tomás Oliveira e Silva of the Universidade de Aveiro in Portugal, who was a guest of our group and my roommate for a period of three months. During his stay at our group and our intensive correspondence through email we have done the work leading to a joint conference paper and Chapter 5 of this thesis.

Veel dank ben ik bovendien verschuldigd aan de afstudeerders en stagiaires met wie ik het genoegen heb gehad te mogen werken, te weten Frank Benders, Patrick Meuwissen, Martijn Houkes, Jeroen Lammerts, Erwin Kuijpers, Sjaak Derksen, Dion Cornelissen en Maurice de Château. Many thanks also to the international students who visited our group for a practical traineeship and whom I had the pleasure to work with, namely Gilles Henry from Bordeaux in France, Martin Leyh from Erlangen in Germany, and Pedro Ignacho Gracia Latorre from Zaragoza in Spain.

Ik ben Kees Janse van het Philips Nat.Lab. zeer erkentelijk voor ons vriendschappelijke contact tijdens mijn promotieperiode en voor zijn inspanningen om mij uiteindelijk aan mijn huidige baan te helpen.

cont.

Tenslotte wil ik het 'thuisfront', pap, mam, Renske en Aukje, bedanken voor al hun stimuleringen en voor het bieden van een altijd gezellige thuishaven. Zonder hun was dit proefschrift er nooit gekomen. In het bijzonder ben ik Arlette dankbaar voor al haar begrip en steun. Zij heeft mij enorm bijgestaan, zeker op de vele drukke avonden en in de weekenden tijdens het schrijven van dit proefschrift.

Gerwen, 14 maart 1997.

Summary

In the field of adaptive filtering the most commonly applied filter structure is the transversal filter, also referred to as the tapped-delay line (TDL). The TDL is composed of a cascade of unit delay elements that are tapped, weighted and then summed. Thus, the output of a TDL is formed by a linear combination of its input signal at various delays. The weights in this linear combination are called the tap weights. The number of delay elements, or equivalently the number of tap weights, determines the duration of the impulse response of the TDL. For this reason, one often speaks of a finite impulse response (FIR) filter. In a general adaptive filtering scheme the adaptive filter aims to minimize a certain measure of error between its output and a desired signal. Usually, a quadratic cost criterion is taken: the so-called mean-squared error. There exists an extensive literature on the subject of adaptive optimization of the tap weights.

A problematic aspect of the TDL is that its associated basis functions, delayed versions of a unit pulse function, are extremely localized in time. As a consequence, a large number of delay elements or tap weights is required to mimic the dynamic behavior of systems that exhibit a large memory. For adaptive filtering a large number of weights may be undesirable for the following reasons. First, a lot of costly memory is needed to store the previous input samples and the values of the tap weights. Second, a large number of weights implies a large computational burden to perform the convolution with the input signal. Third, once the adaptive filter has reached its optimum, each adaptive weight fluctuates around its steady state value in this way causing a certain noise contribution at the output of the adaptive filter. The cumulative effect of the noise contributions of a large number of weights is a limiting factor in terms of the performance of the adaptive filter.

In this thesis alternative adaptive filter structures are studied. We specifically investigate linear regression models of which the output is a weighted summation of filtered versions of the input signal, where the tap filters are Infinite Impulse Response (IIR) filters. Due to the similarities between the TDL and the linear regression model, we may use adaptation algorithms such as the Least-Mean-Square (LMS) or the Recursive Least-Squares (RLS) algorithms that were initially developed for the TDL, to optimize the weights of the linear regression model. When the tap filters are chosen appropriately for a specific application, one can suffice with less adaptive weights compared to the TDL. We investigate candidate sets of filters for linear regression models. We find that for the purpose of adaptive filtering specifically those sets of filters are interesting, of which the impulse responses form (complete) systems of orthonormal functions. We consider

(generalized) Laguerre, Kautz, Jacobi, Legendre, and Meixner-like filters and treat their relevant properties. These filters contain parameters (for example poles) that need to be chosen beforehand and therefore we consider some methods to find good values for them. As a by-product of the treated methods we propose a way to find good values for the free parameters in truncated expansions of finite support signals with orthonormal Hermite functions. The behavior of the LMS algorithm for the optimization of the weights in linear regression models is studied, where we consider the rate of convergence and the misadjustment. Further, we propose an adaptive optimization algorithm for the free parameter (a multiple pole) of a Laguerre filter. Finally, the adaptive optimization of a complex pole pair is considered for a specific second-order IIR adaptive filter, namely an adaptive line enhancer.

Contents

Voorwoord	iii
Summary	v
Glossary	xi
1 Introduction	1
1.1 Adaptive Filters in General	1
1.2 Applications of Adaptive Filters	2
1.2.1 Identification	3
1.2.2 Inverse Modelling	3
1.2.3 Prediction	4
1.2.4 Interference Cancelling	5
1.3 The Adaptive Transversal Filter	5
1.3.1 The Wiener Filter	6
1.3.2 The Method of Steepest Descent	9
1.3.3 The LMS Algorithm	10
1.3.4 The Standard RLS Algorithm	11
1.4 Adaptive Linear Regression Models	13
1.5 Filter Length and MSE: an Example	15
1.6 Scope of this Thesis	17
Bibliography	19
2 Orthogonal Filters	21
2.1 Introduction	21
2.2 Some Relevant Hilbert Spaces	21
2.3 Orthogonal Series Expansions	26
2.4 Orthogonal Polynomials	27
2.4.1 Continuous Polynomials	27
2.4.2 Discrete Polynomials	31
2.5 Orthonormal Laguerre Functions	34
2.5.1 The Continuous Laguerre Functions	34
2.5.2 The Discrete Laguerre Functions	37
2.5.3 Optimal Truncated Laguerre Series	40

2.6	Orthonormalized Exponentials	44
2.6.1	Continuous Kautz Functions	44
2.6.2	Discrete Kautz Functions	46
2.6.3	Optimal Truncated Kautz Series	49
2.7	Adaptive Orthonormal Filters	51
	Bibliography	54
3	Jacobi and Legendre Filters	59
3.1	Introduction	59
3.2	Continuous Jacobi Filters	59
3.2.1	Classical Jacobi and Legendre Polynomials	60
3.2.2	Continuous Jacobi and Legendre Functions	61
3.2.3	Continuous Jacobi and Legendre Networks	64
3.3	Discrete Jacobi Filters	66
3.3.1	Discrete Jacobi Functions and Networks	66
3.3.2	Discrete Legendre Functions and Networks	70
3.4	Discussion	72
	Bibliography	73
4	Optimal Generalized Laguerre Filters	75
	Abstract	75
4.1	Introduction	75
4.2	Two Orthonormal Bases	76
4.2.1	The Generalized Laguerre Functions	76
4.2.2	The Meixner-Like Functions	80
4.3	The Derivatives of the Basis Functions	83
4.4	The Optimality Condition	86
4.5	An Example	88
4.6	Discussion	88
	Bibliography	90
5	Optimal Truncated Hermite Expansions	93
	Abstract	93
5.1	Introduction	93
5.2	Hermite Polynomials and Functions with some Properties	94
5.3	Stationarity Conditions for Truncated Hermite Series	95
5.3.1	Approximation of Even and Odd Components of a Function	97
5.4	Optimum Value of λ and t_0 for a Class of Functions	97
5.5	An Example	99
	Bibliography	100

6 Cascaded All-Pass Sections for LMS Adaptive Filtering	103
Abstract	103
6.1 Introduction	103
6.2 The All-Pass Filter Bank	104
6.3 The LMS Adaptive All-Pass Filter	105
6.4 The Weight-Error Correlation Matrix	106
6.5 Performance Analysis	107
6.6 Discussion	108
Appendix	109
Bibliography	110
7 Laguerre Filters with Adaptive Pole Optimization	111
Abstract	111
7.1 Introduction	112
7.2 Laguerre Functions and Filters	112
7.2.1 Laguerre Functions	112
7.2.2 Laguerre Filters	114
7.3 Adaptive Laguerre Filters	116
7.3.1 Adapting the Laguerre Weights	116
7.3.2 Adapting the Laguerre Pole	116
7.4 An Example	121
7.5 Discussion	122
Bibliography	122
8 A Second-Order IIR Adaptive Line Enhancer	125
Abstract	125
8.1 Introduction	125
8.2 The Second-Order IIR Prediction Filter	127
8.3 Adapting the Weights	128
8.4 Adapting the Poles	130
8.5 The Zero of the Notch Transfer	132
8.6 Computer Experiments	134
8.7 Discussion	137
Appendix	138
Bibliography	140
A Optimal Orthonormal Approximations	143
Bibliography	147
Samenvatting	149
List of Scientific Publications	151
Curriculum Vitae	153

Glossary

Used symbols

- k : discrete-time index
- t : continuous-time index
- ω : frequency variable for continuous-time signals
- Ω : frequency variable for discrete-time signals
- $x(k)$: input signal
- $d(k)$: desired signal or reference signal
- $y(k)$: output signal
- $e(k)$: error signal
- \underline{w} : weight vector
- \underline{w}_o : Wiener solution, optimal weight vector
- \mathbf{R} : covariance matrix
- \underline{p} : correlation vector
- $\underline{\mathcal{J}}$: mean-squared error: $\mathcal{J} = E\{e^2(k)\}$
- \mathcal{J}_{\min} : minimum mean-squared error
- $\underline{\nabla}\mathcal{J}$: gradient $\partial\mathcal{J}/\partial\underline{w}$
- μ : step-size for LMS algorithm
- $\tilde{\mu}$: step-size for NLMS algorithm
- \mathbf{R} : covariance matrix
- λ_i : i -th eigenvalue of \mathbf{R}
- \underline{q}_i : corresponding eigenvector of \mathbf{R}
- λ_{\max} : maximum eigenvalue of \mathbf{R}
- λ_{\min} : minimum eigenvalue of \mathbf{R}
- $\mathbf{\Lambda}$: diagonal matrix with eigenvalues λ_i on its main diagonal
- \mathbf{Q} : matrix with the eigenvectors \underline{q}_i in its columns
- η : condition number of \mathbf{R} : $\eta = \lambda_{\max}/\lambda_{\min}$
- $\rho_{xx}(l)$: auto-correlation function at lag l of a wide-sense stationary
: stochastic process $x(k)$
- $\Phi_{xx}(\Omega)$: power spectral density function of $x(k)$
- σ_x^2 : the power of $x(k)$

-
- \mathbb{N}, \mathbb{N}_0 : the sets of positive and nonnegative integers, respectively
 \mathbb{Z} : the set of all integers
 \mathbb{R}, \mathbb{R}^+ : the sets of real numbers and nonnegative real numbers,
: respectively
 $\ell_2(\mathbb{Z}), \ell_2(\mathbb{N}_0)$: the Hilbert spaces of square-summable functions on \mathbb{Z} and \mathbb{N}_0 ,
: respectively
 $L_2(\mathbb{R}), L_2(\mathbb{R}^+)$: the Hilbert spaces of square-integrable functions on \mathbb{R} and \mathbb{R}^+ ,
: respectively
 $l_m(x)$: m -th (continuous) Laguerre polynomial
 $\lambda_m(\sigma; t)$: m -th (continuous) Laguerre function, where σ is the scale
 $\Lambda_m(\sigma; s)$: the Laplace transform of $\lambda_m(\sigma; t)$
 $l_m^{(\alpha)}(x)$: m -th (continuous) generalized Laguerre polynomial, where α
: is the order of generalization
 $\lambda_m^{(\alpha)}(\sigma; t)$: m -th (continuous) generalized Laguerre function
 $\Lambda_m^{(\alpha)}(\sigma; s)$: the Laplace transform of $\lambda_m^{(\alpha)}(\sigma; t)$
 $\gamma_m(k)$: m -th discrete Laguerre polynomial
 $g_m(\xi; k)$: m -th discrete Laguerre function, where ξ acts in a similar
: way as a scale in the continuous domain
 $G_m(\xi; z)$: the z -transform of $g_m(\xi; k)$
 $\gamma_m^{(a)}(k)$: m -th Meixner-like polynomial, where a is the order of
: generalization
 $g_m^{(a)}(\xi; k)$: m -th Meixner-like function
 $G_m^{(a)}(\xi; z)$: the z -transform of $g_m^{(a)}(\xi; k)$
 $\mathcal{P}_m^{(\alpha, \gamma)}(x)$: m -th Jacobi polynomial
 $p_m^{(\alpha, \gamma)}(\sigma; t)$: m -th Jacobi function
 $P_m^{(\alpha, \gamma)}(\sigma; s)$: Laplace transform of $p_m^{(\alpha, \gamma)}(\sigma; t)$
 $\mathcal{T}_m(x)$: m -th (shifted) Legendre polynomial
 $t_m(\sigma; t)$: m -th Legendre function
 $T_m(\sigma; s)$: Laplace transform of $t_m(\sigma; t)$
 $q_m^{(a, c)}(\theta; k)$: m -th discrete Jacobi function
 $Q_m^{(a, c)}(\theta; z)$: z -transform of $q_m^{(a, c)}(\theta; k)$
 $q_m(\theta; k)$: m -th discrete Legendre function
 $Q_m(\theta; z)$: z -transform of $q_m(\theta; k)$
 $H_m(x)$: m -th Hermite polynomial
 $\mathcal{H}_m(\lambda, t_0; t)$: Hermite function with scale σ and center t_0
 $\mathcal{C}_m(k)$: m -th Chebyshev polynomial
 $\mathcal{K}_m(k)$: m -th Krawtchouk polynomial
 $\mathcal{H}a_m(k)$: m -th Hahn polynomial
 $\mathcal{C}_m(k)$: m -th Charlier polynomial
 $\mathcal{M}_m(k)$: m -th Meixner polynomial

-
- $\phi_m^{(1)}(t), \phi_m^{(2)}(t)$: m -th continuous Kautz function of the first and second kind,
: respectively
 $\Phi_m^{(1)}(s), \Phi_m^{(2)}(s)$: Laplace transforms of $\phi_m^{(1)}(t)$ and $\phi_m^{(2)}(t)$
 $\psi_m^{(1)}(k), \psi_m^{(2)}(k)$: m -th discrete Kautz function of the first and second kind,
: respectively
 $\Psi_m^{(1)}(z), \Psi_m^{(2)}(z)$: z -transforms of $\psi_m^{(1)}(k)$ and $\psi_m^{(2)}(k)$

Notational conventions

- \mathbf{X} : matrices are boldfaced
 \mathbf{X}^T : matrix transpose
 $\text{trace}\{\mathbf{X}\}$: the trace of the matrix \mathbf{X} (the sum of its diagonal elements)
 \underline{x} : vectors are underlined
 \underline{x}^T : vector transpose
 x_m : the $(m + 1)$ -th element of the vector \underline{x} , with $m = 0, 1, 2, \dots$
 X_{mn} : the $(m + 1, n + 1)$ -th element of the matrix \mathbf{X} , with $m, n = 0, 1, 2, \dots$
 $\underline{u}(k)$: vector of signals: $\underline{u}(k) = [u_0(k), u_1(k), \dots]^T$
 $E\{x\}$: expected value of x
 $\Delta^n f(k)$: n -th forward difference operator: $\Delta^n f(k) = \Delta^{n-1} f(k+1) - \Delta^{n-1} f(k)$
with $n = 1, 2, \dots$ and $\Delta^0 f(k) = f(k)$
 $(x)_n$: Pochhammer symbol or forward factorial function:
 $(x)_n = x(x+1) \dots (x+n-1)$
 $\binom{b}{a}$: binomial coefficient defined by $b(b-1) \dots (b-a+1)/a!$
 $\Gamma(\alpha)$: Gamma function
 δ_{mn} : Kronecker delta symbol: $\delta_{mn} = 0$ if $m \neq n$ and $\delta_{mm} = 1$
 $\delta(t)$: Dirac's delta function
 $\delta(k)$: unit pulse function
 $\epsilon(t)$: unit step function: $\epsilon(t) = 0$ if $t < 0$ and $\epsilon(t) = 1$ if $t \geq 0$
 $\text{Re}\{p\}$: the real part of a complex number p
 $\text{Im}\{p\}$: the imaginary part of a complex number p

Abbreviations

- DSP : Digital Signal Processor
TDL : Tapped-Delay Line
FIR : Finite Impulse Response
IIR : Infinite Impulse Response
LMS : Least-Mean-Square algorithm
NLMS : Normalized Least-Mean-Square algorithm
RLS : Recursive Least-Squares algorithm

MSE	:	Mean-Squared Error
LRM	:	Linear Regression Model
ALE	:	Adaptive Line Enhancer
FDAF	:	Frequency-Domain Adaptive Filter
SNR	:	Signal-to-Noise Ratio
SNIR	:	Signal-to-Noise Improvement Ratio
MBT	:	Modified Bilinear Transform
DT	:	Discrete-time
CT	:	Continuous-time
LTI	:	Linear Time-Invariant
WECM	:	Weight-Error Correlation Matrix

Chapter 1

Introduction

1.1 Adaptive Filters in General

An adaptive filter is a data-manipulating device that relies on a recursive algorithm to adjust its characteristics to an unknown environment. An adaptive filter can be trained to perform a specific filtering task and in this respect an adaptive filter is self-designing. Also, it can automatically adjust itself in the face of a time-varying environment. It is for these properties that adaptive filters perform better than fixed filters in those situations where complete knowledge about the environment is lacking or where the environment is changing in time.

In the past decade, technological advances in electronic circuit design and production have resulted in cheap, powerful and versatile Digital Signal Processors (DSP's). This development has set the path for a rapid-growing field of digital signal processing applications, including adaptive filters. Adaptive filters have been successfully applied in fields as communications, radar, sonar, seismology and biomedical electronics. Due to their versatility and low cost, adaptive filters have earned an important place in digital signal processing applications.

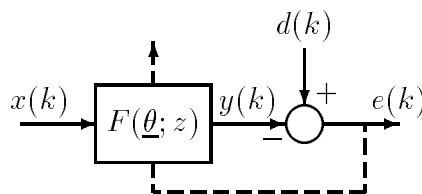


Figure 1.1: General scheme of an adaptive filter.

Fig. 1.1 shows the general scheme of an adaptive filter with the system function $F(\underline{\theta}; z)$. The adaptive filter contains a set of free parameters denoted by the vector $\underline{\theta}$. The scalar input signals $d(k)$ and $x(k)$ are sampled values of some real continuous-time signals. The output of the adaptive filter is denoted by $y(k)$.

The so-called *desired response* $d(k)$ is partly correlated with the input signal $x(k)$ via some unknown dynamical system called the *reference filter*. An *error signal* $e(k)$ is formed by subtracting $y(k)$ from $d(k)$:

$$e(k) = d(k) - y(k).$$

By appropriately updating the parameter vector $\underline{\theta}$, the adaptive filter aims to remove from $e(k)$ those signal components that are correlated with $x(k)$. Ideally, the output $y(k)$ of the adaptive filter represents the correlated part of $d(k)$ and, conversely, $e(k)$ represents the uncorrelated part of $d(k)$. The mechanism just described operates by virtue of the minimization of the so-called *mean-squared error* (MSE), given by

$$\mathcal{J} = E\{e^2(k)\},$$

where $E\{\cdot\}$ stands for expectation.

Many recursive optimization algorithms to minimize \mathcal{J} are found in the literature. Most of them revolve around a standard coefficient update formula of the form

$$\underline{\theta}(k+1) = \underline{\theta}(k) + \mu(k) e(k) \underline{\nabla}(k),$$

where $\mu(k)$ is a sequence of so-called *step-sizes* and $\underline{\nabla}(k)$ is a gradient vector. Generally speaking, large step-sizes provide the adaptive filter with the ability to learn fast during the initial learning phase or track fast in a non-stationary environment. However, in a stationary environment large step-sizes imply large asymptotical fluctuations of the adaptive parameters around their steady-state solution. In other words, the choice of the step-sizes involves a trade-off between learning speed and accuracy.

The degree to which the signal components in $e(k)$ which are correlated with $x(k)$ are removed depends on how well the adaptive filter is able to imitate the behaviour of the reference system under the given excitation $x(k)$. Better resemblance of the reference system usually imposes more complexity on the adaptive filter. Among other difficulties, a large complexity may result in a large number of parameters that need to be adapted. Similar to large step-size parameters, a large number of adaptive coefficients leads to large fluctuations in the behaviour of the adaptive filter around its steady-state solution. For this reason, one could search for that structure of F that, with the smallest possible number of adaptive coefficients, can resemble the reference system satisfactorily well under all occurring conditions. This is the problem of selecting the proper *model set*, the collection of attainable models. The chosen model set should at the same time permit the use of efficient, well-performing and easy-to-implement adaptive optimization methods.

1.2 Applications of Adaptive Filters

Adaptive filters find a wide range of applications. In (Haykin 1996), four basic classes of adaptive filtering are distinguished:

- Identification,
- Inverse modelling,
- Prediction,
- Interference cancelling.

They will be described next, together with some applications.

1.2.1 Identification

System identification deals with the problem of building a mathematical model that describes the behaviour of a dynamical system using observed data from the system (Eykhoff 1974; Ljung 1987). Such a model should describe the behaviour of the system as closely as possible within its intended use. When a model of a system is available, it can be used for various purposes, e.g. for controller design or diagnosis.

In practice the environment of the system (and thus its excitation) often varies in time. Also, the system itself may be subject to time variations, e.g. due to wear of the system components. This calls for the need of modelling schemes that can adjust the model parameters when the current parameters are no longer optimal. In Fig. 1.2 it is shown how an adaptive filter can be employed. The adaptive filter aims to imitate the behaviour of the unknown system by recursive minimization of the power of the error signal $e(k)$.

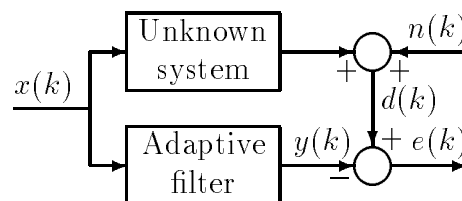


Figure 1.2: System identification or adaptive modelling.

In order to arrive at a good choice for the model set, the designer should use all available *a priori* knowledge of the unknown system and occurring operating conditions. The choice of the model set is very important for various reasons, such as keeping the model uncertainty small and ensuring good tracking capabilities for adaptive modelling. It is probably the most important, and at the same time most difficult step in system identification.

1.2.2 Inverse Modelling

Inverse modelling deals with providing an inverse model of an unknown system that is possibly corrupted by noise. In Fig. 1.3 the general scheme of adaptive inverse modelling is shown. Ideally, the inverse model yields in cascade with the unknown system a perfect transmission medium.

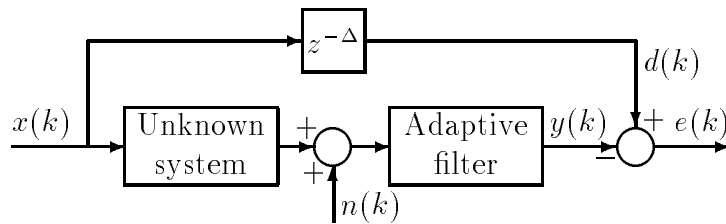


Figure 1.3: Inverse modelling.

An example of inverse modelling is predictive deconvolution, which deals with removing the effect of some previously performed convolution on a given time series. Predictive deconvolution can e.g. be applied to seismic data to arrive at a layered earth model (Haykin 1996). Another example is adaptive equalization in digital communication systems: a higher data transmission rate can be achieved by removing (or at least mitigating) intersymbol interference (ISI) caused by dispersion in the transmission line. Once proper ISI cancelling is achieved, small variations in the transmission line characteristics can be tracked with an adaptive filter.

Again, for a good performance of the adaptive filter, the model set should be matched as closely as possible to all occurring characteristics of the unknown system (in the previous example the transmission line) and its excitation.

1.2.3 Prediction

In Fig. 1.4 the general adaptive prediction scheme is depicted. The adaptive filter is used here to predict the current value of a signal $x(k)$ on the basis of past values of the signal only. To this end, the input of the adaptive filter is formed by a delayed version of $x(k)$, while the desired response is $x(k)$ itself.

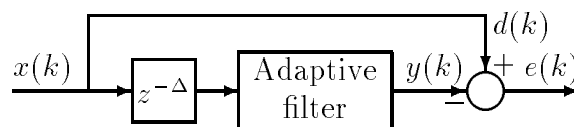


Figure 1.4: Prediction.

An application of adaptive prediction filters is signal detection. Consider a signal composed of a sinusoid corrupted by additive broad-band noise. On the basis of the difference in correlation lengths between the two signal components, the sinusoid can be separated from the noise with the aid of an adaptive prediction filter. Such a filter is called an adaptive line enhancer (ALE). In the optimal situation it forms a bandfilter with center frequency equal to the frequency of the sinusoid. For a high signal-to-noise ratio (SNR) at the output it is important that the adaptive filter can obtain a high quality factor, in other words: a sharp band-pass filter must be in the model set. Chapter 8 of this thesis

deals with an IIR (infinite impulse response) adaptive line enhancer, see also (den Brinker, Belt, and Benders 1994; Belt, den Brinker, and Benders 1995).

1.2.4 Interference Cancelling

Finally, an adaptive filter can be employed to suppress an undesired *interference signal* from a *primary signal*, see Fig. 1.5. The primary signal $d(k)$, composed of an information bearing signal and the interference signal, serves as the desired response for the adaptive filter. A sensor is placed near the source of the interference signal that feeds the adaptive filter with the input $x(k)$. In the ideal situation the adaptive filter has adjusted itself in such a way that the primary signal is disposed of the interference signal.

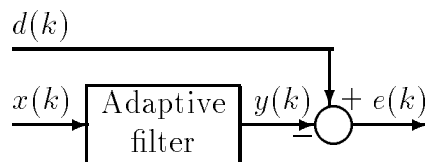


Figure 1.5: Interference cancelling.

An application is adaptive noise cancelling, see e.g. (Widrow *et al.* 1975). As an example, suppose the primary signal $d(k)$ is a microphone signal, say the voice of the captain of an aircraft. The noise in the cockpit originating from the engines can considerably reduce the intelligibility of the captain on the ground. A second microphone is placed near the engine to yield the input signal $x(k)$ of the adaptive filter. The adaptive filter 'learns' to imitate the behaviour of the acoustic propagation path from the engine through the airplane to the cockpit microphone. In the optimal situation the engine noise is cancelled and the signal $e(k)$, the captain's voice, can be transmitted to the ground. Another application is found in the cancellation of echos caused by improper balancing of the hybrids in two-way communication systems, see e.g. (Haykin 1996).

1.3 The Adaptive Transversal Filter

In the field of adaptive filtering the most commonly used filter has an impulse response of finite duration. For this reason such a filter is referred to as a Finite Impulse Response (FIR) filter. Examples of adaptive FIR filters comprise the Tapped-Delay-Line (TDL) or transversal filter, the lattice filter and the Frequency Domain Adaptive Filter (FDAF). FIR filters are characterized by the fact that they don't contain any feedback loops. Their popularity can be contributed to the fact that they are always stable, easy-to-implement and linear-in-the-parameters (these parameters are the so-called *weights*). In combination with a quadratic error criterion, this last property is especially desirable since it leads to simple adaptation algorithms and a unique optimal solution for the weights. In Fig. 1.6 a TDL of length M is shown.

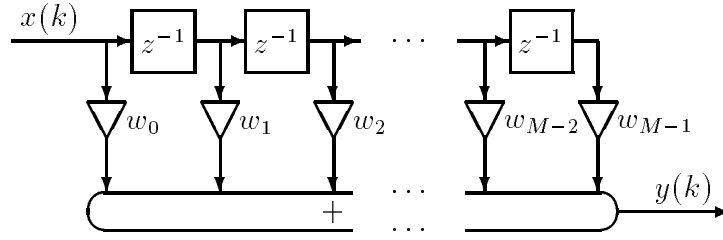


Figure 1.6: The tapped-delay line.

The output $y(k)$ of the TDL is formed by a weighted summation of the M tap signals, delayed versions of the input signal $x(k)$. The tap signals and the weights are written in vector notation¹ as

$$\begin{aligned}\underline{x}(k) &= [x(k), x(k-1), \dots, x(k-M+1)]^T, \\ \underline{w} &= [w_0, w_1, \dots, w_{M-1}]^T,\end{aligned}$$

where T denotes a transpose. The output of the TDL is a linear function of the tap signals and the weights:

$$y(k) = \sum_{m=0}^{M-1} w_m x(k-m) = \underline{w}^T \underline{x}(k).$$

For the error signal we may thus write

$$e(k) = d(k) - \underline{w}^T \underline{x}(k).$$

1.3.1 The Wiener Filter

Consider the minimization of the MSE, given by

$$\mathcal{J} = E\{e^2(k)\} = E\{[d(k) - \underline{w}^T \underline{x}(k)]^2\}. \quad (1.1)$$

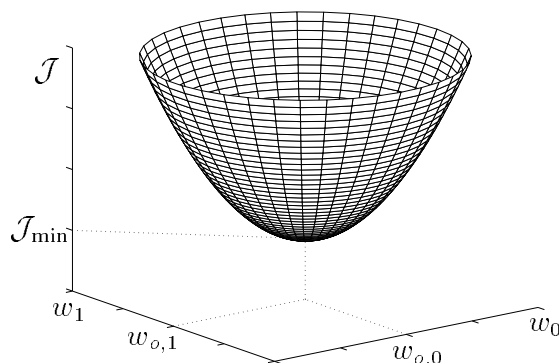
It is assumed that the input $x(k)$ of the TDL is a zero-mean, wide-sense stationary stochastic process. Its auto-correlation function for lag l is given by

$$\rho_{xx}(l) = E\{x(k)x(k-l)\}.$$

Since $\rho_{xx}(l)$ is an even function of the lag l , the power spectral density function $\Phi_{xx}(\Omega)$ of $x(k)$, obtained by Fourier transforming $\rho_{xx}(l)$, is a real function of the frequency Ω :

$$\Phi_{xx}(\Omega) = \sum_{l=-\infty}^{\infty} \rho_{xx}(l) e^{-j\Omega l} = \sum_{l=0}^{\infty} \rho_{xx}(l) \cos(\Omega l).$$

¹Care should be taken with the notation used here. Henceforth, w_m (with $m = 0, 1, 2, \dots$) will denote the $(m+1)$ -th element of the vector \underline{w} . Likewise, R_{mn} (with $m, n = 0, 1, 2, \dots$) will denote the $(m+1, n+1)$ -th element of the matrix \mathbf{R} .

Figure 1.7: The cost function \mathcal{J} for two weights.

The power of $x(k)$, given by $\rho_{xx}(0) = E\{x^2(k)\}$, will henceforth be denoted by σ_x^2 .

Let \mathbf{R} denote the $M \times M$ (auto-)correlation matrix of $x(k)$:

$$\mathbf{R} = E\{\underline{x}(k)\underline{x}^T(k)\} = \begin{pmatrix} \rho_{xx}(0) & \rho_{xx}(1) & \rho_{xx}(2) & \dots & \rho_{xx}(M-1) \\ \rho_{xx}(1) & \rho_{xx}(0) & \rho_{xx}(1) & \dots & \rho_{xx}(M-2) \\ \rho_{xx}(2) & \rho_{xx}(1) & \rho_{xx}(0) & \dots & \rho_{xx}(M-3) \\ \vdots & \vdots & \vdots & \ddots & \vdots \\ \rho_{xx}(M-1) & \rho_{xx}(M-2) & \rho_{xx}(M-3) & \dots & \rho_{xx}(0) \end{pmatrix}.$$

Clearly, the matrix \mathbf{R} is symmetric, meaning that $\mathbf{R} = \mathbf{R}^T$. Also, \mathbf{R} has a Toeplitz structure as a result of $x(k)$ being wide-sense stationary. Finally, \mathbf{R} is nonnegative definite as a consequence of the dyadic form of $\underline{x}(k)\underline{x}^T(k)$.

Let \underline{p} denote the following correlation vector

$$\underline{p} = E\{d(k)\underline{x}(k)\}.$$

Now the MSE in (1.1), also often referred to as the *cost function*, can be explicitly written as a quadratic form, reading

$$\mathcal{J} = E\{d^2(k)\} + \underline{w}^T \mathbf{R} \underline{w} - 2\underline{w}^T \underline{p}.$$

When \mathbf{R} is positive definite the cost function \mathcal{J} is convex, implying that there exists only one stationary point with respect to \underline{w} . This stationary point corresponds to the global minimum of \mathcal{J} . A typical cost function is plotted in Fig. 1.7 for the case that there are two weights. The two horizontal axes represent the values of two weights w_0 and w_1 , and the vertical axis represents the corresponding value of \mathcal{J} . This so-called *performance surface* has the shape of a paraboloid. If there are more than two weights, the performance surface becomes a hyper-paraboloid.

At the bottom of the performance surface the function \mathcal{J} attains its minimum value, denoted by \mathcal{J}_{\min} . This minimum can be found by setting the derivative of \mathcal{J} with respect

to \underline{w} equal to zero. This yields a set of M linear equations, the so-called *Wiener-Hopf equations* (Wiener 1949), which read in matrix form:

$$\mathbf{R}\underline{w}_o = \underline{p}. \quad (1.2)$$

The weight vector $\underline{w}_o = [w_{o,0}, w_{o,1}, \dots, w_{o,M-1}]^T$ is called the *Wiener solution* and the corresponding optimal filter is called the *Wiener filter*. The minimum MSE is given by

$$\mathcal{J}_{\min} = \mathcal{J}|_{\underline{w}=\underline{w}_o} = E\{d^2(k)\} - \underline{p}^T \underline{w}_o.$$

Solving the Wiener-Hopf equations in (1.2) implies a matrix inversion, which can be cumbersome. However, there exists an efficient recursive method to solve (1.2) exploiting the fact that \mathbf{R} is a symmetric Toeplitz matrix (Levinson 1947).

Some other interesting properties of \mathbf{R} related to its eigenvalues are described next. Let the M eigenvalues of \mathbf{R} be denoted by λ_m ($m = 0, 1, \dots, M-1$) and the M corresponding eigenvectors by \underline{q}_m , which are assumed to be normalized so that $\underline{q}_m^T \underline{q}_m = 1$. Note that all eigenvalues are real because \mathbf{R} is real and symmetric². Consequently, the eigenvectors of \mathbf{R} are also real. We compose an $M \times M$ diagonal matrix $\mathbf{\Lambda}$ from the eigenvalues:

$$\mathbf{\Lambda} = \text{diag}\{\lambda_0, \dots, \lambda_{M-1}\},$$

and an $M \times M$ matrix \mathbf{Q} with the M corresponding eigenvectors as its columns:

$$\mathbf{Q} = [\underline{q}_0, \underline{q}_1, \dots, \underline{q}_{M-1}].$$

For the case that all eigenvalues of \mathbf{R} are distinct, it is a simple matter to prove that the eigenvectors of \mathbf{R} are mutually orthonormal. Consider two distinct eigenvalues of \mathbf{R} , say λ_i and λ_j , with their corresponding eigenvectors \underline{q}_i and \underline{q}_j . We may write

$$\begin{aligned} \mathbf{R}\underline{q}_i &= \lambda_i \underline{q}_i &\rightarrow & \underline{q}_j^T \mathbf{R}\underline{q}_i &= \lambda_i \underline{q}_j^T \underline{q}_i, \\ \mathbf{R}\underline{q}_j &= \lambda_j \underline{q}_j &\rightarrow & \underline{q}_j^T \mathbf{R}^T \underline{q}_i &= \lambda_j \underline{q}_j^T \underline{q}_i. \end{aligned}$$

With $\mathbf{R} = \mathbf{R}^T$ we see that the left-hand sides of the two equations on the right are identical. Therefore, since $\lambda_i \neq \lambda_j$ for $i \neq j$ we must have that $\underline{q}_j^T \underline{q}_i = \delta_{ij}$ which implies that the eigenvectors of \mathbf{R} are mutually orthonormal. With \mathbf{I} the identity matrix, the orthonormality of the eigenvectors can also be expressed in matrix notation by

$$\mathbf{Q}\mathbf{Q}^T = \mathbf{I}.$$

With $\mathbf{R}\mathbf{Q} = \mathbf{Q}\mathbf{\Lambda}$, \mathbf{R} can be decomposed as $\mathbf{R} = \mathbf{Q}\mathbf{\Lambda}\mathbf{Q}^T$. Since the trace of a matrix is invariant under an orthogonal transformation, we find

$$M\sigma_x^2 = \text{trace}\{\mathbf{R}\} = \text{trace}\{\mathbf{Q}\mathbf{\Lambda}\mathbf{Q}^T\} = \sum_{m=0}^{M-1} \lambda_m.$$

²In fact, the eigenvalues of any Hermitian matrix are real.

Even when the eigenvalues are *not distinct*, it is still possible to obtain a diagonalization of \mathbf{R} of the form $\mathbf{R} = \mathbf{Q}\mathbf{\Lambda}\mathbf{Q}^{-1}$, where $\mathbf{Q}^{-1} = \mathbf{Q}^T$. Proof of this can be found in standard books on matrix theory, e.g. in (Franklin 1968).

Another useful property of the matrix \mathbf{R} is that its eigenvalues are bounded by the maximum and the minimum of the power spectrum of $x(k)$:

$$\lambda_{\max} = \max_m \{\lambda_m\} \leq \max_{\Omega} \{\Phi_{xx}(\Omega)\} \quad (1.3)$$

$$\lambda_{\min} = \min_m \{\lambda_m\} \geq \min_{\Omega} \{\Phi_{xx}(\Omega)\} \quad (1.4)$$

This property will be proved in Chapter 2 in a more general context. In this thesis the signal $x(k)$ is always assumed to be *persistently exciting*: $\Phi_{xx}(\Omega) > 0$ for all frequencies and thus $\lambda_{\min} > 0$. This means that \mathbf{R} is assumed to be strictly positive definite and thus its inverse \mathbf{R}^{-1} exists.

An important quantity is the eigenvalue ratio η :

$$\eta = \frac{\lambda_{\max}}{\lambda_{\min}}.$$

This ratio is called the *condition number* of the correlation matrix \mathbf{R} of the signal $x(k)$; it determines how well the Wiener-Hopf equations can be solved numerically. Also, η will turn out to be important with respect to the convergence properties of adaptive optimization algorithms for the weights. With (1.3) and (1.4) we see that η is upper bounded, which means that adding more weights does at a certain point not decrease the accuracy of a numerical solution of the Wiener-Hopf equations, nor does it influence the convergence properties of adaptive optimization algorithms for the weights. In the ideal situation we have $\eta = 1$, which corresponds to $x(k)$ being white noise.

Much can be said about the asymptotic distribution of the eigenvalues of a (symmetric and Toeplitz) correlation matrix of a wide-sense stationary process. These eigenvalues can be shown to asymptotically follow the distribution of the power spectral density $\Phi_{xx}(\Omega)$, see (Gray 1972).

1.3.2 The Method of Steepest Descent

Solving the Wiener-Hopf equations by inversion of the correlation matrix in (1.2) may be a tedious job due to computational difficulties, especially when the number of weights is large or when \mathbf{R} is ill-conditioned. Instead of directly solving the Wiener-Hopf equations, the *method of steepest descent*, which is an iterative gradient-based optimization procedure, can be adopted to *search* for the minimum MSE \mathcal{J}_{\min} (see e.g. (Widrow *et al.* 1975)). The method proceeds as follows. An initial weight vector $\underline{w}(0)$ is chosen as a first estimate of the Wiener solution. In most cases, when no *a priori* knowledge is available that could give a good idea about the Wiener solution, the initial weights are made zero. Starting from the initial weight vector, a new weight vector $\underline{w}(1)$ is formed by taking a small step in the direction opposite to that of the gradient vector of \mathcal{J} at $\underline{w}(0)$. Subsequently, the new

weight vector $\underline{w}(1)$ is the starting-point for the formation of the next weight vector $\underline{w}(2)$. Iteratively applying the procedure just described yields the method of steepest descent:

$$\underline{w}(k+1) = \underline{w}(k) - \frac{1}{2}\mu\underline{\nabla}\mathcal{J}, \quad k = 0, 1, 2, \dots, \quad (1.5)$$

where μ is a small positive number (the step-size) and $\underline{\nabla}\mathcal{J}$ is the gradient vector, given by

$$\underline{\nabla}\mathcal{J} \triangleq \partial\mathcal{J}/\partial\underline{w} = 2(\mathbf{R}\underline{w}(k) - \underline{p}). \quad (1.6)$$

The method strives to make the gradient equal to zero, so that ultimately the weights become such that the Wiener-Hopf equations in (1.2) are (nearly) satisfied.

Of course, in practical situations the exact gradient in (1.6), determined by \mathbf{R} and \underline{p} , is unknown. Consequently, the gradient must be approximated with the aid of some sort of estimation procedure. In addition, the environment of the adaptive filter is generally non-stationary and the performance surface is subject to some drift. The gradient estimation procedure must be designed in such a way that it can cope with the nonstationarities.

1.3.3 The LMS Algorithm

The method of steepest descent makes use of a purely deterministic gradient for the optimization of the weights, given by (1.6). The Least-Mean-Square (LMS) algorithm on the other hand, relies on a stochastic gradient. The expected values in the matrix \mathbf{R} and in the vector \underline{p} are simply replaced by the instantaneous values of their arguments. The estimates of \mathbf{R} and \underline{p} at instant k , to be denoted by $\hat{\mathbf{R}}(k)$ and $\hat{\underline{p}}(k)$ respectively, then become

$$\hat{\mathbf{R}}(k) = \underline{x}(k)\underline{x}^T(k) \quad \text{and} \quad \hat{\underline{p}}(k) = \underline{x}(k)d(k).$$

Also the expectation $E\{e^2(k)\}$ is replaced by the instantaneous value $e^2(k)$. At each instant k an estimate for the gradient $\underline{\nabla}\mathcal{J}$ is obtained with

$$\frac{\partial e^2(k)}{\partial\underline{w}} = 2e(k)\nabla e(k) = -2e(k)\underline{x}(k). \quad (1.7)$$

Inserting (1.7) in (1.5) results in the following updating rule for the LMS algorithm, see e.g. (Widrow *et al.* 1975) or (Haykin 1996):

$$\underline{w}(k+1) = \underline{w}(k) + \mu\underline{x}(k)e(k). \quad (1.8)$$

It is for its robustness and extreme simplicity that the LMS algorithm is the most widely used optimization algorithm in the field of adaptive filtering. Unfortunately, the implementational simplicity of the LMS-algorithm does not imply a simple analysis of its behaviour. For such an analysis, most authors rely on an (improper) *independence assumption*, stating that successive input vectors $\underline{x}(k)$ are statistically independent. Due to the shifting mechanism of a TDL this is never true: successive input vectors are even dependent in a deterministic way! In (Butterweck 1995; Butterweck 1996c; Butterweck 1996b) a steady-state analysis of the LMS-algorithm (for small step-sizes) is performed without making use of this disputed independence assumption.

To study the convergence behaviour of the LMS algorithm operating in a steady-state environment, one needs a convergence criterion. Usually, *convergence in the mean square* is considered. The LMS algorithm is convergent in the mean square when

$$\lim_{k \rightarrow \infty} E\{e^2(k)\} = \text{constant}.$$

To ensure convergence in the mean-square of the LMS algorithm, the step-size μ must satisfy (Haykin 1996):

$$0 < \mu < \frac{2}{\lambda_{\max}}.$$

The analysis leading to the upper bound for the step-size is unfortunately based on the independence assumption again. As a simple working rule, a more conservative upper bound is also given, of which the correctness is justified by computer simulations:

$$0 < \mu < \frac{2}{\text{trace}\{\mathbf{R}\}} = \frac{2}{M\sigma_x^2}.$$

In (Douglas 1995) a method is presented to determine the exact statistical expectations of an FIR LMS adaptive filter. With this method an exact step-size bound for stability can be found, and this bound is tighter than that derived with the independence assumption. Unfortunately, the method does not yield an analytical bound; moreover, it is computationally extremely demanding for filter lengths larger than only a few taps.

The step-size parameter μ involves a trade-off between convergence speed and accuracy: a large value for μ yields fast convergence, but the weight fluctuations around the Wiener solution in the steady state are large and vice versa. The correction term $\mu \underline{x}(k)e(k)$ in (1.8) is responsible for these weight fluctuations. This term is dependent on the power of the input signal $x(k)$. To overcome this, the correction term can be normalized leading to the so-called *Normalized Least-Mean-Square* (NLMS) algorithm (Haykin 1996):

$$\underline{w}(k+1) = \underline{w}(k) + \tilde{\mu} \frac{\underline{x}(k)e(k)}{\epsilon + \underline{x}^T(k)\underline{x}(k)}.$$

Here, $\tilde{\mu}$ is the NLMS step-size and ϵ is a small positive constant to prevent division by zero. Under the independence assumption, convergence in the mean square requires $0 < \tilde{\mu} < 2$ (Haykin 1996).

1.3.4 The Standard RLS Algorithm

The standard Recursive Least-Squares (RLS) algorithm is characterized by a deterministic error criterion for each sampling instant k , given by

$$\mathcal{J}_{\text{RLS}}(k) = \sum_{l=-\infty}^k \lambda^{k-l} (d(l) - \underline{w}(k+1)^T \underline{x}(l))^2, \quad (1.9)$$

where λ is the so-called *forgetting factor* with $0 < \lambda < 1$. By setting the derivatives of $\mathcal{J}_{\text{RLS}}(k)$ with respect to the elements of the weight vector $\underline{w}(k+1)$ equal to zero, we find that the minimum of $\mathcal{J}_{\text{RLS}}(k)$ is attained when

$$\underline{w}(k+1) = \hat{\mathbf{R}}^{-1}(k) \hat{\underline{p}}(k), \quad (1.10)$$

where

$$\begin{aligned} \hat{\mathbf{R}}(k) &= \sum_{l=-\infty}^k \lambda^{k-l} \underline{x}(l) \underline{x}^T(l) = \lambda \hat{\mathbf{R}}(k-1) + \underline{x}(k) \underline{x}^T(k), \\ \hat{\underline{p}}(k) &= \sum_{l=-\infty}^k \lambda^{k-l} d(l) \underline{x}(l) = \lambda \hat{\underline{p}}(k-1) + d(k) \underline{x}(k). \end{aligned}$$

Equation (1.10) gives the standard RLS algorithm. In contrast with the method of steepest descent and the LMS algorithm, the RLS algorithm does not perform a gradient search. Instead, it directly optimizes the cost function in (1.9) that is, however, slightly different at each sampling instant.

The RLS algorithm in (1.10) may be formulated in a recursive way by observing that

$$\hat{\mathbf{R}}(k) \underline{w}(k+1) = \hat{\underline{p}}(k), \quad (1.11)$$

$$\text{and} \quad \hat{\mathbf{R}}(k-1) \underline{w}(k) = \hat{\underline{p}}(k-1). \quad (1.12)$$

We multiply (1.12) by λ and subtract the result from (1.11). Then with $\hat{\underline{p}}(k) - \lambda \hat{\underline{p}}(k-1) = d(k) \underline{x}(k)$ and with $\lambda \hat{\mathbf{R}}(k-1) = \hat{\mathbf{R}}(k) - \underline{x}(k) \underline{x}^T(k)$ the resulting equation yields the following updating rule for the RLS algorithm:

$$\underline{w}(k+1) = \underline{w}(k) + \hat{\mathbf{R}}^{-1}(k) \underline{x}(k) e(k).$$

Note that when comparing the RLS algorithm with the LMS algorithm in (1.8) the step-size μ has been replaced by the inverse of $\hat{\mathbf{R}}(k)$. In some cases the RLS algorithm outperforms the LMS algorithm. The price to pay is an increase in computational complexity. With the aid of the matrix inversion lemma it is possible to track the inverse of $\hat{\mathbf{R}}$, avoiding the need of matrix inversion, see e.g. (Haykin 1996):

$$\hat{\mathbf{R}}^{-1}(k) = \frac{1}{\lambda} \left\{ \hat{\mathbf{R}}^{-1}(k-1) - \frac{\hat{\mathbf{R}}^{-1}(k-1) \underline{x}(k) \underline{x}^T(k) \hat{\mathbf{R}}^{-1}(k-1)}{\lambda + \underline{x}^T(k) \hat{\mathbf{R}}^{-1}(k-1) \underline{x}(k)} \right\}.$$

For use of the RLS algorithm an initialization is required. Usually, $\hat{\mathbf{R}}^{-1}(0) = \delta^{-1} \mathbf{I}$ is taken, where δ is a small positive number (Haykin 1996).

Similar to the choice of the step-size μ for the LMS algorithm described in the previous section, the choice of the forgetting factor λ for the RLS algorithm involves a trade-off between convergence speed and accuracy: a small value for λ yields fast convergence but large fluctuations around the steady-state solution, and vice versa.

The convergence behaviour of the RLS algorithm is greatly influenced by the numerical precision with which the calculations are performed. For instance, due to round-off errors $\hat{\mathbf{R}}(k)$ may lose its symmetry property resulting in bad or no convergence of the RLS algorithm. Numerous modifications of the RLS algorithm have been reported in the literature that yield an increase in the robustness of the RLS algorithm for finite wordlength implementations.

1.4 Adaptive Linear Regression Models

The major drawback of adaptive TDLs is that many taps are required in case the reference filter has a long memory. The use of many taps has a few undesirable implications. First, a lot of costly memory is needed to store the previous input samples and the adaptive weights. Second, the calculation of the convolution yielding $y(k)$ and the calculation of the weight updates involves a large computational burden. Third, each adaptive weight fluctuating in the steady state gives rise to a certain noise contribution at the output of the adaptive filter. A large number of adaptive weights thus limits the performance of the adaptive filter in the sense that the *misadjustment* becomes large (Haykin 1996).

For these reasons interest has grown for adaptive Infinite Impulse Response (IIR) filters. IIR filters are well suited to approximate systems with infinitely long impulse responses using only a few (recursive) parameters. However, the adaptation of these parameters is far more complicated. Generally, the error function is multimodal, meaning that local minima exist. As a consequence a gradient based adaptation algorithm can get stuck in such a local minimum giving rise to poor performance of the adaptive filter. Another obstacle for adaptive IIR filters is formed by the potentially unstable behaviour of the adaptation algorithm.

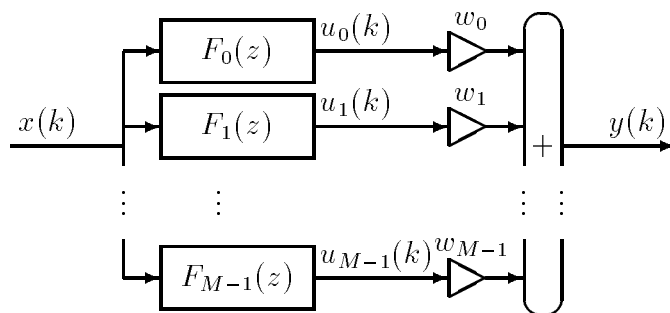


Figure 1.8: Discrete linear regression model.

Fortunately, the attractive properties of the adaptive TDL and the adaptive IIR filters can be combined in an adaptive Linear Regression Model (LRM). In Fig. 1.8 the general scheme of an LRM is shown. The input signal $x(k)$ is filtered by the set of linearly independent and stable tap filters $F_0(z)$ to $F_{M-1}(z)$ resulting in the tap signals $u_0(k)$ to $u_{M-1}(k)$. The output signal $y(k)$ is obtained as a weighted sum of the tap signals. Due

to the structural similarities between the TDL and the LRM, most of the adaptation algorithms for the TDL (such as the LMS or the standard RLS algorithm) can be applied to an LRM with adaptive weights.

The tap filters $F_0(z)$ to $F_{M-1}(z)$ can either be of the FIR or the IIR type, as long as they are stable. Since we are interested in applying adaptive filters to those situations where the reference filter has a long memory, we will concentrate on tap filters of the IIR type. These tap filters contain one or more (fixed) parameters (e.g. in the form of pole(s)) that need to be chosen beforehand.

The tap signals of the LRM are combined in the following tap signal vector:

$$\underline{u}(k) = [u_0(k), u_1(k), \dots, u_{M-1}(k)]^T.$$

As in a TDL, the output signal $y(k)$ is formed by a weighted summation of the tap signals and is thus linear in the weights:

$$y(k) = \sum_{m=0}^{M-1} w_m u_m(k) = \underline{w}^T \underline{u}(k).$$

With reference to Fig. 1.1, we may now write for the error signal

$$e(k) = d(k) - \underline{w}^T \underline{u}(k)$$

and the mean-squared error (MSE) becomes

$$\begin{aligned} \mathcal{J} &= E\{e^2(k)\} = E\{[d(k) - \underline{w}^T(k)\underline{u}(k)]^2\} \\ &= E\{d^2(k)\} + \underline{w}^T \mathbf{R} \underline{w} - 2\underline{w}^T \underline{p}. \end{aligned} \quad (1.13)$$

Here the vector \underline{p} is given by

$$\underline{p} = E\{d(k)\underline{u}(k)\},$$

where the $(p+1)$ -th element denotes the covariance between the desired signal $d(k)$ and the tap signal $u_p(k)$. The matrix \mathbf{R} is the $M \times M$ covariance matrix of the tap signal vector $\underline{u}(k)$:

$$\mathbf{R} = E\{\underline{u}(k)\underline{u}^T(k)\}, \quad (1.14)$$

and thus the $(p+1, q+1)$ -th element of \mathbf{R} is given by $\mathbf{R}_{pq} = E\{u_p(k)u_q(k)\}$. The covariance matrix \mathbf{R} again is symmetric ($\mathbf{R} = \mathbf{R}^T$) and nonnegative definite, but not necessarily Toeplitz. However, certain choices for the filters $F_m(z)$ yield a Toeplitz covariance matrix \mathbf{R} , as will be shown in Chapter 2. This is true if $F_{m+1}(z) = A(z)F_m(z)$, where $A(z)$ is an all-pass function, independent of m .

For the LRM the LMS updating algorithm reads

$$\underline{w}(k+1) = \underline{w}(k) + \mu \underline{u}(k) e(k),$$

while for the NLMS algorithm we have

$$\underline{w}(k+1) = \underline{w}(k) + \tilde{\mu} \frac{\underline{u}(k)e(k)}{\epsilon + \underline{u}^T(k)\underline{u}(k)},$$

where ϵ is a small positive number. Under the independence assumption, convergence in the mean square requires $0 < \mu < 2/\text{trace}\{\mathbf{R}\}$ and $0 < \tilde{\mu} < 2$.

The standard RLS algorithm is given by

$$\underline{w}(k+1) = \underline{w}(k) + \hat{\mathbf{R}}^{-1}(k) \underline{u}(k) e(k),$$

where $\hat{\mathbf{R}}^{-1}(k) = \sum_{l=-\infty}^k \lambda^{k-l} \underline{u}(l) \underline{u}^T(l)$, with λ the forgetting factor satisfying $0 < \lambda < 1$.

1.5 Filter Length and MSE: an Example

In the previous section it has been made clear that the adaptive TDL has its shortcomings in that its FIR structure may not particularly be matched to the unknown reference system that it is required to resemble. If the reference system has an (infinitely) long memory, a large filter length M is required for a small approximation error. Next, an illustrative example will show that a large number M of required adaptive weights is indeed a limiting factor in terms of the performance of an LMS adaptive TDL.

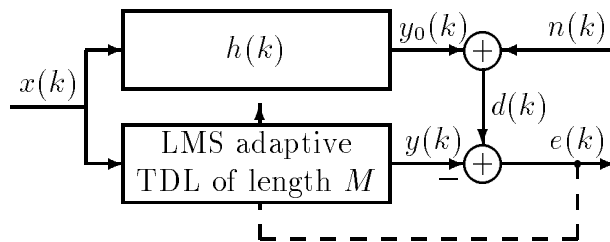


Figure 1.9: Adaptive filter configuration. The reference filter is not in the model set.

Consider the adaptive filtering configuration depicted in Fig. 1.9. The reference filter is assumed to be stable, linear and time-invariant. Its impulse response, denoted by $h(k)$, is of infinite duration. In this example we take a first-order low-pass filter $h(k) = \sqrt{1 - \xi^2} \xi^k$ with $\xi = 0.995$ (note that $\sum_{k=0}^{\infty} h^2(k) = 1$). The excitation signal $x(k)$ has power σ_x^2 and is assumed to be white to make this example mathematically tractable. The signal $n(k)$ with power σ_n^2 is independent of $x(k)$ and need not be white.

The adaptive filter is of the TDL type with M taps. The weights $w_m(k)$ with $m = 0, 1, \dots, M-1$ are updated using the LMS algorithm in (1.8) with step-size μ . It is assumed that the adaptation process has been finished implying that the weights have reached a steady state in which they fluctuate around the Wiener solution³. Since $x(k)$ is white, the

³Actually, in contrast to common belief, the weights do not fluctuate symmetrically around the Wiener solution in the steady state in the sense that the Wiener solution is the mean value of the fluctuating weight vector: this is true only if *the reference system is in the model set!* However, when the adaptive filter contains enough weights to be able to approximate the reference system to a relatively high degree, the deviation from the Wiener solution is small compared to the fluctuations of the weights (without proof).

Wiener solution is the truncated version (length M) of $h(k)$. For the error signal we may now write

$$\begin{aligned} e(k) &= d(k) - y(k) \\ &= n(k) + r(k) - y_f(k), \end{aligned}$$

where $r(k) = \sum_{m=M}^{\infty} h(m)x(k-m)$ is due to the unmodelled part of the reference filter and $y_f(k) = \sum_{m=0}^{M-1} (w_m(k) - h(m))x(k-m)$ is due to the weight fluctuations around the Wiener solution. For white $x(k)$ it can be verified that $E\{r(k)y_f(k)\} = 0$ and thus we may apply superposition of powers when evaluating the MSE:

$$E\{e^2(k)\} = \sigma_n^2 + E\{r^2(k)\} + E\{y_f^2(k)\}. \quad (1.15)$$

The power of $r(k)$ is a *decreasing* function of the number of taps M (remember that $x(k)$ is white):

$$E\{r^2(k)\} = \sigma_r^2(M) = \sigma_x^2 \sum_{m=M}^{\infty} h^2(m).$$

As will be shown in Section 7, for sufficiently small values of μ the power of $y_f(k)$ is given by (see also (Butterweck 1996a; Belt and Butterweck 1996)):

$$E\{y_f^2(k)\} \approx \frac{1}{2}\mu M \sigma_x^2 (\sigma_n^2 + \sigma_r^2(M)). \quad (1.16)$$

In the very exceptional case that $\sigma_n^2 = 0$, $E\{y_f^2(k)\}$ becomes a monotone decreasing function of M , and thus for an MSE in (1.15) as small as possible M should be taken as large as possible. In practice however, we always have $\sigma_n^2 > 0$. In applications of adaptive interference cancelling (see Section 1.2.4), $n(k)$ even is the signal of interest! For larger values of M the power $\sigma_r^2(M)$ becomes smaller and at a certain point σ_n^2 is dominant in the expression for $E\{y_f^2(k)\}$. From this point on the MSE will grow without bound when M is increased.

In Fig. 1.10 the MSE

$$\begin{aligned} E\{e^2(k)\} &= \sigma_n^2 + \sigma_r^2(M) + E\{y_f^2(k)\} \\ &= \left(1 + \frac{1}{2}\mu M \sigma_x^2\right) (\sigma_n^2 + \sigma_r^2(M)) \end{aligned} \quad (1.17)$$

is plotted as a function of the number of taps M in the TDL for three different values of the step-size μ . Here, we took white noise for $n(k)$ with power $\sigma_n^2 = 1$, and $\sigma_x^2 = 1$ so that $\sigma_r^2(0) = 1$. The maximum considered number of taps is 600, so that for stability it is required that $\mu < 2/(M\sigma_x^2) = 1/300$.

For low values of M the MSE in Fig. 1.10 is mostly determined by the modelling error of the adaptive filter, see equation (1.17). For larger values of M the power of the noise $y_f(k)$ due to the weight fluctuations becomes dominant, which limits the number of useful adaptive weights: above a certain number of adaptive weights an additional tap weight results in a higher MSE.

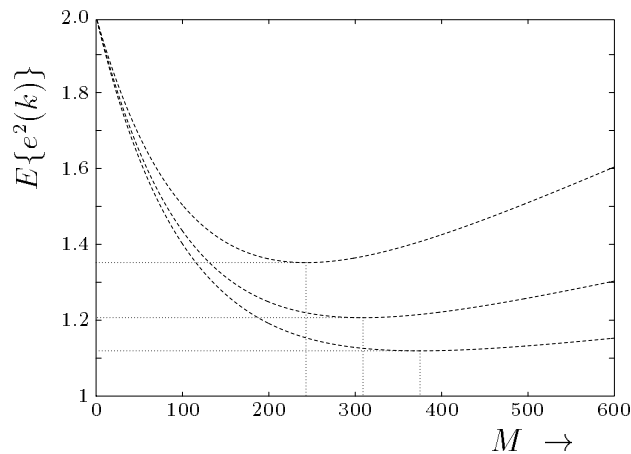


Figure 1.10: The MSE as a function of the number of adaptive weights for three different step-sizes. The upper, middle and lower curves correspond to $\mu = 10^{-4}$, $\mu = 10^{-3}$ and $\mu = 2 \cdot 10^{-3}$, respectively.

In practical adaptive filtering applications the designer demands a certain speed of convergence, and thus μ is given before-hand. The designer can then use a plot like Fig. 1.10 to determine the optimal number of adaptive weights in a TDL. In some cases this yields an MSE that is unsatisfactorily high. A possible approach towards a solution would be a modification of the LMS algorithm so that with the same convergence speed a lower value for $E\{y_f^2(k)\}$ in (1.16) can be obtained (e.g. with a variable step-size LMS algorithm). However, such an approach does not tackle the problem at its source, that is a large number M of adaptive weights. Thus, this example clearly motivates the research of IIR alternatives to the adaptive TDL, especially, as motivated before, adaptive LRMs.

1.6 Scope of this Thesis

The aim of this thesis is to investigate adaptive filters based on linear regression models (LRMs) that may serve as alternatives to the commonly applied adaptive tapped-delay line (TDL). More specifically, we will study adaptive LRMs that, by their nature, are better suited than the adaptive TDL to imitate systems with a long memory.

We will investigate several sets of orthonormal basis functions that can be generated as the impulse responses of (IIR) filters with rational transfer functions. These orthogonal filters contain free design parameters, e.g. in the form of poles. The choice of the set of orthonormal filters for a specific application and their parametrization are of crucial importance towards better adaptive filters.

In Chapter 2 a few general concepts concerning orthogonal series expansions and approximations are treated. In this context some theory on orthogonal polynomials is presented, with emphasis on classical orthogonal polynomials. Two specific sets of orthonor-

mal functions, namely Laguerre and Kautz functions, are treated. The Laguerre and Kautz functions can be generated as the impulse responses of a Laguerre and Kautz network, respectively. The suitability of Laguerre and Kautz networks for adaptive filtering is demonstrated. Also, some methods known in literature to parametrize these filters are briefly discussed.

Chapter 3 deals with orthonormal Jacobi functions constructed from the classical Jacobi polynomials, that can be generated as the impulse responses of a network of filters with rational transfer functions. A special case of this so-called Jacobi network is given by the Legendre network. Being constructed from continuous polynomials, the Jacobi network is continuous. We search for a discrete-time equivalent of the Jacobi (and the Legendre) network, so that it can serve as the basis of an adaptive filter.

As was indicated above, a good parametrization of the IIR filters in the LRM is important. In Chapter 4 so-called generalized Laguerre networks (CT) and Meixner-like networks (DT) are considered. These are generalizations of the (CT and DT) Laguerre networks. The generalized Laguerre networks and Meixner-like networks have a free design parameter in the form of a pole. The problem of how to choose this pole is considered and an optimality condition is found. Chapter 4 is a slightly extended version of a paper in cooperation with A.C. den Brinker (Belt and den Brinker 1995).

In Chapter 5 we consider approximations of functions that are rather concentrated in time by truncated Hermite series. The (classical) Hermite polynomials are orthogonal on $(-\infty, \infty)$ under the weight function e^{-x^2} . The Hermite functions used in the approximation are constructed by multiplying the Hermite polynomials with the weight function, followed by a translation and a change of scale in the x -axis and finally, a normalization. The choice of the scale and the translation is important in view of a fast convergence of the series. A method is given to arrive at a good scale and translation for the Hermite functions on the basis of a few moments of the function to be approximated. Chapter 5 is the precise text of a paper in cooperation with T. Oliveira e Silva (Oliveira e Silva and Belt 1996).

So far we have only concentrated on the bases for the adaptive LRMs. In Chapter 6 the behaviour of the LMS adaptive algorithm applied to orthonormal LRMs is studied. We look at convergence speed and steady-state weight fluctuations. It is argued that the orthonormal adaptive LRM can outperform the adaptive TDL in those situations where *a priori* available knowledge of the unknown system can be used to parametrize the LRM. Chapter 6 is the (slightly modified version of the) text of a paper in cooperation with H.J. Butterweck (Belt and Butterweck 1996).

Chapter 7 is concerned with an adaptive Laguerre filter. A Laguerre filter has a free design variable in the form of a real pole. A method described in Chapter 2 can be used to select this pole based on off-line measurements performed on the unknown reference system. However, after some time this pole may no longer be optimal. To this end an adaptive optimization procedure for the Laguerre pole is proposed. Chapter 7 is based on a paper in cooperation with A.C. den Brinker (Belt and den Brinker 1996).

As was indicated in Section 1.2, an application of adaptive filters is adaptive prediction. In Chapter 8 we will present a certain adaptive prediction filter that is used for signal

detection, namely an adaptive line enhancer (ALE). An ALE can separate a narrow-band signal from additive broadband noise on the basis of their difference in correlation lengths. The proposed ALE is a second-order IIR filter, of which the center frequency and bandwidth can be controlled separately. The convergence and tracking capabilities of the ALE are demonstrated with computer experiments. Chapter 8 is based on a paper in cooperation with A.C. den Brinker and F.P.A. Benders (Belt, den Brinker, and Benders 1995).

In this thesis Chapters 4, 5, 6, 7 and 8 are based on scientific publications. Consequently, now and then the reader can expect to encounter small portions of previously presented material.

Bibliography

- Belt, H. J. W. and H. J. Butterweck (1996). Cascaded all-pass sections for LMS adaptive filtering. In *Signal Processing VIII: Theories and Applications, Proc. EUSIPCO-96, Eighth European Signal Processing Conference*, Trieste, Italy, pp. 1219–1222.
- Belt, H. J. W. and A. C. den Brinker (1995). Optimality condition for truncated generalized Laguerre networks. *Int. J. Circuit Theory Appl.* *23*, 227–235.
- Belt, H. J. W. and A. C. den Brinker (1996). Laguerre filters with adaptive pole optimization. In *Proc. IEEE International Symposium on Circuits and Systems (ISCAS)*, Atlanta (GA), U.S.A., pp. 37–40.
- Belt, H. J. W., A. C. den Brinker, and F. P. A. Benders (1995). Adaptive line enhancement using a second-order IIR filter. In *Proc. IEEE International Conference on Acoustics, Speech and Signal Processing (ICASSP)*, Detroit (MI), U.S.A., pp. 1444–1447.
- Butterweck, H. J. (1995). A steady-state analysis of the LMS adaptive algorithm without use of the independence assumption. In *Proc. IEEE International Conference on Acoustics, Speech and Signal Processing (ICASSP)*, Detroit (MI), U.S.A., pp. 1404–1407.
- Butterweck, H. J. (1996a). A new interpretation of the misadjustment in adaptive filtering. In *Proc. IEEE International Conference on Acoustics, Speech and Signal Processing (ICASSP)*, Atlanta (GA), U.S.A., pp. 1641–1643.
- Butterweck, H. J. (1996b). An approach to LMS adaptive filtering without use of the independence assumption. In *Signal Processing VIII: Theories and Applications, Proc. EUSIPCO-96, Eighth European Signal Processing Conference*, Trieste, Italy, pp. 1223–1226.
- Butterweck, H. J. (1996c). Iterative analysis of the steady-state weight fluctuations in LMS-type adaptive filters. Technical Report 96-E-299, Eindhoven University of Technology.

- den Brinker, A. C., H. J. W. Belt, and F. P. A. Benders (1994). An adaptive line enhancer based on a second-order IIR filter. In *Proc. ProRISC/IEEE Benelux Workshop on Circuits, Systems and Signal Processing*, Arnhem, Netherlands, pp. 59–65.
- Douglas, S. C. (1995). Exact expectation analysis of the LMS adaptive filter. *IEEE Trans. Signal Process.* 43, 2863–2871.
- Eykhoff, P. (1974). *System Identification: Parameter and State Estimation*. London, U.K.: John Wiley and Sons.
- Franklin, J. N. (1968). *Matrix Theory*. Englewood Cliffs (NJ), U.S.A.: Prentice-Hall.
- Gray, R. M. (1972). On the asymptotic eigenvalue distribution of Toeplitz matrices. *IEEE Trans. I.T.* 18, 725–730.
- Haykin, S. (1996). *Adaptive Filter Theory, Third Edition*. London, U.K.: Prentice-Hall Int.
- Levinson, N. (1947). The Wiener RMS error criterion in filter design and prediction. *J. Math. Phys.* 25, 261–278.
- Ljung, L. (1987). *System Identification: Theory for the user*. Englewood Cliffs (NJ), U.S.A.: Prentice-Hall.
- Oliveira e Silva, T. and H. J. W. Belt (1996). On the determination of the optimal center and scale factor for truncated hermite series. In *Signal Processing VIII: Theories and Applications, Proc. EUSIPCO-96, Eighth European Signal Processing Conference*, Trieste, Italy, pp. 1563–1566.
- Widrow *et al.*, B. (1975). Adaptive noise cancelling: principles and applications. *Proc. IEEE* 63, 1692–1716.
- Wiener, N. (1949). *Extrapolation, Interpolation and Smoothing of Stationary Time Series, with Engineering Applications*. New York (NY), U.S.A.: John Wiley and Sons.

Chapter 2

Orthogonal Filters

2.1 Introduction

In Chapter 1 we have presented a brief introduction to adaptive filters. It was demonstrated that the character of the commonly used FIR filter can be problematic when systems with long memory need to be approximated. To cope with such systems, an adaptive filter of a more general form was introduced, namely the *adaptive linear regression model* (LRM). The adaptive LRM can, under some circumstances, suffice with much less adaptive parameters than an adaptive FIR filter.

This chapter deals with the choice of the set of (IIR) filters in an LRM. First, some notational conventions will be introduced. Next, orthogonal expansions of some relevant Hilbert spaces related to continuous-time (CT) and discrete-time (DT) signals and their connections will be considered. A function belonging to such a Hilbert space can be represented by an orthogonal series expansion. This leads to a treatment of orthogonal polynomials and their most relevant properties. Some of the *classical* orthogonal polynomials form the origin of orthonormal basis functions that appear to be very well suited as a basis for the construction of adaptive LRMs.

2.2 Some Relevant Hilbert Spaces

“A Hilbert space is an inner product space which is a complete metric space with respect to the metric induced by its inner product” (Young 1988). An inner product space (or pre-Hilbert space) is a linear vector space with an inner product defined between any two of its elements. The inner product is used to define a *norm* of an element of the inner product space. This norm is then used to define a *distance* (a *metric*) between any two elements of the inner product space. Finally, a Hilbert space is a *complete* inner product space, which means that any convergent Cauchy sequence of elements of that space converges towards an element of that space. For a first introduction to Hilbert spaces see (Young 1988).

In this section some Hilbert spaces are introduced that are relevant to the remaining chapters. Henceforth, \mathbb{R} will denote the set of real numbers and \mathbb{R}^+ the set of positive real

numbers. The set of integers will be denoted by \mathbb{Z} and the set of nonnegative integers by \mathbb{N}_0 .

A continuous-time (CT) signal $x(t)$ with $t \in \mathbb{R}$ is square-integrable if

$$\int_{-\infty}^{\infty} |x(t)|^2 dt < \infty. \quad (2.1)$$

The Laplace transform of $x(t)$ and its inverse transform are defined by

$$X(s) = \mathcal{L}\{x(t)\} = \int_{-\infty}^{\infty} x(t) e^{-st} dt, \quad (2.2)$$

$$x(t) = \mathcal{L}^{-1}\{X(s)\} = \frac{1}{2\pi j} \int_{-j\infty}^{j\infty} X(s) e^{st} ds. \quad (2.3)$$

A discrete-time (DT) signal $x(k)$ with $k \in \mathbb{Z}$ is square-summable if

$$\sum_{k=-\infty}^{\infty} |x(k)|^2 < \infty. \quad (2.4)$$

The z -transform of $x(k)$ and its inverse transform are defined by

$$X(z) = \mathcal{Z}\{x(k)\} = \sum_{k=-\infty}^{\infty} x(k) z^{-k}, \quad (2.5)$$

$$x(k) = \mathcal{Z}^{-1}\{X(z)\} = \frac{1}{2\pi j} \oint_C X(z) z^k \frac{dz}{z}, \quad (2.6)$$

where the contour integral C is taken counter-clockwise around the unit circle.

The Hilbert space of square-integrable functions on \mathbb{R} is denoted by $L_2(\mathbb{R})$. An inner product between two functions belonging to $L_2(\mathbb{R})$, say $g_1(t)$ and $g_2(t)$, is defined by

$$\langle g_1(t), g_2(t) \rangle = \int_{-\infty}^{\infty} g_1(t) g_2^*(t) dt. \quad (2.7)$$

In this thesis we often consider impulse responses of causal stable filters. Such an impulse response, say $h(t)$, is only defined for $t \in \mathbb{R}^+$. The Hilbert space of square-integrable causal functions is denoted by $L_2(\mathbb{R}^+)$. We define for a causal function that $h(t) = 0$ for $t < 0$, so that the inner product definition of (2.7) can be used for square-integrable causal functions, where the integral effectively extends from 0 to ∞ .

The *norm* of a member of $L_2(\mathbb{R})$, say $g(t)$, is defined as the square root of the inner product of $g(t)$ with itself:

$$\|g(t)\| = \sqrt{\langle g(t), g(t) \rangle}.$$

The *distance* between two members of $L_2(\mathbb{R})$, say $g_1(t)$ and $g_2(t)$, is then defined by $\|g_1(t) - g_2(t)\|$. If the inner product between two functions vanishes, the two functions are said to be *orthogonal*. If, in addition, these functions have unity norms they are said to be *orthonormal*.

According to Parseval's theorem the inner product between two functions in $L_2(\mathbb{R})$, say $g_1(t)$ and $g_2(t)$, can be written as

$$\langle g_1(t), g_2(t) \rangle = \frac{1}{2\pi j} \int_{-j\infty}^{j\infty} G_1(s) G_2^*(-s^*) ds = \frac{1}{2\pi} \int_{-\infty}^{\infty} G_1(j\omega) G_2^*(j\omega) d\omega.$$

This can be seen as follows:

$$\begin{aligned} \langle g_1(t), g_2(t) \rangle &= \int_{-\infty}^{\infty} g_1(t) g_2^*(t) dt = \int_{-\infty}^{\infty} \left\{ \frac{1}{2\pi j} \int_{-j\infty}^{j\infty} G_1(s) e^{st} ds \right\} g_2^*(t) dt \\ &= \frac{1}{2\pi j} \int_{-j\infty}^{j\infty} G_1(s) \left\{ \int_{-\infty}^{\infty} g_2(t) e^{s^*t} dt \right\}^* ds = \frac{1}{2\pi j} \int_{-j\infty}^{j\infty} G_1(s) G_2^*(-s^*) ds. \end{aligned}$$

The Hilbert space of square-summable functions on \mathbb{Z} is denoted by $\ell_2(\mathbb{Z})$. The inner product between two members of $\ell_2(\mathbb{Z})$, say $f_1(k)$ and $f_2(k)$, is defined as¹

$$\langle f_1(k), f_2(k) \rangle = \sum_{k=-\infty}^{\infty} f_1(k) f_2^*(k). \quad (2.8)$$

In this thesis we often consider impulse responses of causal stable systems. Stability of a DT system is ensured by the requirement that its impulse response is absolutely summable². This is sufficient to ensure that such an impulse response is a member of $\ell_2(\mathbb{N}_0)$, the Hilbert space of causal square-summable functions³. We define for a causal function that $h(k) = 0$ for $k < 0$, so that the inner product definition of (2.8) can be used for square-summable causal functions, where the summation effectively extends from 0 to ∞ .

A norm of a member of $\ell_2(\mathbb{Z})$ and a distance measure between two members of $\ell_2(\mathbb{Z})$ can be defined in a similar way as for members of $L_2(\mathbb{R})$. With Parseval's theorem we have that the inner product between two functions belonging to $\ell_2(\mathbb{Z})$, say $f_1(k)$ and $f_2(k)$, can be written as

$$\langle f_1(k), f_2(k) \rangle = \frac{1}{2\pi j} \oint_C F_1(z) F_2^*(1/z^*) \frac{dz}{z} = \frac{1}{2\pi} \int_{-\pi}^{\pi} F_1(e^{j\Omega}) F_2^*(e^{j\Omega}) d\Omega. \quad (2.9)$$

¹For clarity it is mentioned here that all inner products appearing in this thesis are taken with respect to either the continuous time index t or the discrete time index k .

²This requirement implies that a bounded input of the system yields a bounded output.

³A causal absolutely summable function $h(k)$ satisfies $\sum_{k=0}^{\infty} |h(k)| < \infty$, which implies that $h(k)$ is absolutely bounded: $|h(k)| < M \forall k \in \mathbb{N}_0$. Consequently, $\sum_{k=0}^{\infty} |h(k)|^2 \leq M \sum_{k=0}^{\infty} |h(k)| < \infty$, and thus $h(k)$ is a member of $\ell_2(\mathbb{N}_0)$.

A specific isomorphism can be considered between the CT signal space and the DT signal space via Laplace and z -transforms, see (Steiglitz 1965). Let's start with the bilinear transformation that maps the variable s onto z according to

$$s = a \frac{z-1}{z+1}, \quad \text{so that} \quad ds = \frac{2a}{(z+1)^2} dz. \quad (2.10)$$

The inverse transformation is given by

$$z = \frac{a+s}{a-s}, \quad \text{so that} \quad dz = \frac{2a}{(a-s)^2} ds.$$

With $a \in \mathbb{R}^+$, the bilinear transformation maps the left-half s -plane onto the unit disc in the z -plane and the imaginary axis onto the unit circle. This means that a transfer function $G(s)$ of a causal and stable CT system is mapped onto a transfer functions $F(z)$ of a causal and stable DT system.

We consider the functions $g_1(t)$ and $g_2(t)$ belonging to $L_2(\mathbb{R})$ with Laplace transforms $G_1(s)$ and $G_2(s)$ according to (2.3), and the functions $f_1(k)$ and $f_2(k)$ in $\ell_2(\mathbb{Z})$ with z -transforms $F_1(z)$ and $F_2(z)$ according to (2.6). By making a change of variable with (2.10), we can write for the inner product between $g_1(t)$ and $g_2(t)$:

$$\begin{aligned} \langle g_1(t), g_2(t) \rangle &= \frac{1}{2\pi j} \int_{-j\infty}^{j\infty} G_1(s) G_2^*(-s^*) ds \\ &= \frac{1}{2\pi j} \oint_C G_1\left(a \frac{z-1}{z+1}\right) G_2^*\left(a \frac{1/z^*-1}{1/z^*+1}\right) \frac{2a}{(z+1)^2} dz \\ &= \frac{1}{2\pi j} \oint_C \left\{ \frac{\sqrt{2a} z}{z+1} G_1\left(a \frac{z-1}{z+1}\right) \right\} \left\{ \frac{\sqrt{2a} 1/z^*}{1/z^*+1} G_2\left(a \frac{1/z^*-1}{1/z^*+1}\right) \right\}^* \frac{dz}{z} \\ &= \frac{1}{2\pi j} \oint_C F_1(z) F_2^*(1/z^*) \frac{dz}{z}. \end{aligned}$$

Thus, via the mapping \mathcal{M} of a function $G(s)$ onto a function $F(z)$ according to

$$\mathcal{M} : G(s) \mapsto \frac{\sqrt{2a} z}{z+1} G\left(a \frac{z-1}{z+1}\right) = F(z), \quad (2.11)$$

it is found that

$$\frac{1}{2\pi j} \int_{-\infty}^{\infty} G_1(s) G_2^*(-s^*) ds = \frac{1}{2\pi j} \oint_C F_1(z) F_2^*(1/z^*) \frac{dz}{z},$$

see (Steiglitz 1965). This mapping is called the *Modified Bilinear Transform* (MBT). The MBT produces an isomorphism that preserves inner products between the CT and DT signal spaces.

Along similar lines of reasoning an inverse mapping \mathcal{M}^{-1} is found that maps a function $F(z)$ onto a function $G(s)$ with preservation of inner products:

$$\mathcal{M}^{-1} : F(z) \mapsto \frac{\sqrt{2a}}{a+s} F\left(\frac{a+s}{a-s}\right) = G(s). \quad (2.12)$$

Further, we will need the Hilbert space of all zero-mean, stationary stochastic processes with finite variances. Here we confine ourselves to the DT case. The inner product between two such stochastic processes $f_1(k)$ and $f_2(k)$ is defined by their covariance:

$$E\{f_1(k) f_2^*(k)\}, \quad k \in \mathbb{Z}.$$

If, in addition, $f_1(k)$ and $f_2(k)$ are ergodic, the ensemble average may be replaced by a time average denoted by $A\{\cdot\}$. The *cross-correlation* function of two (wide-sense stationary) stochastic signals $x(k)$ and $y(k)$ is defined by

$$\rho_{xy}(l) = E\{x(k) y^*(k+l)\}, \quad k, l \in \mathbb{Z}.$$

The corresponding *cross-power spectral density* function $\Phi_{xy}(\Omega)$ is obtained after Fourier transformation of $\rho_{xy}(l)$,

$$\Phi_{xy}(\Omega) = \sum_{l=-\infty}^{\infty} \rho_{xy}(l) e^{-j\Omega l},$$

and has periodicity 2π . In a similar way the *auto-correlation* function $\rho_{xx}(l)$ of a wide-sense stationary stochastic process $x(k)$ and the corresponding power spectral density function $\Phi_{xx}(\Omega)$ are defined.

We now consider the output $y(k)$ of a causal linear time-invariant (LTI) system with (real) impulse response $h(k)$. The output $y(k)$ is related to the input $x(k)$ through a convolution:

$$y(k) = h(k) * x(k) = \sum_{l=0}^{\infty} h(l) x(k-l).$$

Consider two LTI systems with impulse responses $h_1(k)$ and $h_2(k)$, that are excited by the stationary stochastic excitations $x_1(k)$ and $x_2(k)$, respectively. For the covariance matrix of an LRM in (1.14), we need to determine covariances of the form $E\{y_1(k) y_2^*(k)\}$. These can be calculated as follows:

$$\begin{aligned} E\{y_1(k) y_2^*(k)\} &= E\{[h_1(k) * x_1(k)] [h_2(k) * x_2^*(k)]\} \\ &= E\left\{ \sum_{l_1=0}^{\infty} h_1(l_1) x_1(k-l_1) \sum_{l_2=0}^{\infty} h_2(l_2) x_2^*(k-l_2) \right\} \\ &= \sum_{l_2=0}^{\infty} \left[\sum_{l_1=0}^{\infty} h_1(l_1) E\{x_1(k-l_1) x_2^*(k-l_2)\} \right] h_2(l_2) \\ &= \langle h_1(l) * \rho_{x_1 x_2}(l), h_2(l) \rangle \\ &= \frac{1}{2\pi} \int_{-\pi}^{\pi} H_1(e^{j\Omega}) H_2^*(e^{j\Omega}) \Phi_{x_1 x_2}(\Omega) d\Omega. \end{aligned} \quad (2.13)$$

Note that apart from the additional weight function $\Phi_{x_1 x_2}(\Omega)$, the covariance in (2.13) is similar to the inner product in (2.9).

2.3 Orthogonal Series Expansions

For the approximation of the impulse responses of stable causal systems, expansions in terms of orthogonal functions are of great interest. We treat such expansions in discrete time. The treatment of continuous-time systems follows similar lines of reasoning.

We start with a causal function $h(k)$ belonging to $\ell_2(\mathbb{N}_0)$, the sampled impulse response of a stable causal system, and a set of orthonormal functions $\{\phi_m(k)\}_{m=0}^{\infty}$ belonging to $\ell_2(\mathbb{N}_0)$. The approximation of $h(k)$ by a linear combination of the first M orthonormal functions $\phi_m(k)$ involves the minimization of the error

$$\zeta_M = \sum_{k=0}^{\infty} \left| h(k) - \sum_{m=0}^{M-1} c_m \phi_m(k) \right|^2. \quad (2.14)$$

The minimum of (2.14) is achieved when the coefficients c_m are given by

$$c_m = \langle h(k), \phi_m(k) \rangle, \quad m = 0, 1, \dots, M-1.$$

It has the value $\min \zeta_M = \|h(k)\|^2 - \sum_{m=0}^{M-1} |c_m|^2$, so that

$$\sum_{m=0}^{M-1} |c_m|^2 \leq \|h(k)\|^2.$$

Particularly, with $M \rightarrow \infty$, we obtain *Bessel's inequality*

$$\sum_{m=0}^{\infty} |c_m|^2 \leq \|h(k)\|^2. \quad (2.15)$$

As a consequence of the orthogonality of the basis functions, the value of c_m minimizing (2.14) does not depend on the order M of the approximation. Therefore, addition of an extra term $c_M \phi_M(k)$ improves the approximation without the necessity to recalculate all previous coefficients c_m ($m = 0, 1, \dots, M-1$).

Apart from the orthogonality of the basis functions, an important desired property is that of *completeness*. The set of basis functions $\{\phi_m(k)\}_{m=0}^{\infty}$ is complete in $\ell_2(\mathbb{N}_0)$ if any function $h(k)$ belonging to $\ell_2(\mathbb{N}_0)$ can be approximated to any desired accuracy by a linear combination of the functions $\phi_m(k)$. Consequently, the set of functions $\{\phi_m(k)\}_{m=0}^{\infty}$ is complete in $\ell_2(\mathbb{N}_0)$ if

$$\langle h(k), \phi_m(k) \rangle = 0 \quad \forall m \in \mathbb{N}_0$$

implies that $h(k) \in \ell_2(\mathbb{N}_0)$ vanishes. When functions $\phi_m(k)$ are orthonormal and complete in $\ell_2(\mathbb{N}_0)$, they form a so-called orthonormal *basis* of $\ell_2(\mathbb{N}_0)$. In this case Bessel's inequality

in (2.15) becomes an equality and we may write for the squared norm of $h(k)$

$$\sum_{m=0}^{\infty} |c_m|^2 = \|h(k)\|^2. \quad (2.16)$$

Eq. 2.16 is known as *Parseval's relation*.

2.4 Orthogonal Polynomials

We will now seek for sets of complete orthogonal functions, starting with some theory on (classical) orthogonal polynomials. First we focus on the continuous orthogonal polynomials in Section 2.4.1, and then we treat the discrete orthogonal polynomials in Section 2.4.2.

2.4.1 Continuous Polynomials

Let's consider a so-called *weight function* or *norm function* $w(x)$, that is real, nonnegative and integrable on the interval (a, b) . It is also assumed that $w(x) > 0$ on a sufficiently large sub-interval of (a, b) , so that

$$\int_a^b w(x) dx > 0.$$

Further, in the case that the interval (a, b) is infinite (meaning that $a = -\infty$ and/or $b = \infty$), we require that all following moments of $w(x)$ are finite:

$$\int_a^b x^m w(x) dx < \infty, \quad \forall m \in \mathbb{N}_0.$$

Now, we associate with $w(x)$ a sequence of m -th order polynomials of the form

$$p_m(x) = \alpha_{m,m} x^m + \alpha_{m,m-1} x^{m-1} + \dots + \alpha_{m,0}, \quad m = 0, 1, 2, \dots,$$

that obeys the generalized orthogonality relation

$$\int_a^b p_m(x) p_n(x) w(x) dx = \begin{cases} 0, & \text{for } m \neq n, \\ h_m^2, & \text{for } m = n, \end{cases} \quad (2.17)$$

where h_m is a (nonzero) normalization constant called the *norm*. The polynomial $p_m(x)$ is of order m and its leading coefficient is strictly positive ($\alpha_{m,m} > 0$). The polynomials $p_m(x)$ are said to constitute a system of orthogonal polynomials on the interval (a, b) with

weight function $w(x)$ (Szegő 1959; Gradshteyn and Ryzhik 1980). For an inner product of the form in (2.17) a short-hand notation is introduced:

$$\langle f(x), g(x) \rangle_{w(x)} = \int_a^b f(x) g(x) w(x) dx.$$

According to the theorem of Weierstrass, the system of orthogonal polynomials $p_m(x)$ is complete when the orthogonality interval (a, b) is finite, see (Szegő 1959; Beckmann 1973). When the interval (a, b) is infinite the system is not necessarily incomplete: such a system requires a special investigation to check completeness. The orthogonal polynomials on an infinite interval that will be described hereafter, namely the (generalized) Laguerre polynomials and the Hermite polynomials, can both be shown to form complete systems, see (Beckmann 1973).

We may define functions $f_m(x)$ as the polynomials $p_m(x)$ multiplied by the square root of the weight function $w(x)$. In this way, a new system of orthogonal functions is obtained that is complete in the Hilbert space of square-integrable functions on the interval (a, b) . When $a = 0$ and $b = \infty$ this corresponds to the Hilbert space $L_2(\mathbb{R}^+)$.

An arbitrary polynomial $g_r(x)$ of degree r can be expressed as a linear combination of polynomials $p_0(x), p_1(x), \dots, p_r(x)$:

$$g_r(x) = \sum_{n=0}^r c_n p_n(x),$$

with $c_n = \langle g_r(x), p_n(x) \rangle_{w(x)}$. As a consequence, an orthogonal polynomial $p_m(x)$ is orthogonal (with weight $w(x)$) to any polynomial $g(x)$ of degree r lower than m , since when $r < m$

$$\langle p_m(x), g_r(x) \rangle_{w(x)} = \langle p_m(x), \sum_{n=0}^r c_n p_n(x) \rangle_{w(x)} = \sum_{n=0}^r c_n \langle p_m(x), p_n(x) \rangle_{w(x)} = 0.$$

We now show that all orthogonal polynomials satisfy a recurrence relation of the form ($m \in \mathbb{N}_0$)

$$p_{m+1}(x) = \{A_m + B_m x\} p_m(x) - C_m p_{m-1}(x), \quad (2.18)$$

where we define $p_{-1}(x) = 0$. Since the function $x p_m(x)$ is a polynomial of order $m+1$ it may be expanded as follows:

$$x p_m(x) = \sum_{n=0}^{m+1} c_n p_n(x),$$

where the expansion coefficients c_n are given by

$$c_n = \langle x p_m(x), p_n(x) \rangle = \langle p_m(x), x p_n(x) \rangle, \quad n = 0, 1, \dots, m+1.$$

Since the polynomial $p_m(x)$ is orthogonal to all polynomials of order lower than m , we find $c_n = 0$ for $n = 0, 1, \dots, m - 2$, thus proving (2.18).

Next we consider a subclass of all orthogonal polynomials, called the *classical* orthogonal polynomials, containing the *Jacobi* polynomials, the *Hermite* polynomials and the *generalized Laguerre* polynomials. In Table 2.1 the weight functions for these polynomials are presented, together with the orthogonality interval. The corresponding normalization constants are given in Table 2.2. In this table, $\Gamma(x)$ stands for the Gamma function (Abramowitz and Stegun 1970). Explicit expressions for the classical orthogonal polynomials are provided in Table 2.3.⁴ Finally, Table 2.4 presents the coefficients for the recurrence relation (2.18). In this table, $(x)_n$ stands for the Pochhammer symbol⁵.

Special cases can be considered. The Jacobi polynomials contain the (shifted) *Legendre* polynomials for $a = c = 1$, the (shifted) *Chebyshev* polynomials of the first kind for $\alpha = 0$, $\gamma = \frac{1}{2}$ and of the second kind for $\alpha = 2$, $\gamma = \frac{3}{2}$, and the shifted *Gegenbauer* polynomials for $\alpha = 2\beta$, $\gamma = \beta + \frac{1}{2}$ with $\beta > \frac{1}{2}$. The generalized Laguerre polynomials contain the Laguerre polynomials for $\alpha = 0$ (Szegő 1959; Beckmann 1973).

All classical orthogonal polynomials satisfy a differential equation of the form ($m = 0, 1, 2, \dots$)

$$f_2(x)p_m''(x) + f_1(x)p_m'(x) + f_0(x)p_m(x) = 0, \quad (2.19)$$

where a prime denotes differentiation with respect to x . Historically, (2.19) served as the starting point of the classical orthogonal polynomials. The functions $f_0(x)$, $f_1(x)$ and $f_2(x)$ are specified for the classical orthogonal polynomials in Table 2.5.

Name	Symbol	(a, b)	Weight $w(x)$	Conditions
Jacobi	$\mathcal{P}_m^{(\alpha, \gamma)}(x)$	$(0, 1)$	$(1 - x)^{\alpha - \gamma} x^{\gamma - 1}$	$\alpha - \gamma > -1$ $\gamma > 0$
(shifted) Legendre	$\mathcal{T}_m(x)$	$(0, 1)$	1	
(generalized) Laguerre	$l_m^{(\alpha)}(x)$	$(0, \infty)$	$x^\alpha e^{-x}$	$\alpha > -1$
Hermite	$H_m(x)$	$(-\infty, \infty)$	e^{-x^2}	

Table 2.1: The classical orthogonal polynomials.

As we notice from Table 2.1, the orthogonality intervals of the sets of orthogonal polynomials differ. We are particularly interested in an orthogonality interval of $(0, \infty)$

⁴The binomial coefficients in Table 2.3 are defined by $\binom{b}{a} = b(b-1)\dots(b-a+1)/a!$, so that b is not necessarily an integer.

⁵The Pochhammer symbol $(x)_n$, with $x \in \mathbb{R}$ and $n \in \mathbb{N}_0$, is defined by $(x)_n = x(x+1)\dots(x+n-1)$.

Symbol	h_m^2
$\mathcal{P}_m^{(\alpha,\gamma)}(x)$	$\frac{m!\Gamma(m+\gamma)\Gamma(m+\alpha)\Gamma(m+\alpha-\gamma+1)}{(2m+\alpha)\Gamma^2(2m+\alpha)}$
$\mathcal{T}_m(x)$	$\frac{1}{2m+1}$
$l_m^{(\alpha)}(x)$	$\frac{\Gamma(m+a+1)}{m!}$
$H_m(x)$	$\sqrt{\pi}2^m m!$

Table 2.2: Normalization constants of the classical orthogonal polynomials.

$p_m(x)$	N	d_m	c_n	$g_n(x)$
$\mathcal{P}_m^{(\alpha,\gamma)}(x)$	m	$\frac{\Gamma(\gamma+m)}{\Gamma(\alpha+2m)}$	$(-1)^{m+n} \binom{m}{n} \frac{\Gamma(\alpha+m+n)}{\Gamma(\gamma+n)}$	x^n
$\mathcal{T}_m(x)$	m	1	$(-1)^{m+n} \binom{m}{n} \binom{m+n}{n}$	x^n
$l_m^{(\alpha)}(x)$	m	1	$(-1)^n \binom{m+\alpha}{m-n} \frac{1}{n!}$	x^n
$H_m(x)$	$\lfloor \frac{m}{2} \rfloor$	$m!$	$(-1)^n \frac{1}{n!(m-2n)!}$	$(2x)^{m-2n}$

Table 2.3: Explicit expressions for the classical orthogonal polynomials of the form $p_m(x) = d_m \sum_{n=0}^N c_n g_n(x)$.

to represent impulse responses of causal LTI systems. The orthogonality interval $(0, 1)$ of the Jacobi polynomials and their special cases can easily be changed to the interval $(0, \infty)$ by scaling the independent variable x according to $x = e^{-\sigma t}$, where $\sigma, t \in \mathbb{R}^+$. The orthogonality relation in (2.17) then becomes

$$\int_0^{\infty} \mathcal{P}_m^{(a,c)}(e^{-\sigma t}) \mathcal{P}_n^{(a,c)}(e^{-\sigma t}) w(e^{-\sigma t}) \sigma e^{-\sigma t} dt = \begin{cases} 0, & \text{for } m \neq n, \\ h_m^2, & \text{for } m = n. \end{cases}$$

$p_m(x)$	A_m	B_m	C_m
$\mathcal{P}_m^{(\alpha, \gamma)}(x)$	$\frac{-[2m(m+\alpha)+\gamma(\alpha-1)]}{(2m+\alpha-1)(2m+\alpha+1)}$	1	$\frac{m(m+\alpha-1)(m+\gamma-1)(m+\alpha-\gamma)}{(2m+\alpha-2)_3(2m+\alpha-1)}$
$\mathcal{T}_m(x)$	$\frac{-2m-1}{m+1}$	$\frac{4m+2}{m+1}$	$\frac{m}{m+1}$
$l_m^{(\alpha)}(x)$	$\frac{2m+\alpha+1}{m+1}$	$\frac{-1}{m+1}$	$\frac{m+\alpha}{m+1}$
$H_m(x)$	0	2	$2m$

Table 2.4: Coefficients in the recurrence relations for the classical orthogonal polynomials of the form $p_{m+1}(x) = \{A_m + B_m x\} p_m(x) - C_m p_{m-1}(x)$, where $p_0(x) = 1$.

$p_m(x)$	$f_2(x)$	$f_1(x)$	$f_0(x)$
$\mathcal{P}_m^{(\alpha, \gamma)}(x)$	$x(1-x)$	$\gamma - (\alpha + 1)x$	$m(m + \alpha)$
$\mathcal{T}_m(x)$	$x(1-x)$	$(1-2x)$	$m(m+1)$
$l_m^{(\alpha)}(x)$	x	$\alpha + 1 - x$	m
$H_m(x)$	1	$-2x$	$2m$

Table 2.5: Coefficients in the differential equations for the classical orthogonal polynomials of the form $f_2(x)p_m''(x) + f_1(x)p_m'(x) + f_0(x)p_m(x) = 0$.

2.4.2 Discrete Polynomials

Analogous to the continuous orthogonal polynomials discussed in the preceding section such polynomials can also be constructed for a discrete variable.

We consider the weight function $v(k)$ defined on the interval $[A, B]$, which is required to be real, nonnegative and finite for $k \in [A, B]$. It is assumed that $v(k) > 0$ on a subset of $[A, B]$, so that

$$\sum_{k=A}^B v(k) > 0.$$

Further, if the interval $[A, B]$ is infinite (meaning $A = -\infty$ and/or $B = \infty$) we require

that all following moments of $v(k)$ are finite:

$$\sum_{k=A}^B k^m v(k) < \infty, \quad \forall m \in \mathbb{N}_0.$$

Now, a sequence of discrete polynomials $q_m(k)$ associated with $v(k)$, with

$$q_m(k) = a_{m,m}k^m + a_{m,m-1}k^{m-1} + \dots + a_{m,0}, \quad m \in \mathbb{N}_0,$$

can be constructed, that satisfy the following orthogonality relation:

$$\sum_{k=A}^B q_m(k)q_n(k)v(k) = \begin{cases} 0, & \text{for } m \neq n, \\ h_m^2, & \text{for } m = n. \end{cases}$$

Here, h_m is a (nonzero) normalization constant called the *norm*. The polynomial $q_m(k)$ is of order m and its leading coefficient is strictly positive ($a_{m,m} > 0$). The discrete polynomials $q_m(k)$ are said to constitute a system of orthogonal polynomials on the interval $[A, B]$ with weight function $v(k)$. An inner product as above is henceforth written in short-hand notation as

$$\langle f(k), g(k) \rangle_{v(k)} = \sum_{k=A}^B f(k)g(k)v(k).$$

Note that if the orthogonality interval $[A, B]$ is finite, the system of discrete orthogonal polynomials $q_m(k)$ contains a finite number (namely $B - A + 1$) of elements.

All discrete orthogonal polynomials satisfy a recurrence relation of the form ($m = 0, 1, \dots, B - A - 1$):

$$q_{m+1}(k) = \{A_m + B_m k\} q_m(k) - C_m q_{m-1}(k). \quad (2.20)$$

where we define $q_{-1}(k) = 0$. Proof of this can be obtained in a similar way as in Section 2.4 for continuous polynomials.

Next we consider the *classical discrete* orthogonal polynomials, containing the *Chebyshev*, the *Krawtchouk*, the *Hahn*, the *Charlier* and the *Meixner* polynomials (Beckmann 1973). In Table 2.6 the weight functions for these polynomials are presented, together with the orthogonality interval. We see that for all classical discrete orthogonal polynomials the orthogonality interval starts at $A = 0$. The corresponding normalization constants are given in Table 2.7⁶. The coefficients for the recurrence relation in (2.20) are shown in Table 2.8. Note that for $b = 1$ the weight function belonging to the Meixner polynomials becomes an exponential decay. This corresponds to the weight function of the continuous Laguerre polynomials. The Meixner polynomials with $b = 1$ are therefore called the discrete *Laguerre* polynomials.

⁶The Hahn polynomials are omitted in Tables 2.7, 2.8, and 2.9, since the expressions are of an unelegant form, see e.g. (Weber and Erdélyi 1952).

Name	Symbol	A	B	Weight $v(k)$	Conditions
Chebyshev	$\mathcal{C}_m(k)$	0	$N - 1$	1	
Krawtchouk	$\mathcal{K}_m(k)$	0	N	$\binom{N}{k} p^k q^{N-k}$	$p, q > 0, p + q = 1$
Hahn	$\mathcal{H}_m(k)$	0	N	$\frac{(-N)_k (\beta)_k}{k! (\delta)_k}$	$0 < \beta, \delta < 1 - N$
Charlier	$\mathcal{C}_m(k)$	0	∞	$e^{-a} a^k / k!$	$a > 0$
Meixner	$\mathcal{M}_m(k)$	0	∞	$\theta^k (b)_k / k!$	$0 < \theta < 1, b > 0$

Table 2.6: The classical discrete orthogonal polynomials. In the expression for the weight function of the Hahn polynomials, $(\beta)_k$ stands for the Pochhammer symbol or forward factorial function: $(\beta)_n = \beta(\beta + 1) \cdots (\beta + n - 1)$.

All classical discrete orthogonal polynomials satisfy a difference equation of the form

$$f_2(k)q_m(k + 1) + f_1(k)q_m(k) + f_0(k)q_m(k - 1) = 0, \quad k, m \in [0, B].$$

Note that B may be finite or infinite. The functions $f_0(k)$, $f_1(k)$ and $f_2(k)$ are specified in Table 2.9. In the difference equation a problem may arise when $k = 0$ or when $k = B$ if B is finite, since $q_m(-1)$ and $q_m(B + 1)$ have not been defined. Fortunately, for none of the classical discrete polynomials it is necessary to define $q_m(-1)$ nor $q_m(B + 1)$, since it can be deduced from Table 2.9 that $f_0(0) = 0$ and $f_2(B) = 0$.

As stated before, we are particularly interested in orthogonal bases on the semi-infinite interval $[0, \infty)$. Unlike the situation in the continuous case, in the discrete case a finite orthogonality interval cannot be mapped onto a semi-infinite interval by scaling of the (discrete) independent variable. Therefore, of the classical discrete orthogonal polynomials only the Charlier polynomials and the Meixner polynomials are suitable for the representation of physical impulse responses. From the Charlier and the Meixner polynomials, the square root of their weight function and a normalization constant, so-called *Charlier* and *Meixner functions* can be obtained that form an orthonormal basis on $[0, \infty)$. For the purpose of filter synthesis it is important that the basis functions have rational z -transforms. Of all Charlier and Meixner functions, only the Meixner functions with $b = 1$ (these are the so-called *Laguerre functions* and will be treated hereafter) have rational z -transforms. In Chapter 4 so-called *Meixner-like functions* (den Brinker 1995) will be introduced, that are very similar to the Meixner functions, but have rational z -transforms.

Symbol	h_m^2
$\mathcal{C}b_m(k)$	$\frac{N(N^2 - 1^2)(N^2 - 2^2) \dots (N^2 - m^2)}{2m + 1}$
$\mathcal{K}_m(k)$	$\binom{N}{m} p^m q^m$
$\mathcal{C}_m(k)$	1
$\mathcal{M}_m(k)$	$m!(b)_m \theta^{-m} (1 - \theta)^{-b}$

Table 2.7: Normalization constants of the classical discrete orthogonal polynomials.

$q_m(k)$	A_m	B_m	C_m
$\mathcal{C}b_m(k)$	$-(N - 1) \frac{2m + 1}{m + 1}$	$2 \frac{2m + 1}{m + 1}$	$(N^2 - m^2) \frac{m}{m + 1}$
$\mathcal{K}_m(k)$	$-\frac{p(N - m) + qm}{m + 1}$	$\frac{1}{m + 1}$	$pq \frac{N - m + 1}{m + 1}$
$\mathcal{C}_m(k)$	$-\frac{m + a}{\sqrt{a(m + 1)}}$	$\frac{1}{\sqrt{a(m + 1)}}$	$\sqrt{\frac{m}{m + 1}}$
$\mathcal{M}_m(k)$	$b + m \frac{\theta + 1}{\theta}$	$\frac{\theta - 1}{\theta}$	$\frac{m}{\theta} (b + m - 1)$

Table 2.8: Coefficients in the recurrence relations for the classical discrete orthogonal polynomials of the form $q_{m+1}(k) = \{A_m + B_m k\} q_m(k) - C_m q_{m-1}(k)$, where $q_0(k) = 1$.

2.5 Orthonormal Laguerre Functions

2.5.1 The Continuous Laguerre Functions

In Section 2.4.1 the classical Laguerre polynomials were discussed. The Laguerre polynomials can also be defined by Rodriguez' formula for the classical orthogonal polynomials, see (Szegő 1959) or (Abramowitz and Stegun 1970):

$$l_m(x) = \frac{1}{m!} e^x \frac{d^m}{dx^m} [x^m e^{-x}] = \sum_{n=0}^m (-1)^n \binom{m}{n} \frac{x^n}{n!},$$

$q_m(k)$	$f_2(k)$	$f_1(k)$	$f_0(k)$
$\mathcal{C}_m(k)$	$(k+1)(N-1-k)$	$2k^2 - (2k+1)(N-1) + m(m+1)$	$k(N-k)$
$\mathcal{K}_m(k)$	$p(N-k)$	$m - p(N-k) - qk$	qk
$\mathcal{C}_m(k)$	a	$m - a - k$	k
$\mathcal{M}_m(k)$	$\theta(k+b)$	$m(1-\theta) - b\theta - (1+\theta)k$	k

Table 2.9: Coefficients in the difference equations for the classical discrete orthogonal polynomials of the form $f_2(k)q_m(k+1) + f_1(k)q_m(k) + f_0(k)q_m(k-1) = 0$.

where $m \in \mathbb{N}_0$ and $x \in \mathbb{R}^+$. From Section 2.4.1 we know that the Laguerre polynomials are orthonormal under the weight $w(x) = e^{-x}$, thus

$$\int_0^{\infty} e^{-x} l_m(x) l_n(x) dx = \delta_{mn}.$$

Here, δ_{mn} is the Kronecker delta symbol⁷. The Laguerre polynomials satisfy the recurrence relation (see Table 2.4 with $\alpha = 0$)

$$(m+1)l_{m+1}(x) = \{2m+1-x\}l_m(x) - ml_{m-1}(x), \quad (2.21)$$

and the differential equation (see Table 2.5 with $\alpha = 0$)

$$xl_m''(x) + (1-x)l_m'(x) + ml_m(x) = 0, \quad (2.22)$$

where a prime denotes differentiation with respect to x .

From the Laguerre polynomials $l_m(x)$ and the weight function $w(x)$ we construct functions on the interval $(0, \infty)$ that are orthonormal with respect to a unity weight function. These functions are obtained by multiplying the Laguerre polynomials by the square root of their weight function and changing the scale of the independent variable x according to $x = \sigma t$ with $\sigma > 0$ and $t \in \mathbb{R}^+$, followed by a normalization. As a result we obtain the (continuous) *Laguerre functions* (see (Lee 1932; Kautz 1954; Lee 1960))

$$\lambda_m(\sigma; t) = \sqrt{\sigma} l_m(\sigma t) e^{-\sigma t/2} = \sqrt{\sigma} \sum_{n=0}^m (-1)^n \binom{m}{n} \frac{(\sigma t)^n}{n!} e^{-\sigma t/2}, \quad (2.23)$$

which form a complete orthonormal set for each fixed σ in the Hilbert space $L_2(\mathbb{R}^+)$, see (Clement 1963) and Section 2.6.1. Therefore, any function $f(t)$ in $L_2(\mathbb{R}^+)$ can be approximated to any desired degree by a linear combination of Laguerre functions.

⁷The Kronecker delta symbol is defined by: $\delta_{mn} = 1$ for $m = n$ and $\delta_{mn} = 0$ for $m \neq n$.

An important property of the Laguerre functions is that they have rational Laplace transforms, given by (Lee 1932; Kautz 1954)

$$\Lambda_m(\sigma; s) = \frac{\sqrt{\sigma}}{s + \sigma/2} \left(\frac{s - \sigma/2}{s + \sigma/2} \right)^m, \quad \sigma > 0. \quad (2.24)$$

With (2.24) it is a simple matter to verify the orthonormality of the Laguerre functions. We find for the inner product between $\lambda_n(\sigma; t)$ and $\lambda_m(\sigma; t)$ that

$$\begin{aligned} \langle \lambda_n(\sigma; t), \lambda_m(\sigma; t) \rangle &= \frac{1}{2\pi j} \int_{-j\infty}^{j\infty} \Lambda_n(\sigma; s) \Lambda_m^*(\sigma; -s^*) ds \\ &= \frac{\sigma}{2\pi j} \int_{-j\infty}^{j\infty} \frac{1}{s + \sigma/2} \frac{1}{-s + \sigma/2} \left(\frac{s - \sigma/2}{s + \sigma/2} \right)^{n-m} ds. \end{aligned}$$

The integral can be evaluated by closing the contour over the left half s -plane and applying Cauchy's residue theorem. For $n < m$ the singularity in the left half s -plane is cancelled and the integral vanishes. For $n = m$ it is found that $\|\lambda_m(\sigma; t)\|^2 = 1$, which proves that the Laguerre functions are orthonormal.

The specific form of (2.24) allows a very efficient cascade implementation of the set of filters that have the Laguerre functions as their impulse responses. This so-called *Laguerre network* is depicted in Fig. 2.1, see e.g. (Lee 1960; Eykhoff 1974). Note that the Laguerre network is composed of a first-order low-pass section followed by a cascade of identical first-order all-pass sections. In the Laguerre network the parameter $-\sigma/2$ appears as a pole, and will therefore be referred to as the *Laguerre pole*. Hereafter, we will mean by a continuous *Laguerre filter* the combination of a continuous counterpart of the LRM in Fig. 1.8 with a Laguerre network. Thus, the output of a continuous Laguerre filter is formed by a weighted sum of the individual outputs of a continuous Laguerre network.

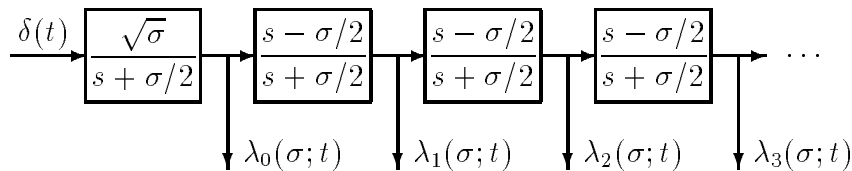


Figure 2.1: Laguerre network composed of a first-order low-pass section followed by a filter line of identical first-order all-pass sections. The individual impulse responses are the Laguerre functions.

The Laguerre functions can also be generated with the aid of the following recurrence relation that is directly obtained from (2.21) and (2.23):

$$(m + 1)\lambda_{m+1}(\sigma; t) = \{(2m + 1) - \sigma t\} \lambda_m(\sigma; t) - m\lambda_{m-1}(\sigma; t),$$

with $\lambda_0(\sigma; t) = \sqrt{\sigma}e^{-\sigma t/2}$. Note that it is not necessary to define $\lambda_{-1}(\sigma; t)$.

Also, the following useful differential equation for the Laguerre functions can be derived from (2.22) and (2.23):

$$t\lambda_m''(\sigma; t) + \lambda_m'(\sigma; t) + (m\sigma + \frac{1}{2}\sigma - \frac{1}{4}\sigma^2 t) \lambda_m(\sigma; t) = 0. \quad (2.25)$$

A further useful result is obtained when a Laguerre function is differentiated with respect to its scale σ (King and O'Canainn 1969; Oliveira e Silva 1994b; Wang and Cluett 1994):

$$\frac{\partial \lambda_m(\sigma; t)}{\partial \sigma} = \frac{(m+1)\lambda_{m+1}(\sigma; t) - m\lambda_{m-1}(\sigma; t)}{\sigma}. \quad (2.26)$$

Again it is not necessary to define $\lambda_{-1}(\sigma; t)$. Higher-order derivatives can be obtained by iterative application of (2.26).

2.5.2 The Discrete Laguerre Functions

The discrete Laguerre polynomials are a special case of the Meixner polynomials described in Section 2.4.2, namely with $b = 1$: The discrete Laguerre polynomials are here defined by the discrete counterpart of Rodriguez' formula for the classical (continuous) orthogonal polynomials, see (Abramowitz and Stegun 1970):

$$\gamma_m(k) = \frac{m!}{\theta^{m+k}} \Delta^m \left[\binom{k}{m} \theta^k \right],$$

where $0 < \theta < 1$, $m, k \in \mathbb{N}_0$, and Δ^m is the m -th forward difference operator⁸. The discrete Laguerre polynomials satisfy the following orthogonality relation:

$$\sum_{k=0}^{\infty} \theta^k \gamma_m(k) \gamma_n(k) = \delta_{mn} \frac{(m!)^2}{\theta^m (1-\theta)}.$$

It is noted that alternative discrete Laguerre polynomials are defined by Gottlieb as $(\theta^m/m!) \gamma_m(k)$ with normalization constant $h_m^2 = \theta^m/(1-\theta)$ (Gottlieb 1938).

The recurrence relation for the discrete Laguerre polynomials can be found by setting $b = 1$ in the recurrence relation for the Meixner polynomials, see Table 2.8:

$$\theta \gamma_{m+1}(k) = \{(\theta - 1)k + \theta + m(1 + \theta)\} \gamma_m(k) - m^2 \gamma_{m-1}(k). \quad (2.27)$$

From Table 2.9 we conclude that the discrete Laguerre polynomials satisfy the difference equation

$$\theta(k+1)\gamma_m(k+1) + [m(1-\theta) - \theta - (1+\theta)k]\gamma_m(k) + k\gamma_m(k-1) = 0. \quad (2.28)$$

Through multiplication of the discrete Laguerre polynomials by the square root of the weight function and a normalization constant, discrete functions can be constructed that

⁸The m -th forward difference operator is recursively defined by $\Delta^m [f(k)] = \Delta^{m-1} [f(k+1) - f(k)]$, with $\Delta^0 [f(k)] = f(k)$.

are orthonormal on the interval $[0, \infty)$ with respect to a unity weight function. These functions are given by (Gottlieb 1938; Broome 1965)

$$g_m(\xi; k) = \frac{(-1)^m}{m!} \sqrt{1 - \xi^2} \xi^{m+k} \gamma_m(k), \quad -1 < \xi < 1, \quad (2.29)$$

where $\xi = \pm\sqrt{\theta}$. For $\xi = \sqrt{\theta}$ the functions are called the (discrete) *Laguerre functions*. For $\xi = -\sqrt{\theta}$ the functions are often called the *alternating Laguerre functions*. Henceforth, for simplicity, the alternating Laguerre functions will also be referred to as the Laguerre functions.

The discrete Laguerre functions form a complete set in the Hilbert space $\ell_2(\mathbb{N}_0)$. Proof of completeness is given in a more general context in (Oliveira e Silva 1995c), see also Section 2.6.2. Any function $h(k)$ in $\ell_2(\mathbb{N}_0)$ can be approximated arbitrarily well by a linear combination of discrete Laguerre functions.

The discrete Laguerre functions have rational z -transforms, given by (Broome 1965):

$$G_m(\xi; z) = \frac{\sqrt{1 - \xi^2} z}{z - \xi} \left(\frac{1 - \xi z}{z - \xi} \right)^m. \quad (2.30)$$

Although $\xi = 0$ is not allowed for the Laguerre *polynomials*, we will allow this value as a natural extension for the Laguerre *functions*. We can use (2.30) to verify that the discrete Laguerre functions are indeed orthonormal. For the inner product between $g_n(\xi; k)$ and $g_m(\xi; k)$ we obtain

$$\begin{aligned} \langle g_n(\xi; k), g_m(\xi; k) \rangle &= \frac{1}{2\pi j} \oint_C G_n(\xi; z) G_m^*(\xi; 1/z^*) \frac{dz}{z} \\ &= \frac{1 - \xi^2}{2\pi j} \oint_C \frac{z}{z - \xi} \frac{1}{1 - \xi z} \left(\frac{1 - \xi z}{z - \xi} \right)^{n-m} \frac{dz}{z}. \end{aligned}$$

For $n < m$ the integral vanishes with Cauchy's residue theorem. For $n = m$ it is found that $\|g_m(\xi; k)\|^2 = 1$, which completes the proof of the orthonormality of the discrete Laguerre functions.

Similar to the case of the Laplace transforms of the continuous Laguerre functions in (2.24), the specific form of the z -transforms in (2.30) of the discrete Laguerre functions allows an efficient implementation of a filter to generate the Laguerre functions. This so-called *discrete Laguerre network*, depicted in Fig. 2.2, is composed of a first-order low-pass section followed by a cascade of identical first-order all-pass sections (King and Paraskevopoulos 1977). In the Laguerre network the parameter ξ appears as a pole. For this reason the parameter ξ will throughout be referred to as the *Laguerre pole*. Note that when $\xi = 0$ the Laguerre functions simply become delays and the Laguerre network reduces to a delay line. Hereafter, we will mean by a discrete *Laguerre filter* the combination of the LRM in Fig. 1.8 with a discrete Laguerre network. Thus, the output of a discrete Laguerre filter is formed by a weighted sum of the individual outputs of a discrete Laguerre network.

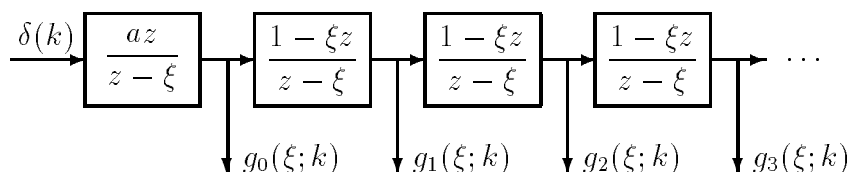


Figure 2.2: Discrete Laguerre network composed of a first-order low-pass section followed by a filter line of first-order all-pass sections. The individual impulse responses $g_m(\xi; k)$ are the discrete Laguerre functions.

Using the recurrence relation for the discrete Laguerre polynomials in (2.27) and the relation between the discrete Laguerre polynomials and the functions in (2.29), a recurrence relation for the Laguerre functions can be derived. This recurrence relation yields another way to generate the discrete Laguerre functions:

$$(m+1)\xi g_{m+1}(\xi; k) = \{(1-\xi^2)k - \xi^2 - (1+\xi^2)m\} g_m(\xi; k) - m\xi g_{m-1}(\xi; k),$$

with $g_0(\xi; k) = \sqrt{1-\xi^2} \xi^k$. Note that it is not necessary to define $g_{-1}(\xi; k)$.

In Fig. 2.3 the first four discrete Laguerre functions ($m = 0, 1, 2, 3$) with $\xi = 0.9$ are shown. As can be seen from this plot, Laguerre functions are well-suited for approximations of exponentially decaying functions, when the rate of decay—determined by ξ —is properly chosen. In other words: the convergence rate of a Laguerre series of an exponentially decaying function is expected to be high.

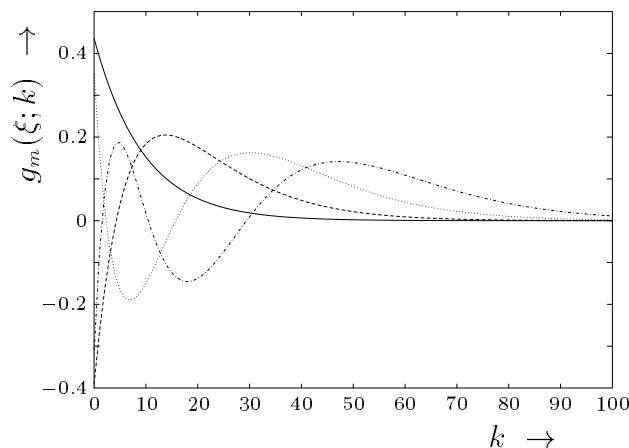


Figure 2.3: An example of the first four discrete Laguerre functions $g_m(\xi; k)$ with $\xi = 0.9$. The continuous, dotted, dashed and dash-dotted lines correspond to $m = 0$, $m = 1$, $m = 2$ and $m = 3$, respectively.

For later use the difference equation for the Laguerre functions is given, derived from (2.28) and (2.29):

$$-(k+1)\xi g_m(\xi; k+1) + \{k-m+\xi^2(k+m+1)\} g_m(\xi; k) - k\xi g_m(\xi; k-1) = 0. \quad (2.31)$$

Differentiating a discrete Laguerre function with respect to ξ yields the following useful identity (Oliveira e Silva 1994b):

$$\frac{\partial g_m(\xi; k)}{\partial \xi} = \frac{(m+1)g_{m+1}(\xi; k) - mg_{m-1}(\xi; k)}{1 - \xi^2}. \quad (2.32)$$

We see that $g_{-1}(\xi; k)$ need not be defined. Higher-order derivatives can be obtained by iterative application of (2.32).

Using the MBT in (2.11) and the inverse mapping in (2.12) the discrete and the continuous Laguerre functions can be mapped onto each other via their z - and Laplace transforms and

$$\mathcal{M} : \Lambda_m(\sigma; s) \mapsto \frac{\sqrt{2a}z}{z+1} \Lambda_m\left(\sigma; a\frac{z-1}{z+1}\right) = (-1)^m G_m\left(\frac{a-\sigma/2}{a+\sigma/2}; z\right), \quad (2.33)$$

$$\mathcal{M}^{-1} : G_m(\xi; z) \mapsto \frac{\sqrt{2a}}{a+s} G_m\left(\xi; \frac{a+s}{a-s}\right) = (-1)^m \Lambda_m\left(2a\frac{1-\xi}{1+\xi}; s\right). \quad (2.34)$$

Note the remarkable fact that the functions z^{-m} , the z -transforms of the *discrete* Laguerre functions with $\xi = 0$, are mapped onto the Laplace transforms of *continuous* Laguerre functions with $\sigma = 2a$.

2.5.3 Optimal Truncated Laguerre Series

The exact representation of an impulse response of a causal stable system by a Laguerre series is in practice not feasible. The series must be truncated to a finite number of terms resulting in an approximation. In view of a small approximation error, it is important that the scale factor σ for the continuous Laguerre functions or the ξ for the discrete Laguerre functions, is optimally chosen.

First we consider the DT case. The impulse response $h(k)$ of a DT causal stable system can be approximated by an M -term truncated Laguerre series according to

$$h(k) \approx h_M(k) = \sum_{m=0}^{M-1} c_m(\xi) g_m(\xi; k).$$

The coefficients $c_m(\xi)$ are given by $c_m(\xi) = \langle h(k), g_m(\xi; k) \rangle$. The squared norm of $h_M(k)$ is a function of the Laguerre pole:

$$E_M(\xi) = \|h_M(k)\|^2 = \sum_{m=0}^{M-1} c_m^2(\xi).$$

To synthesize $h_M(k)$, the impulse response of a Laguerre filter with weights $c_m(\xi)$ can be used.

Remark: When approximating a DT function $h(k)$ by a truncated Laguerre series, usually only a limited number of samples, say N , of $h(k)$ is available. Assuming N is large enough so that all the

Laguerre functions in the expansion are sufficiently close to zero for $k > N$, we may approximate the expansion coefficients by

$$c_m(\xi) \approx \sum_{k=0}^{N-1} h(k) g_m(\xi; k), \quad m = 0, 1, \dots, M-1.$$

These inner products can be calculated efficiently in the following way. The N samples of $h(k)$ are fed in reverse order to the Laguerre network in Fig. 2.2. The M expansion coefficients are then given by the M outputs of the Laguerre network at instant $k = N - 1$.

The M -term truncation error is a function of the Laguerre parameter ξ :

$$\zeta_M(\xi) = \|h(k) - h_M(k)\|^2 = \|h(k)\|^2 - E_M(\xi) = \sum_{m=M}^{\infty} c_m^2(\xi).$$

For a small truncation error given a certain number M of expansion terms, or equivalently, for a small number of expansion terms given a certain truncation error, $\zeta_M(\xi)$ needs to be minimized. Minimization of $\zeta_M(\xi)$ is equivalent to maximization of $E_M(\xi)$. As a first step, one could search for the stationary points of $E_M(\xi)$ by setting its derivative with respect to the Laguerre parameter ξ equal to zero:

$$\frac{\partial E_M(\xi)}{\partial \xi} = 0 \quad \rightarrow \quad 2 \sum_{m=0}^{M-1} c_m(\xi) \frac{\partial c_m(\xi)}{\partial \xi} = 0. \quad (2.35)$$

Knowing that $c_m(\xi) = \langle h(k), g_m(\xi; k) \rangle$ and with the aid of the specific form of the derivative of a Laguerre function with respect to ξ in (2.32) we find

$$\frac{\partial c_m(\xi)}{\partial \xi} = \frac{(m+1)c_{m+1}(\xi) - mc_{m-1}(\xi)}{1 - \xi^2}. \quad (2.36)$$

Using this, eq. (2.35) becomes

$$\frac{\partial E_M(\xi)}{\partial \xi} = 2 \sum_{m=0}^{M-1} c_m(\xi) \frac{(m+1)c_{m+1}(\xi) - mc_{m-1}(\xi)}{1 - \xi^2},$$

a telescopic series of which only the last term remains uncanceled, so that

$$\frac{\partial E_M(\xi)}{\partial \xi} = \frac{2M}{1 - \xi^2} c_{M-1}(\xi) c_M(\xi).$$

Thus, for any stationary point of $E_M(\xi)$ (and of $\zeta_M(\xi)$) with respect to ξ it is necessary and sufficient that at least one of the following two conditions is satisfied (Masnadi-Shirazi and Ahmed 1991; Oliveira e Silva 1995a):

$$c_{M-1}(\xi) = 0 \quad \text{or} \quad c_M(\xi) = 0. \quad (2.37)$$

In words: The truncation error associated with an M -term Laguerre expansion of a discrete function in $\ell_2(\mathbb{N}_0)$ has a stationary point with respect to the free parameter ξ if the last

coefficient $c_{M-1}(\xi)$ in the expansion is zero or if the last coefficient $c_M(\xi)$ of an $(M+1)$ -term expansion is zero (or both). Consequently, when $c_M(\xi) = 0$, the M -term and $(M+1)$ -term Laguerre approximations of $h(k)$ are identical. Similarly, when $c_{M-1}(\xi) = 0$, the $(M-1)$ -term Laguerre approximation of $h(k)$ is identical to the M -term Laguerre approximation. This is further made clear by an example. Let $h(k)$ be the impulse response of the system

$$H(z) = \left(\frac{z}{z-p} \right)^4 + \left(\frac{z}{z-p^*} \right)^4, \quad \text{where } p = 0.9 + 0.1i.$$

In Fig. 2.4 the normalized M -term truncation error $\zeta_M(\xi)/\|h(k)\|^2$ is plotted for the first eight values of M . Note that a pair of curves pertaining to neighbouring M -values touches at the stationary points with respect to ξ . For clarity, the curve corresponding to $\zeta_5(\xi)$ is highlighted. The stationary points of $\zeta_5(\xi)$ are local minima when $c_5(\xi) = 0$, which correspond to local maxima of $\zeta_6(\xi)$. Similarly, the stationary points of $\zeta_5(\xi)$ are local maxima when $c_4(\xi) = 0$, which are the local minima of $\zeta_4(\xi)$. [From this example one might suspect that $c_{M-1}(\xi) = 0$ and $c_M(\xi) = 0$ always correspond to local maxima and local minima of $\zeta_M(\xi)$, respectively. However, this is not true in general.]

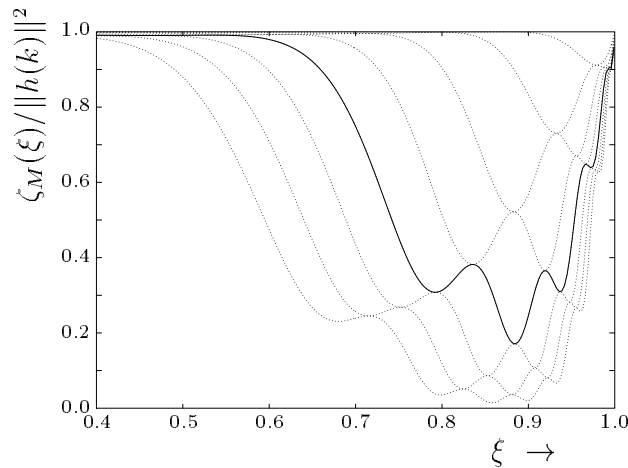


Figure 2.4: The normalized truncation error curves associated with the M -term truncated Laguerre expansions of the impulse response $h(k)$ in the example, where $M = 1, 2, \dots, 8$. The top curve corresponds with $M = 1$, the bottom curve with $M = 8$. The curve corresponding with $M = 5$ is highlighted.

The problem of finding a stationary point of the truncation error with respect to ξ is now reduced to finding the zeros of either $c_{M-1}(\xi)$ or $c_M(\xi)$ with respect to ξ . To this end, the gradient in (2.36) can be used. Higher-order derivatives can readily be obtained by iterative application of (2.36). If an idea of a good pole ξ is available, a better one can be found using one or more iterations of Newton's method.

In the CT case an equivalent result is obtained. The truncation error of an M -term Laguerre expansion of $h(t)$ is given by $\zeta_M(\sigma) = \sum_{m=M}^{\infty} c_m^2(\sigma)$, where the expansion coefficients are given by $c_m(\sigma) = \langle h(t), \lambda_m(\sigma; t) \rangle$. For any stationary point of $\zeta_M(\sigma)$ with

respect to σ it is necessary and sufficient that at least one of the two following conditions is satisfied (Clowes 1965; King and O'Canainn 1969; Wang and Cluett 1994):

$$c_{M-1}(\sigma) = 0 \quad \text{or} \quad c_M(\sigma) = 0. \quad (2.38)$$

The optimality conditions in (2.37) and in (2.38) are associated with the problem of approximating the output of a causal stable system with the output of a Laguerre filter under an impulsive excitation. Curiously, the problem of approximating the system output with the output of a Laguerre filter under (almost) any excitation yields optimality conditions of the same form (Oliveira e Silva 1994b; Oliveira e Silva 1995a). Let $c_{M-1,m}(\sigma)$ with $m = 0, 1, \dots, M-1$ be the optimal weights of an M -tap Laguerre filter. Since $x(k)$ is generally non-white, these optimal weights are dependent on M , hence the extra index. In the CT case, for any stationary point of the mean-squared error $E\{e^2(t)\}$ with respect to the Laguerre parameter σ it is necessary and sufficient that at least one of the two following conditions is satisfied:

$$c_{M-1,M-1}(\sigma) = 0 \quad \text{or} \quad c_{M,M}(\sigma) = 0,$$

In the DT case, for any stationary point of the mean-squared error $E\{e^2(k)\}$ with respect to the Laguerre pole ξ it is necessary and sufficient that at least one of the two following conditions is satisfied:

$$c_{M-1,M-1}(\xi) = 0 \quad \text{or} \quad c_{M,M}(\xi) = 0,$$

where $c_{M-1,M-1}(\xi)$ and $c_{M,M}(\xi)$ are the M -th and $(M+1)$ -th optimal weights of a Laguerre filter with M and $M+1$ taps, respectively. In Chapter 4 the details will be presented in a more general context.

In (Parks 1971) a method is presented to make a choice for σ on the basis of certain moments of $h(t)$. The σ that is found is the best for the class of functions $h(t)$ with the same moments. For the derivation leading to this result it is essential that the Laguerre functions are orthonormal and that they satisfy a second-order differential equation of a specific form, see eq. (2.25).

An alternative procedure to find a pole for Laguerre expansions has been presented in (Fu and Dumont 1993a; Fu and Dumont 1993b). The authors consider a weighted quadratic error criterion of the form $\mathcal{J}(\xi) = \sum_{m=0}^{\infty} (m+1)c_m^2(\xi)$. Intuitively, a fast convergence rate of the Laguerre expansion is then expected. This specific error criterion results in an explicit expression for the optimal Laguerre pole in terms of certain moments of the function to be approximated. For the derivation leading to this optimal Laguerre pole it is essential that the Laguerre functions are orthonormal and satisfy a second-order difference equation of a specific form, see eq. (2.31).

In (Tanguy, Vilbé, and Calvez 1995) it is shown that if the number of basis functions is chosen sufficiently large, then the weighted error criterion presented in (Fu and Dumont 1993a) is related to a certain upper bound of the truncation error. This upper bound is precisely that minimized in (Parks 1971). Then, a general method is given to minimize the upper bound of the truncation error for a wide class of CT or DT orthonormal basis

functions which depend on one or more free parameters. The basis functions must satisfy a differential (CT) or difference equation (DT) of a specific form. It is observed that several basis functions related to the classical orthogonal polynomials are suitable. The method by Tanguy *et al.* is presented in Appendix A, and is applied in (Belt and den Brinker 1997) to parametrize the *generalized Laguerre functions* (see Chapter 4) in truncated generalized Laguerre series of functions in $L_2(\mathbb{R}^+)$.

2.6 Orthonormalized Exponentials

In the previous section the continuous and discrete Laguerre functions were introduced. It was stated that any function in $L_2(\mathbb{R}^+)$ or $\ell_2(\mathbb{N}_0)$ can be approximated to any desired degree by a linear combination of (discrete) Laguerre functions. Unfortunately, because the Laguerre pole is real, the Laguerre functions are not particularly suited for approximations of functions that show a strong oscillatory behaviour. In this section more general orthonormal basis functions will be introduced that are associated with complex poles. These basis functions are much better suited for approximations of functions with oscillatory behaviour.

2.6.1 Continuous Kautz Functions

Consider the sequence $\{\sigma_m\}_{m=0}^{\infty}$ of complex numbers with positive real parts. These complex numbers need not necessarily be distinct. Let n_m be the number of times that σ_m appeared before in the sequence. Then the (generalized) exponentials $t^{n_m} e^{-\sigma_m t}$ are linearly independent. A Gram-Schmidt orthonormalization procedure can be applied to these (generalized) exponentials. The resulting functions, denoted by $\phi_m(t)$, are hereafter called the *Kautz functions* and have Laplace transforms given by (Kautz 1954; Oliveira e Silva 1994a)

$$\Phi_m(s) = \kappa_m \frac{\alpha_m}{s + \sigma_m} \prod_{n=0}^{m-1} \frac{s - \sigma_n^*}{s + \sigma_n}, \quad (2.39)$$

where $\alpha_m = \sqrt{\sigma_m + \sigma_m^*}$ and κ_m is a complex number with $|\kappa_m| = 1$. For convenience we take $\kappa_m = 1$. We see that in the special case that all σ_n are equal and real-valued ($\sigma_n = \sigma/2$ for $n = 0, 1, 2, \dots$ with $\sigma > 0$) the Laguerre functions in (2.24) are obtained.

To prove the orthogonality of the continuous Kautz functions it is sufficient to show that the m -th Kautz function $\phi_m(t)$ is orthogonal to all previous Kautz functions $\phi_n(t)$ ($0 \leq n < m$). Taking the inner product between the n -th and the m -th Kautz function and using Parseval's theorem we find

$$\langle \phi_n(t), \phi_m(t) \rangle = \frac{1}{2\pi j} \int_{-j\infty}^{j\infty} \Phi_n(s) \Phi_m^*(-s^*) ds$$

$$= \frac{\alpha_n \alpha_m}{2\pi j} \int_{-j\infty}^{j\infty} \frac{1}{s + \sigma_n} \frac{1}{-s + \sigma_m^*} \prod_{u=0}^{n-1} \frac{s - \sigma_u^*}{s + \sigma_u} \prod_{v=0}^{m-1} \frac{s + \sigma_v}{s - \sigma_v^*} ds.$$

The integral can be evaluated by closing the contour over the left half s -plane and applying Cauchy's residue theorem. For $n < m$ all singularities in the left half s -plane are cancelled and the integral vanishes. When we take $m = n$ we find

$$\langle \phi_m(t), \phi_m(t) \rangle = \frac{\alpha_m^2}{2\pi j} \int_{-j\infty}^{j\infty} \frac{1}{s + \sigma_m} \frac{1}{-s + \sigma_m^*} ds = \frac{\alpha_m^2}{\sigma_m + \sigma_m^*} = 1,$$

which proves that the continuous Kautz functions are orthonormal.

The continuous Kautz functions can be generated as the impulse responses of the so-called continuous *Kautz network* depicted in Fig. 2.5. In the Kautz network the complex parameters $-\sigma_m$ appear as poles, and are therefore called *Kautz poles*. Hereafter, we will mean by a continuous *Kautz filter* the combination of a continuous counterpart of the LRM in Fig. 1.8 with the continuous Kautz network of Fig. 2.5. Thus, the output of a continuous Kautz filter is formed by a weighted sum of the individual outputs of a continuous Kautz network.

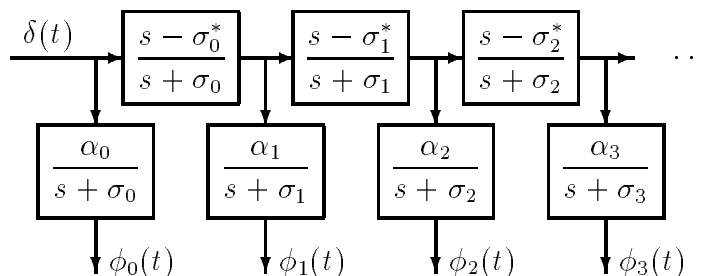


Figure 2.5: Continuous Kautz network composed of a filter line of first-order all-pass sections tapped by first-order low-pass sections. The individual impulse responses $\phi_m(t)$ are the continuous Kautz functions.

For the exact representation of functions in $L_2(\mathbb{R}^+)$ by a Kautz series, it is important that the Kautz functions $\phi_m(t)$ form a complete set. If the σ_m are distinct ($\sigma_m \neq \sigma_n$ when $m \neq n$), the exponentials $e^{-\sigma_m t}$ form a complete set in $L_2(\mathbb{R}^+)$ if and only if (Huggins 1956; Clement 1963; Young 1968)

$$\sum_{m=0}^{\infty} \frac{\operatorname{Re}(\sigma_m)}{1 + |\sigma_m - \frac{1}{2}|^2} = \infty. \quad (2.40)$$

Because a Gram-Schmidt orthonormalization procedure applied to the exponentials $e^{-\sigma_m t}$ yields precisely the Kautz functions $\phi_m(t)$, it follows directly that the Kautz functions with distinct σ_m are complete in $L_2(\mathbb{R}^+)$ if and only if (2.40) is satisfied. It was proved in

(Oliveira e Silva 1995c) and in (Sarroukh 1996) that the Kautz functions are complete in $L_2(\mathbb{R}^+)$ under the condition (2.40), even when the σ_m have arbitrary multiplicities. Note that this also guarantees the completeness of the Laguerre functions $\lambda_m(\sigma; t)$.

To represent real impulse responses with a Kautz series, we require that the Kautz poles σ_m are either real or appear in complex-conjugated pairs. In the latter case a unitary transformation can be applied to the set of Kautz functions such that the resulting set contains real functions only. This set of real functions is subdivided in two sets containing the so-called Kautz functions of the first and second kind, denoted by $\phi_m^{(1)}(t)$ and $\phi_m^{(2)}(t)$, respectively. Their Laplace transforms are given by ($m = 0, 1, 2, \dots$):

$$\Phi_m^{(1)}(s) = D_m^{(1)} \frac{s}{(s + \sigma_m)(s + \sigma_m^*)} \prod_{n=0}^{m-1} \frac{(s - \sigma_n)(s - \sigma_n^*)}{(s + \sigma_n)(s + \sigma_n^*)}, \quad (2.41)$$

$$\Phi_m^{(2)}(s) = D_m^{(2)} \frac{1}{(s + \sigma_m)(s + \sigma_m^*)} \prod_{n=0}^{m-1} \frac{(s - \sigma_n)(s - \sigma_n^*)}{(s + \sigma_n)(s + \sigma_n^*)}, \quad (2.42)$$

where $D_m^{(1)}$ and $D_m^{(2)}$ are the following normalization constants:

$$D_m^{(1)} = \sqrt{2(\sigma_m + \sigma_m^*)}, \quad D_m^{(2)} = \sqrt{2(\sigma_m + \sigma_m^*)\sigma_m\sigma_m^*}.$$

In the case that $\sigma_m = \sigma_m^* = \sigma/2$ for all m , where $\sigma/2 > 0$, we find that the continuous Kautz functions above are related to the continuous Laguerre functions defined in (2.24) according to

$$\Lambda_{2m}(\sigma; s) = \frac{\Phi_m^{(1)}(s) + \Phi_m^{(2)}(s)}{\sqrt{2}}, \quad \Lambda_{2m+1}(\sigma; s) = \frac{\Phi_m^{(1)}(s) - \Phi_m^{(2)}(s)}{\sqrt{2}}.$$

2.6.2 Discrete Kautz Functions

Consider the sequence $\{p_m\}_{m=0}^{\infty}$ of complex numbers that all satisfy $|p_m| < 1$. These complex numbers need not necessarily be distinct. Let n_m be the number of times that p_m appeared before in the sequence. Then the sequence of (linearly independent) generalized geometric progressions $(k+1)^{n_m} p_m^k$ with $k = 0, 1, 2, \dots$ can be formed. In (Broome 1965) a Gram-Schmidt orthonormalization procedure is applied to these generalized geometric progressions, resulting in the so-called Kautz functions $\psi_m(k)$ with z -transforms (see also (Oliveira e Silva 1994a))

$$\Psi_m(z) = \kappa_m \frac{a_m z}{z - p_m} \prod_{n=0}^{m-1} \frac{1 - p_n^* z}{z - p_n} \quad (2.43)$$

where $a_m = \sqrt{1 - p_m p_m^*}$ and κ_m a complex number with $|\kappa_m| = 1$. For convenience we henceforth take $\kappa_m = 1$. In (Heuberger and Bosgra 1990; Heuberger 1991; Heuberger, van den Hof, and Bosgra 1993; Heuberger, van den Hof, and Bosgra 1995; van den Hof,

Heuberger, and Bokor 1995) the authors take a sequence p_m that is periodic. The obtained functions are called the *generalized orthonormal basis functions*.

To prove the orthogonality of the discrete Kautz functions it is sufficient to show that the m -th Kautz function $\psi_m(k)$ is orthogonal to all previous Kautz functions $\psi_n(k)$ ($0 \leq n < m$). Taking the inner product between the n -th and the m -th Kautz function leads to

$$\begin{aligned} \langle \psi_n(k), \psi_m(k) \rangle &= \frac{1}{2\pi j} \oint_C \Psi_n(z) \Psi_m^*(1/z^*) \frac{dz}{z} \\ &= \frac{a_n a_m}{2\pi j} \oint_C \frac{z}{z - p_n} \frac{1}{1 - p_m^* z} \prod_{u=0}^{n-1} \frac{1 - p_u^* z}{z - p_u} \prod_{v=0}^{m-1} \frac{z - p_v}{1 - p_v^* z} \frac{dz}{z}. \end{aligned}$$

With $n < m$ all singularities of the integrand inside the unit circle are cancelled. Consequently, with Cauchy's residue theorem the integral vanishes. For $m = n$ we obtain, again using Cauchy's residue theorem,

$$\langle \psi_m(k), \psi_m(k) \rangle = \frac{a_m^2}{2\pi j} \oint_C \frac{z}{z - p_m} \frac{1}{1 - p_m^* z} \frac{dz}{z} = \frac{a_m^2}{1 - p_m p_m^*} = 1,$$

which proves that the Kautz functions are orthonormal.

The discrete Kautz functions can be generated as the impulse responses of the so-called discrete *Kautz network* depicted in Fig. 2.6. In the Kautz network, the complex parameters p_m appear as poles and will therefore be called *Kautz poles*. Hereafter, we will mean by a discrete *Kautz filter* the combination of the LRM in Fig. 1.8 with the discrete Kautz network of Fig. 2.6. Thus, the output of a discrete Kautz filter is formed by a weighted sum of the individual outputs of a discrete Kautz network.

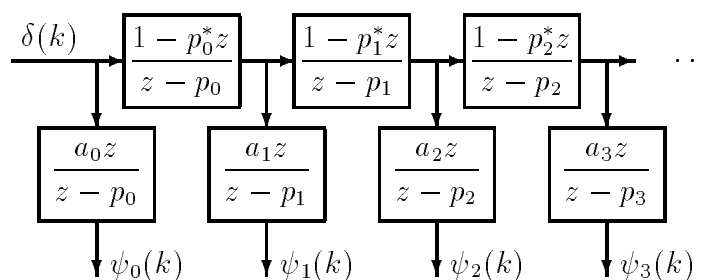


Figure 2.6: Discrete Kautz network composed of a filter line of first-order all-pass sections tapped by first-order low-pass sections. The individual impulse responses $\psi_m(k)$ are the discrete Kautz functions.

The functions $\psi_m(k)$ form a *complete* (orthonormal) set in the Hilbert space $\ell_2(\mathbb{N}_0)$ if and only if the following condition is satisfied (Oliveira e Silva 1995c; Sarroukh 1996):

$$\sum_{m=0}^{\infty} (1 - |p_m|) = \infty. \quad (2.44)$$

Therefore, if the sequence $\{p_m\}_{m=0}^{\infty}$ has an accumulation point within the unit circle or if this sequence approaches the unit circle sufficiently slowly, then the Kautz functions form a complete set in $\ell_2(\mathbb{N}_0)$. Note that with this the completeness of the discrete Laguerre functions $g_m(\xi; k)$ is guaranteed.

The Laplace transforms of the continuous Kautz functions in (2.39) can be mapped onto the z -transforms of the discrete Kautz functions in (2.43) using the modified bilinear transform:

$$\mathcal{M} : \Phi_m(s) \mapsto \frac{\sqrt{2a}z}{z+1} \Phi_m\left(a \frac{z-1}{z+1}\right) = (-1)^m \sqrt{\frac{1+p_m}{1+p_m^*}} \Psi_m(z), \quad (2.45)$$

where $p_m = (1 - \sigma_m/a)/(1 + \sigma_m/a)$. Note that the constant preceding $\Psi_m(z)$ has unity modulus. The inverse MBT yields

$$\mathcal{M}^{-1} : \Psi_m(z) \mapsto \frac{\sqrt{2a}}{a+s} \Psi_m\left(\frac{a+s}{a-s}\right) = (-1)^m \sqrt{\frac{1+\sigma_m/a}{1+\sigma_m^*/a}} \Phi_m(s), \quad (2.46)$$

where $\sigma_m/a = (1 - p_m)/(1 + p_m)$. The constant preceding $\Phi_m(s)$ has unity modulus.

To represent real impulse responses the numbers p_m must either be real or appear in complex conjugate pairs. In the latter case a unitary transformation can be applied to the set of Kautz functions such that the resulting set contains real functions only. These functions are the discrete Kautz functions of the first and second kind, and are denoted by $\psi_m^{(1)}(k)$ and $\psi_m^{(2)}(k)$, respectively (see also (Young and Huggins 1962)). Their z -transforms are given by

$$\Psi_m^{(1)}(z) = C_m^{(1)} \frac{z(z-1)}{(z-p_m)(z-p_m^*)} \prod_{n=1}^m \frac{(1-p_n z)(1-p_n^* z)}{(z-p_n)(z-p_n^*)}, \quad (2.47)$$

$$\Psi_m^{(2)}(z) = C_m^{(2)} \frac{z(z+1)}{(z-p_m)(z-p_m^*)} \prod_{n=1}^m \frac{(1-p_n z)(1-p_n^* z)}{(z-p_n)(z-p_n^*)}, \quad (2.48)$$

where $C_m^{(1)}$ and $C_m^{(2)}$ are the normalization constants given by

$$\begin{aligned} C_m^{(1)} &= \sqrt{(1+p_m)(1+p_m^*)(1-p_m p_m^*)/2}, \\ C_m^{(2)} &= \sqrt{(1-p_m)(1-p_m^*)(1-p_m p_m^*)/2}. \end{aligned}$$

If all poles p_m are identical and real, $p_m = p_m^* = \xi$ for $m = 0, 1, \dots, M-1$ with $|\xi| < 1$, we find that the Kautz functions are related to the Laguerre functions defined in (2.30) according to

$$G_{2m}(\xi; z) = \frac{\Psi_m^{(2)}(z) + \Psi_m^{(1)}(z)}{\sqrt{2}}, \quad G_{2m+1}(\xi; z) = \frac{\Psi_m^{(2)}(z) - \Psi_m^{(1)}(z)}{\sqrt{2}}.$$

Using the MBT in (2.11) the Laplace transforms of the continuous Kautz functions in (2.41) and (2.42) can be mapped onto the z -transforms of the discrete Kautz functions in

(2.41) and (2.48) as follows:

$$\begin{aligned}\mathcal{M} : \Phi_m^{(1)}(s) &\mapsto \frac{\sqrt{2a}z}{z+1} \Phi_m^{(1)}\left(a \frac{z-1}{z+1}\right) = \Psi_m^{(1)}(z), \\ \mathcal{M} : \Phi_m^{(2)}(s) &\mapsto \frac{\sqrt{2a}z}{z+1} \Phi_m^{(2)}\left(a \frac{z-1}{z+1}\right) = \Psi_m^{(2)}(z),\end{aligned}$$

with $p_n = (a - \sigma_n)/(a + \sigma_n)$ for $n = 0, 1, 2, \dots, m$. The inverse mapping according to (2.12) is given by

$$\begin{aligned}\mathcal{M}^{-1} : \Psi_m^{(1)}(z) &\mapsto \frac{\sqrt{2a}}{a+s} \Psi_m^{(1)}\left(\frac{a+s}{a-s}\right) = \Phi_m^{(1)}(s), \\ \mathcal{M}^{-1} : \Psi_m^{(2)}(z) &\mapsto \frac{\sqrt{2a}}{a+s} \Psi_m^{(2)}\left(\frac{a+s}{a-s}\right) = \Phi_m^{(2)}(s),\end{aligned}$$

with $\sigma_n = a(1 - p_n)/(1 + p_n)$ for $n = 0, 1, 2, \dots, m$.

In Fig. 2.7 an example of the first two discrete Kautz functions of the first kind and the first two discrete Kautz functions of the second kind is presented. As can be seen from this plot, Kautz functions are well-suited for approximations of exponentially decaying functions with an oscillatory behaviour.

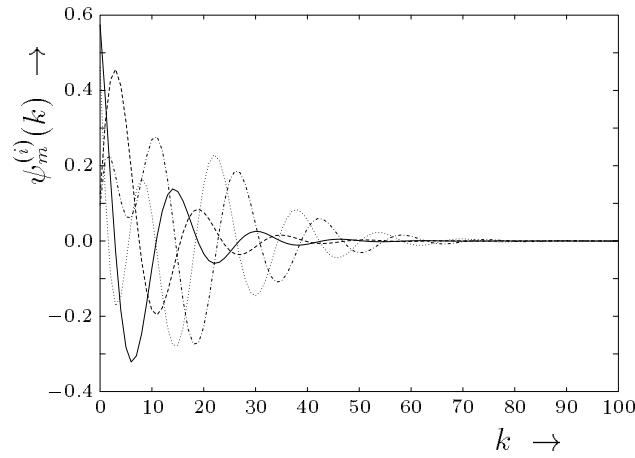


Figure 2.7: An example of the first two discrete Kautz functions of the first ($i = 1$) and of the second kind ($i = 2$) with $p_0 = p_1 = 0.9e^{j\pi/8}$. The continuous, dotted, dashed and dash-dotted lines correspond to $\psi_0^{(1)}(k)$, $\psi_0^{(2)}(k)$, $\psi_1^{(1)}(k)$ and $\psi_1^{(2)}(k)$, respectively.

2.6.3 Optimal Truncated Kautz Series

An exact Kautz series representation of a function is in practical situations not feasible. The Kautz series must be truncated to a finite number of terms resulting in an approximation. In view of a small approximation error, it is important that the free design parameters in the Kautz functions are chosen well.

We will concentrate on discrete Kautz approximations of real functions in $\ell_2(\mathbb{N}_0)$. The results to be presented next are very similar for continuous Kautz approximations of real functions in $L_2(\mathbb{R}^+)$ and are therefore omitted. Consider the Kautz functions given in (2.47) and (2.48), with $p_m = p$ and $p_m^* = p^*$ ($|p| < 1$). With these poles the completeness condition in (2.44) is satisfied and thus any real function $h(k) \in \ell_2(\mathbb{N}_0)$ can be approximated to any desired degree by a linear combination of these Kautz functions. In an M -term Kautz expansion the following approximation $h_M(k)$ of $h(k)$ is obtained:

$$h(k) \approx h_M(k) = \sum_{m=0}^{M-1} \{c_m^{(1)}\psi_m^{(1)}(k) + c_m^{(2)}\psi_m^{(2)}(k)\}.$$

The expansion coefficients are given by $c_m^{(1)} = \langle h(k), \psi_m^{(1)}(k) \rangle$ and $c_m^{(2)} = \langle h(k), \psi_m^{(2)}(k) \rangle$. The squared norm $E_M(p)$ of the approximation $h_M(k)$ is a function of p :

$$E_M(p) = \|h_M(k)\|^2 = \sum_{m=0}^{M-1} \left(\{c_m^{(1)}\}^2 + \{c_m^{(2)}\}^2 \right).$$

Minimization of the error $\|h(k) - h_M(k)\|^2$ is equivalent to maximization of $E_M(p)$ with respect to the complex parameter p . In (den Brinker, Benders, and Oliveira e Silva 1996) it is found that for a stationary point of $E_M(p)$ with respect to p it is necessary and sufficient that at least one of the two following conditions is satisfied:

$$c_{M-1}^{(1)} = c_{M-1}^{(2)} = 0 \quad \text{or} \quad c_M^{(1)} = c_M^{(2)} = 0. \quad (2.49)$$

This result is also found when p and p^* are replaced by p_1 and p_2 , respectively, where both p_1 and p_2 are real-valued and $|p_1|, |p_2| < 1$ (den Brinker, Benders, and Oliveira e Silva 1996).

Remark: The optimality conditions in (2.49) are associated with the problem of approximating the output of a causal stable system with the output of a Kautz filter (with $p_m = p$ and $p_m^* = p^*$) under an impulsive excitation. In a more general system identification framework, the problem of approximating the system output with the output of the Kautz filter under (almost) any excitation yields optimality conditions of the same form, see (Oliveira e Silva 1995b).

In (den Brinker 1994) and (den Brinker 1996) the optimality conditions for a more general truncated Kautz series are derived. The Kautz functions are obtained as the impulse responses of a Kautz network based on identical N -th order all-pass sections. It is found that for a stationary point of E_M with respect to the N complex poles it is sufficient that at least one of the following two conditions is satisfied:

$$c_{M-1}^{(i)} = 0 \quad \text{or} \quad c_M^{(i)} = 0,$$

where $i = 1, 2, \dots, N$. These conditions are sufficient, however for $N > 2$ they are not necessary. See also (Oliveira e Silva 1994a) and (Oliveira e Silva 1995c).

2.7 Adaptive Orthonormal Filters

The networks treated in this chapter all have orthonormal impulse responses at their tap outputs. As we will see, this property is very attractive for the behaviour of adaptive optimization algorithms for the weights in an LRM. Let's again consider the LRM with M tap outputs, depicted in Fig. 1.8. The M orthonormal impulse responses are denoted by $g_m(k)$ ($m = 0, 1, \dots, M-1$) with Fourier transforms $G_m(e^{j\Omega})$. The excitation $x(k)$ is a zero-mean, stationary stochastic signal with power σ_x^2 . Its power spectral density function is denoted by $\Phi_{xx}(\Omega)$. Furthermore, it is assumed that the LRM operates in the steady state, so that all initial conditions can be neglected and the M tap outputs can be considered stationary.

The tap outputs are written in vector notation as $\underline{u}(k) = [u_0(k), u_1(k), \dots, u_{M-1}(k)]^T$. The corresponding $M \times M$ covariance matrix $\mathbf{R} = E\{\underline{u}(k)\underline{u}^T(k)\}$ is symmetric and (semi-)positive definite. In general \mathbf{R} is not Toeplitz. However, the Kautz network with identical poles $p_m = p$ in (2.43) (when $p_m = \xi$ with ξ a real number satisfying $0 < \xi < 1$ a Laguerre network is obtained) yields a Toeplitz covariance matrix. Such Kautz functions can be written as

$$\Psi_m(z) = \frac{az}{z-p} A^m(z),$$

where $a = \sqrt{1-|p|^2}$ and $A(z) = (1-p^*z)/(z-p)$ an all-pass function. Thus we find for the $(p+1, q+1)$ -th element of \mathbf{R} that

$$E\{u_p(k)u_q(k)\} = \frac{a^2}{2\pi} \int_{-\pi}^{\pi} \frac{e^{j\Omega}}{e^{j\Omega}-p} \frac{1}{1-p^*e^{j\Omega}} \left(\frac{1-p^*e^{j\Omega}}{e^{j\Omega}-p^*} \right)^{p-q} \Phi_{xx}(\Omega) d\Omega,$$

which is a function of $p-q$ only. Consequently, the covariance matrix of a Kautz network with identical poles is Toeplitz.

We know from Chapter 1 that the eigenvalues of \mathbf{R} determine the convergence behaviour of the adaptive filter, in particular the maximum eigenvalue λ_{\max} and the minimum eigenvalue λ_{\min} . A consequence of the orthonormality of the basis functions is that these are bounded by

$$\lambda_{\max} \leq \max_{\Omega} \Phi_{xx}(\Omega), \quad (2.50)$$

$$\lambda_{\min} \geq \min_{\Omega} \Phi_{xx}(\Omega). \quad (2.51)$$

Proof: The maximum and minimum eigenvalues of a symmetric matrix \mathbf{R} are given by the maximum and minimum values of the Rayleigh quotient (see e.g. (Franklin 1968)):

$$\lambda_{\max} = \max_{\underline{a}} \frac{\langle \mathbf{R}\underline{a}, \underline{a} \rangle}{\langle \underline{a}, \underline{a} \rangle}, \quad (2.52)$$

$$\lambda_{\min} = \min_{\underline{a}} \frac{\langle \mathbf{R}\underline{a}, \underline{a} \rangle}{\langle \underline{a}, \underline{a} \rangle}, \quad (2.53)$$

where $\underline{a} = [a_0, a_1, \dots, a_{M-1}]^T$ and $\underline{a} \neq \underline{0}$. With (2.13), the $(p+1, q+1)$ -th element of \mathbf{R} is given by

$$\mathbf{R}_{pq} = E\{u_p(k)u_q(k)\} = \frac{1}{2\pi} \int_{-\pi}^{\pi} G_p(e^{j\Omega}) G_q^*(e^{j\Omega}) \Phi_{xx}(\Omega) d\Omega,$$

so that we may now write

$$\begin{aligned} \langle \mathbf{R}\underline{a}, \underline{a} \rangle &= \sum_{p=0}^{M-1} \sum_{q=0}^{M-1} a_p \mathbf{R}_{pq} a_q = \frac{1}{2\pi} \int_{-\pi}^{\pi} \left| \sum_{m=0}^{M-1} a_m G_m(e^{j\Omega}) \right|^2 \Phi_{xx}(\Omega) d\Omega \\ &\leq \frac{1}{2\pi} \int_{-\pi}^{\pi} \left| \sum_{m=0}^{M-1} a_m G_m(e^{j\Omega}) \right|^2 d\Omega \max_{\Omega} \Phi_{xx}(\Omega) = \langle \underline{a}, \underline{a} \rangle \max_{\Omega} \Phi_{xx}(\Omega) \end{aligned}$$

We have used that the functions $g_m(k)$ are orthonormal. By combination of (2.54) and (2.52) the proof of (2.50) is completed. The same line of reasoning can be used to prove (2.51). Note that this proof also holds for the TDL, see eq. 1.3 and eq. 1.4.

With the discrete Laguerre and Kautz networks we now have at our disposal a few filter structures that may serve as the basis of an adaptive linear regression model (LRM). We have indicated that adaptive Laguerre filters are well suited to imitate systems with impulse responses that show a certain exponential decay towards infinity, see e.g. (den Brinker 1993). Of course, before the adaptive Laguerre filter can be used, one needs to make a choice of the (fixed) Laguerre pole ξ . The Laguerre pole should be in accordance with the memory of the unknown reference system. In practice, this choice will often be made on the basis of some off-line measurements performed on the unknown reference system. With the collected input/output data, a choice for ξ can be made using the method described in (Oliveira e Silva 1995a), see also Section 2.5.3. If the collected data is in the impulse response form, one can use the alternative method in (Fu and Dumont 1993a; Fu and Dumont 1993b) to directly arrive at the Laguerre pole that minimizes the criterion $\sum_{m=0}^{\infty} (m+1)c_m^2(\xi)$, see also Appendix A of this thesis.

By using a fixed Laguerre pole, it is assumed that the environment of the adaptive filter is stationary or at most weakly nonstationary. In the situation where, for example, the memory of the unknown reference system changes in time, the advantage of using an adaptive Laguerre filter instead of an adaptive TDL is lost. In Chapter 7 an algorithm is presented for the adaptive optimization of the Laguerre pole, so that slow variations of the environment of the adaptive filter can be tracked.

To imitate systems with impulse responses that, in addition to an exponential decay, show strong oscillatory behaviour, adaptive Kautz filters are expected to do better for obvious reasons, see also (den Brinker 1993). For a good performance of an adaptive Kautz filter, it is crucial to select good positions of the Kautz poles. Again, off-line measurements can be performed on the unknown reference system to yield the input/output data on the

basis of which the Kautz poles are selected. To this end, standard system identification techniques can be adopted to arrive at some sort of system description, e.g. an impulse response, a transfer function or a state space description (Williamson and Zimmerman 1996).

An example of such an identification technique is the popular method by Steiglitz and McBride (Steiglitz and McBride 1965). The popularity of this method can be contributed to the fact that it is a simple and robust iterative procedure, yet it gives (if it converges) the solution to the difficult nonlinear output error problem. After convergence, a model of the unknown system is found in the form of a rational transfer function, say $H(z)$, of a prescribed order. The poles for the Kautz filter can then be obtained as the roots of the denominator polynomial of $H(z)$.

Sometimes an impulse response of the reference system is available. In (Beliczynski, Kale, and Cain 1992) a method is proposed to obtain from a high-order FIR model a low-order IIR model. First, a balanced state space realization is constructed from the FIR model. Second, by inspection of the Hankel singular values the reduced system order is determined. This is then followed by truncation of the high-order state space form to a lower-order state space form. Finally, the suitable poles for the Kautz filter can be obtained as the eigenvalues of the system matrix of the state space equations.

As was already indicated by Kautz (Kautz 1954), an alternative way to arrive at an IIR model from a (noisy) impulse response, say $h(k)$, is via Prony's method, see e.g. (Marple 1987). This (non-iterative) method consists of establishing a linear difference equation of prescribed order that is nearly satisfied by $h(k)$. It is well known that if we use Prony's method with an order close to the order of the reference system, then the damping parameters of the poles tend to be overestimated (van Blaricum and Mitra 1978). However, we can use Prony's method with an order that is substantially larger than the order of the reference system. As a consequence, not only the system dynamics are modelled but also the noise. It turns out that if the Prony order is substantially larger than the order of the reference system, a subset of the poles given by the denominator polynomial are close to the true system poles (Marple 1987). These poles can be found with the method for model reduction proposed in (den Brinker and Belt 1996), from which we cite: "The method is based on the representation of the original model in an (exact) Kautz series. ... The Kautz model is nonunique: it depends on the ordering of the poles. The ordering of the poles can be chosen such that the first sections contribute most to the overall impulse response of the original system in a quadratic sense. Having a specific ordering, the reduced model order, say n , can be chosen by considering the energy contained in a truncated representation. The resulting reduced order model is obtained simply by truncation of the Kautz series at the n -th term."

An important short-coming of the Laguerre and Kautz functions is that they have an abrupt start at $k = 0$. This means that a Laguerre or Kautz filter is not well suited to imitate a system that has an impulse response with a gradual start. In Chapter 3 and Chapter 4 two other networks will be introduced that may serve as the basis of an adaptive LRM. These are the so-called *Jacobi* networks (with the special case of *Legendre networks*) and the Meixner-like networks. The Jacobi and the Meixner-like functions have a gradual

start and an exponential decay towards $k = \infty$. Therefore, if properly parametrized, Jacobi and Meixner-like filters are well suited to model systems of which the impulse responses have a gradual start and a certain exponential decay towards $k = \infty$.

Bibliography

- Abramowitz, M. and I. A. Stegun (1970). *Handbook of Mathematical Functions*. New York (NY), U.S.A.: Dover Publications.
- Beckmann, P. (1973). *Orthogonal Polynomials for Engineers and Physicist*. Boulder (CO), U.S.A.: The Golem Press.
- Beliczynski, B., I. Kale, and G. D. Cain (1992). Approximation of FIR by IIR digital filters: an algorithm based on balanced model reduction. *IEEE Trans. Signal Process.* 40, 532–542.
- Belt, H. J. W. and A. C. den Brinker (1997). Optimal parametrization of truncated generalized Laguerre series. In *Proc. IEEE International Conference on Acoustics, Speech and Signal Processing (ICASSP)*, Munich, Germany. To appear in April 1997.
- Broome, P. W. (1965). Discrete orthonormal sequences. *Journal of the Association for Computing Machinery* 12, 151–168.
- Clement, P. R. (1963). On completeness of basis functions used for signal analysis. *SIAM Rev.* 5, 131–139.
- Clowes, G. J. (1965). Choice of the time-scaling factor for linear system approximations using orthonormal Laguerre functions. *IEEE Trans. Automat. Contr.* 10, 487–489.
- den Brinker, A. C. (1993). Adaptive orthonormal filters. In *Preprints Proc. 12th World Congress of the International Federation of Automatic Control (IFAC)*, Volume 5, Sydney, Australia, pp. 287–292.
- den Brinker, A. C. (1994). Optimality conditions for truncated Kautz series based on n th order all-pass sections. In *Signal Processing VII: Theories and Applications, Proc. EUSIPCO-94, Seventh European Signal Processing Conference*, Edinburgh, Scotland U.K., pp. 1086–1089.
- den Brinker, A. C. (1995). Meixner-like functions having a rational z -transform. *Int. J. Circuit Theory Appl.* 23, 237–246.
- den Brinker, A. C. (1996). Optimality conditions for a specific class of truncated Kautz series. *IEEE Trans. Circuits Syst.-II* 43, 597–600.
- den Brinker, A. C. and H. J. W. Belt (1996). Model reduction by orthogonalized exponential sequences. In *Proc. ProRISC/IEEE Benelux Workshop on Circuits, Systems and Signal Processing*, Mierlo, Netherlands, pp. 77–82.
- den Brinker, A. C., F. P. A. Benders, and T. Oliveira e Silva (1996). Optimality conditions for truncated Kautz series. *IEEE Trans. Circuits Syst.-II* 43, 117–122.

- Eykhoff, P. (1974). *System Identification: Parameter and State Estimation*. London, U.K.: John Wiley and Sons.
- Franklin, J. N. (1968). *Matrix Theory*. Englewood Cliffs (NJ), U.S.A.: Prentice-Hall.
- Fu, Y. and G. A. Dumont (1993a). An optimum time scale for discrete Laguerre network. *IEEE Trans. Automat. Contr.* 38, 934–938.
- Fu, Y. and G. A. Dumont (1993b). On determination of Laguerre filter pole through step or impulse response data. In *Preprints Proc. 12th World Congress of the International Federation of Automatic Control (IFAC)*, Volume 5, Sydney, Australia, pp. 303–307.
- Gottlieb, M. J. (1938). Concerning some polynomials orthogonal on a finite or enumerable set of points. *Am. J. Math.* 60, 453–458.
- Gradshteyn, I. S. and I. M. Ryzhik (1980). *Table of Integrals, Series and Products, corrected and enlarged edition*. Orlando (FL), U.S.A.: Academic Press, Inc.
- Heuberger, P. S. C. (1991). *On approximate system identification using system based orthonormal functions*. Ph. D. thesis, Delft University of Technology.
- Heuberger, P. S. C. and O. H. Bosgra (1990). Approximate system identification using system based orthonormal functions. In *Proc. of the 29th Conference on Decision and Control*, Honolulu, Hawaii, pp. 1086–1092.
- Heuberger, P. S. C., P. M. J. van den Hof, and O. H. Bosgra (1993). Modelling linear dynamical systems through generalized orthonormal basis functions. In *Preprints Proc. 12th World Congress of the International Federation of Automatic Control (IFAC)*, Volume 5, Sydney, Australia, pp. 283–286.
- Heuberger, P. S. C., P. M. J. van den Hof, and O. H. Bosgra (1995). A generalized orthonormal basis for linear dynamical systems. *IEEE Trans. Automat. Contr.* 40, 451–465.
- Huggins, W. H. (1956). Signal theory. *IRE Trans. Circuit Theory* 3, 210–216.
- Kautz, W. (1954). Transient synthesis in the time domain. *IRE Trans. Circuit Theory* 1, 29–39.
- King, J. J. and T. O’Canainn (1969). Optimum pole positions for Laguerre-function models. *Electronics Letters* 5, 601–602.
- King, R. E. and P. N. Paraskevopoulos (1977). Digital Laguerre filters. *Int. J. Circuit Theory Appl.* 5, 81–91.
- Lee, Y. W. (1932). Synthesis of electrical networks by means of the Fourier transforms of Laguerre functions. *J. Math. Phys.* 11, 83–113.
- Lee, Y. W. (1960). *Statistical Theory of Communication*. New York (NY), U.S.A.: John Wiley and Sons.
- Marple, Jr., S. L. (1987). *Digital Spectral Analysis with Applications*. Englewood Cliffs (NJ), U.S.A.: Prentice-Hall.

- Masnadi-Shirazi, M. A. and N. Ahmed (1991). Optimum Laguerre networks for a class of discrete-time systems. *IEEE Trans. Signal Process.* 39, 2104–2108.
- Oliveira e Silva, T. (1994a). Kautz filters. English translation of a work written in Portuguese for the “Prémio Científico IBM 94”.
URL: <ftp://inesca.inesca.pt/pub/tos/English/ibm94e.ps.gz>.
- Oliveira e Silva, T. (1994b). Optimality conditions for truncated Laguerre networks. *IEEE Trans. Signal Process.* 42, 2528–2530.
- Oliveira e Silva, T. (1995a). On the determination of the optimal pole position of Laguerre filters. *IEEE Trans. Signal Process.* 43, 2079–2087.
- Oliveira e Silva, T. (1995b). Optimality conditions for truncated Kautz networks with two periodically repeating complex conjugate poles. *IEEE Trans. Automat. Contr.* 40, 342–346.
- Oliveira e Silva, T. (1995c). Rational orthonormal functions on the unit circle and on the imaginary axis, with applications in system identification.
URL: <ftp://inesca.inesca.pt/pub/tos/English/rof.ps.gz>.
- Parks, T. W. (1971). Choice of time scale in Laguerre approximations using signal measurements. *IEEE Trans. Automat. Contr.* 16, 511–513.
- Sarroukh, B. E. (1996). Filter banks induced by unitary integral transformations. Master’s thesis, Eindhoven University of Technology.
- Steiglitz, K. (1965). The equivalence of digital and analog signal processing. *Information and Control* 8, 455–467.
- Steiglitz, K. and L. E. McBride (1965). A technique for the identification of linear systems. *IEEE Trans. Automat. Contr.* 10, 461–464.
- Szegő, G. (1959). *Orthogonal Polynomials*. New York (NY), U.S.A.: American Mathematical Society.
- Tanguy, N., P. Vilbé, and L. C. Calvez (1995). Optimum choice of free parameter in orthonormal approximations. *IEEE Trans. Automat. Contr.* 40, 1811–1813.
- van Blaricum, M. L. and R. Mitra (1978). Problems and solutions associated with Prony’s method for processing transient data. *IEEE Trans. Antennas Propag.* 26, 174–182.
- van den Hof, P. M. J., P. S. C. Heuberger, and J. Bokor (1995). System identification with generalized orthonormal basis functions. *Automatica* 31, 1821–1834.
- Wang, L. and W. R. Cluett (1994). Optimal choice of time-scaling factor for linear system approximations using Laguerre models. *IEEE Trans. Automat. Contr.* 39, 1463–1467.
- Weber, M. and A. Erdélyi (1952). On the finite difference analogue of Rodrigues’ formula. *Am. Math. Monthly* 59, 163–168.

- Williamson, G. A. and S. Zimmerman (1996). Globally convergent adaptive IIR filters based on fixed pole locations. *IEEE Trans. Signal Process.* 44, 1418–1427.
- Young, N. (1988). *An Introduction to Hilbert Space*. Cambridge, U.K.: Cambridge University Press.
- Young, T. Y. (1968). An extension of Szász's theorem for random signal representation. *Proc. IEEE* 56, 2195–2196.
- Young, T. Y. and W. H. Huggins (1962). Discrete orthonormal sequences. In *Proc. of the National Electronics Conference*, Chicago, Illinois, pp. 10–18.

Chapter 3

Jacobi and Legendre Filters

3.1 Introduction

In Chapter 2 the Laguerre and Kautz filters were introduced. It was demonstrated that these filters are well suited to imitate systems that have impulse responses with an exponential decay. A Laguerre filter contains a (multiple) real pole, and is therefore less suited to approximate systems with oscillatory impulse responses. Such systems are much better approximated by Kautz filters, because Kautz filters may contain a whole set of complex-valued poles. However, due to the abrupt start of their basis functions, neither Kautz filters nor Laguerre filters are suitable to imitate systems with gradually starting impulse responses.

In this chapter we construct a continuous-time and a discrete-time linear regression model (LRM) based on a set of orthonormal functions on a semi-infinite interval which exhibit a gradual start and an exponential decay towards infinity. In Section 3.2 we construct a set of continuous orthonormal functions from the classical Jacobi polynomials, in a way similar to the construction of the Laguerre functions from the classical Laguerre polynomials in Section 2.5.1. The obtained orthonormal functions show a gradual start and then an exponential decay. In Section 3.3 we develop a (new) discrete counterpart of the continuous Jacobi functions. Based on these discrete Jacobi functions we construct a discrete LRM for adaptive filtering purposes.

3.2 Continuous Jacobi Filters

First we introduce the system of classical Jacobi polynomials with the system of classical Legendre polynomials as a special case. We then construct, from the system of Jacobi polynomials and the associated weight function, a set of orthonormal functions on the interval $(0, \infty)$, the continuous Jacobi functions, with the continuous Legendre functions as a special case. If the parameters satisfy certain conditions, the Laplace transforms of the obtained orthonormal functions are rational functions of s . Then, the continuous Jacobi functions can be generated as impulse responses of a realizable network. This network

may serve as the basis of a linear regression model resulting in what will be called a *Jacobi filter* which, under a certain parametrization, reduces to a *Legendre filter*.

3.2.1 Classical Jacobi and Legendre Polynomials

The classical *Jacobi polynomials* are orthogonal under the weight function given by

$$\tilde{w}(x) = (1-x)^\lambda(1+x)^\mu,$$

with orthogonality interval $(-1, 1)$, see (Szegő 1959). Integrability of $\tilde{w}(x)$ is guaranteed for $\lambda > -1$ and $\mu > -1$. The classical Jacobi polynomials include as special cases the Gegenbauer or ultraspherical polynomials ($\lambda = \mu = \delta - \frac{1}{2}$ with $\delta > -\frac{1}{2}$), the Chebyshev polynomials of the first kind ($\lambda = \mu = -\frac{1}{2}$), the Chebyshev polynomials of the second kind ($\lambda = \mu = \frac{1}{2}$), and the Legendre or spherical polynomials ($\lambda = \mu = 0$) (Abramowitz and Stegun 1970).

The classical *shifted Jacobi polynomials* (Abramowitz and Stegun 1970; Beckmann 1973) are orthogonal on the interval $(0, 1)$ under the weight function

$$w(x) = x^{\gamma-1}(1-x)^{\alpha-\gamma},$$

and follow from the Jacobi polynomials by the substitution $x = 2y + 1$. For integrability of $w(x)$ it is required that $\alpha - \gamma > -1$ and $\gamma > 0$. The shifted Jacobi polynomials, denoted by $\mathcal{P}_m^{(\alpha, \gamma)}(x)$ with $m = 0, 1, 2, \dots$, are given by (see also Table 2.3)

$$\begin{aligned} \mathcal{P}_m^{(\alpha, \gamma)}(x) &= \frac{\Gamma(\gamma + m)}{\Gamma(\alpha + 2m)} \sum_{n=0}^m (-1)^n \binom{m}{n} \frac{\Gamma(\alpha + 2m - n)}{\Gamma(\gamma + m - n)} x^{m-n} \\ &= \frac{\Gamma(\gamma + m)}{\Gamma(\alpha + 2m)} \sum_{n=0}^m (-1)^{m+n} \binom{m}{n} \frac{\Gamma(\alpha + m + n)}{\Gamma(\gamma + n)} x^n. \end{aligned} \quad (3.1)$$

Special cases of the shifted Jacobi polynomials are the shifted Chebyshev polynomials of the first kind ($\alpha = 0$ and $\gamma = \frac{1}{2}$), the shifted Chebyshev polynomials of the second kind ($\alpha = 2$ and $\gamma = \frac{3}{2}$), the shifted Gegenbauer polynomials ($\alpha = 2\beta$ and $\gamma = \beta + \frac{1}{2}$ with $\beta > \frac{1}{2}$), and the shifted Legendre polynomials ($\alpha = \gamma = 1$).

The orthogonality relation of the shifted Jacobi polynomials reads ($\forall m, n \in \mathbb{N}_0$):

$$\int_0^1 w(x) \mathcal{P}_m^{(\alpha, \gamma)}(x) \mathcal{P}_n^{(\alpha, \gamma)}(x) dx = \delta_{mn} h_m^2, \quad (3.2)$$

where δ_{mn} is the Kronecker delta. The normalization constant is given by (see Table 2.2)

$$h_m^2 = \frac{m! \Gamma(m + \gamma) \Gamma(m + \alpha) \Gamma(m + \alpha - \gamma + 1)}{(2m + \alpha) \Gamma^2(2m + \alpha)}.$$

For our purposes the shifted Legendre polynomials $\mathcal{T}_m(x)$ appear to be of special interest. Following Table 2.3 they are defined as

$$\mathcal{T}_m(x) = \frac{(2m)!}{(m!)^2} \mathcal{P}_m^{(1,1)}(x) = \sum_{n=0}^m (-1)^{m+n} \binom{m}{n} \binom{m+n}{n} x^n. \quad (3.3)$$

Thus apart from a constant multiplier, they are shifted Jacobi polynomials for $\alpha = \gamma = 1$. The constant multiplier is so chosen that they satisfy the orthogonality relations

$$\int_0^1 \mathcal{T}_m(x) \mathcal{T}_n(x) dx = \frac{1}{2m+1} \delta_{mn}.$$

3.2.2 Continuous Jacobi and Legendre Functions

Consider the orthogonality relation of the shifted Jacobi polynomials in (3.2). After the substitution $x = e^{-\sigma t}$ with $\sigma > 0$, the orthogonality interval is changed from $(0, 1)$ to $(0, \infty)$. Note that with this substitution the weight function becomes

$$w(e^{-\sigma t}) = e^{-\sigma(\gamma-1)t} (1 - e^{-\sigma t})^{\alpha-\gamma}. \quad (3.4)$$

Clearly, this weight function exhibits an exponential decay for large t . Also, note that when $\alpha - \gamma > n$ with $n = 0, 1, \dots$, all m -th order derivatives $\partial^m w(e^{-\sigma t}) / \partial t^m$ with $m = 0, 1, \dots, n$ vanish at $t = 0$. This means that with $\alpha - \gamma$ we can control the "speed" with which $w(e^{-\sigma t})$ starts.

Multiplied by the square root of the weight function in (3.4) and a normalization constant, the shifted Jacobi polynomials in (3.1) with $x = e^{-\sigma t}$ pass into orthonormal functions on $(0, \infty)$. These *continuous Jacobi functions* are given by (Armstrong 1957; Armstrong 1959; Mendel 1964)

$$p_m^{(\alpha, \gamma)}(\sigma; t) = \frac{\sqrt{\sigma}}{h_m} e^{-(\sigma\gamma/2)t} (1 - e^{-\sigma t})^{(\alpha-\gamma)/2} \mathcal{P}_m^{(\alpha, \gamma)}(e^{-\sigma t}). \quad (3.5)$$

Since the shifted Jacobi polynomials are complete on $(0, 1)$, the continuous Jacobi functions form a complete orthonormal set in the Hilbert space $L_2(\mathbb{R}^+)$. Consequently, any function $h(t)$ belonging to $L_2(\mathbb{R}^+)$ can be approximated to any desired degree by a linear combination of continuous Jacobi functions.

Using the recurrence relation of the shifted Jacobi polynomials in Table 2.4 and the definition of the Jacobi functions in (3.5) we find a recurrence relation for the Jacobi functions:

$$p_{m+1}^{(\alpha, \gamma)}(\sigma; t) = \{A_m + B_m e^{-\sigma t}\} p_m^{(\alpha, \gamma)}(\sigma; t) - C_m p_{m-1}^{(\alpha, \gamma)}(\sigma; t), \quad m = 0, 1, 2, \dots, \quad (3.6)$$

where

$$\begin{aligned} A_m &= -[2m(m + \alpha) + \gamma(\alpha - 1)] \sqrt{2m + \alpha} F(m, \alpha, \gamma), \\ B_m &= (2m + \alpha + 1)(2m + \alpha - 1) \sqrt{2m + \alpha} F(m, \alpha, \gamma), \\ C_m &= (2m + \alpha + 1) \sqrt{\frac{m(m + \alpha - 1)(m + \gamma - 1)(m + \alpha - \gamma)}{(2m + \alpha - 2)}} F(m, \alpha, \gamma), \end{aligned}$$

and

$$F(m, \alpha, \gamma) = \frac{1}{2m + \alpha - 1} \sqrt{\frac{2m + \alpha + 2}{(m + 1)(m + \alpha)(m + \gamma)(m + \alpha - \gamma + 1)}}.$$

Note that $C_0 = 0$ so that it is not necessary to define $p_{-1}^{(\alpha, \gamma)}(\sigma; t)$. The function $p_0^{(\alpha, \gamma)}(\sigma; t)$ follows from (3.5).

The first four continuous Jacobi functions for four different choices of α and γ are depicted in Fig. 3.1. In Fig. 3.1A and Fig. 3.1C we have $(\alpha, \gamma) = (5, 1)$ and $(\alpha, \gamma) = (10, 6)$, respectively, so that $\alpha - \gamma = 4$ in both cases. Similarly, in Fig. 3.1B and Fig. 3.1D we have $(\alpha, \gamma) = (10, 1)$ and $(\alpha, \gamma) = (15, 6)$ so that $\alpha - \gamma = 9$. We see that with a larger value for $\alpha - \gamma$ the functions have a more gradual start. Further, a larger value for γ results in a faster exponential decay, as was to be expected from (3.4).

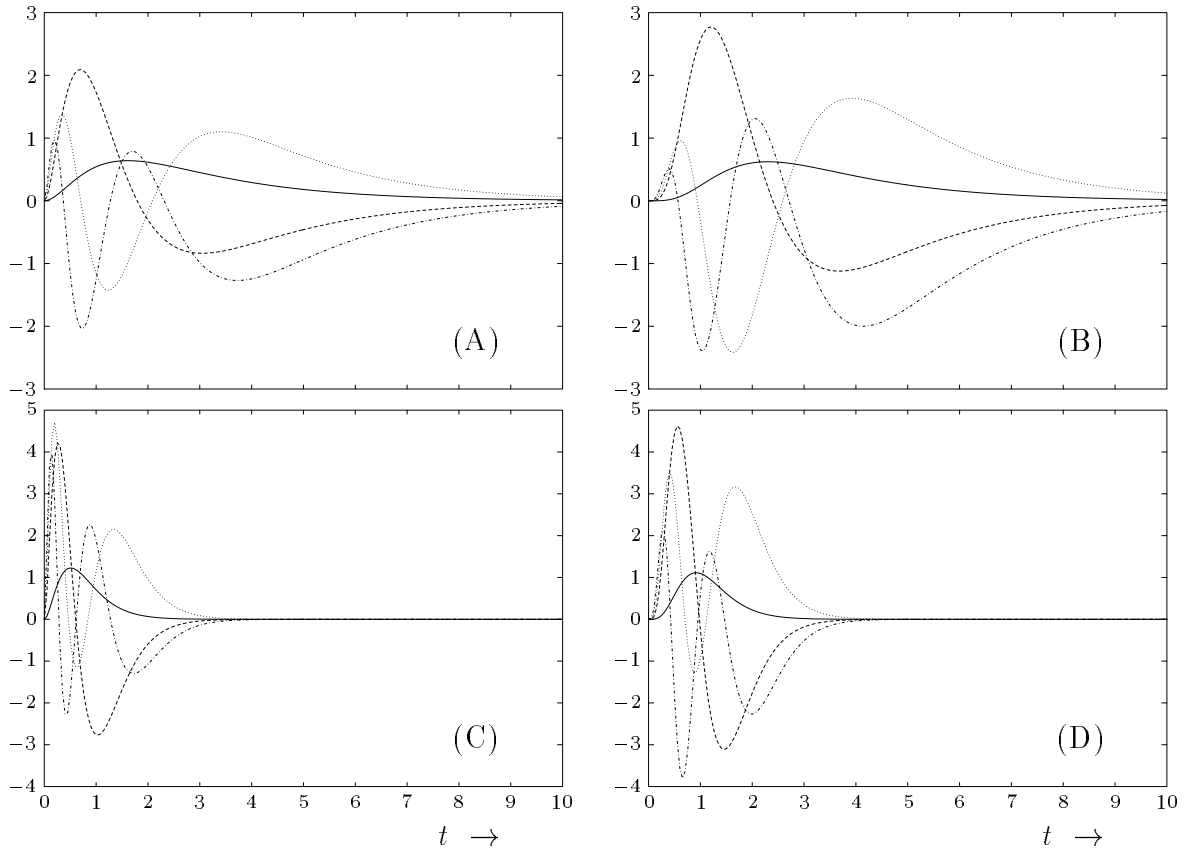


Figure 3.1: Examples of the first four continuous Jacobi functions $p_m^{(\alpha, \gamma)}(\sigma; t)$ with $\sigma = 1$. The solid, dashed, dotted and dash-dotted lines correspond to $m = 0$, $m = 1$, $m = 2$ and $m = 3$, respectively. Further, (A) $\alpha = 5$ and $\gamma = 1$, (B) $\alpha = 10$ and $\gamma = 1$, (C) $\alpha = 10$ and $\gamma = 6$, (D) $\alpha = 15$ and $\gamma = 6$.

With (3.3) the shifted Jacobi polynomials $\mathcal{P}^{(\alpha, \gamma)}(x)$ with $\alpha = \gamma = 1$ pass into the

shifted Legendre polynomials $\mathcal{T}(x)$ (apart from a constant multiplier). Likewise, with $\alpha = \gamma = 1$ the continuous Jacobi functions $p_m^{(\alpha, \gamma)}(\sigma; t)$ reduce to the so-called *continuous Legendre functions*, henceforth denoted by $t_m(\sigma; t)$. The continuous Legendre functions are given by

$$\begin{aligned} t_m(\sigma; t) &= p_m^{(1,1)}(\sigma; t) \\ &= \sqrt{\sigma(2m+1)} \sum_{n=0}^m (-1)^{m+n} \binom{m}{n} \binom{m+n}{n} e^{-\sigma(n+1/2)t}, \end{aligned} \quad (3.7)$$

and form an orthonormal basis of $L_2(\mathbb{R}^+)$. They are related to the shifted Legendre polynomials according to

$$t_m(\sigma; t) = \sqrt{\sigma(2m+1)} e^{-\sigma t/2} \mathcal{T}_m(e^{-\sigma t}). \quad (3.8)$$

By combining the recurrence relation of the shifted Legendre polynomials (see Table 2.4) with the relation between the continuous Legendre functions and the shifted Legendre polynomials in (3.8), we arrive at the following recurrence relation:

$$(m+1)t_{m+1}(\sigma; t) = \sqrt{(2m+1)(2m+3)} (-1 + 2e^{-\sigma t}) t_m(\sigma; t) - m \sqrt{\frac{2m+3}{2m-1}} t_{m-1}(\sigma; t), \quad (3.9)$$

with $m = 0, 1, 2, \dots$ and $t_0(\sigma; t) = \sqrt{\sigma} e^{-\sigma t/2}$. Note that it is not necessary to define $t_{-1}(\sigma; t)$.

The first four continuous Legendre functions $t_m(\sigma; t)$ with $\sigma = 1$ are plotted in Fig. 3.2. We observe that the functions jump at $t = 0$ and decay exponentially. Also, for larger m the functions $t_m(\sigma; t)$ become more oscillatory.

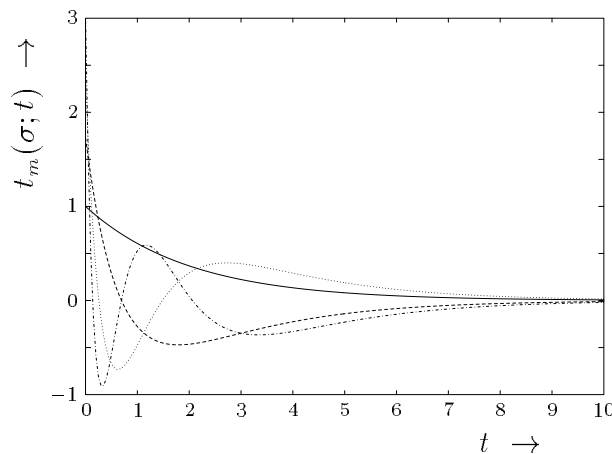


Figure 3.2: The first four continuous Legendre functions with $\sigma = 1$. The solid, dashed, dotted and dash-dotted lines correspond to $t_0(\sigma; t)$, $t_1(\sigma; t)$, $t_2(\sigma; t)$ and $t_3(\sigma; t)$, respectively.

Finally, the continuous Legendre functions satisfy a differential equation that can be obtained from the differential equation for the Legendre polynomials in Table 2.5 and the relation between the continuous Legendre functions and the Legendre polynomials in (3.8):

$$\frac{1 - e^{-\sigma t}}{\sigma^2} t_m''(\sigma; t) + \frac{1}{\sigma} t_m'(\sigma; t) + \left[\frac{1}{4}(1 + e^{-\sigma t}) + e^{-\sigma t} m(m+1) \right] t_m(\sigma; t) = 0.$$

3.2.3 Continuous Jacobi and Legendre Networks

In this section we present the Laplace transforms of the continuous Jacobi functions with $(\alpha - \gamma)/2 \in \mathbb{N}_0$ and of the continuous Legendre functions ($\alpha = \gamma = 1$). Using these Laplace transforms we construct networks with the continuous Jacobi functions and Legendre functions as impulse responses. These networks may serve as the basis of a linear regression model (LRM) as that depicted in Fig. 1.8.

For $(\alpha - \gamma)/2 \in \mathbb{N}_0$ the continuous Jacobi functions in (3.5) can be written with the aid of (3.1) in the following form:

$$p_m^{(\alpha, \gamma)}(\sigma; t) = \sum_{n=0}^m L_{m,n}^{(\alpha, \gamma)}(\sigma) \sum_{l=0}^{(\alpha-\gamma)/2} B_{n,n+l}^{(\alpha-\gamma)} e^{-\sigma(l+\gamma/2+n)t}. \quad (3.10)$$

Here, $L_{m,n}^{(\alpha, \gamma)}$ is given by

$$L_{m,n}^{(\alpha, \gamma)}(\sigma) = \begin{cases} 0, & \text{if } m < n, \\ (-1)^n \binom{m}{n} \frac{(\alpha + m)_n}{\Gamma(\gamma + n)} b_m^{(\alpha, \gamma)}(\sigma), & \text{if } m \geq n, \end{cases}$$

where

$$b_m^{(\alpha, \gamma)}(\sigma) = (-1)^m \sqrt{\frac{\sigma(2m + \alpha) \Gamma(m + \gamma) \Gamma(m + \alpha)}{m! \Gamma(m + \alpha - \gamma + 1)}},$$

while $B_{n,n+l}^{(\alpha-\gamma)}$ is given by

$$B_{n,n+l}^{(\alpha-\gamma)} = \begin{cases} 0, & \text{if } -n \leq l < 0, \\ (-1)^l \binom{(\alpha-\gamma)/2}{l}, & \text{if } 0 \leq l \leq (\alpha-\gamma)/2, \\ 0, & \text{if } l > (\alpha-\gamma)/2. \end{cases}$$

The coefficients $L_{m,n}^{(\alpha, \gamma)}$ are the entries of the lower-triangular matrix $\mathbf{L}^{(\alpha, \gamma)}$, with the understanding that the subscript $\{m, n\}$ denotes the $(m+1, n+1)$ -th element. The coefficients $B_{n,n+l}^{(\alpha-\gamma)}$ are the entries of the upper-band matrix $\mathbf{B}^{(\alpha-\gamma)}$.

After introducing the vector functions

$$\underline{p}^{(\alpha, \gamma)} = \left[p_0^{(\alpha, \gamma)}(\sigma; t), p_1^{(\alpha, \gamma)}(\sigma; t), p_2^{(\alpha, \gamma)}(\sigma; t), \dots \right]^T, \\ \underline{f} = \left[e^{-\sigma(\gamma/2)t}, e^{-\sigma(\gamma/2+1)t}, e^{-\sigma(\gamma/2+2)t}, \dots \right]^T$$

we can express the Jacobi functions in (3.10) in the product form

$$\underline{p}^{(\alpha,\gamma)} = \underline{L}^{(\alpha,\gamma)} \underline{B}^{(\alpha-\gamma)} \underline{f}.$$

The Laplace transforms of the Jacobi functions in (3.10) with $(\alpha - \gamma)/2 \in \mathbb{N}_0$ are rational functions of s :

$$P_m^{(\alpha,\gamma)}(\sigma; s) = \sum_{n=0}^m L_{m,n}^{(\alpha,\gamma)}(\sigma) \sum_{l=0}^{(\alpha-\gamma)/2} B_{n,n+l}^{(\alpha-\gamma)} \frac{1}{s + \sigma(l + \gamma/2 + n)},$$

so that the Jacobi functions can be generated as the impulse responses of the *Jacobi network* shown in Fig. 3.3.

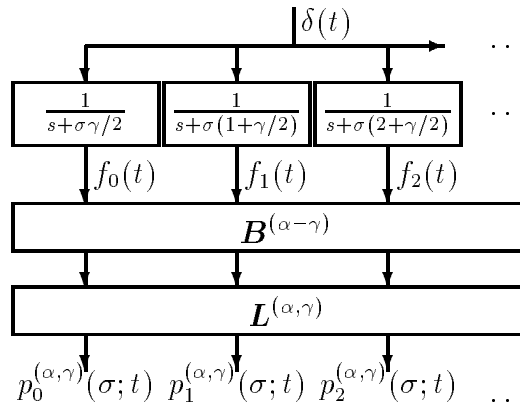


Figure 3.3: Continuous Jacobi network. The impulse responses $p_m^{(\alpha,\gamma)}(\sigma; t)$ are the continuous Jacobi functions for $(\alpha - \gamma)/2 \in \mathbb{N}_0$.

Hereafter, we will mean by a *continuous Jacobi filter* the combination of the LRM in Fig. 1.8 with a continuous Jacobi network. Thus, the output of a continuous Jacobi filter is formed by a weighted sum of the individual outputs of a Jacobi network.

The Laplace transforms of the continuous Legendre functions in (3.7) are given by

$$\begin{aligned} T_m(\sigma; s) &= \sqrt{2\sigma_m} (-1)^m \sum_{n=0}^m (-1)^n \binom{m}{n} \binom{m+n}{n} \frac{1}{s + \sigma_n} \\ &= \sqrt{2\sigma_m} \frac{1}{s + \sigma_m} \prod_{l=0}^{m-1} \frac{s - \sigma_l}{s + \sigma_l}, \end{aligned} \tag{3.11}$$

where $\sigma_m = \sigma(m + \frac{1}{2})$. The continuous Legendre functions can be generated as the impulse responses of a so-called *continuous Legendre network* (Lee 1960), cf. Fig. 3.4. It consists of a cascade of first-order all-pass sections tapped by first-order low-pass filters. Due to the specific relation between the poles of successive sections, the transfer function from the input to the $(m + 1)$ -th output ($m = 0, 1, 2, \dots$) has a low-pass character with (-3 dB)

cut-off frequency $\omega_c = \sigma_m = \sigma(m + \frac{1}{2})$. When comparing Fig. 3.4 and Fig. 2.5 we see that the continuous Legendre network is a specific continuous Kautz network. Note that in the continuous Legendre network only one parameter, namely σ , can be chosen and that all filter sections then directly follow from this choice.

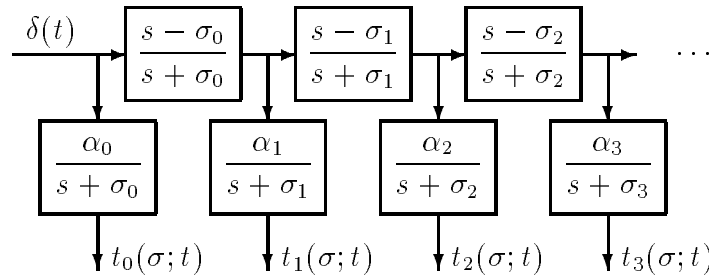


Figure 3.4: A continuous Legendre network composed of a filter line of first-order all-pass sections tapped by first-order low-pass sections with $\sigma_m = \sigma(m + \frac{1}{2})$ and $\alpha_m = (\sigma(2m + 1))^{1/2}$ for $m \in \mathbb{N}_0$. The impulse responses $t_m(\sigma; t)$ are the continuous Legendre functions.

Hereafter, we will mean by a *continuous Legendre filter* the combination of the LRM in Fig. 1.8 and a continuous Legendre network. Thus, the output of a continuous Legendre filter is formed by a weighted sum of the individual outputs of a continuous Legendre network.

3.3 Discrete Jacobi Filters

We search for a discrete-time counterpart of the system of continuous Jacobi functions which should meet the following constraints. First, we require that the discrete functions can be generated as impulse responses of a discrete network. This implies that their z -transforms must be rational functions of z with all singularities inside the unit circle in the complex z -plane. Second, in conformity with the continuous Jacobi functions we demand that the discrete functions can be expressed as the square root of a weight function $v(k)$ times polynomials orthogonal under $v(k)$.

3.3.1 Discrete Jacobi Functions and Networks

A possible approach towards discrete Jacobi functions would be to start with the Laplace transforms of the continuous Jacobi functions and apply to these Laplace transforms the modified bilinear transformation (MBT) in (2.11). The resulting functions are the z -transforms of discrete orthonormal functions. These are rational stable transfer functions, because the MBT maps rational stable transfer functions in the s -domain (which the Laplace transforms of the continuous Jacobi functions are) onto rational stable transfer functions in the z -domain. Unfortunately, the discrete Jacobi functions obtained in this

way do not meet our second requirement: they cannot be expressed as the square root of a weight function times a polynomial.

We will follow an alternative approach to arrive at a discrete-time counterpart of the continuous Jacobi functions. We start with the weight function

$$v^{(a,c)}(\theta; k) = \theta^{2ck}(1 - \theta^{k+1})^{2a}, \quad (3.12)$$

where $k, a \in \mathbb{N}_0$, $0 < \theta < 1$ and $c > 0$. This weight function resembles the weight function associated with the continuous Jacobi polynomials after the substitution $x = e^{-\sigma t}$ (see (3.4)): for large values of k it decreases exponentially, and the speed with which it starts at $k = 0$ can be controlled with the parameter a .

Discrete functions, called the *discrete Jacobi functions*, can be constructed from the square root of the weight function in (3.12) and polynomials in θ^k :

$$\begin{aligned} q_m^{(a,c)}(\theta; k) &= \theta^{ck}(1 - \theta^{k+1})^a \sum_{n=0}^m M_{m,n}^{(a,c)} \theta^{kn} \\ &= \sum_{n=0}^m M_{m,n}^{(a,c)} \sum_{l=0}^a C_{n,n+l}^{(a)} \theta^{(l+c+n)k}. \end{aligned} \quad (3.13)$$

Here, $C_{n,n+l}^{(a)}$ is given by

$$C_{n,n+l}^{(a)} = \begin{cases} 0, & \text{if } -n < l < 0, \\ (-\theta)^l \binom{a}{l}, & \text{if } 0 \leq l \leq a, \\ 0, & \text{if } l > a. \end{cases}$$

The not yet specified coefficients $M_{m,n}^{(a,c)}$ are the entries of the lower-triangular matrix $\mathbf{M}^{(a,c)}$, with the understanding that the subscript $\{m, n\}$ denotes the $(m+1, n+1)$ -th element. Likewise, the coefficients $C_{n,n+l}$ are the entries of the upper-band matrix $\mathbf{C}^{(a)}$.

Note the similar form of the discrete Jacobi functions in (3.13) and the continuous Jacobi functions for $(\alpha - \gamma) \in \mathbb{N}_0$ in (3.10).

From (3.13) we conclude that the system of discrete Jacobi functions is obtained from the system of sequences p_m^k with $p_m = \theta^{c+m}$, $m = 0, 1, 2, \dots$, $0 < \theta < 1$ and $c > 0$. Conversely, the system of sequences p_m^k can always be recovered from the system of discrete Jacobi functions. The system of sequences p_m^k is complete in $\ell_2(\mathbb{N}_0)$ if

$$\sum_{m=0}^{\infty} (1 - |p_m|) = \infty. \quad (3.14)$$

Since

$$\sum_{m=0}^{\infty} (1 - \theta^{(c+m)}) > \sum_{m=0}^{\infty} (1 - \theta^c) = \infty,$$

we may conclude that the discrete Jacobi functions form a complete orthonormal set on $\ell_2(\mathbb{N}_0)$. Thus, any function belonging to $\ell_2(\mathbb{N}_0)$ can be approximated to any desired degree by a linear combination of discrete Jacobi functions.

After introducing the following vector functions

$$\begin{aligned}\underline{q}^{(a,c)} &= [q_0^{(a,c)}(\theta; k), q_1^{(a,c)}(\theta; k), q_2^{(a,c)}(\theta; k), \dots]^T \\ \underline{g} &= [\theta^{ck}, \theta^{(c+1)k}, \theta^{(c+2)k}, \dots]^T\end{aligned}$$

we can express the discrete Jacobi functions in the following product form:

$$\underline{q}^{(a,c)} = \mathbf{M}^{(a,c)} \mathbf{C}^{(a)} \underline{g}.$$

The matrix $\mathbf{M}^{(a,c)}$ is such that the functions $\underline{q}^{(a,c)}$ are orthonormal. Therefore, $\mathbf{M}^{(a,c)}$ satisfies

$$\underline{q}^{(a,c)} \{\underline{q}^{(a,c)}\}^T = \mathbf{M}^{(a,c)} \mathbf{C}^{(a)} \underline{g} \underline{g}^T \{\mathbf{C}^{(a)}\}^T \{\mathbf{M}^{(a,c)}\}^T = \mathbf{I},$$

where $\mathbf{M}^{(a,c)}$ is calculated as the inverse of the first Cholesky factor of $\mathbf{C}^{(a)} \underline{g} \underline{g}^T \{\mathbf{C}^{(a)}\}^T$. We did not find an explicit expression for $\mathbf{M}^{(a,c)}$, but with the wide availability of well-behaving numerical algorithms $\mathbf{M}^{(a,c)}$ can be determined numerically once a choice for a and c has been made.

The calculation of $\mathbf{M}^{(a,c)}$ becomes numerically unstable when θ is close to unity since then the matrix $\underline{g} \underline{g}^T$ is ill-conditioned. To avoid this, we may start with a near-orthogonal set of functions $\tilde{\underline{g}}$ given by

$$\tilde{\underline{g}} = \tilde{\mathbf{M}}^{(a,c)} \mathbf{C}^{(a)} \underline{g}$$

where $\tilde{\mathbf{M}}^{(a,c)}$ is proportional to $\mathbf{L}^{(\alpha,\gamma)}$ with $\alpha = 2a + 2c$ and $\gamma = 2c$:

$$\tilde{M}_{m,n}^{(a,c)} = (-1)^n \binom{m}{n} \frac{(2a + 2c + m)_n}{\Gamma(2c + n)}.$$

The obtained discrete functions are almost orthogonal. They can be considered as sampled continuous Jacobi functions with $t = kD$, $\alpha = 2a + 2c$, $\gamma = 2c$ and $e^{-\sigma D} = \theta$. For shorter sampling intervals (smaller value for D thus θ closer to but smaller than unity) these functions form a better resemblance of the orthonormal continuous Jacobi functions and are therefore closer to being orthogonal. A Gram-Schmidt orthonormalization procedure can be applied to orthonormalize the set of functions $\tilde{\underline{g}}$, after which $\mathbf{M}^{(a,c)}$ can be calculated.

The z -transforms of the discrete Jacobi functions are given by

$$Q_m^{(a,c)}(\theta; z) = \sum_{n=0}^m M_{m,n}^{(a,c)} \sum_{j=0}^a C_{n,n+j}^{(a)} \frac{z}{z - \theta^{j+c+n}}$$

The discrete Jacobi functions can be generated as the impulse responses of the *discrete Jacobi network* shown in Fig. 3.5.

In Fig. 3.6 four examples of the first four discrete Jacobi functions are plotted. We conclude, as we had already expected from (3.12), that for larger value for a the functions become more gradually starting. Further, a larger value for c results in a faster exponential decay for large k .

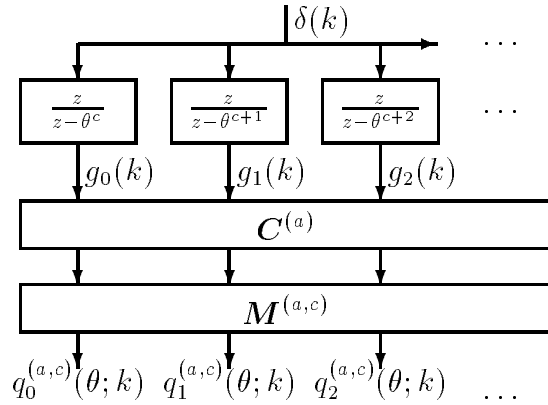


Figure 3.5: Discrete Jacobi network. The impulse responses $q_m^{(a,c)}(\theta; k)$ are the discrete Jacobi functions.

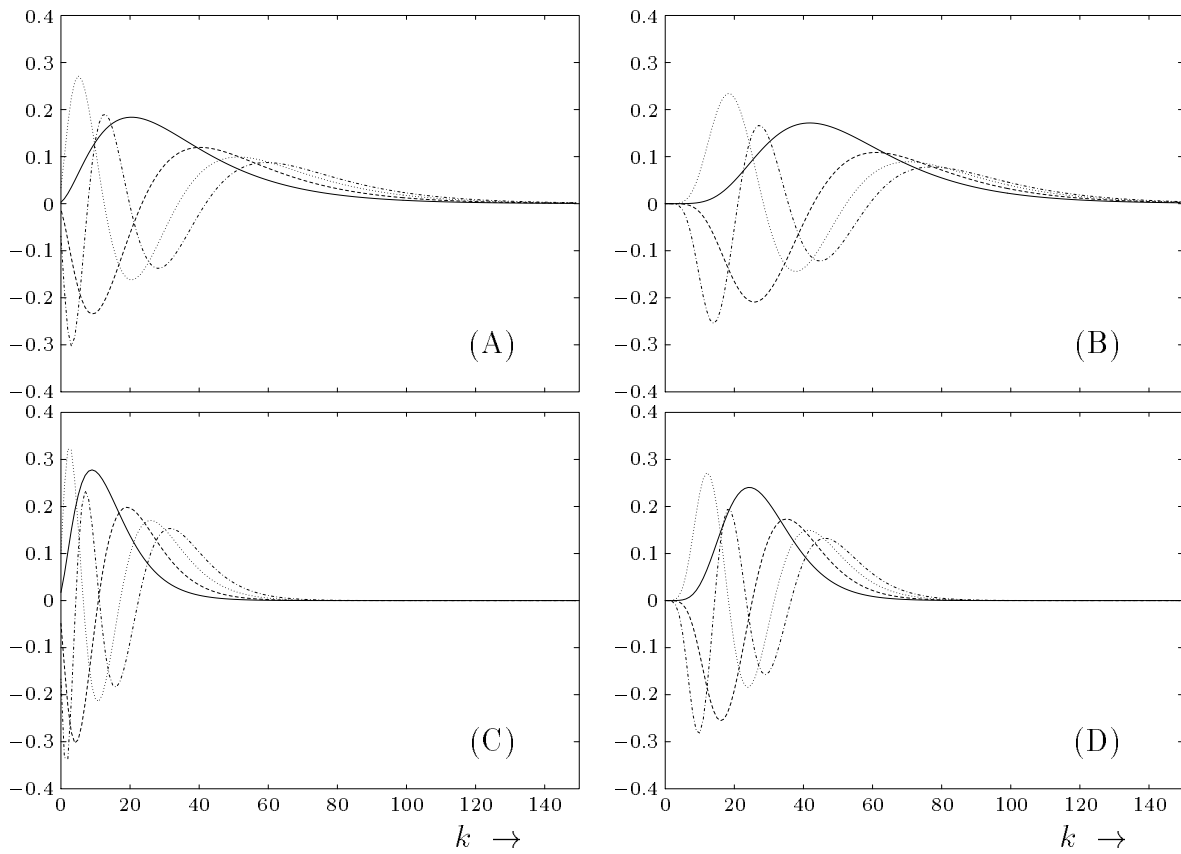


Figure 3.6: Examples of the first four discrete Jacobi functions $q_m^{(a,c)}(\theta; k)$ with $\theta = 0.95$. The solid, dashed, dotted and dash-dotted lines correspond to $m = 0$, $m = 1$, $m = 2$ and $m = 3$, respectively. Further, (A) $a = 2$ and $c = 1$, (B) $a = 8$ and $c = 1$, (C) $a = 2$ and $c = 3$, (D) $a = 8$ and $c = 3$.

3.3.2 Discrete Legendre Functions and Networks

In conformity with the continuous Legendre functions that are a special case of the continuous Jacobi functions, the *discrete Legendre functions* (Perez and Tsujii 1988; Perez and Tsujii 1991; Davidson and Falconer 1991) are a special case of the discrete Jacobi functions, namely for $a = 0$ and $c = \frac{1}{2}$ (compare with (3.13) and observe that $\mathbf{C}^{(0)}$ is the identity matrix):

$$q_m(\theta; k) = q_m^{(0, \frac{1}{2})}(\theta; k) = \sum_{n=0}^m M_{m,n}^{(0, \frac{1}{2})} \theta^{(n+\frac{1}{2})k}.$$

The z -transforms of the discrete Legendre functions read:

$$Q_m(\theta; z) = Q_m^{(0, \frac{1}{2})}(\theta; z) = \sum_{n=0}^m M_{m,n}^{(0, \frac{1}{2})} \frac{z}{z - \theta_n} \quad (3.15)$$

where $\theta_m = \theta^{m+\frac{1}{2}}$. The matrix $\mathbf{M}^{(0, \frac{1}{2})}$ is given by

$$M_{m,n}^{(0, \frac{1}{2})} = \begin{cases} \sqrt{1 - \theta_m^2} \frac{1 - \theta_n}{\theta_n - \theta_m} \prod_{l=0, l \neq n}^{m-1} \frac{1 - \theta_n \theta_l}{\theta_n - \theta_l}, & \text{if } n < m, \\ \sqrt{1 - \theta_m^2} \prod_{l=0}^{m-1} \frac{1 - \theta_m \theta_l}{\theta_m - \theta_l}, & \text{if } n = m, \\ 0, & \text{if } n > m, \end{cases}$$

which after substitution in (3.15) yields for the z -transforms of the discrete Legendre functions:

$$Q_m(\theta; z) = Q_m^{(0, \frac{1}{2})}(\theta; z) = \sqrt{1 - \theta_m^2} \frac{z}{z - \theta_m} \prod_{l=0}^{m-1} \frac{1 - z \theta_l}{z - \theta_l}, \quad (3.16)$$

Due to the specific form of the z -transforms in (3.16), the discrete Legendre functions can be generated as the impulse responses of the elegant network presented in 3.7 called a *discrete Legendre network*. The network is composed of a cascade of first-order all-pass sections tapped by first-order low-pass sections. Similar to the continuous Legendre network that is a specific continuous Kautz network, the discrete Legendre network is a specific discrete Kautz network (compare Fig. 3.7 and Fig. 2.6). Note that in the discrete Legendre network only one parameter, namely θ , can be chosen and that all filter sections directly follow from this choice.

We have used a discrete Legendre network to generate an example of the first four discrete Legendre functions with $\theta = 0.95$. These functions are depicted in Fig. 3.8. We observe that with an increasing function index m the discrete Legendre functions become more oscillatory. In conformity with this, the transfer function from the input of the discrete Legendre network to the $(m+1)$ -th output ($m = 0, 1, 2, \dots$) is a low-pass function of which the (-3 dB) cut-off frequency grows for larger m .

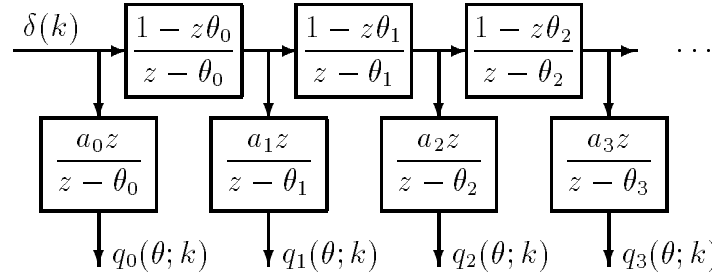


Figure 3.7: A discrete Legendre network composed of a filter line of first-order all-pass sections tapped by first-order low-pass sections. The impulse responses $q_m(\theta; k)$ are the discrete Legendre functions. Further, $\theta_m = \theta^{m+1/2}$ and $a_m = (1 - \theta^{2m+1})^{1/2}$ with $m \in \mathbb{N}_0$.

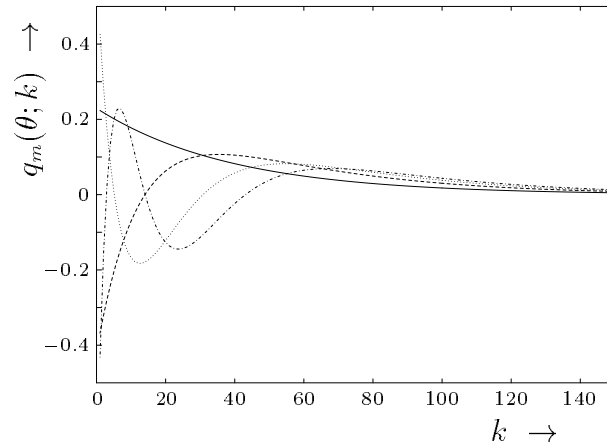


Figure 3.8: The first four discrete Legendre functions with $\theta = 0.95$. The solid, dashed, dotted and dash-dotted lines correspond to $q_0(\theta; k)$, $q_1(\theta; k)$, $q_2(\theta; k)$ and $q_3(\theta; k)$, respectively.

In Chapter 2 it was demonstrated that via the MBT the Laplace transforms of the continuous Laguerre functions are mapped onto the z -transforms of the discrete Laguerre functions, see (2.33). The inverse mapping was given in (2.34). It was also demonstrated in (2.45) and (2.46) that such a mapping exists between the Laplace transforms of the continuous Kautz functions and the z -transforms of the discrete Kautz functions.

When the MBT is applied to the Laplace transforms of the continuous Legendre functions in (3.11), we find

$$T_m(\sigma; s) \mapsto \frac{\sqrt{2}az}{z+1} T_m\left(\sigma; a \frac{z-1}{z+1}\right) = \sqrt{1-\vartheta_m^2} \frac{z}{z-\vartheta_m} \prod_{l=0}^{m-1} \frac{1-z\vartheta_l}{z-\vartheta_l},$$

where $\vartheta_m = (1 - \sigma_m/a)/(1 + \sigma_m/a)$. At first sight these functions appear to be the z -transforms of the discrete Legendre functions as in (3.16). However, we see that for large m the poles ϑ_m accumulate towards -1 , while the poles θ_m in (3.16) accumulate towards

0. Therefore, the MBT does not map the Laplace transforms of the continuous Legendre functions defined in (3.11) onto the z -transforms of the discrete Legendre functions in (3.16).

3.4 Discussion

In this chapter we have introduced the continuous Jacobi functions and a special case of these functions, namely the continuous Legendre functions. These functions were obtained from the classical Jacobi and Legendre polynomials and are orthonormal bases of the Hilbert space $L_2(\mathbb{R}^+)$. It was demonstrated that under certain restrictions of their parameters the continuous Jacobi functions have Laplace transforms that are rational functions of s , and that these functions can be generated as the impulse responses of a continuous Jacobi network. Likewise, being a special case of the continuous Jacobi functions, the continuous Legendre functions have Laplace transforms that are rational functions of s and can be generated as the impulse responses of a simple continuous Legendre network.

We have presented a discrete counterpart of the continuous Jacobi functions. These discrete Jacobi functions are also associated with orthogonal polynomials and form an orthonormal basis of the Hilbert space $\ell_2(\mathbb{N}_0)$. We have demonstrated that the discrete Jacobi functions have z -transforms that are rational functions of z so that they can be generated as the impulse responses of a so-called discrete Jacobi network. The discrete Legendre functions are a special case of the discrete Jacobi functions and can be generated as the impulse responses of a discrete Legendre network that resemble the continuous Legendre network.

A discrete Legendre filter is a discrete Legendre network of which the tap outputs are weighted and summed to yield the filter output. In an adaptive (discrete) Legendre filter the weights are adaptively optimized using algorithms as (N)LMS (Perez and Tsujii 1988; Perez and Tsujii 1991) or standard RLS. Before an adaptive Legendre filter can be used, one has to make a choice of the parameter θ . If, e.g. an impulse response of the reference system is available, one could select θ on the basis of the asymptotic exponential decay of this impulse response. An NLMS adaptive Legendre filter was proposed by Davidson and Falconer (1991) for the cancellation of echos in two-way communication systems. The authors found a considerable reduction in the required number of adaptive weights compared to the adaptive TDL.

A discrete Jacobi filter is a discrete Jacobi network of which the tap outputs are weighted and summed to yield the filter output. Again, the weights can be adaptively optimized using (N)LMS or standard RLS. Before the adaptive Jacobi filter can be used, three parameters need to be chosen. These are a , c , and θ . We do not have available a ready-to-use procedure to select these parameters from e.g. measured impulse response data. Instead, these parameters must be roughly chosen on the basis of *a priori* knowledge and physical insight concerning the reference system. A further fine-tuning can be performed with off-line numerical search algorithms using measured input/output data of the reference system in operation.

Concerning practical use of continuous and discrete Jacobi filters there is an important remark to make. For higher values of $\alpha - \gamma$ and a , the continuous and discrete Jacobi functions become more gradually starting, see Fig. 3.1 and Fig. 3.6, respectively. From Fig. 3.3 and Fig. 3.5 we observe that the Jacobi functions are synthesized by a linear combination of the abruptly starting impulse responses of first-order filters. In order to arrive at the desired gradual start of the Jacobi functions by a linear combination of abruptly starting functions, there must be destructive interference near the start. This leads to high demands on the accuracy of the coefficients in the matrices $\mathbf{B}^{(\alpha-\gamma)}$ and $\mathbf{L}^{(\alpha,\gamma)}$ or $\mathbf{C}^{(a)}$ and $\mathbf{M}^{(a,c)}$.

Bibliography

- Abramowitz, M. and I. A. Stegun (1970). *Handbook of Mathematical Functions*. New York (NY), U.S.A.: Dover Publications.
- Armstrong, H. L. (1957). On finding an orthonormal basis for representing transients. *IRE Trans. Circuit Theory* 4, 286–287.
- Armstrong, H. L. (1959). On the representation of transients by series of orthogonal functions. *IRE Trans. Circuit Theory* 6, 351–354.
- Beckmann, P. (1973). *Orthogonal Polynomials for Engineers and Physicist*. Boulder (CO), U.S.A.: The Golem Press.
- Davidson, G. W. and D. D. Falconer (1991). Reduced complexity echo cancellation using orthonormal functions. *IEEE Trans. Circuits Syst.* 38, 20–28.
- Lee, Y. W. (1960). *Statistical Theory of Communication*. New York (NY), U.S.A.: John Wiley and Sons.
- Mendel, J. M. (1964). On the use of orthogonal exponentials in a feedback application. *IEEE Trans. Automat. Contr.* 9, 310–312.
- Perez, H. and S. Tsujii (1988). IIR adaptive filtering via discrete Legendre functions. *Electronics Letters* 24, 450–451.
- Perez, H. and S. Tsujii (1991). A System Identification Algorithm Using Orthogonal Functions. *IEEE Trans. Signal Process.* 39, 752–755.
- Szegö, G. (1959). *Orthogonal Polynomials*. New York (NY), U.S.A.: American Mathematical Society.

Chapter 4

Optimal Generalized Laguerre Filters*

Abstract

The optimality condition for the pole in a Laguerre filter both in continuous-time and discrete-time has recently been established. This condition is of a very simple form and is independent of the power spectrum of the input signal, which makes it attractive for system identification purposes. The simple form of the optimality condition stems from the following property. The derivative of a Laguerre function with respect to the pole parameter can be expressed in the previous and next Laguerre function. We show that this property not only applies to the Laguerre functions but also to specific generalizations of the Laguerre functions. In particular we consider the generalized Laguerre functions and what will be called the Meixner-like functions. Further, we derive the optimality conditions for the pole in a generalized Laguerre filter and in a Meixner-like filter.

4.1 Introduction

It is sometimes desirable to have a compact description of a function defined on either the continuous interval \mathbb{R}^+ or the discrete interval \mathbb{N}_0 that exhibits an exponential decay towards infinity. Such a function could for example be the impulse response of a time-invariant stable system. A good approach is to approximate the function with a truncated Laguerre series, because the Laguerre functions also show an exponential decay. The rate

*This chapter is based on a paper with A.C. den Brinker, entitled "Optimality Condition for Truncated Generalized Laguerre Networks", *Int. J. Circuit Theory Appl.*, Vol. 23, pp. 227–235, 1995. Part of this work, entitled "Optimal Truncated Meixner-Like Networks", was presented in cooperation with A.C. den Brinker at the ProRISC/IEEE Benelux Workshop Circuits, Systems and Signal Processing, Mierlo, The Netherlands, March 23-24, 1995. Another part of this work, entitled "Filter Synthesis by Discrete-Time Generalized Laguerre Networks", was presented in cooperation with A.C. den Brinker at the European Conference on Circuit Theory and Design (ECCTD), Istanbul, Turkey, August 27-31, 1995. See references (Belt and den Brinker 1995c; Belt and den Brinker 1995b; Belt and den Brinker 1995a).

of decay of the Laguerre functions is determined by a free design parameter (the "pole"). For fast convergence of the series expansion, the choice of this Laguerre parameter is essential.

The best possible choice of the Laguerre parameter must satisfy a certain condition. This so-called *optimality condition* has been derived for both continuous Laguerre expansions (Clowes 1965; King and O'Canainn 1969) and discrete Laguerre expansions (Masnadi-Shirazi and Ahmed 1991; den Brinker 1994), see also Section 2.5.3 of this thesis. The result is obtained for an impulsive input signal of the system and is therefore of limited use in the field of system identification. Oliveira e Silva (1994) demonstrates that a similar optimality condition holds for any deterministic or stationary stochastic input signal satisfying some mild conditions.

Some systems have impulse responses that show a gradual start and an exponential decay towards infinity. A Laguerre series expansion of such an impulse response cannot be expected to show a fast convergence, since the basis functions have an abrupt start. A much better basis in these cases would be the set of *generalized Laguerre functions* in the continuous time or as a discrete-time counterpart the set of the recently introduced *Meixner-like functions* (den Brinker 1995) in the discrete time. These basis functions can be obtained as the impulse responses of a network. Like the Laguerre functions, they contain a free design parameter (a pole) that determines the rate of decay towards infinity. Additionally, they contain a parameter that determines how fast the functions start.

In this chapter we extend the result obtained by Oliveira e Silva (1994) to generalized Laguerre and Meixner-like approximations of systems under any excitation satisfying some mild conditions. The chapter is organized as follows. In Section 4.2 the generalized Laguerre functions and the Meixner-like functions are introduced. In Section 4.3 the derivatives of the basis functions with respect to the pole are determined. In Section 4.4 the optimality condition for a generalized Laguerre filter and the optimality condition for a Meixner-like filter are derived. The results are illustrated with an example in Section 4.5. Finally, some concluding remarks are made in Section 4.6.

4.2 Two Orthonormal Bases

In this section two sets of orthonormal functions are presented. For the continuous case the generalized Laguerre functions are considered. For the discrete case we use the recently introduced Meixner-like functions. We will see that the two sets of functions can be generated as the impulse responses of very similar networks.

4.2.1 The Generalized Laguerre Functions

The generalized Laguerre polynomials $l_m^{(\alpha)}(x)$ belong to the class of the classical orthogonal polynomials and are given by (Szegő 1959)

$$l_m^{(\alpha)}(x) = \sum_{n=0}^m (-1)^n \binom{m+\alpha}{m-n} \frac{x^n}{n!}, \quad (4.1)$$

with $m \in \mathbb{N}_0$, α a real parameter satisfying $\alpha > -1$, and $x \in \mathbb{R}^+$. The parameter α is called the *order of generalization*. In the special case where $\alpha = 0$ the polynomials in (4.1) reduce to the Laguerre polynomials $l_m(x)$, see (Szegö 1959; Abramowitz and Stegun 1970).

The generalized Laguerre polynomials are orthogonal under the window $w^{(\alpha)}(x) = x^\alpha e^{-x}$, in particular

$$\int_0^\infty l_m^{(\alpha)}(x) l_n^{(\alpha)}(x) w^{(\alpha)}(x) dx = \delta_{mn} \frac{\Gamma(m + \alpha + 1)}{m!},$$

where δ_{mn} is the Kronecker delta.

From the generalized Laguerre polynomials and the weight function $w^{(\alpha)}(x)$ it is possible to construct functions on \mathbb{R}^+ that are orthonormal with respect to a unity weight function. These functions are obtained by multiplying the generalized Laguerre polynomials by the square root of their weight function, followed by a change of scale in the x -axis ($x = \sigma t$) and a normalization. As a result we obtain the so-called *generalized Laguerre functions*, given by

$$\lambda_m^{(\alpha)}(\sigma; t) = \sqrt{\frac{\sigma m!}{\Gamma(m + \alpha + 1)}} \sum_{n=0}^m (-1)^n \binom{m + \alpha}{m - n} \frac{(\sigma t)^{n + \alpha/2}}{n!} e^{-\sigma t/2}, \quad (4.2)$$

where t stands for the time variable ($t \in \mathbb{R}^+$). These functions have two free parameters, namely the order α ($\alpha > -1$) and the scale factor σ ($\sigma > 0$). For $\alpha = 0$ the functions in (4.2) reduce to the Laguerre functions (Lee 1932), denoted by $\lambda_m(\sigma; t)$. The orthonormality of the generalized Laguerre functions is expressed by

$$\langle \lambda_m^{(\alpha)}(\sigma; t), \lambda_n^{(\alpha)}(\sigma; t) \rangle = \int_0^\infty \lambda_m^{(\alpha)}(\sigma; t) \lambda_n^{(\alpha)}(\sigma; t) dt = \delta_{mn}.$$

The generalized Laguerre functions form a complete orthonormal set in the Hilbert space $L_2(\mathbb{R}^+)$ of square-integrable functions on \mathbb{R}^+ (Clement 1963). Consequently, any function $h(t)$ belonging to $L_2(\mathbb{R}^+)$, e.g. the impulse response of a time-invariant stable system, can be approximated to any desired accuracy by a linear combination of generalized Laguerre functions.

After Laplace transformation of (4.2) we obtain

$$\Lambda_m^{(\alpha)}(\sigma; s) = \beta^{(\alpha)} \left(\frac{1}{s + \sigma/2} \right)^{1 + \alpha/2} \sum_{n=0}^m M_{m,n}^{(\alpha)} \left(\frac{\sigma}{s + \sigma/2} \right)^n. \quad (4.3)$$

Here $\beta^{(\alpha)} = \sigma^{(1+\alpha)/2}$ and $M_{m,n}^{(\alpha)}$ is given by

$$M_{m,n}^{(\alpha)} = \begin{cases} 0, & \text{if } m < n, \\ (-1)^n \binom{m}{n} \frac{\Gamma(n + \alpha/2 + 1)}{\Gamma(n + \alpha + 1)} \sqrt{\frac{\Gamma(m + \alpha + 1)}{m!}}, & \text{if } m \geq n. \end{cases}$$

The coefficient $M_{m,n}^{(\alpha)}$ can be regarded as the $(m+1, n+1)$ -th element of a lower-triangular matrix $\mathbf{M}^{(\alpha)}$

When α is even ($\alpha = 0, 2, 4, \dots$) the Laplace transform in (4.3) is a rational function of s , and the generalized Laguerre functions in (4.2) can be generated as the impulse responses of the so-called *generalized Laguerre network* shown in Fig. 4.1.

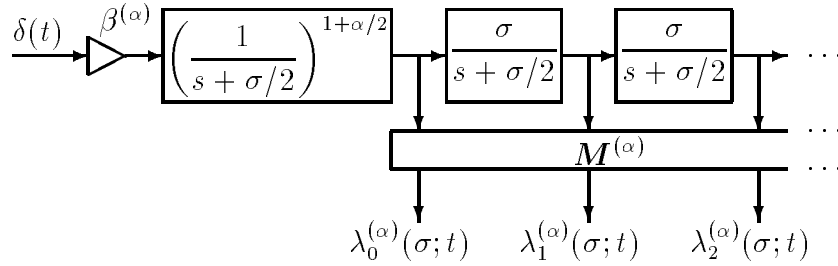


Figure 4.1: Generalized Laguerre network. The individual impulse responses are the generalized Laguerre functions. The constant α may only take on the even values $0, 2, 4, \dots$. Further, $\beta^{(\alpha)} = \sigma^{(1+\alpha)/2}$ and $\mathbf{M}^{(\alpha)}$ is a (memoryless) lower-triangular matrix.

Note that the generalized Laguerre network is constructed around a cascade of identical first-order low-pass sections. This can be transformed to a cascade of identical first-order all-pass sections using the identity¹

$$\left(\frac{\sigma}{s + \sigma/2}\right)^m = \sum_{n=0}^m \binom{m}{n} (-1)^n \left(\frac{s - \sigma/2}{s + \sigma/2}\right)^n, \quad m \in \mathbb{N}_0. \quad (4.4)$$

The resultant network, equivalent to the network in Fig 4.1, is depicted in Fig. 4.2A. The lower-triangular matrix $\mathbf{L}^{(\alpha)}$ can be written as $\mathbf{L}^{(\alpha)} = \mathbf{M}^{(\alpha)}\mathbf{Q}$, where \mathbf{Q} is also a lower-triangular matrix of which the $(m+1, n+1)$ -th element follows from (4.4) and is given by

$$Q_{m,n} = \begin{cases} 0, & \text{if } m < n, \\ \binom{m}{n} (-1)^n, & \text{if } m \geq n. \end{cases}$$

Finally, the network presented in Fig. 4.2B is also equivalent to the network of Fig. 4.1 and it demonstrates that the system of generalized Laguerre functions $\lambda_m^{(\alpha)}(\sigma; t)$ is obtained from the system of Laguerre functions $\lambda_m(\sigma; t)$ by the transformation with the matrix $\mathbf{A}^{(\alpha)}$ given by $\mathbf{A}^{(\alpha)} = \mathbf{L}^{(\alpha)}\mathbf{U}^{(\alpha)}$, where

$$\mathbf{U}^{(\alpha)} = \begin{pmatrix} 1 & -1 & & \emptyset \\ & 1 & -1 & \\ & & 1 & -1 \\ \emptyset & & & \ddots & \ddots \end{pmatrix}^{\alpha/2}.$$

¹The relation in (4.4) follows from $(1-x)^m = \sum_{n=0}^m \binom{m}{n} (-1)^n x^n$ with the substitution $x = (s - \sigma/2)/(s + \sigma/2)$. Note the interesting inverse relation when $x = \sigma/(s + \sigma/2)$ is substituted instead.

Since both the Laguerre and the generalized Laguerre functions form orthonormal sets, we conclude that $\mathbf{A}^{(\alpha)}$ is orthonormal:

$$\mathbf{A}^{(\alpha)}\{\mathbf{A}^{(\alpha)}\}^T = \mathbf{M}^{(\alpha)}\mathbf{Q}\mathbf{U}^{(\alpha)}\{\mathbf{U}^{(\alpha)}\}^T\mathbf{Q}^T\{\mathbf{M}^{(\alpha)}\}^T = \mathbf{I}.$$

The fact that the Laguerre functions form a complete orthonormal set in $L_2(\mathbb{R}^+)$ (see (Clement 1963) or also Section 2.6.1 of this thesis), and the fact that the generalized Laguerre functions with even α are obtained from the Laguerre functions by a (reversible) orthonormal transformation, confirms the statement by Clement (1963) that for even α the generalized Laguerre functions are also complete.

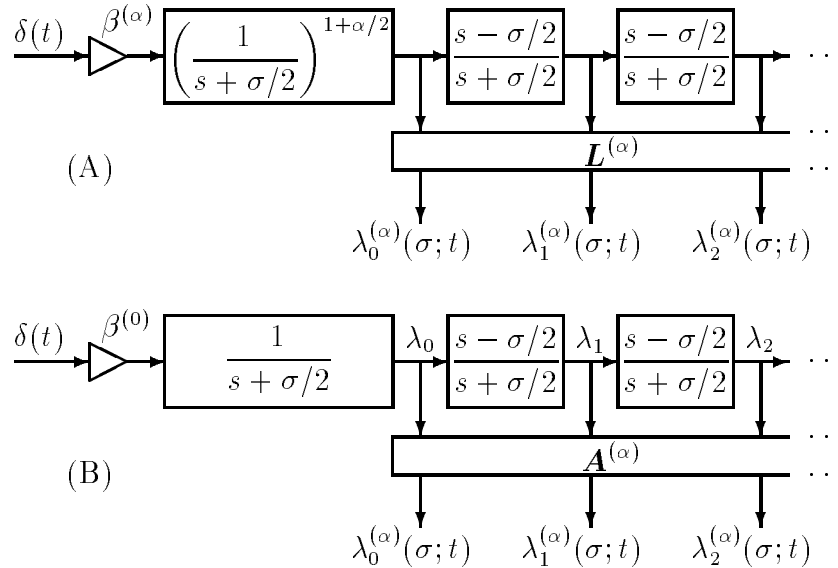


Figure 4.2: Equivalent generalized Laguerre networks. (A) The cascade of first-order low-pass sections in Fig. 4.1 is transformed to a cascade of first-order all-pass sections; (B) The system of generalized Laguerre functions $\lambda_m^{(\alpha)}(\sigma; t)$ is obtained from the system of Laguerre functions $\lambda_m(\sigma; t)$ by an orthonormal transformation.

Increasing the value of α results in a more gradually starting weight function $x^\alpha e^{-x}$ under which the generalized Laguerre polynomials are constructed. This leads to more gradually starting generalized Laguerre functions. Thus, with α , the center of gravity of these functions can be shifted in time. Equivalently, a larger value for α results in more emphasis on the lower frequency components of the basis functions at the expense of the higher frequency components. In Fig. 4.3 four examples are presented of the first four generalized Laguerre functions with different orders of generalization.

Finally, from a generalized Laguerre network we may construct what will be called a *generalized Laguerre filter*. Let $x(t)$ be the excitation signal of the network. The output of the generalized Laguerre filter is then formed by a linear combination of the outputs of

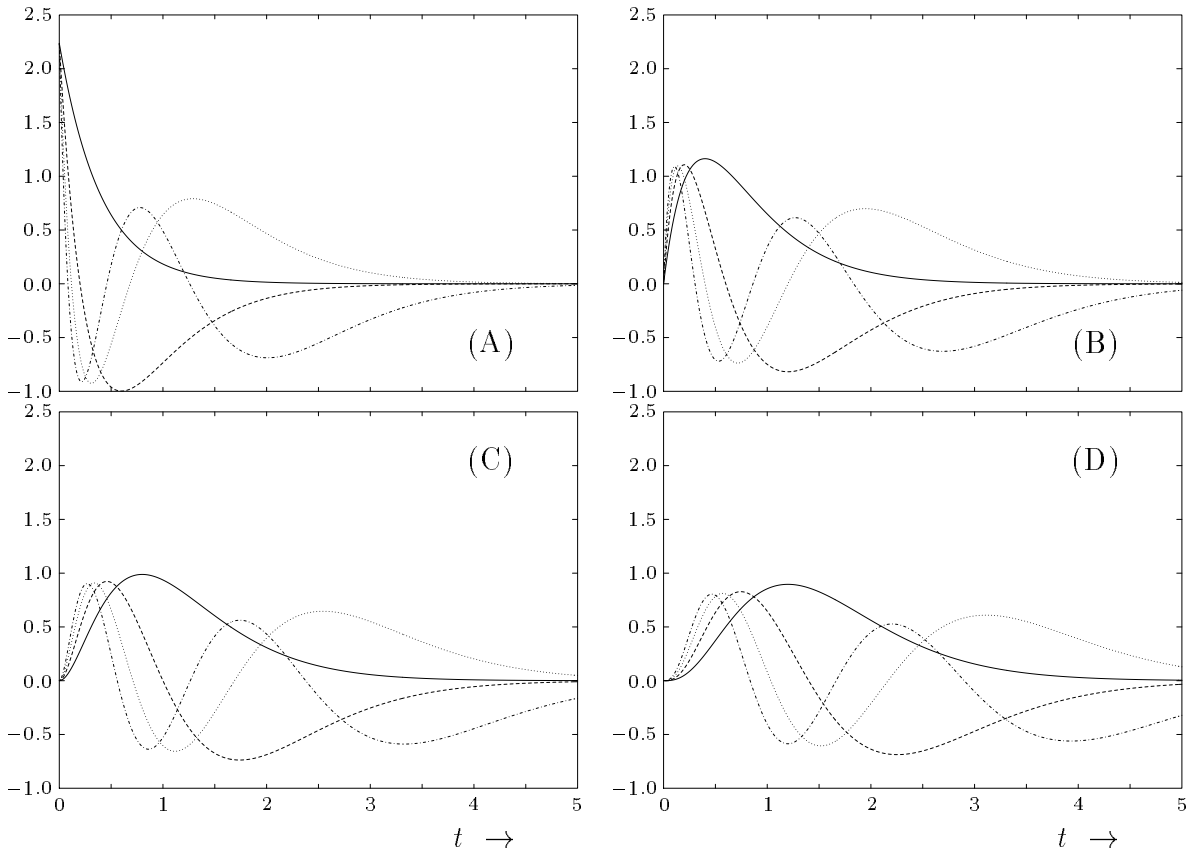


Figure 4.3: Examples of the first four generalized Laguerre functions $\lambda_m^{(\alpha)}(\sigma; t)$ with $\sigma = 5$. The solid, dashed, dotted and dash-dotted lines correspond to $m = 0$, $m = 1$, $m = 2$ and $m = 3$, respectively. The orders of generalization are given by (A) $\alpha = 0$, (B) $\alpha = 2$, (C) $\alpha = 4$ and (D) $\alpha = 6$.

the generalized Laguerre network, according to

$$y_M(t) = \sum_{m=0}^M w_m \lambda_m^{(\alpha)}(\sigma; t) * x(t),$$

where $*$ denotes a convolution. For $\alpha = 0$ the generalized Laguerre filter reduces to a *Laguerre filter*.

4.2.2 The Meixner-Like Functions

In the previous section it was shown that the generalized Laguerre functions $l_m^{(\alpha)}(\sigma; t)$ are obtained from the Laguerre functions $l_m(\sigma; t)$ by an orthonormal transformation. The *discrete Laguerre functions*, denoted by $g_m(\xi; k)$ with $m, k \in \mathbb{N}_0$, are the inverse z -transforms

of (see (2.30) or (Broome 1965))

$$G_m(\xi; z) = \frac{\sqrt{1 - \xi^2} z}{z - \xi} \left(\frac{1 - \xi z}{z - \xi} \right)^m,$$

where ξ is the Laguerre parameter satisfying $-1 < \xi < 1$. In this section we consider an orthonormal transformation applied to the discrete Laguerre functions as proposed by den Brinker (1995). The obtained orthonormal functions will be denoted by $g_m^{(a)}(\xi; k)$ with z -transforms $G_m^{(a)}(\xi; z)$. Analogous to the parameter α in the previous section, a is called the *order of generalization* ($a \in \mathbb{N}_0$). Again, for $a = 0$ the generalized functions reduce to the discrete Laguerre functions: $g_m^{(0)}(\xi; k) = g_m(\xi; k)$. The orthonormality of the functions $g_m^{(a)}(\xi; k)$ is expressed by

$$\langle g_m^{(a)}(\xi; k), g_n^{(a)}(\xi; k) \rangle = \sum_{k=0}^{\infty} g_m^{(a)}(\xi; k) g_n^{(a)}(\xi; k) = \delta_{mn}.$$

The functions $g_m^{(a)}(\xi; k)$ are called the *Meixner-like functions* (den Brinker 1995) for the following reason. In Chapter 2 the classical Meixner polynomials were introduced. The Meixner polynomials contain a free parameter b , and for $b = 1$ the Meixner polynomials reduce to the discrete Laguerre polynomials. By multiplying the Meixner polynomials with the square root of their weight function $w^{(b)}(\theta; k) = \theta^k b_k / k!$ followed by a normalization *Meixner functions* are obtained that form an orthonormal set on \mathbb{N}_0 . However, among all Meixner functions only the discrete Laguerre functions ($b = 1$) have rational z -transforms. Therefore, the Meixner functions cannot be generated as the impulse responses of a digital network. The Meixner-like functions on the other hand, do have rational z -transforms. As demonstrated by den Brinker (1995) they are associated with orthogonal polynomials and weight function $v^{(a)}(\xi; k) = [(k+1)_a]^2 \xi^{2k}$. The weight functions $w^{(b)}(\theta; k)$ with $b = 2a + 1$, and $v^{(a)}(\xi; k)$ with $\xi^2 = \theta$ are both polynomials in k of order $2a$ multiplied by the exponential sequence θ^k . Also, these functions are very similar of shape. As a consequence, the Meixner-like functions look very much like the Meixner functions, which justifies the choice of their name.

The Meixner-like functions $g_m^{(a)}(\xi; k)$ can be obtained as the impulse responses of the *Meixner-like network* depicted in Fig. 4.4A, where $\mathbf{L}^{(a)}$ is a lower-triangular matrix (den Brinker 1995). Similar to the generalized Laguerre network in Fig 4.2A, the Meixner-like network of Fig. 4.4A is constructed around a filter line composed of a cascade of identical first-order all-pass sections preceded by a low-pass filter of order $a + 1$. The z -transforms of the Meixner-like functions $g_m^{(a)}(\xi; k)$ are given by

$$G_m^{(a)}(\xi; z) = b^{(a)} \left(\frac{z}{z - \xi} \right)^{a+1} \sum_{n=0}^m L_{m,n}^{(a)} \left(\frac{1 - \xi z}{z - \xi} \right)^n, \quad (4.5)$$

where $b^{(a)} = (1 - \xi^2)^{a+1/2}$ and $L_{m,n}^{(a)}$ is the $(m + 1, n + 1)$ -th element of the matrix $\mathbf{L}^{(a)}$. Since

$$b^{(a)} \left(\frac{z}{z - \xi} \right)^a = b^{(0)} \sum_{n=0}^a \binom{a}{n} \xi^n \left(\frac{1 - \xi z}{z - \xi} \right)^n,$$

we see that the Meixner-like functions are obtained by a transformation on the Laguerre domain. The resulting equivalent Meixner-like network is presented in Fig. 4.4B. The matrix $\mathbf{A}^{(a)}$ is given by $\mathbf{A}^{(a)} = \mathbf{L}^{(a)}\mathbf{U}^{(a)}$, where

$$\mathbf{U}^{(a)} = \begin{pmatrix} 1 & \xi & & \emptyset \\ & 1 & \xi & \\ & & 1 & \xi \\ \emptyset & & & \ddots & \ddots \end{pmatrix}^a.$$

The matrix $\mathbf{A}^{(a)}$ has at its m -th row $m + a + 1$ non-zero elements, which implies that the system function $G_m^{(a)}(\xi; z)$ has a pole in $z = \xi$ with multiplicity $m + a + 1$. Unfortunately, no closed-form solution of $\mathbf{L}^{(a)}$ (and thus $\mathbf{A}^{(a)}$) is known. We do know that $\mathbf{A}^{(a)}$ must be orthonormal, and therefore

$$\mathbf{A}^{(a)}\{\mathbf{A}^{(a)}\}^T = \mathbf{L}^{(a)}\mathbf{U}^{(a)}\{\mathbf{U}^{(a)}\}^T\{\mathbf{L}^{(a)}\}^T = \mathbf{I}. \quad (4.6)$$

The matrix $\mathbf{U}^{(a)}\{\mathbf{U}^{(a)}\}^T$ is positive definite. With (4.6) we may determine $\mathbf{L}^{(a)}$ as the inverse of the first Cholesky factor of $\mathbf{U}^{(a)}\{\mathbf{U}^{(a)}\}^T$. This can be done with stable numerical algorithms.

When the order of generalization $a = 0$, we obtain from the trivial Cholesky decomposition of the identity matrix that $\mathbf{L}^{(0)} = \mathbf{I}$, and in (4.5) the discrete Laguerre functions are obtained. In the special case where $\xi = 0$ we obtain $\mathbf{L}^{(a)} = \mathbf{I}$, and with $G_m^{(a)}(0; z) = z^{-m}$ the Meixner-like network reduces to a delay line for all values of a .

The facts that the discrete Laguerre functions form a complete orthonormal set in $\ell_2(\mathbb{N}_0)$ (see (Oliveira e Silva 1995) or also Section 2.6.2 of this thesis), and that the Meixner-like functions are obtained from the discrete Laguerre functions by a (reversible) orthonormal transformation, imply that the Meixner-like functions also constitute a complete orthonormal set in $\ell_2(\mathbb{N}_0)$.

In Fig. 4.5 four examples are presented of the first four Meixner-like functions with different orders of generalization. We notice that a has a similar effect on the Meixner-like functions as α has on the generalized Laguerre functions. With a , the speed with which the basis functions start can be controlled. Equivalently in the frequency domain, the lower-frequency components of the basis functions can be emphasized at the expense of the higher-frequency components.

From a Meixner-like network we may construct what will be called a *Meixner-like filter*. Let $x(k)$ be the excitation signal of the network. The output of the Meixner-like filter is then formed by a linear combination of the outputs of the Meixner-like network, according to

$$y_M(k) = \sum_{m=0}^M w_m g_m^{(a)}(\xi; k) * x(k),$$

For $a = 0$ the Meixner-like filter reduces to the (discrete) *Laguerre filter* (King and Paraskevopoulos 1977).

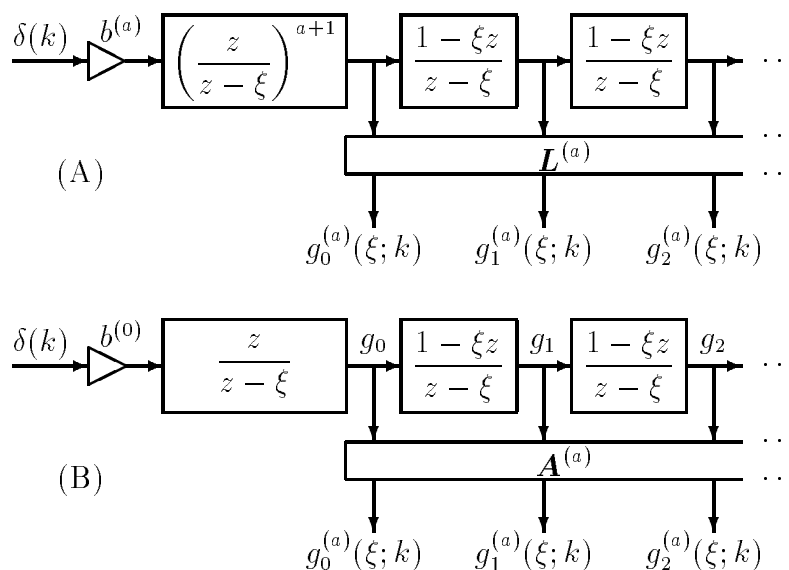


Figure 4.4: Two equivalent Meixner-like networks. The individual impulse responses are the Meixner-like functions. The order of generalization a may take on the values $0, 1, 2, \dots$. Further, $b^{(a)} = (1 - \xi^2)^{a+1/2}$.

4.3 The Derivatives of the Basis Functions

The remainder of this chapter will be devoted to the problem of how to choose σ in generalized Laguerre filters and ξ in Meixner-like filters. For this, we will need the derivatives of the generalized Laguerre functions with respect to σ and the derivatives of the Meixner-like functions with respect to ξ . In this section it will be shown that these derivatives are of a remarkably simple form.

Consider the set of real-valued orthonormal functions $f_m(\chi; \tau)$ that constitute a complete basis in $L^2(\mathbb{R}^+)$ or $\ell^2(\mathbb{N}_0)$ for the continuous-time case and discrete-time case, respectively. Here, m is the function index with $m \in \mathbb{N}_0$; χ is the free parameter that needs to be optimized, and τ stands for the continuous-time variable $t \in \mathbb{R}^+$ or the discrete-time variable $k \in \mathbb{N}_0$. We demand that $f_m(\chi; \tau)$ be a continuously differentiable function of χ . We introduce the vector $\underline{f}(\chi; \tau)$ (with infinite length) as

$$\underline{f}(\chi; \tau) = [f_0(\chi; \tau), f_1(\chi; \tau), \dots]^T.$$

The orthonormality of the functions $f_m(\chi; \tau)$ can be expressed by the following property of the corresponding inner product matrix:

$$\langle \underline{f}(\chi; \tau), \underline{f}^T(\chi; \tau) \rangle = \mathbf{I}. \tag{4.7}$$

The $(m + 1, n + 1)$ -th element of the inner product matrix is given by $\langle f_m(\chi; \tau), f_n(\chi; \tau) \rangle$, the inner product between $f_m(\chi; \tau)$ and $f_n(\chi; \tau)$ with respect to the time variable τ . With

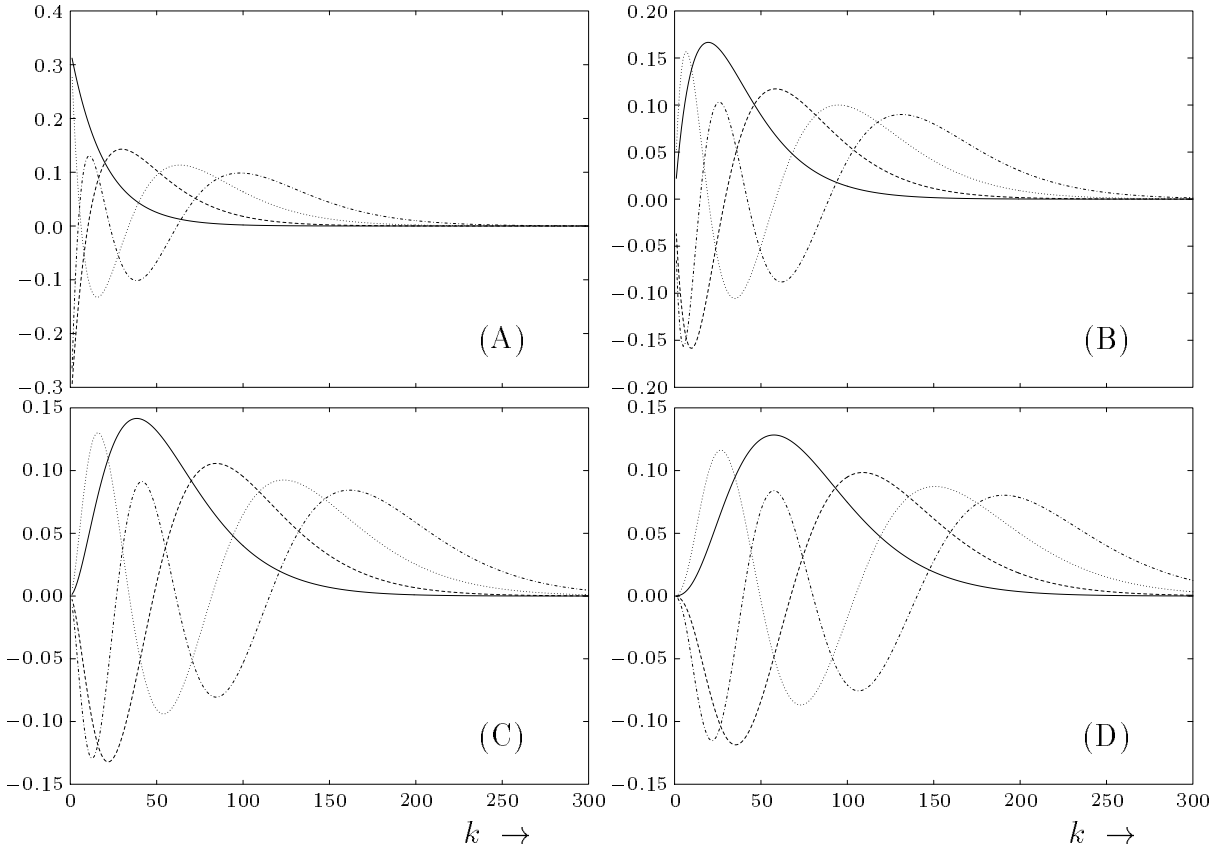


Figure 4.5: Examples of the first four Meixner-like functions $g_m^{(a)}(\xi; k)$ with $\xi = 0.95$. The solid, dashed, dotted and dash-dotted lines correspond to $m = 0$, $m = 1$, $m = 2$ and $m = 3$, respectively. The orders of generalization are given by (A) $a = 0$, (B) $a = 1$, (C) $a = 2$ and (D) $a = 3$.

the definition of the matrix

$$\mathbf{D}(\chi) = \left\langle \frac{\partial \underline{f}(\chi; \tau)}{\partial \chi}, \underline{f}^T(\chi; \tau) \right\rangle.$$

we obtain, after differentiating (4.7) with respect to χ ,

$$\mathbf{D}(\chi) = -\{\mathbf{D}(\chi)\}^T.$$

Thus $\mathbf{D}(\chi)$ is skew-symmetric. Consequently, the diagonal elements of $\mathbf{D}(\chi)$ all vanish. The derivative of the n -th basis function with respect to χ can be expanded according to

$$\frac{\partial f_n(\chi; \tau)}{\partial \chi} = \sum_{m=0}^{\infty} \left\langle \frac{\partial f_n(\chi; \tau)}{\partial \chi}, f_m(\chi; \tau) \right\rangle f_m(\chi; \tau).$$

Such an expansion can be obtained for the derivatives of all basis functions with respect

to χ , leading to

$$\frac{\partial \underline{f}(\chi; \tau)}{\partial \chi} = \mathbf{D}(\chi) \underline{f}(\chi; \tau). \quad (4.8)$$

We now derive the \mathbf{D} -matrices of the generalized Laguerre functions and the Meixner-like functions, denoted by $\mathbf{D}^{(\alpha)}(\sigma)$ and $\mathbf{D}^{(\alpha)}(\xi)$, respectively.

Inspection of (4.3) reveals that the derivative of the m -th generalized Laguerre function $\Lambda_m^{(\alpha)}(\sigma; s)$ with respect to σ is a power series of $\sigma/(s + \sigma/2)$. The lowest and highest powers in this series are $\alpha/2 + 1$ and $m + \alpha/2 + 2$, respectively. This implies that the derivative can be expressed in a finite series of generalized Laguerre basis functions (with order of generalization α) up to and including $\Lambda_{m+1}^{(\alpha)}(\sigma; s)$. Using the skew-symmetry property of the matrix $\mathbf{D}^{(\alpha)}(\sigma)$, we conclude that the matrix must be of the form

$$\mathbf{D}^{(\alpha)}(\sigma) = \begin{pmatrix} 0 & D_{0,1}^{(\alpha)}(\sigma) & & & \emptyset \\ -D_{0,1}^{(\alpha)}(\sigma) & 0 & D_{1,2}^{(\alpha)}(\sigma) & & \\ & -D_{1,2}^{(\alpha)}(\sigma) & 0 & D_{2,3}^{(\alpha)}(\sigma) & \\ \emptyset & & & \ddots & \ddots & \ddots \end{pmatrix}, \quad (4.9)$$

where the elements $D_{m,m+1}^{(\alpha)}(\sigma)$ are functions of m , α , and σ , only. In particular, the derivative of the m -th basis function can be expressed in the $(m-1)$ -th and $(m+1)$ -th basis function according to

$$\frac{\partial \Lambda_m^{(\alpha)}(\sigma; s)}{\partial \sigma} = -D_{m-1,m}^{(\alpha)}(\sigma) \Lambda_{m-1}^{(\alpha)}(\sigma; s) + D_{m,m+1}^{(\alpha)}(\sigma) \Lambda_{m+1}^{(\alpha)}(\sigma; s). \quad (4.10)$$

with the definition $D_{-1,0}^{(\alpha)}(\sigma) = 0$. Differentiating the functions $\Lambda_m^{(\alpha)}(\sigma; s)$ in (4.3) with respect to σ gives

$$\frac{\partial \Lambda_m^{(\alpha)}(\sigma; s)}{\partial \sigma} = -\frac{m + \alpha/2 + 1}{2\sigma} \beta^{(\alpha)} M_{m,m}^{(\alpha)} \left(\frac{1}{s + \sigma/2} \right)^{1+\alpha/2} \left(\frac{\sigma}{s + \sigma/2} \right)^{m+1} + \text{lower-order terms.} \quad (4.11)$$

We also know that

$$\Lambda_{m+1}^{(\alpha)}(\sigma; s) = \beta^{(\alpha)} M_{m+1,m+1}^{(\alpha)} \left(\frac{1}{s + \sigma/2} \right)^{1+\alpha/2} \left(\frac{\sigma}{s + \sigma/2} \right)^{m+1} + \text{lower-order terms.} \quad (4.12)$$

Substituting (4.12) in (4.10) and then combining (4.10) and (4.11) yields

$$\begin{aligned} D_{m-1,m}^{(\alpha)}(\sigma) &= -\frac{m + \alpha/2}{2\sigma} \frac{M_{m-1,m-1}^{(\alpha)}}{M_{m,m}^{(\alpha)}} \\ &= \frac{\sqrt{m(m + \alpha)}}{2\sigma} \end{aligned} \quad (4.13)$$

For $\alpha = 0$, we obtain $D_{m-1,m}^{(0)}(\sigma) = m/2\sigma$, and (4.13) reduces to the result obtained by Oliveira e Silva (1994).

In a similar way we arrive at the \mathbf{D} -matrix of the Meixner-like functions, given by

$$\mathbf{D}^{(a)}(\xi) = \begin{pmatrix} 0 & D_{0,1}^{(a)}(\xi) & & & \emptyset \\ -D_{0,1}^{(a)}(\xi) & 0 & D_{1,2}^{(a)}(\xi) & & \\ & -D_{1,2}^{(a)}(\xi) & 0 & D_{2,3}^{(a)}(\xi) & \\ \emptyset & & \ddots & \ddots & \ddots \end{pmatrix}, \quad (4.14)$$

with

$$D_{m-1,m}^{(a)}(\xi) = \frac{m+a}{1-\xi^2} \frac{L_{m-1,m-1}^{(a)}}{L_{m,m}^{(a)}}, \quad (4.15)$$

and $D_{-1,0}^{(a)}(\xi) = 0$. When $a = 0$, we obtain $D_{m-1,m}^{(0)}(\xi) = m/(1-\xi^2)$, and (4.15) reduces to the result obtained by Oliveira e Silva (1994).

4.4 The Optimality Condition

In this section we look at the problem of finding the best values of σ and ξ in generalized Laguerre filters and Meixner-like filters, respectively. As in the previous section, τ will denote either t or k , and χ will denote either σ or ξ . Let $x(\tau)$ be a stationary stochastic signal with a strictly positive power spectral density function. For the output of either a generalized Laguerre filter or a Meixner-like filter we write

$$\begin{aligned} y_M(\chi; \tau) &= \sum_{m=0}^M w_{M,m}(\chi) \phi_m(\chi; \tau) * x(\tau) \\ &= \sum_{m=0}^M w_{M,m}(\chi) u_m(\chi; \tau). \end{aligned}$$

The functions $\phi_m(\chi; \tau)$ are the $M+1$ individual impulse responses of the orthogonal network and the $w_{M,m}(\chi)$ are the weights.

The *desired signal* is denoted by $d(\tau)$. For the *error signal* we write

$$e_M(\chi; \tau) = d(\tau) - y_M(\chi; \tau).$$

The optimization goal is to minimize the mean-squared error (MSE) given by

$$\mathcal{J}_M(\chi) = E \{e_M^2(\chi; \tau)\}.$$

The optimal weights follow from the so-called *normal equations*:

$$E \{e_M(\chi; \tau) u_m(\chi; \tau)\} = 0, \quad m = 0, 1, \dots, M. \quad (4.16)$$

The optimal weights depend on the number of filter sections (note the additional subscript M in $w_{M,m}$), since the filter outputs are not orthogonal for non-white excitations $x(\tau)$.

We seek the stationary points of $\mathcal{J}_M(\chi)$ with respect to χ . Thus

$$\frac{\partial \mathcal{J}_M(\chi)}{\partial \chi} = 2E \left\{ e_M(\chi; \tau) \frac{\partial e_M(\chi; \tau)}{\partial \chi} \right\} = 0.$$

When the normal equations in (4.16) are satisfied, we may write this as

$$\frac{\partial \mathcal{J}_M(\chi)}{\partial \chi} = -2E \left\{ e_M(\chi; \tau) \sum_{m=0}^M w_{M,m}(\chi) \frac{\partial}{\partial \chi} \{u_m(\chi; \tau)\} \right\} = 0.$$

Using (4.8) with the knowledge that the matrix \mathbf{D} has the special form as in (4.9) and (4.14) and again using the fact that the normal equations in (4.16) are satisfied, we obtain the gradient as

$$\frac{\partial \mathcal{J}_M(\chi)}{\partial \chi} = -2 w_{M,M}(\chi) D_{M,M+1} E \{e_M(\chi; \tau) u_{M+1}(\chi; \tau)\} = 0. \quad (4.17)$$

Here, $D_{M,M+1}$ denotes either $D_{M,M+1}^{(\alpha)}(\sigma)$ or $D_{M,M+1}^{(a)}(\xi)$. We now know that the stationary points of $\mathcal{J}_M(\chi)$ satisfy the normal equations (4.16) and

$$w_{M,M}(\chi) = 0 \quad \text{or} \quad E \{e_M(\chi; \tau) u_{M+1}(\chi; \tau)\} = 0. \quad (4.18)$$

The second equation in (4.18) tells us that a proper choice for χ , say $\chi = \chi_0$, makes the error signal orthogonal to $u_{M+1}(\chi_0; \tau)$. We will now prove that $E \{e_M(\chi_0; \tau) u_{M+1}(\chi_0; \tau)\} = 0$ implies that $w_{M+1,M+1}(\chi_0) = 0$. For this, consider a filter with one extra section and with weights

$$\begin{aligned} w_{M+1,m}(\chi_0) &= w_{M,m}(\chi_0), & m = 0, 1, \dots, M, \\ w_{M+1,M+1}(\chi_0) &= 0. \end{aligned} \quad (4.19)$$

Then $e_{M+1}(\chi_0; \tau) = e_M(\chi_0; \tau)$ and as a consequence of (4.16) and the second equation in (4.18)

$$E \{e_{M+1}(\chi_0; \tau) u_m(\chi_0; \tau)\} = 0, \quad (4.20)$$

with $m = 0, 1, \dots, M+1$. Thus, using the weights defined by (4.19), the normal equations in (4.20) are satisfied for a filter with one extra section. Therefore, using one extra section with $\chi = \chi_0$, the weights in (4.19) are the optimal weights in the sense that $\mathcal{J}_{M+1}(\chi_0)$ is minimal.

Consequently the stationary points of the mean-squared error $\mathcal{J}_M^{(\alpha)}(\sigma)$ of the generalized Laguerre filter satisfy the normal equations in (4.16) and

$$w_{M,M}^{(\alpha)}(\sigma) = 0 \quad \text{or} \quad w_{M+1,M+1}^{(\alpha)}(\sigma) = 0.$$

Similarly, the stationary points of the mean-squared error $\mathcal{J}_M^{(a)}(\xi)$ of the Meixner-like filter satisfy the normal equations (4.16) and

$$w_{M,M}^{(a)}(\xi) = 0 \quad \text{or} \quad w_{M+1,M+1}^{(a)}(\xi) = 0. \quad (4.21)$$

This optimality condition is exactly the same as the one obtained by Oliveira e Silva (1994). In fact, any filter based on a set of orthogonal functions of which the matrix $\mathbf{D}(\chi)$ has the same structure as in (4.9) and (4.14) will yield this optimality condition, since the analysis in this section depends solely on the specific structure of $\mathbf{D}(\chi)$.

4.5 An Example

As an example we consider the system given by the transfer function

$$H(z) = \left(\frac{z}{z-p}\right)^4 + \left(\frac{z}{z-p^*}\right)^4, \quad (4.22)$$

where $p = 0.9 + 0.1i$. This system is not within the model set of the Meixner-like filters because the poles are complex-valued. However, a good approximation should be feasible, since p is chosen close to the real axis. For this example the system in (4.22) is excited by colored noise $x(k)$ obtained by low-pass filtering white noise with normal distribution $N(0, 1)$. The low-pass filter that is used here is given by

$$G(z) = \frac{z}{z-0.5}.$$

The system $H(z)$ in (4.22), excited by $x(k)$, is imitated by Meixner-like filters with a different number of sections ranging from one to four. The following results are obtained with a single run of 5000 samples. The first 2000 samples are only used to initialize the filters in order to avoid problems with initial conditions. The remaining 3000 samples are used to solve the normal equations (4.16) for the determination of the optimal weights. In Fig. 4.6A an approximation of the normalized MSE

$$\frac{E\{e_M^2(\xi; k)\}}{E\{d^2(k)\}}$$

is plotted for $a = 3$ and $M = 0, 1, 2, 3$ as a function of the pole ξ . From the plot with $M = 3$ we see that in the optimal situation, namely when $\xi \approx 0.84$, the normalized MSE is approximately given by 0.07 (or -11.5 dB). In Fig. 4.6B the weight product $w_{M,M}^{(a)}(\xi)w_{M+1,M+1}^{(a)}(\xi)$ is plotted for $a = 3$ and $M = 3$. As expected from (4.21), we notice that the zero-crossings in this plot correspond to the extrema of the normalized MSE for $M = 3$ in Fig. 4.6A.

4.6 Discussion

In this chapter the optimality condition for the pole of generalized Laguerre filters in continuous time and of Meixner-like filters in discrete time has been derived. The result is valid for any stationary stochastic input signal satisfying some mild conditions. We conclude that the optimality condition is exactly the same as that for continuous-time and discrete-time Laguerre filters (Oliveira e Silva 1994). We have shown that, very generally, a filter based on an orthogonal set of functions for which the derivative of the m -th basis function with respect to any free parameter can be expressed as a linear combination of the $(m-1)$ -th and $(m+1)$ -th basis function satisfies the same optimality condition.

The use of a generalized Laguerre filter (continuous-time) or a Meixner-like filter (discrete-time) rather than a more restricted Laguerre filter (continuous-time and discrete-time) gives the designer an extra free parameter, namely the order of generalization. As

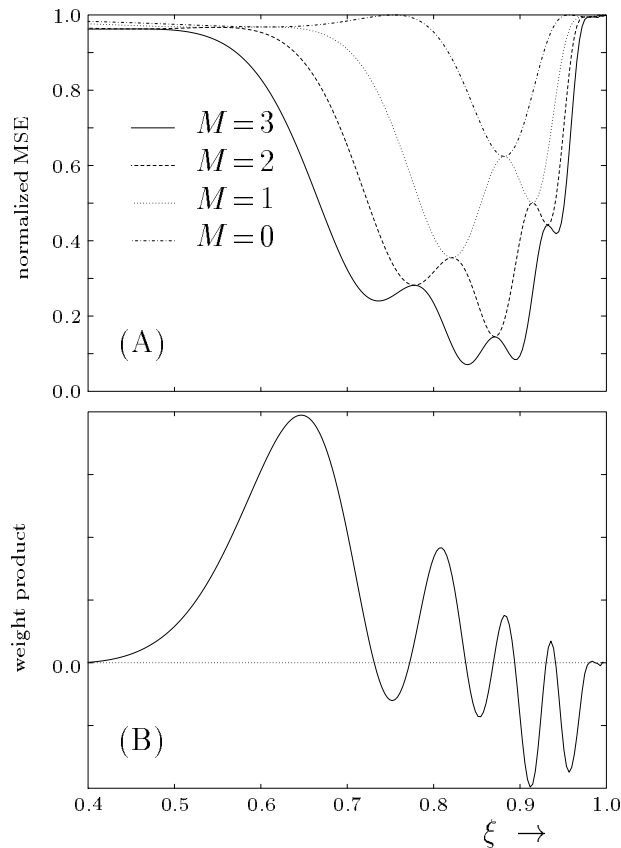


Figure 4.6: (A) Normalized MSE curves of the approximation of the output of the system $H(z)$ by the output of a Meixner-like filter excited by $x(k)$; (B) The weight product $w_{3,3}^{(3)}(\xi) w_{4,4}^{(3)}(\xi)$.

has been indicated in Section 4.2, this parameter can be used to enhance the low-frequency components of the basis functions at the expense of the high-frequency components. Equivalently, in the time domain the basis functions can be made more gradually starting. The problem of finding the optimal order of generalization is not addressed in this chapter. In (Belt and den Brinker 1997) a method is presented to obtain the best order of generalization for truncated generalized Laguerre expansions of a class of $L_2(\mathbb{R}^+)$ -functions satisfying certain moments.

The Meixner-like filter can be employed advantageously for adaptive filtering purposes. The weights can be optimized adaptively using algorithms such as LMS and RLS (Haykin 1996). For adaptive optimization of the pole the gradient given by (4.17) can be used. The expected value can be estimated by time averaging over the product $e_M(\xi; k)u_{M+1}(\xi; k)$. Care must be taken to ensure that the normal equations in (4.16) are (within a good approximation) always satisfied while the pole is adjusted, since only then the derived gradient is applicable. Belt and den Brinker (1996) proposed an algorithm for the adaptation of the pole in a Laguerre filter, see also Chapter 7 of this thesis.

Bibliography

- Abramowitz, M. and I. A. Stegun (1970). *Handbook of Mathematical Functions*. New York (NY), U.S.A.: Dover Publications.
- Belt, H. J. W. and A. C. den Brinker (1995a). Filter synthesis by discrete-time generalized Laguerre networks. In *Proc. 12th European Conference on Circuit Theory & Design (ECCTD)*, Istanbul, Turkey, pp. 971–974.
- Belt, H. J. W. and A. C. den Brinker (1995b). Optimal truncated Meixner-like networks. In *Proc. ProRISC/IEEE Benelux Workshop on Circuits, Systems and Signal Processing*, Mierlo, Netherlands, pp. 25–32.
- Belt, H. J. W. and A. C. den Brinker (1995c). Optimality condition for truncated generalized Laguerre networks. *Int. J. Circuit Theory Appl.* *23*, 227–235.
- Belt, H. J. W. and A. C. den Brinker (1996). Laguerre filters with adaptive pole optimization. In *Proc. IEEE International Symposium on Circuits and Systems (ISCAS)*, Atlanta (GA), U.S.A., pp. 37–40.
- Belt, H. J. W. and A. C. den Brinker (1997). Optimal parametrization of truncated generalized Laguerre series. In *Proc. IEEE International Conference on Acoustics, Speech and Signal Processing (ICASSP)*, Munich, Germany. To appear in April 1997.
- Broome, P. W. (1965). Discrete orthonormal sequences. *Journal of the Association for Computing Machinery* *12*, 151–168.
- Clement, P. R. (1963). On completeness of basis functions used for signal analysis. *SIAM Rev.* *5*, 131–139.
- Clowes, G. J. (1965). Choice of the time-scaling factor for linear system approximations using orthonormal Laguerre functions. *IEEE Trans. Automat. Contr.* *10*, 487–489.
- den Brinker, A. C. (1994). Optimality conditions for truncated Kautz series based on n th order all-pass sections. In *Signal Processing VII: Theories and Applications, Proc. EUSIPCO-94, Seventh European Signal Processing Conference*, Edinburgh, Scotland U.K., pp. 1086–1089.
- den Brinker, A. C. (1995). Meixner-like functions having a rational z -transform. *Int. J. Circuit Theory Appl.* *23*, 237–246.
- Haykin, S. (1996). *Adaptive Filter Theory, Third Edition*. London, U.K.: Prentice-Hall Int.
- King, J. J. and T. O’Canainn (1969). Optimum pole positions for Laguerre-function models. *Electronics Letters* *5*, 601–602.
- King, R. E. and P. N. Paraskevopoulos (1977). Digital Laguerre filters. *Int. J. Circuit Theory Appl.* *5*, 81–91.
- Lee, Y. W. (1932). Synthesis of electrical networks by means of the Fourier transforms of Laguerre functions. *J. Math. Phys.* *11*, 83–113.

-
- Masnadi-Shirazi, M. A. and N. Ahmed (1991). Optimum Laguerre networks for a class of discrete-time systems. *IEEE Trans. Signal Process.* 39, 2104–2108.
- Oliveira e Silva, T. (1994). Optimality conditions for truncated Laguerre networks. *IEEE Trans. Signal Process.* 42, 2528–2530.
- Oliveira e Silva, T. (1995). Rational orthonormal functions on the unit circle and on the imaginary axis, with applications in system identification.
URL: <ftp://inesca.inesca.pt/pub/tos/English/rof.ps.gz>.
- Szegő, G. (1959). *Orthogonal Polynomials*. New York (NY), U.S.A.: American Mathematical Society.

Chapter 5

Optimal Truncated Hermite Expansions*

Abstract

Signals that are fairly concentrated in time or space can often be conveniently described by a truncated Hermite series. The rate of convergence of such series depends on the center and scale factor of the Hermite functions. In this paper we present some results concerning the determination of the optimal values of these two important parameters. We address the problem of the approximation of one-dimensional functions defined in the continuous interval $(-\infty, \infty)$.

5.1 Introduction

In some signal and image processing applications it is necessary to approximate signals which either have a finite support or are very concentrated (in time or space). One way to approximate this type of signals is to use a truncated Hermite series, since the factor $\exp(-x^2/2)$ in the Hermite functions approaches zero rather quickly when $|x|$ is substantially larger than 1. There is, however, one problem with this approach: it is necessary to find a good center and a good scale factor for the Hermite functions in order to have fast convergence of the series. This is the point we will address in this paper. We note that truncated Hermite expansions were used recently in the approximation of biomedical signals (Lo Conte, Merletti, and Sandri 1994). Other applications of Hermite series can be found in (Martens 1990b; Martens 1990a).

*This chapter is the precise text of a paper by T. Oliveira e Silva** and H.J.W. Belt that appeared under the title "On the Determination of the Optimal Center and Scale Factor for Truncated Hermite Series" in *Signal Processing VIII, Theories and Applications, Proc. EUSIPCO-96, Eighth European Signal Processing Conference*, Trieste, Italy, pp. 1563–1566, 1996. See reference (Oliveira e Silva and Belt 1996).

**Dr. T. Oliveira e Silva is with the Departamento de Electrónica e Telecomunicações/INESC-Aveiro, Universidade de Aveiro, Portugal.

The results of this paper were inspired by similar results for truncated Laguerre expansions (Clowes 1965; King and O'Canainn 1969; Parks 1971; Wang and Cluett 1994). Due to lack of space we will discuss the approximation of one-dimensional signals only.

The structure of this paper is the following. Section 5.2 is concerned with the Hermite functions, and with some of their properties. Section 5.3 presents the stationarity conditions of the squared error of a truncated Hermite series. In Section 5.4 we describe a method to find a “good” center and a “good” scale factor for the Hermite functions based on measurements of the function to be approximated. Lastly, in Section 5.5 we present a simple example of the main results of the paper.

5.2 Hermite Polynomials and Functions with some Properties

The Hermite polynomials form one of the families of classical orthogonal polynomials and may be defined for $n > 0$ by the recurrence relation (Szegő 1959)

$$H_{n+1}(x) = 2x H_n(x) - 2n H_{n-1}(x) \quad (5.1)$$

with $H_0(x) = 1$. Another useful recurrence relation is

$$H_{n+2}(x) = [4x^2 - 2(2n + 1)] H_n(x) - 4n(n - 1) H_{n-2}(x) \quad (5.2)$$

with $H_0(x) = 1$ and $H_1(x) = 2x$, and for $n \geq 0$. It is also easy to prove that

$$H'_n(x) = 2n H_{n-1}(x). \quad (5.3)$$

It is well known that the Hermite polynomials obey the orthogonality condition

$$\int_{-\infty}^{\infty} H_m(x) H_n(x) e^{-x^2} dx = 2^n n! \sqrt{\pi} \delta_{mn}, \quad m, n \geq 0. \quad (5.4)$$

From the Hermite polynomials, which are orthogonal w.r.t. the weighting function e^{-x^2} , it is possible to construct families of functions in the interval $(-\infty, \infty)$ which are orthonormal with respect to a unity weighting function. These functions are obtained by multiplying the Hermite polynomials by the square root of their weighting function, followed by a translation and a change of scale in the x axis, and, finally, by a normalization. The end result of all these operations are the so-called Hermite functions, given by

$$\mathcal{H}_n(\lambda, t_0; t) = \alpha_n H_n(x) e^{-x^2/2} \quad (5.5)$$

where $x = (t - t_0)/\lambda$ and $\alpha_n = (2^n n! \lambda \sqrt{\pi})^{-1/2}$. These functions have two free parameters: t_0 , the center of the functions; and λ , their scale factor.

The Hermite functions form a complete orthonormal set in $L^2(-\infty, \infty)$, i.e., any square integrable function $f(t)$ can be expressed in the form

$$f(t) = \sum_{n=0}^{\infty} c_n(\lambda, t_0) \mathcal{H}_n(\lambda, t_0; t) \quad (5.6)$$

where

$$c_n(\lambda, t_0) = \int_{-\infty}^{\infty} f(t) \mathcal{H}_n(\lambda, t_0; t) dt. \quad (5.7)$$

The partial derivatives of the Hermite functions w.r.t. their three parameters are given by the following interesting formulas

$$\frac{\partial \mathcal{H}_n(\lambda, t_0; t)}{\partial t} = \beta_n \mathcal{H}_{n-1}(\lambda, t_0; t) - \beta_{n+1} \mathcal{H}_{n+1}(\lambda, t_0; t), \quad (5.8)$$

$$\frac{\partial \mathcal{H}_n(\lambda, t_0; t)}{\partial t_0} = -\frac{\partial \mathcal{H}_n(\lambda, t_0; t)}{\partial t}, \quad (5.9)$$

and

$$\frac{\partial \mathcal{H}_n(\lambda, t_0; t)}{\partial \lambda} = \gamma_n \mathcal{H}_{n-2}(\lambda, t_0; t) - \gamma_{n+2} \mathcal{H}_{n+2}(\lambda, t_0; t), \quad (5.10)$$

where

$$\beta_n = \frac{\sqrt{n}}{\lambda\sqrt{2}}, \quad \text{and} \quad \gamma_n = -\frac{\sqrt{n}\sqrt{n-1}}{2\lambda}. \quad (5.11)$$

These formulas express the partial derivatives of the Hermite functions as linear combinations of other Hermite functions, and can be proven easily by differentiating (5.5) w.r.t. the appropriate variables and simplifying the results with (5.1), (5.2), and (5.3). In a few words, these formulas are a consequence of the special form of the Fourier transform of the Hermite functions and of their orthonormality. Note that a similar result exists for the Laguerre functions (King and O'Canainn 1969; Wang and Cluett 1994; Oliveira e Silva 1995).

The Hermite functions satisfy the following differential equation (a prime denotes differentiation w.r.t. t)

$$x^2 \mathcal{H}_n(\lambda, t_0; t) - \lambda^2 \mathcal{H}_n''(\lambda, t_0; t) = (2n + 1) \mathcal{H}_n(\lambda, t_0; t) \quad (5.12)$$

[remember that $x = (t - t_0)/\lambda$]. This follows from the differentiation of (5.8) w.r.t. t and from (5.1) and (5.3).

5.3 Stationarity Conditions for Truncated Hermite Series

In practice we are forced to use a finite number of terms, say $N + 1$, in (5.6). We then obtain an approximation to $f(t)$ of the form

$$f_N(\lambda, t_0; t) = \sum_{n=0}^N c_n(\lambda, t_0) \mathcal{H}_n(\lambda, t_0; t) \quad (5.13)$$

that has a squared error of

$$\xi_N(\lambda, t_0) = \int_{-\infty}^{\infty} f^2(t) dt - \sum_{n=0}^N c_n^2(\lambda, t_0). \quad (5.14)$$

This squared error is clearly a function of the center and of the scale factor of the Hermite functions. It makes then sense to try to minimize it w.r.t. these two parameters. A preliminary step towards this goal is the deduction of the stationarity conditions of the squared error w.r.t. λ and to t_0 .

Let $\theta = \lambda$ or $\theta = t_0$. Then we have

$$\frac{\partial \xi_N(\lambda, t_0)}{\partial \theta} = -2 \sum_{n=0}^N c_n(\lambda, t_0) \frac{\partial c_n(\lambda, t_0)}{\partial \theta} \quad (5.15)$$

and [cf. (5.7)]

$$\frac{\partial c_n(\lambda, t_0)}{\partial \theta} = \int_{-\infty}^{\infty} f(t) \frac{\partial \mathcal{H}_n(\lambda, t_0; t)}{\partial \theta} dt. \quad (5.16)$$

Using (5.9) and (5.10) in the previous formula yields

$$\frac{\partial c_n(\lambda, t_0)}{\partial t_0} = -\beta_n c_{n-1}(\lambda, t_0) + \beta_{n+1} c_{n+1}(\lambda, t_0), \quad (5.17)$$

and

$$\frac{\partial c_n(\lambda, t_0)}{\partial \lambda} = \gamma_n c_{n-2}(\lambda, t_0) + \gamma_{n+2} c_{n+2}(\lambda, t_0). \quad (5.18)$$

Using these remarkable formulas in (5.15) it is possible to verify that in both cases the summation appearing there becomes a telescopic series, giving the simple results

$$\frac{\partial \xi_N(\lambda, t_0)}{\partial t_0} = -2 \beta_{N+1} c_N(\lambda, t_0) c_{N+1}(\lambda, t_0) \quad (5.19)$$

and

$$\begin{aligned} \frac{\partial \xi_N(\lambda, t_0)}{\partial \lambda} &= 2 \gamma_{N+1} c_{N-1}(\lambda, t_0) c_{N+1}(\lambda, t_0) \\ &\quad + 2 \gamma_{N+2} c_N(\lambda, t_0) c_{N+2}(\lambda, t_0). \end{aligned} \quad (5.20)$$

It is easy to prove that these two partial derivatives vanish simultaneously if and only if at least one of the following three conditions is satisfied

$$c_k(\lambda, t_0) = c_{k+1}(\lambda, t_0) = 0, \quad k = N-1, N, N+1. \quad (5.21)$$

Intuitively, we would expect that at local minima of $\xi_N(\lambda, t_0)$ the condition corresponding to $k = N+1$ is the one satisfied, since for the other two cases one or more coefficients used in the approximation vanish. Unfortunately, this is not always the case.

If we suspect that the global minimum of $\xi_N(\lambda, t_0)$ satisfies condition (5.21) for a specific k , and if we have one reasonably good estimate of the optimal values of λ and t_0 , then it is possible to refine these estimates using one or more iterations of Newton's method to solve a system of (two) nonlinear equations. This is possible because it is very easy to compute the partial derivatives of $\xi_N(\lambda, t_0)$ w.r.t. these two parameters [it is only necessary to compute two extra coefficients of the Hermite series, cf. (5.19) and (5.20)]. Of course, we can also use Newton's method to try to find solutions of (5.21) by starting at some random values of λ and t_0 .

5.3.1 Approximation of Even and Odd Components of a Function

If it is known that a function is even (or odd) around a certain point t_0 then half of the expansion coefficients of the truncated Hermite series will be zero. In such cases it makes sense to use in the approximation only even (or odd) Hermite functions, which can be computed directly with recursion (5.2). Again, the partial derivative of the squared error of the approximation w.r.t. λ will be a telescopic series, and the stationarity condition will simply be

$$c_N(\lambda, t_0) c_{N+2}(\lambda, t_0) = 0 \quad (5.22)$$

where N is the index of the last term used in the expansion.

Since even and odd functions (around the same point) are orthogonal to each other it is possible to approximate the even and odd components of a function using even and odd truncated Hermite expansions with different scale factors and with different numbers of terms (but with the same center). The two independent stationarity conditions will have the same form as (5.22). This idea was suggested to the authors by Dr. A. C. den Brinker.

5.4 Optimum Value of λ and t_0 for a Class of Functions

Based on the ideas of (Parks 1971) (see also (Tanguy, Vilbé, and Calvez 1995) for a more general result) it is possible to estimate a “good” center and scale factor for the Hermite functions used in the approximation of a function $f(t)$. Let

$$m_i = \int_{-\infty}^{\infty} t^i f^2(t) dt, \quad i = 0, 1, 2, \quad (5.23)$$

and

$$m_3 = \int_{-\infty}^{\infty} [f'(t)]^2 dt = - \int_{-\infty}^{\infty} f(t) f''(t) dt. \quad (5.24)$$

We assume that these integrals exist and are absolutely convergent. The purpose of this section is to derive formulas for the best center and scale of the Hermite functions when the only information about $f(t)$ is the four “measurements” m_0, \dots, m_3 introduced above. Note that m_0 is the energy of $f(t)$ and that m_1 will vanish if $f(t)$ is an even or an odd function. Note also that a translation and change of scale affect these measurements in the way shown in Table 5.1.

$f(t)$	m_0	m_1	m_2	m_3
$f(x)$	$m_0 \lambda$	$m_1 \lambda^2 + t_0 m_0 \lambda$	$m_2 \lambda^3 + 2t_0 m_1 \lambda^2 + t_0^2 m_0 \lambda$	m_3 / λ

Table 5.1: Effect of a translation and change of scale in the measurements m_k . Note that $x = (t - t_0)/\lambda$. The second line of this table then represents a translation of $f(t)$ by t_0 followed by an amplification of the t axis by a factor of λ .

Using the differential equation (5.12) that the Hermite functions satisfy it is possible to prove that

$$\sum_{n=0}^{\infty} (2n+1)c_n^2(\lambda, t_0) = \frac{m_2 - 2t_0 m_1 + t_0^2 m_0}{\lambda^2} + \lambda^2 m_3.$$

But

$$(2N+3)\xi_N(\lambda, t_0) \leq \sum_{n=N+1}^{\infty} (2n+1)c_n^2(\lambda, t_0)$$

with equality if and only if $c_n(\lambda, t_0) = 0$ for $n > N+1$. Also

$$\sum_{n=0}^N (2n+1)c_n^2(\lambda, t_0) \geq \sum_{n=0}^N c_n^2(\lambda, t_0)$$

with equality if and only if $c_n(\lambda, t_0) = 0$ for $1 \leq n \leq N$. Combining all these results yields

$$\xi_N(\lambda, t_0) \leq \frac{m_3 \lambda^4 - m_0 \lambda^2 + (m_2 - 2t_0 m_1 + t_0^2 m_0)}{2(N+1)\lambda^2} \quad (5.25)$$

This upper bound for $\xi_N(\lambda, t_0)$ is attained if $f(t)$ is a linear combination of $\mathcal{H}_0(\lambda, t_0; t)$ and $\mathcal{H}_{N+1}(\lambda, t_0; t)$. Minimizing this bound w.r.t. t_0 yields

$$\hat{t}_0 = \frac{m_1}{m_0}, \quad (5.26)$$

which is independent of λ . Hence the “best” center for the expansion can be determined quite easily and requires only two measurements. Note that (5.26) has a very simple and elegant interpretation, and is widely used in wavelet theory. Minimizing the upper bound also w.r.t. λ yields

$$\hat{\lambda}^4 = \frac{m_0 m_2 - m_1^2}{m_0 m_3}. \quad (5.27)$$

Using the data presented in Table 5.1 it is reassuring to verify that translations and changes of scale of $f(t)$ are reflected in the appropriate way in the values of \hat{t}_0 and $\hat{\lambda}$, as we invite the reader to check. Also, for the Hermite functions themselves we have $m_0 = 1$, $m_1 = t_0$, $m_2 = \frac{2n+1}{2}\lambda^2 + t_0^2$, and $m_3 = \frac{2n+1}{2\lambda^2}$, which gives $\hat{t}_0 = t_0$ and $\hat{\lambda} = \lambda$, which is also reassuring.

These results can be extended easily to the problem of the determination of a “good” center and scale factor for the simultaneous approximation of several functions by truncated Hermite series (with the same center and scale factor). Let

$$M_k = \sum_{l=1}^L w_l m_{k,l}, \quad k = 0, 1, 2, 3, \quad (5.28)$$

where $m_{k,l}$ is the k -th measurement for the l -th function and w_l is a positive weight that quantifies the relative importance of the l -th function. Then, estimates for a “good” center and scale factor for the Hermite functions can be obtained using (5.26) and (5.27), but replacing the (individual) lower-case m_k “measurements” by the (collective) upper-case M_k “measurements”.

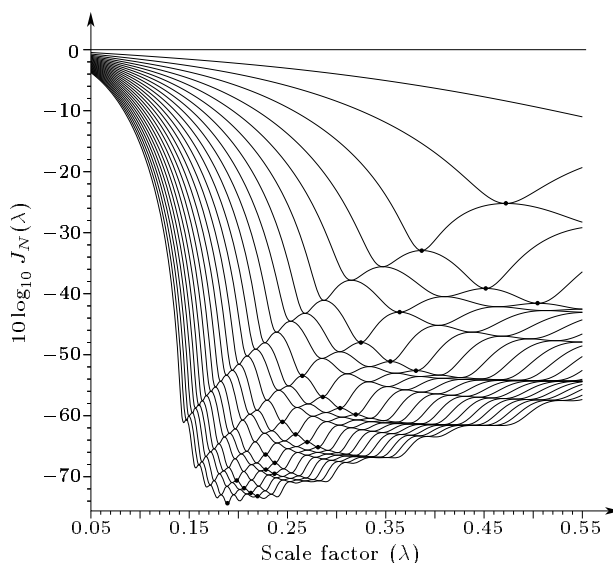


Figure 5.1: Normalized squared error of the approximation of $f_{1/2}(t)$ by truncated Hermite series with up to 26 even terms, i.e., for $N = 0, 2, \dots, 50$. Note that consecutive curves touch only in stationary points (in this case, local extrema) of both curves. This is a consequence of (5.22).

5.5 An Example

Consider the problem of approximating the following function (a raised cosine)

$$f_b(t) = \begin{cases} 1, & \text{if } |t| < 1 - b \\ \frac{1}{2} [1 - \sin(\frac{\pi}{2} \frac{|t|-1}{b})], & \text{if } 1 - b \leq |t| < 1 + b \\ 0, & \text{otherwise} \end{cases}$$

by a truncated Hermite expansion. Since this is an even function around $t = 0$ we will set $t_0 = 0$ and work with Hermite series with even terms only. In Fig. 5.1 we depict the normalized squared error, which is given by $J_N(\lambda) = \xi_N(\lambda, 0)/m_0$, for several values of N . Although it may be dangerous to extrapolate, the figure suggests that the optimal λ approaches zero when N increases. If true, this may be explained by the fact that the Hermite functions become wider and wider when N increases, with a “width” that is roughly proportional to $\sqrt{2N+1}$ [the magnitude of their largest zero, cf. (5.3)]. If the function being approximated has finite support, which is the case here, then it may happen that the best λ decreases to compensate for this increase in the “width” of the last Hermite functions used in the approximation.

For $f_b(t)$ it is possible to show that

$$\begin{aligned} m_0 &= \frac{4-b}{2} \\ m_1 &= 0 \\ m_2 &= \frac{(6-\pi^2)b^3 + (12\pi^2-96)b^2 - 3\pi^2 b + 4\pi^2}{6\pi^2} \end{aligned}$$

$$m_3 = \frac{\pi^2}{8b},$$

giving

$$\begin{aligned} \hat{t}_0 &= 0 \\ \hat{\lambda}^4 &= \frac{4b[6 - \pi^2]b^3 + (12\pi^2 - 96)b^2 - 3\pi^2 b + 4\pi^2}{3\pi^4} \end{aligned}$$

as a “good” center and a “good” scale factor for the Hermite functions. Note that $\hat{\lambda}$ tends to zero when b tends to zero, i.e., when $f_b(t)$ tends to a rectangular function. We believe that the same phenomenon occurs for other discontinuous functions, since for these the “natural” value of m_3 is infinity. For $b = 1/2$ we have $\hat{\lambda} \approx 0.672$, which is not a good estimate of the best λ for almost all values of N (cf. Fig. 5.1). However, for small N , it gives a reasonably good indication of the magnitude of the optimal values of the scale factor.

Bibliography

- Clowes, G. J. (1965). Choice of the time-scaling factor for linear system approximations using orthonormal Laguerre functions. *IEEE Trans. Automat. Contr.* 10, 487–489.
- King, J. J. and T. O’Canainn (1969). Optimum pole positions for Laguerre-function models. *Electronics Letters* 5, 601–602.
- Lo Conte, L. R., R. Merletti, and G. V. Sandri (1994). Hermite expansions of compact support waveforms: Applications to myoelectric signals. *IEEE Trans. Biomed. Eng.* 41, 1147–1159.
- Martens, J.-B. (1990a). The Hermite transform – Applications. *IEEE Trans. Acoust. Speech Signal Process.* 38, 1607–1618.
- Martens, J.-B. (1990b). The Hermite transform – Theory. *IEEE Trans. Acoust. Speech Signal Process.* 38, 1595–1606.
- Oliveira e Silva, T. (1995). On the determination of the optimal pole position of Laguerre filters. *IEEE Trans. Signal Process.* 43, 2079–2087.
- Oliveira e Silva, T. and H. J. W. Belt (1996). On the determination of the optimal center and scale factor for truncated hermite series. In *Signal Processing VIII: Theories and Applications, Proc. EUSIPCO-96, Eighth European Signal Processing Conference*, Trieste, Italy, pp. 1563–1566.
- Parks, T. W. (1971). Choice of time scale in Laguerre approximations using signal measurements. *IEEE Trans. Automat. Contr.* 16, 511–513.
- Szegö, G. (1959). *Orthogonal Polynomials*. New York (NY), U.S.A.: American Mathematical Society.

-
- Tanguy, N., P. Vilbé, and L. C. Calvez (1995). Optimum choice of free parameter in orthonormal approximations. *IEEE Trans. Automat. Contr.* *40*, 1811–1813.
- Wang, L. and W. R. Cluett (1994). Optimal choice of time-scaling factor for linear system approximations using Laguerre models. *IEEE Trans. Automat. Contr.* *39*, 1463–1467.

Chapter 6

Cascaded All-Pass Sections for LMS Adaptive Filtering*

Abstract

The behaviour of the LMS adaptive algorithm is analyzed for a class of adaptive filters that is based on a cascade of identical N -th order all-pass sections. The well-known tapped-delay-line is a special case of this class. We look at the rate of convergence and the steady-state weight fluctuations. It is shown that in the steady state the weight-error correlation matrix satisfies a Lyapounov equation for sufficiently small values of the step-size. Sometimes *a priori* knowledge of the unknown reference system is available that can be used to select the N parameters of the all-pass section. It is motivated that in these cases the LMS adaptive filter based on a cascade of identical all-pass sections can outperform the LMS adaptive tapped-delay-line.

6.1 Introduction

The widespread use of the LMS adaptive algorithm applied to a tapped-delay-line (TDL) is a direct consequence of its simplicity and good performance. For the analysis of the behaviour of the LMS algorithm most authors rely on an "independence assumption" stating statistical independence of successive input vectors (Haykin 1996). It is argued that for the analysis to be tractable this assumption must be made. However, due to the (deterministic) coherence between successive input vectors, the independence assumption cannot be justified. This logical inconsistency has recently led to alternative approaches. Particularly the weight fluctuations in the fully adapted state are studied by Butterweck (1995) *without* making use of the independence assumption. An iterative procedure is used

*This chapter is the (slightly modified version of the) paper in cooperation with H.J. Butterweck that appeared under the same title in *Signal Processing VIII, Theories and Applications, Proc. EUSIPCO-96, Eighth European Signal Processing Conference*, Trieste, Italy, pp. 1219–1222, 1996. See reference (Belt and Butterweck 1996).

to arrive at a power series of the weight-error correlation matrix (WECM) in terms of the step-size.

In this paper we study the behaviour of the LMS algorithm applied to a more general class of adaptive filters. The delay line is replaced by a cascade of identical all-pass sections of order N and each tap signal is filtered to yield N outputs. In Section 2 this structure is introduced and a few relevant properties are given. In Section 3 some notational aspects concerning the LMS algorithm applied to the all-pass filter bank are treated. Section 4 deals with the WECM, which is shown to be the solution of a Lyapounov equation. Two explicitly solvable cases of the Lyapounov equation are considered. Section 5 contains a performance analysis of the LMS algorithm applied to the all-pass filter bank in terms of adaptation speed and misadjustment. Finally, some concluding remarks are made in the Discussion.

6.2 The All-Pass Filter Bank

Consider a filter bank of P sections, cf. Fig. 6.1. Compared to the TDL each delay element has been replaced by an N -th order all-pass section with the transfer function

$$A(z) = \frac{\prod_{i=1}^N (1 - z p_i)}{\prod_{i=1}^N (z - p_i)}.$$

The (not necessarily distinct) poles p_i are real or occur in complex conjugate pairs and lie inside the unit circle. Each tap signal in the cascade is filtered by a section $B(z)$ with one input and N outputs. The latter is chosen such that the NP impulse responses of the filter bank form an orthonormal set. These functions are usually referred to as "Kautz functions" (Kautz 1954; Broome 1965).

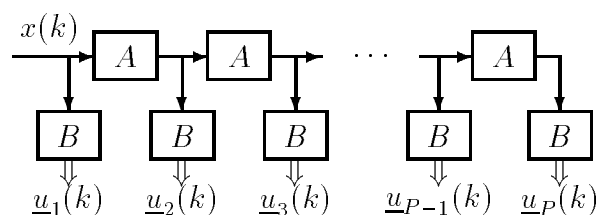


Figure 6.1: Orthonormal Kautz network based on a cascade of identical N -th order all-pass sections

If we take $A(z) = (1 - \xi z)/(z - \xi)$ and $B(z) = \sqrt{1 - \xi^2} z/(z - \xi)$ with $|\xi| < 1$ we have $N = 1$ and we obtain a "Laguerre network" (King and Paraskevopoulos 1977). Its orthonormal impulse responses are called the "discrete Laguerre functions" (Broome 1965). Note that for $\xi = 0$ the Laguerre network degenerates into a TDL.

Although most of the following analysis applies to more general structures, that of Fig. 6.1 deserves special attention: all-passes imply energy conservation along the filter line and good numerical properties, while the repetitive structure can be easily implemented.

The Kautz network is assumed to be excited by a zero-mean, stationary stochastic signal $x(k)$ with autocorrelation function $X_l = E\{x(k)x(k-l)\}$, power $\sigma_x^2 = X_0$, and power spectral density function $\Phi_{xx}(\Omega)$. Furthermore, it operates in the steady state such that also the $M = NP$ outputs of the filter bank can be viewed as stationary. These outputs are written in vector notation as $\underline{u}(k) = [\underline{u}_1^T(k), \dots, \underline{u}_P^T(k)]^T$, where $\underline{u}_p(k)$ denotes the $N \times 1$ output vector of the $(p+1)$ -th section ($p = 0, 1, \dots, P-1$). The corresponding $M \times M$ covariance matrix $\mathbf{R} = E\{\underline{u}(k)\underline{u}^T(k)\}$ is symmetric and (semi-)positive definite. It has a block-Toeplitz structure where the size of the blocks is $N \times N$. Its eigenvectors are orthogonal and its eigenvalues λ_0 to λ_{M-1} are non-negative. For white $x(k)$ the covariance matrix becomes $\mathbf{R} = \sigma_x^2 \mathbf{I}$ because the filter bank is orthonormal.

We now show that the smallest eigenvalue λ_{\min} of \mathbf{R} satisfies the inequality (Oliveira e Silva 1994)

$$\lambda_{\min} = \min_{\underline{a} \neq \underline{0}} \frac{\underline{a}^T \mathbf{R} \underline{a}}{\underline{a}^T \underline{a}} \geq \min\{\Phi_{xx}(\Omega)\}. \quad (6.1)$$

Let $g_m(k)$ with $m = 0, 1, \dots, M-1$ denote the impulse response of the $(m+1)$ -th filter bank output, and $G_m(e^{j\Omega})$ its Fourier transform. We then find

$$\begin{aligned} \underline{a}^T \mathbf{R} \underline{a} &= \frac{1}{2\pi} \int_{-\pi}^{\pi} \left| \sum_{m=0}^{M-1} a_m G_m(e^{j\Omega}) \right|^2 \Phi_{xx}(\Omega) d\Omega \\ &\geq \frac{1}{2\pi} \int_{-\pi}^{\pi} \left| \sum_{m=0}^{M-1} a_m G_m(e^{j\Omega}) \right|^2 d\Omega \min\{\Phi_{xx}(\Omega)\}, \end{aligned}$$

where the a_m are the M components of the vector \underline{a} . Using the orthogonality of the impulse responses $g_m(k)$ implying that of the system functions $G_m(e^{j\Omega})$, we easily obtain

$$\underline{a}^T \mathbf{R} \underline{a} \geq \underline{a}^T \underline{a} \min\{\Phi_{xx}(\Omega)\},$$

which implies (6.1). The counterpart of (6.1), not used in this paper, reads as (Oliveira e Silva 1994)

$$\lambda_{\max} \leq \max\{\Phi_{xx}(\Omega)\}.$$

Hereafter we assume that $x(k)$ is "persistently exciting", which means that $\Phi_{xx}(\Omega) > 0$ for all frequencies, or equivalently, $\lambda_{\min} > 0$.

6.3 The LMS Adaptive All-Pass Filter

Let $x(k)$ simultaneously excite an adaptive filter of the above-mentioned type and a linear and time-invariant "reference system" whose output, corrupted by additive noise $n(k)$, yields the "desired signal" $d(k)$. The noise $n(k)$ is a zero-mean, stationary stochastic process with autocorrelation function $N_l = E\{n(k)n(k-l)\}$, power $\sigma_n^2 = N_0$, and power spectral density function $\Phi_{nn}(\Omega)$. The weight vector of the adaptive filter is denoted by $\underline{w}(k) = [w_1(k), \dots, w_M(k)]^T$. The output $y(k)$ of the adaptive filter can be written as

$\underline{w}^T(k) \underline{u}(k)$. By subtracting $y(k)$ from the desired signal we construct the "error signal" $e(k) = d(k) - y(k)$, which can be used to update $\underline{w}(k)$. In the (optimal) Wiener solution $\underline{w} = \underline{w}_o$ the weights are such that the Mean-Squared Error (MSE) $E\{e^2(k)\}$ is minimal.

The weight error vector $\underline{v}(k)$ is defined as the instantaneous difference between the weight vector of the adaptive filter and the Wiener solution: $\underline{v}(k) = \underline{w}(k) - \underline{w}_o$. Assuming that the reference system can be modelled by the Kautz filter set used for the adaptive filter, so that its output equals $\underline{w}_o^T \underline{u}(k)$, the error signal can be written as

$$\begin{aligned} e(k) &= n(k) + \underline{w}_o^T \underline{u}(k) - \underline{w}^T \underline{u}(k) \\ &= n(k) - \underline{v}^T(k) \underline{u}(k). \end{aligned}$$

The LMS adaptive algorithm is given by

$$\underline{w}(k+1) = \underline{w}(k) + \mu e(k) \underline{u}(k).$$

Here μ is the adaptation constant or step-size. We may write for the weight-error vector:

$$\begin{aligned} \underline{v}(k+1) &= \underline{v}(k) - \mu \underline{u}(k) \underline{u}^T(k) \underline{v}(k) + \mu n(k) \underline{u}(k) \\ &= (\mathbf{I} - \mu \mathbf{R}(k)) \underline{v}(k) + \mu \underline{f}(k), \end{aligned} \quad (6.2)$$

where we have used the short-hand notation $\mathbf{R}(k) = \underline{u}(k) \underline{u}^T(k)$ and $\underline{f}(k) = n(k) \underline{u}(k)$. As in (Butterweck 1995), equation (6.2) is the starting point for the determination of the positive (semi-)definite WECM, given by $\mathbf{V} = E\{\underline{v}(k) \underline{v}^T(k)\}$.

6.4 The Weight-Error Correlation Matrix

For sufficiently small values of μ the time-varying term $\mathbf{R}(k)$ in (6.2) can be replaced by its constant average \mathbf{R} . Then in the limiting case $\mu \rightarrow 0$, the WECM satisfies a Lyapounov equation (henceforth all summations extend from $-\infty$ to ∞ unless stated otherwise):

$$\mathbf{R} \mathbf{V} + \mathbf{V} \mathbf{R} = \mu \mathbf{F}, \quad (6.3)$$

where $\mathbf{F} = \sum_l \mathbf{F}_l$, $\mathbf{F}_l = N_l \mathbf{R}_l$, $\mathbf{R}_l = E\{\underline{u}(k) \underline{u}^T(k-l)\}$, and $\mathbf{R} = \mathbf{R}_0$. Proof of this is presented in the appendix to this chapter. This Lyapounov equation was already found in (Butterweck 1995) and (Butterweck 1996b) for the special case of the TDL. We consider two explicitly solvable cases:

- If $n(k)$ is white, the right-hand side of equation (6.3) equals $\mu \sigma_n^2 \mathbf{R}$, and the WECM becomes

$$\mathbf{V} = \frac{1}{2} \mu \sigma_n^2 \mathbf{I}.$$

- If $x(k)$ is white we get

$$\mathbf{V} = \frac{1}{2} \mu \tilde{\mathbf{R}}, \quad (6.4)$$

where $\tilde{\mathbf{R}}$ is the covariance matrix of the outputs $u_0(k)$ to $u_{M-1}(k)$ of the Kautz network in the imaginary situation that it is excited by $n(k)$ instead of $x(k)$. Here we have used that the impulse responses of the filter bank are orthonormal.

Proof: For the $(p+1, q+1)$ -th element of the matrix \mathbf{F} in (6.3) we may write

$$\begin{aligned} \{\mathbf{F}\}_{pq} &= \sum_l N_l E\{u_p(k)u_q(k-l)\} = \sum_l N_l \sum_{s=0}^{\infty} \sum_{t=0}^{\infty} g_p(s)g_q(t)X_{s-l-t} \\ &= \sigma_x^2 \sum_{s=0}^{\infty} \sum_{t=0}^{\infty} g_p(s)g_q(t)N_{s-t}, \end{aligned} \quad (6.5)$$

which represents σ_x^2 times the covariance between the $(p+1)$ -th and the $(q+1)$ -th output of the filter bank as if it had been excited by $n(k)$ instead of $x(k)$. Also, from (6.3) with $\mathbf{R} = \sigma_x^2 \mathbf{I}$ we know that

$$\mu\{\mathbf{F}\}_{pq} = 2\sigma_x^2\{\mathbf{V}\}_{pq}. \quad (6.6)$$

Combination of (6.5) and (6.6) concludes the proof of (6.4).

6.5 Performance Analysis

In this section our interest will be focussed on the terminal behaviour of the LMS algorithm. The performance of an adaptation algorithm is usually characterized by two measures: the rate of convergence and the misadjustment. As is well known, the rate of convergence of the LMS algorithm is determined by the smallest eigenvalue of \mathbf{R} , which, in our case, is lower-bounded by the minimum of $\Phi_{xx}(\Omega)$, see (6.1). Therefore, the rate of convergence of the LMS algorithm remains bounded even when the number of adaptive weights M is continuously increased.

For a discussion of the misadjustment we decompose the steady-state output of the adaptive filter as

$$\begin{aligned} y(k) &= \underline{w}_o^T \underline{u}(k) + \underline{v}^T(k) \underline{u}(k) \\ &= y_w(k) + y_f(k), \end{aligned}$$

where $y_w(k)$ is the contribution due to the Wiener coefficients \underline{w}_o and $y_f(k)$ is that due to the weight fluctuations. As proposed by Butterweck (1996a), for a small step-size μ the misadjustment should be defined as

$$\text{misadjustment} = \frac{E\{y_f^2(k)\}}{\sigma_n^2}.$$

We then obtain

$$E\{y_f^2(k)\} = E\{\underline{u}^T(k) \underline{v}(k) \underline{v}^T(k) \underline{u}(k)\}.$$

For sufficiently small values of μ the vector $\underline{v}(k)$ varies so much slower than $\underline{u}(k)$ that we may write (Butterweck 1996b), using (6.3)

$$E\{y_f^2(k)\} \approx E\{\underline{u}^T(k) \mathbf{V} \underline{u}(k)\} = \frac{1}{2} \text{trace}\{\mathbf{R}\mathbf{V} + \mathbf{V}\mathbf{R}\}$$

$$\begin{aligned}
&= \frac{\mu}{2} \sum_l N_l E\{ \underline{u}^T(k) \underline{u}(k-l) \} \\
&= \frac{\mu}{2} \sum_{m=0}^{M-1} \frac{1}{2\pi} \int_{-\pi}^{\pi} \Phi_{nn}(\Omega) \Phi_{xx}(\Omega) |G_m(e^{j\Omega})|^2 d\Omega. \tag{6.7}
\end{aligned}$$

Note the symmetry with respect to the excitation signal and the additive noise signal. Because all contributions to the summation in (6.7) are strictly positive, we can draw the important conclusion that the misadjustment grows without bound with increasing M .

In the special case " $x(k)$ white" the result in (6.7) becomes $\frac{1}{2}\mu M \sigma_x^2 \text{trace}\{\hat{\mathbf{R}}\}$. When $n(k)$ is white we obtain $\frac{1}{2}\mu M \sigma_n^2 \text{trace}\{\mathbf{R}\}$. When both $x(k)$ and $n(k)$ are white the result in (6.7) reduces to $\frac{1}{2}\mu M \sigma_n^2 \sigma_x^2$.

In the Laguerre case where $N = 1$ we have that $|G_m(e^{j\Omega})|^2 = |B(e^{j\Omega})|^2$ for all frequencies, which is a consequence of the all-pass structure. As a result we obtain

$$E\{y_f^2(k)\} = \frac{\mu M}{2} \frac{1}{2\pi} \int_{-\pi}^{\pi} \Phi_{nn}(\Omega) \Phi_{xx}(\Omega) |B(e^{j\Omega})|^2 d\Omega.$$

For $\xi = 0$ the Laguerre filter reduces to the TDL, and we find (see also (Butterweck 1996b))

$$E\{y_f^2(k)\} = \frac{\mu M}{2} \frac{1}{2\pi} \int_{-\pi}^{\pi} \Phi_{nn}(\Omega) \Phi_{xx}(\Omega) d\Omega,$$

which becomes $\frac{1}{2}\mu M \sigma_n^2 \sigma_x^2$ when either $x(k)$ or $n(k)$ is white.

6.6 Discussion

We have analyzed the LMS adaptive algorithm for a class of adaptive filters that is based on a cascade of identical N -th order all-pass sections. We have shown that the rate of convergence remains bounded even when the number of weights M is continuously increased. We have also shown that the misadjustment grows without bound with increasing M , and thus for a small misadjustment M should be kept small.

Observe, however, that besides the rate of convergence and the misadjustment a third criterion has to be reckoned with, viz. a good approximation of the reference system. In the Wiener solution, the adaptive filter imitates the reference system such that a properly defined approximation error is minimized. For a given reference system each of the competitive adaptive filter structures yields an approximation error that decreases monotonically with the number of filter sections M . Conversely, for a given approximation error the minimally required number of filter sections M_{\min} depends on the chosen structure. If this structure contains one or more extra free parameters (in our case the poles p_0 to p_{N-1}), M_{\min} becomes a function of these parameters and can be minimized when appropriate *a priori* knowledge of the reference system is available. When this knowledge is not available,

it is sometimes possible to adaptively optimize the free parameters. This is done for the pole of an adaptive Laguerre filter by Belt and den Brinker (1996). Compared with the classical TDL the more general all-pass filter banks often turn out to yield substantially lower values of M_{\min} . As we have shown, a smaller M_{\min} leads to a better LMS adaptive filter.

Appendix

We prove that the WECM satisfies a Lyapounov equation in the limiting case $\mu \rightarrow 0$. It is assumed that the filter operates in the steady state since $-\infty$, such that the influence of the initial conditions can be neglected. With (6.2) we may write for the weight error vector

$$\underline{v}(k+1) = \mu \sum_{l=0}^{\infty} (I - \mu \mathbf{R})^l \underline{f}(k-l) = \mu \sum_{l=0}^{\infty} \mathbf{D}^l \underline{f}(k-l),$$

where \mathbf{D} is the symmetric "damping matrix". We will use the short-hand notation $\mathbf{D}_l = \mathbf{D}^l$ for $l \geq 0$ and $\mathbf{D}_l = 0$ for $l < 0$. For later use the following properties of \mathbf{D}_l are noted here:

$$\mathbf{D}_l^T = \mathbf{D}_l \quad \text{and} \quad \mathbf{D}\mathbf{D}^l = \mathbf{D}^l\mathbf{D} \quad \text{and} \quad \mathbf{D}_{l+1} = \mathbf{D}\mathbf{D}_l + \delta_{l+1}\mathbf{I},$$

where δ_l is the Kronecker delta function. We find for the WECM

$$\begin{aligned} \mathbf{V} &= E\{\underline{v}(k)\underline{v}^T(k)\} = \mu^2 \sum_l \sum_m \mathbf{D}_l E\{\underline{f}(k-l)\underline{f}^T(k-m)\} \mathbf{D}_m^T \\ &= \mu^2 \sum_l \sum_m \mathbf{D}_l \mathbf{F}_m \mathbf{D}_{m+l} = \mu^2 \sum_m \mathbf{T}_m, \end{aligned}$$

where

$$\begin{aligned} \mathbf{T}_m &= \sum_l \mathbf{D}_l \mathbf{F}_m \mathbf{D}_{m+l} = \sum_l \mathbf{D}_{l+1} \mathbf{F}_m \mathbf{D}_{m+l+1} \\ &= \mathbf{D}\mathbf{T}_m\mathbf{D} + \mathbf{F}_m\mathbf{D}\mathbf{D}_{m-1} + \mathbf{D}_{-m-1}\mathbf{F}_m + \mathbf{F}_0\delta_m. \end{aligned} \quad (6.8)$$

For the first term in (6.8) we may use the following approximation when μ is sufficiently small:

$$\mathbf{D}\mathbf{T}_m\mathbf{D} = (\mathbf{I} - \mu\mathbf{R})\mathbf{T}_m(\mathbf{I} - \mu\mathbf{R}) \approx \mathbf{T}_m - \mu\mathbf{R}\mathbf{T}_m - \mu\mathbf{T}_m\mathbf{R}. \quad (6.9)$$

The second and the third term in (6.8) can be approximated as follows:

$$\mathbf{F}_m\mathbf{D}\mathbf{D}_{m-1} \approx \mathbf{F}_m\epsilon(m-1), \quad (6.10)$$

$$\mathbf{D}\mathbf{D}_{-m-1}\mathbf{F}_m \approx \mathbf{F}_m\epsilon(-m-1), \quad (6.11)$$

where $\epsilon(m)$ is the unit step function. This last approximation is valid when it is assumed that the matrix sequence \mathbf{F}_m damps faster than \mathbf{D}_m (this is true for small values of μ). We now obtain from (6.8) with (6.9), (6.10) and (6.11) that

$$\mu\mathbf{R}\mathbf{T}_m + \mu\mathbf{T}_m\mathbf{R} = \mathbf{F}_m\epsilon(m-1) + \mathbf{F}_m\epsilon(-m-1) + \mathbf{F}_0\delta_m = \mathbf{F}_m.$$

Multiplying the previous equation by μ and summing from $-\infty$ to ∞ we find

$$\mu^2 \sum_m \mathbf{R} \mathbf{T}_m + \mu^2 \sum_m \mathbf{T}_m \mathbf{R} = \mu \sum_m \mathbf{F}_m,$$

from which the Lyapounov equation in (6.3) follows directly.

Bibliography

- Belt, H. J. W. and H. J. Butterweck (1996). Cascaded all-pass sections for LMS adaptive filtering. In *Signal Processing VIII: Theories and Applications, Proc. EUSIPCO-96, Eighth European Signal Processing Conference*, Trieste, Italy, pp. 1219–1222.
- Belt, H. J. W. and A. C. den Brinker (1996). Laguerre filters with adaptive pole optimization. In *Proc. IEEE International Symposium on Circuits and Systems (ISCAS)*, Atlanta (GA), U.S.A., pp. 37–40.
- Broome, P. W. (1965). Discrete orthonormal sequences. *Journal of the Association for Computing Machinery* 12, 151–168.
- Butterweck, H. J. (1995). A steady-state analysis of the LMS adaptive algorithm without use of the independence assumption. In *Proc. IEEE International Conference on Acoustics, Speech and Signal Processing (ICASSP)*, Detroit (MI), U.S.A., pp. 1404–1407.
- Butterweck, H. J. (1996a). A new interpretation of the misadjustment in adaptive filtering. In *Proc. IEEE International Conference on Acoustics, Speech and Signal Processing (ICASSP)*, Atlanta (GA), U.S.A., pp. 1641–1643.
- Butterweck, H. J. (1996b). An approach to LMS adaptive filtering without use of the independence assumption. In *Signal Processing VIII: Theories and Applications, Proc. EUSIPCO-96, Eighth European Signal Processing Conference*, Trieste, Italy, pp. 1223–1226.
- Haykin, S. (1996). *Adaptive Filter Theory, Third Edition*. London, U.K.: Prentice-Hall Int.
- Kautz, W. (1954). Transient synthesis in the time domain. *IRE Trans. Circuit Theory* 1, 29–39.
- King, R. E. and P. N. Paraskevopoulos (1977). Digital Laguerre filters. *Int. J. Circuit Theory Appl.* 5, 81–91.
- Oliveira e Silva, T. (1994). Kautz filters. English translation of a work written in Portuguese for the “Prémio Científico IBM 94”.
URL: <ftp://inesca.inesca.pt/pub/tos/English/ibm94e.ps.gz>.

Chapter 7

Laguerre Filters with Adaptive Pole Optimization*

Abstract

In the field of adaptive filtering the most commonly applied structure, the Tapped-Delay Line (TDL) or transversal filter, has an impulse response of finite duration. This is problematic when the adaptive filter is required to resemble a system with long memory. An adaptive Laguerre filter is a specific generalization of the adaptive transversal filter. The delay elements in the transversal filter are replaced by first-order Infinite Impulse Response (IIR) all-pass sections with (real) pole ξ , and the resulting structure is preceded by a first-order IIR low-pass section, again with pole ξ . Due to its IIR character, an adaptive Laguerre filter can show superior performance compared to the TDL when imitating a system with long memory. The degree of superiority depends critically on a proper parametrization of the pole ξ .

In this chapter a new method is proposed to adaptively optimize the pole ξ . To this end we employ a sign algorithm. We perform an analysis of the transients at the output of the Laguerre filter that are caused by the continual tuning of the Laguerre pole. The analysis leads to a choice of the step-size in the sign algorithm. This step-size is such that the cumulative transient signal at the output of the Laguerre filter remains sufficiently small. Also, with this step-size, stability of the Laguerre filter is ensured. A computer experiment shows that the proposed algorithm performs well, both in the steady state and under tracking conditions.

*This chapter is based on a paper with the same title presented in cooperation with A.C. den Brinker at the IEEE International Symposium on Circuits and Systems (ISCAS), Atlanta, GA, USA, May 12-15, 1996. See reference (Belt and den Brinker 1996).

7.1 Introduction

In an adaptive filter the number of weights should be kept as small as possible for three reasons (den Brinker 1993; Belt and Butterweck 1996). First, the use of many weights will result in a large computational load. Second, with many weights the requirements to be imposed on the input signal of the adaptive filter to prevent an ill-conditioned approximation problem might be too severe. Third, the better approximation of the unknown reference filter due to adding more weights might be counteracted by the increase of the total weight fluctuations and the resulting misadjustment.

The TDL is a linear regression model in its simplest form. Its output signal is formed by a linear combination of the input signal at various delays. A more general linear regression model consists of a set of IIR filters of which the outputs are weighted and then summed. A reduction in the number of weights can be achieved when these IIR filters contain the most important characteristics of the reference filter. Among the IIR regression models the discrete Laguerre filters (King and Paraskevopoulos 1977) deserve special attention because of their implementational simplicity. Similar to the impulse responses at the taps of a TDL, the impulse responses at the taps of a discrete Laguerre filter form an orthonormal set of functions. As a consequence, much of the theory developed for the adaptive TDL can be taken over to the adaptive Laguerre filter.

In this chapter we consider an adaptive Laguerre filter. A Laguerre filter contains a recursive parameter in the form of a (multiple) real pole. To obtain a Laguerre filter with only a few adaptive weights, it is useful to adapt the Laguerre pole as well. However, adapting a recursive parameter will result in transients that may deteriorate the adaptation process. We will develop an algorithm to adaptively optimize the Laguerre pole while keeping the transients negligibly small.

In Section 7.2 we introduce the discrete Laguerre functions and the discrete Laguerre filter. Section 7.3 concerns the adaptive use of the Laguerre filter. First, the adaptation of the weights is discussed. Then, the adaptive optimization algorithm for the Laguerre pole is presented. In Section 7.4 the proposed algorithm is illustrated by a computer experiment. Finally, Section 7.5 contains a brief discussion.

7.2 Laguerre Functions and Filters

7.2.1 Laguerre Functions

Let \mathbb{N}_0 denote the set of nonnegative integers. The classical *discrete Laguerre polynomials* are given by (Abramowitz and Stegun 1970)

$$\gamma_m(k) = \frac{m!}{\vartheta^{m+k}} \Delta^m \left[\binom{k}{m} \vartheta^k \right],$$

where $0 < \vartheta < 1$, $m \in \mathbb{N}_0$, $n \in \mathbb{N}_0$; Δ^m is the m -th forward difference operator¹. The polynomials are orthogonal under the weight function ϑ^k :

$$\sum_{k=0}^{\infty} \vartheta^k \gamma_m(k) \gamma_n(k) = \delta_{mn} h_m^2, \quad h_m^2 = \frac{(m!)^2}{\vartheta^m (1 - \vartheta)},$$

where δ_{mn} is the Kronecker delta. From the polynomials and the square root of the weight function and the normalization constant h_m , discrete functions can be constructed that are orthonormal on the interval $[0, \infty)$ with respect to a unity weight function. These function are given by

$$g_m(\xi; k) = \frac{(-1)^m}{m!} \sqrt{1 - \xi^2} \xi^{m+k} \gamma_m(k), \quad (7.1)$$

where $\xi = \sqrt{\vartheta}$ so that $0 < \xi < 1$. The functions in (7.1) are called the *discrete Laguerre functions*, see e.g. (Gottlieb 1938; Broome 1965). The orthonormality of the Laguerre functions is expressed by

$$\sum_{k=0}^{\infty} g_m(\xi; k) g_n(\xi; k) = \delta_{mn}.$$

The Laguerre functions form a complete orthonormal set in the Hilbert space $\ell_2(\mathbb{N}_0)$ of square-summable functions. This means that any function in $\ell_2(\mathbb{N}_0)$ can be approximated to any desired degree by a linear combination of Laguerre functions. An important feature of the Laguerre functions is that they have rational z -transforms:

$$G_m(\xi; z) = B(z) A^m(z), \quad B(z) = \sqrt{1 - \xi^2} \frac{z}{z - \xi}, \quad A(z) = \left(\frac{1 - \xi z}{z - \xi} \right). \quad (7.2)$$

With Parseval's theorem the orthonormality of the Laguerre functions can also be expressed in the z -domain:

$$\sum_{k=0}^{\infty} g_m(\xi; k) g_n(\xi; k) = \frac{1}{2\pi j} \oint G_m(\xi; z) G_n^*(\xi; 1/z^*) \frac{dz}{z} = \delta_{mn}. \quad (7.3)$$

As a result of the specific form of their z -transforms in (7.2), the Laguerre functions can efficiently be generated as the impulse responses of a *Laguerre network*, cf. Fig. 7.1. It consists of a cascade of identical first-order all-pass sections $A(z)$ preceded by a first-order low-pass section $B(z)$. In the Laguerre network the parameter ξ appears as a pole henceforth referred to as the *Laguerre pole*. Note that when $\xi = 0$ the Laguerre functions simply become delays ($G_m(0; z) = z^{-m}$) and the Laguerre network reduces to a delay line.

¹The m -th forward difference operator is recursively defined by $\Delta^m [f(k)] = \Delta^{m-1} [f(k+1) - f(k)]$, with $\Delta^0 [f(k)] = f(k)$.

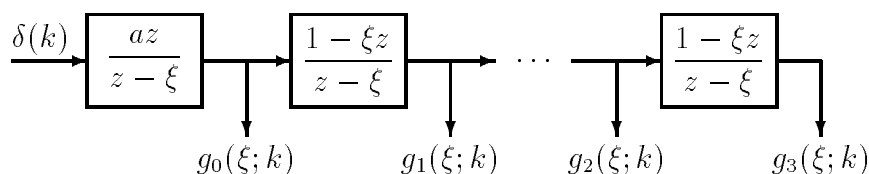


Figure 7.1: Discrete Laguerre network. The impulse responses $g_m(\xi; k)$ are the discrete Laguerre functions. Further, $a = (1 - \xi^2)^{\frac{1}{2}}$.

7.2.2 Laguerre Filters

Consider a Laguerre network with M all-pass sections ($M + 1$ outputs). The excitation $x(k)$ is a zero-mean, stationary stochastic signal with power σ_x^2 . Its power spectral density function is denoted by $\Phi_{xx}(\Omega)$, where Ω is the normalized frequency ($0 < \Omega \leq 2\pi$). The $M + 1$ outputs of the network, henceforth referred to as the *tap signals*, are denoted by $u_m(k)$ with $m = 0, 1, \dots, M$. In vector notation these tap signals are written as

$$\underline{u}(k) = [u_0(k), u_1(k), \dots, u_M(k)]^T.$$

By a linear combination of the tap signals an output signal $y(k)$ is formed. The weights in the linear combination are denoted by w_m with $m = 0, 1, \dots, M$ or, in vector notation,

$$\underline{w} = [w_0, w_1, \dots, w_M]^T.$$

The output signal $y(k)$ is given by

$$y(k) = \sum_{m=0}^M w_m u_m(k) = \underline{w}^T \underline{u}(k).$$

The resulting structure is called a *discrete Laguerre filter*. In Fig. 7.2 the Laguerre filter is depicted in an adaptive filtering setup.

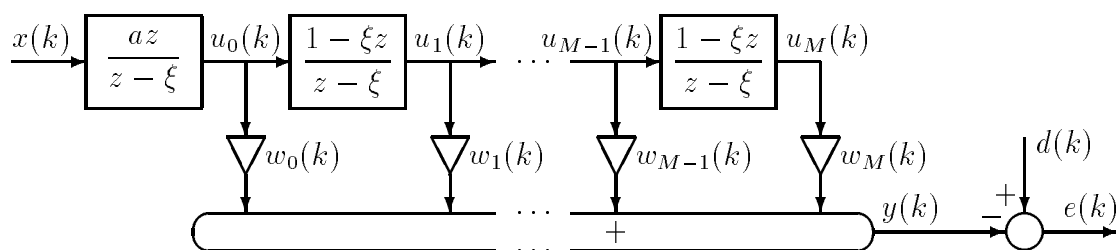


Figure 7.2: Discrete Laguerre filter with $a = (1 - \xi^2)^{\frac{1}{2}}$.

The error signal $e(k)$ is formed by subtracting from the desired signal $d(k)$ the output $y(k)$ of the adaptive filter: $e(k) = d(k) - y(k)$. Consider the minimization of the *Mean-Squared Error* (MSE), given by

$$\mathcal{J} = E\{e^2(k)\}. \quad (7.4)$$

It is well known that the weights that minimize (7.4) are given by the Wiener-Hopf or normal equations, which read in matrix form

$$\mathbf{R}\underline{w} = \underline{p}. \quad (7.5)$$

Here, $\underline{p} = E\{d(k)\underline{u}(k)\}$ and \mathbf{R} is the covariance matrix of the tap signals of the Laguerre network:

$$\mathbf{R} = E\{\underline{u}(k)\underline{u}^T(k)\} = \begin{pmatrix} E\{u_0^2(k)\} & E\{u_0(k)u_1(k)\} & \dots & E\{u_0(k)u_M(k)\} \\ E\{u_1(k)u_0(k)\} & E\{u_1^2(k)\} & \dots & E\{u_1(k)u_M(k)\} \\ \vdots & \vdots & \ddots & \vdots \\ E\{u_M(k)u_0(k)\} & E\{u_M(k)u_1(k)\} & \dots & E\{u_M^2(k)\} \end{pmatrix}.$$

Clearly, the matrix \mathbf{R} is symmetric. Also, because $x(k)$ is stationary the matrix \mathbf{R} is Toeplitz, meaning that all elements on a diagonal are equal. This is a direct consequence of the all-pass structure and can easily be seen as follows:

$$\begin{aligned} E\{u_p(k)u_q(k)\} &= \frac{1}{2\pi} \int_{-\pi}^{\pi} \Phi_{xx}(\Omega) G_p(\xi; e^{j\Omega}) G_q(\xi; e^{-j\Omega}) d\Omega \\ &= \frac{1}{2\pi} \int_{-\pi}^{\pi} \Phi_{xx}(\Omega) |G_0(e^{j\Omega})|^2 |A(e^{j\Omega})|^{p-q} d\Omega, \end{aligned}$$

which is a function of the difference between p and q only.

Solving the normal equations in (7.5) involves the inversion of \mathbf{R} which can be a tedious job, especially when the number of weights is large. Fortunately, the symmetric Toeplitz structure of \mathbf{R} allows an efficient recursive method to solve the normal equations, see (Levinson 1947).

Since \mathbf{R} is associated with a dyadic product the matrix is always nonnegative definite. To ensure that \mathbf{R} is strictly positive definite, so that its inverse exists, its smallest eigenvalue must be strictly positive. Let λ_m with $m = 0, 1, \dots, M$ be the eigenvalues of \mathbf{R} . In Section 2.7 it was proven that the orthonormality of the individual impulse responses of the Laguerre network (the Laguerre functions) implies that the eigenvalues of \mathbf{R} satisfy

$$\min_{\Omega} \Phi_{xx}(\Omega) \leq \lambda_m \leq \max_{\Omega} \Phi_{xx}(\Omega), \quad m = 0, 1, \dots, M.$$

We will henceforth assume that $x(k)$ is *persistently exciting*, meaning that $\Phi_{xx}(\Omega) > 0$ for all frequencies. As a result $\min_m \lambda_m > 0$ and \mathbf{R} is strictly positive definite, so that \mathbf{R}^{-1} exists and the Wiener-Hopf equations can be solved. Note that the condition number of \mathbf{R} , defined by $\max_m \lambda_m / \min_m \lambda_m$, is upper-bounded.

In view of a small MSE the choice of the Laguerre pole is essential. In (Oliveira e Silva 1994) and (Oliveira e Silva 1995) the problem of how to find the optimal Laguerre pole is addressed. Assuming that the normal equations in (7.5) are satisfied, the following useful expression has been derived by Oliveira e Silva (1994):

$$\frac{\partial \mathcal{J}}{\partial \xi} = -\frac{2(M+1)w_M}{1-\xi^2} E\{e(k)u_{M+1}(k)\}. \quad (7.6)$$

The signal $u_{M+1}(k)$ occurring in (7.6) can be obtained using one additional all-pass section.

7.3 Adaptive Laguerre Filters

In this section we study the discrete Laguerre filter in an adaptive environment, as is done in e.g. (den Brinker 1993) or (den Brinker 1994). The weights can be optimized using well-known adaptation algorithms such as the *(Normalized) Least-Mean-Square* ((N)LMS) algorithm or the standard *Recursive Least-Squares* (RLS) algorithm. We will add more flexibility to the adaptive Laguerre filter by simultaneously optimizing the Laguerre pole. To this end the derivative in (7.6) can be used when it is assumed that the weights are (near) optimal. Care must be taken to ensure stability of the Laguerre filter, i.e. $|\xi| < 1$. Also, transients due to the tuning of the recursive parameter must remain sufficiently small in a sense to be discussed below.

7.3.1 Adapting the Laguerre Weights

The Laguerre weights \underline{w} can be optimized adaptively using the LMS algorithm. This algorithm is given by (Haykin 1996)

$$\underline{w}(k+1) = \underline{w}(k) + \mu \underline{u}(k) e(k),$$

where μ is the step-size.

Alternatively, the Laguerre weights can be adapted using the standard RLS algorithm, given by (Haykin 1996)

$$\underline{w}(k+1) = \underline{w}(k) + \hat{\mathbf{R}}^{-1}(k) \underline{u}(k) e(k),$$

where

$$\hat{\mathbf{R}}(k) = \sum_{l=-\infty}^k \lambda^{k-l} \underline{u}(l) \underline{u}^T(l) = \lambda \hat{\mathbf{R}}(k-1) + \underline{u}(k) \underline{u}^T(k),$$

and λ is the exponential weighting or forgetting factor satisfying $0 < \lambda < 1$. Instead of updating $\hat{\mathbf{R}}(k)$ and then performing a matrix inversion for the weight vector update, it is possible to keep track of $\hat{\mathbf{R}}^{-1}(k)$ with

$$\hat{\mathbf{R}}^{-1}(k) = \frac{1}{\lambda} \left\{ \hat{\mathbf{R}}^{-1}(k-1) - \frac{\hat{\mathbf{R}}^{-1}(k-1) \underline{u}(k) \underline{u}^T(k) \hat{\mathbf{R}}^{-1}(k-1)}{\lambda + \underline{u}^T(k) \hat{\mathbf{R}}^{-1}(k-1) \underline{u}(k)} \right\}.$$

7.3.2 Adapting the Laguerre Pole

Similar to the Laguerre weights, the Laguerre pole is updated at each sampling instant. A sign algorithm is used in order to keep complete control of the step-size with which the Laguerre pole is changed. The sign of the derivative given in (7.6) determines the direction of the pole update. With $\mathcal{V}(k)$ an estimate for $E\{e(k) u_{M+1}(k)\}$, the proposed sign algorithm is given by ($0 \leq \theta < 1$):

$$\begin{aligned} \mathcal{V}(k+1) &= \theta \mathcal{V}(k) + (1-\theta) e(k) u_{M+1}(k), \\ \xi(k+1) &= \xi(k) - \Delta \xi(k) \text{sign}\{-w_M(k) \mathcal{V}(k)\}. \end{aligned} \quad (7.7)$$

The update of the pole in (7.7) is thus based on the method of steepest descent: the new pole is formed by the old pole plus a small step in the opposite direction of the derivative of the error criterion with respect to the pole.

Due to the recursive nature of the Laguerre filter, adaptation of the Laguerre pole inevitably leads to transients. Our goal is to design the step-size $\Delta\xi(k)$ in (7.7) in such a way that the effect of these transients remains negligibly small at the output of the adaptive Laguerre filter.

A single abrupt pole change causes a transient in each Laguerre section and each of these transients contributes to the transient in the next section. For this reason we expect the most dominant transient to occur at the output of the last Laguerre section. We will hereafter perform a transient analysis for the Laguerre filter. In this analysis we assume that the Laguerre pole fluctuates around its steady state value, and that subsequent pole fluctuations are uncorrelated. We will investigate at the last output $u_{M+1}(k)$ the power of the *cumulative transient signal* $t_{M+1}(k)$ that is composed of currently and previously evoked transients in all Laguerre sections. The power $E\{t_{M+1}^2(k)\}$ will then be related to the power of the response at the last output to the input $x(k)$. The latter power equals σ_x^2 when $x(k)$ is white because the Laguerre function $g_{M+1}(\xi; k)$ has unity norm.

Let $\Delta\xi(k)$ be a stationary white noise sequence with variance $\sigma_{\Delta\xi}^2$ that is small compared to ξ_0 . We will arrive at the following bound

$$\frac{E\{t_{M+1}^2(k)\}}{\sigma_x^2} < \frac{\sigma_{\Delta\xi}^2}{(1 - \xi_0^2)^3} \left\{ \frac{2(M+2)(2M^2 + 5M + 6)}{3} \right\}. \quad (7.8)$$

This upper bound provides us the means to make a choice for $\Delta\xi(k)$ in (7.7) such that the cumulative transient signal at $u_{M+1}(k)$ remains much smaller in power than the response to $x(k)$, and can therefore be neglected. In (7.7) we take

$$\begin{aligned} \Delta\xi(k) &= \mu_\xi (1 - \xi^2(k))^{\frac{3}{2}}, \\ \mu_\xi &\ll \sqrt{\frac{3}{2(M+2)(2M^2 + 5M + 6)}}. \end{aligned} \quad (7.9)$$

Note that with (7.9) stability of the Laguerre filter is guaranteed.

We now perform the analysis leading to (7.8). Consider a Laguerre network with fixed pole $\xi = \xi_0$ excited by $x(k)$. The network is assumed to operate in the steady state, meaning that all initial conditions have been 'forgotten'. In Fig. 7.3 a direct form implementation of a Laguerre low-pass and a Laguerre all-pass section is shown. The m -th internal state at instant k of the network operating in the steady state with fixed pole ξ is denoted by $s_m(\xi; k)$, where $m = 0, 1, \dots, M, M+1$ (remember that one extra all-pass section is required for the gradient in (7.6)). Now it will be demonstrated that an abrupt change of the pole causes a transient at each tap output, and that such a transient can be expressed in a Laguerre series.

Assume that at instant $k = k_0$ the Laguerre pole is abruptly changed from ξ_0 to $\xi_1 = \xi_0 + \Delta\xi$, where $\Delta\xi$ is a small number ($|\Delta\xi| \ll \xi_0$). This abrupt pole change can be

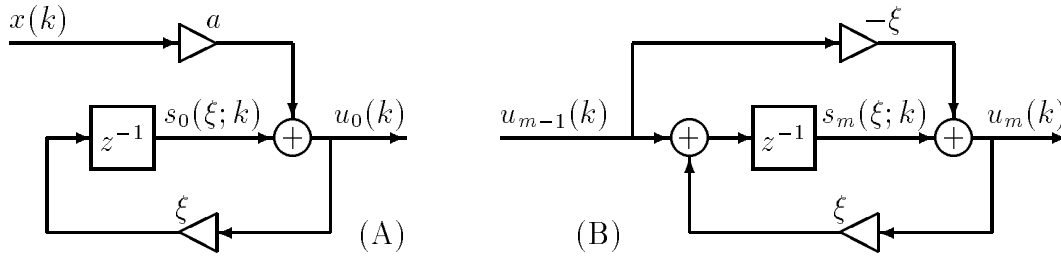


Figure 7.3: (A) Direct form implementation of a Laguerre low-pass section with $a = (1 - \xi^2)^{\frac{1}{2}}$; (B) Direct form implementation of the m -th Laguerre all-pass section with $m = 1, 2, \dots, M + 1$.

expressed by

$$\xi(k) = \xi_0 + \Delta\xi \epsilon(k - k_0),$$

where $\epsilon(k)$ is the unit step function ($\epsilon(k) = 0$ for $k < 0$ and $\epsilon(k) = 1$ for $k \geq 0$). Since the internal states of the Laguerre network are determined by the complete past, they are not associated with the new pole $\xi_1 = \xi_0 + \Delta\xi$; the internal states are erroneous with respect to the pole ξ_1 . We define the m -th *state error* at instant $k = k_0$, denoted by $\Delta s_m(k_0)$, as

$$\Delta s_m(k_0) = s_m(\xi_1; k_0) - s_m(\xi_0; k_0). \tag{7.10}$$

In words: $\Delta s_m(k_0)$ is the difference between the m -th state at instant k_0 of an imaginary Laguerre network that is operating in the steady state with pole ξ_1 (same excitation), and the m -th state at instant $k = k_0$ of the Laguerre network under consideration.

We could replace all erroneous states $s_m(\xi_0; k_0)$ by the correct states $s_m(\xi_1; k_0)$. Then at each state a correction term is required of the form $f_m(k) = -\Delta s_m(k_0)\delta(k - k_0)$, where $\delta(k)$ is the unit pulse function. The situation is depicted in Fig. 7.4.

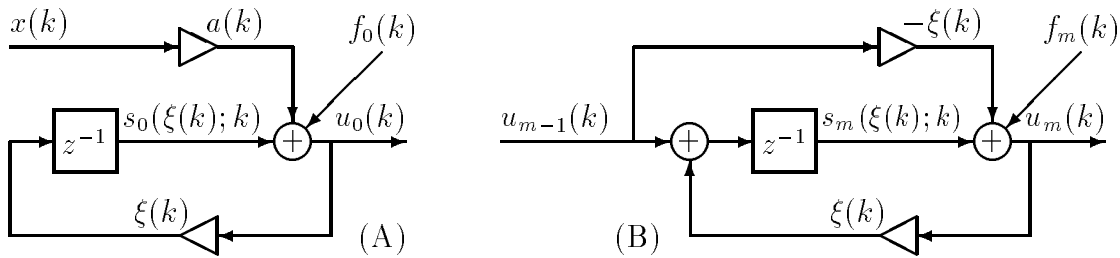


Figure 7.4: Laguerre low-pass (A) and all-pass (B) section. A single abrupt pole change according to $\xi(k) = \xi_0 + \Delta\xi\epsilon(k - k_0)$ causes a transient at each Laguerre section that can be thought of as caused by the impulse excitation $f_m(k)$ at each section.

The impulsive excitation $f_m(k)$ at a summator in the m -th section causes a transient signal starting at instant $k = k_0$ at each following tap output $u_{m+n}(k)$ ($n = 0, 1, \dots, M +$

$1 - m$). Conversely, at each tap output $u_m(k)$ a transient signal $\tau_m(k_0; k)$ is observed that is composed of a sum of transients originating from the section under consideration and all preceding sections. From this we expect the most dominant transient signal to occur at the last tap output $u_{M+1}(k)$.

It can easily be verified that the transfer function from the m -th state to the tap output $u_{m+n}(k)$ is given by $(1 - \xi_1^2)^{-1/2} G_n(\xi_1; z)$. Consequently, the transient $\tau_{M+1}(k_0; k)$ at the tap output $u_{M+1}(k)$ can be expressed by Laguerre series according to

$$\tau_{M+1}(k_0; k) = \frac{-1}{\sqrt{1 - \xi_1^2}} \sum_{m=0}^{M+1} \Delta s_m(k_0) g_{M+1-m}(\xi_1; k - k_0), \quad k \geq k_0.$$

Next we consider the case that at each instant k the Laguerre pole is varied according to $\xi(k) = \xi_0 + \Delta\xi(k)$, where $\Delta\xi(k)$ is zero-mean, stationary white noise with small power $\sigma_{\Delta\xi}^2$ (small compared to ξ_0). In the practical situation where the pole is varied by the sign algorithm in (7.7), subsequent pole variations are not completely uncorrelated. However, for the purpose of a traceable analysis we assume that they are. We look at the cumulative transient signal at the $M+1$ -th tap output, denoted by $t_{M+1}(k)$, as a result of the continual tuning of the Laguerre pole $\xi(k)$ around its steady-state value ξ_0 , and find:

$$\begin{aligned} t_{M+1}(k) &= \sum_{l=-\infty}^k \tau_{M+1}(l; k) \\ &= \sum_{l=-\infty}^k \frac{-1}{\sqrt{1 - \xi^2(l)}} \sum_{m=0}^{M+1} \Delta s_m(l) g_{M+1-m}(\xi(l); k - l). \end{aligned}$$

For the power of $t_{M+1}(k)$ we may thus write

$$E\{t_{M+1}^2(k)\} = E\left\{ \left[\sum_{l=-\infty}^k \frac{1}{1 - \xi^2(l)} \sum_{m=0}^{M+1} \Delta s_m(l) g_{M+1-m}(\xi(l); k - l) \right]^2 \right\}.$$

Replacing $\xi(l)$ by its mean value ξ_0 in the previous expression introduces only a small error (since $\sigma_{\Delta\xi}^2$ is small), and thus

$$E\{t_{M+1}^2(k)\} \approx \frac{1}{1 - \xi_0^2} E\left\{ \left[\sum_{l=-\infty}^k \sum_{m=0}^{M+1} \Delta s_m(l) g_{M+1-m}(\xi_0; k - l) \right]^2 \right\}$$

Further, the whiteness of $\Delta\xi(k)$ implies that $E\{\Delta s_{m_1}(l_1) \Delta s_{m_2}(l_2)\} = 0$ when $l_1 \neq l_2$, meaning that at different sampling instants all state errors are mutually uncorrelated. Using this and the fact that the Laguerre functions are orthonormal we arrive at the following approximate expression for the power of the cumulative transient signal at tap output $u_{M+1}(k)$:

$$E\{t_{M+1}^2(k)\}$$

$$\begin{aligned}
&\approx \frac{1}{1-\xi_0^2} \sum_{m_1, m_2=0}^{M+1} \sum_{l=-\infty}^k E\{\Delta s_{m_1}(l)\Delta s_{m_2}(l)\} g_{M+1-m_1}(\xi_0; k-l) g_{M+1-m_2}(\xi_0; k-l) \\
&= \frac{1}{1-\xi_0^2} \sum_{m_1, m_2=0}^{M+1} E\{\Delta s_{m_1}(k)\Delta s_{m_2}(k)\} \sum_{l=-\infty}^k g_{M+1-m_1}(\xi_0; k-l) g_{M+1-m_2}(\xi_0; k-l) \\
&= \frac{1}{1-\xi_0^2} \sum_{m=0}^{M+1} E\{\Delta s_m^2(k)\}. \tag{7.11}
\end{aligned}$$

Apparently, under our assumption that subsequent pole fluctuations are uncorrelated, the power of the cumulative transient signal is obtained simply by a superposition of the powers of the state errors. This justifies our previous reasoning that the largest transients occur at the output of the last Laguerre all-pass section.

We now determine $E\{\Delta s_m^2(k)\}$. Let $H_m(\xi; z)$ be the transfer function from the input $x(k)$ to the m -th state $s_m(k)$ with impulse response $h_m(\xi; k)$. We may write for $H_m(\xi; z)$ (see Fig. 7.3)

$$H_m(\xi; z) = \begin{cases} z^{-1}\{\xi G_m(\xi; z) + G_{m-1}(\xi; z)\}, & m = 1, 2, \dots \\ z^{-1}\{\xi G_0(\xi; z)\}, & m = 0. \end{cases} \tag{7.12}$$

Further, we need the following remarkable property of the Laguerre functions (Oliveira e Silva 1994):

$$\frac{\partial G_m(\xi; z)}{\partial \xi} = \frac{(m+1)G_{m+1}(\xi; z) - mG_{m-1}(\xi; z)}{1-\xi^2}, \quad m \in \mathbb{N}_0. \tag{7.13}$$

We may write with (7.10) and (7.12)

$$\begin{aligned}
E\{\Delta s_m^2(k)\} &= E\{[s_m(\xi_0 + \Delta\xi; k) - s_m(\xi_0; k)]^2\} \\
&= E\{[h_m(\xi_0 + \Delta\xi; k) * x(k) - h_m(\xi_0; k) * x(k)]^2\}.
\end{aligned}$$

Here the $*$ denotes a convolution. In a first-order approximation we have that

$$H_m(\xi_0 + \Delta\xi; z) - H_m(\xi_0; z) \approx \Delta\xi \frac{\partial H_m(\xi_0; z)}{\partial \xi},$$

so that the whiteness of $\Delta\xi(k)$ leads to

$$E\{\Delta s_m^2(k)\} \approx \frac{\sigma_x^2 \sigma_{\Delta\xi}^2}{2\pi j} \oint_C \left(\frac{\partial H_m(\xi; z)}{\partial \xi} \frac{\partial H_m^*(\xi; 1/z^*)}{\partial \xi} \right) \Big|_{\xi=\xi_0} \frac{dz}{z}, \tag{7.14}$$

where integration is performed counter-clockwise along the unit circle C in the z -plane. We now find from (7.12), (7.13) and (7.14) that

$$E\{\Delta s_m^2(k)\} \approx \frac{\sigma_x^2 \sigma_{\Delta\xi}^2}{(1-\xi_0^2)^2} \{(\xi_0^4 - \xi_0^2 + 2 - \delta(m)) + m^2(2\xi_0^2 + 2)\}. \tag{7.15}$$

With the standard summation

$$\sum_{m=0}^{M+1} m^2 = \frac{(M+1)(M+2)(2M+3)}{6}$$

we find after combining (7.11) and (7.15) that

$$E\{t_{M+1}^2(k)\} \approx \frac{\sigma_x^2 \sigma_{\Delta\xi}^2}{(1-\xi_0^2)^3} \left\{ -1 + (M+2) \frac{3\xi_0^4 + (2M^2 + 5M)(\xi_0^2 + 1) + 9}{3} \right\}.$$

Using the fact that $\xi_0^2 < 1$ we arrive at the bound given in (7.8).

Important remark: To allow simultaneous use of the RLS algorithm for the weights and the sign algorithm for the pole, these two algorithms must operate on completely different time scales. This follows from the fact that in the derivation leading to the gradient in (7.6) the weights are assumed to satisfy the normal equations (7.5). For an accurate determination of the weights θ should be chosen such that the memory of the RLS algorithm² is larger than the memory of the adaptive filter³. The parameter μ_ξ must be chosen sufficiently small to ensure that the weights have converged towards their optimal values given in (7.5) long before the pole can make any relevant change.

7.4 An Example

As an example of the proposed algorithm a computer experiment has been performed. In the experiment both the adaptation and tracking behaviour of the algorithm are tested.

The reference filter used for the experiment was a Laguerre filter with 4 sections and weights $\underline{w} = [-1, 1, 2, 3]^t$. The excitation signal $x(k)$ was zero-mean, white, Gaussian noise with unity variance. Zero-mean, white Gaussian noise with variance 0.1 was added to the output of the reference filter. The pole of the reference filter was varied as indicated by the dotted line in Fig. 7.5A. The adaptation parameters that were used are given by: $\theta = 0.98$, $\lambda = 0.90$ and $\mu_\xi = 10^{-4}$.

As can be seen in Fig. 7.5A, in the initial adaptation phase the Laguerre pole moves from its initial value 0.8 towards its optimal value 0.9. In this adaptation phase the weights (Fig. 7.5B) vary rapidly since the optimal weight vector changes when the pole of the adaptive filter changes. When the pole reaches the steady state the weights settle at their optimal values $[-1, 1, 2, 3]^t$. As can also be seen from Fig. 7.5A the pole adaptation algorithm performs well under tracking conditions.

²The inverse of $1 - \theta$ is, roughly speaking, a measure of the memory of the RLS algorithm (Haykin 1996).

³In this respect it could be advantageous to extend the algorithm such that θ is adapted on the basis of current and past values of the Laguerre pole $\xi(k)$.

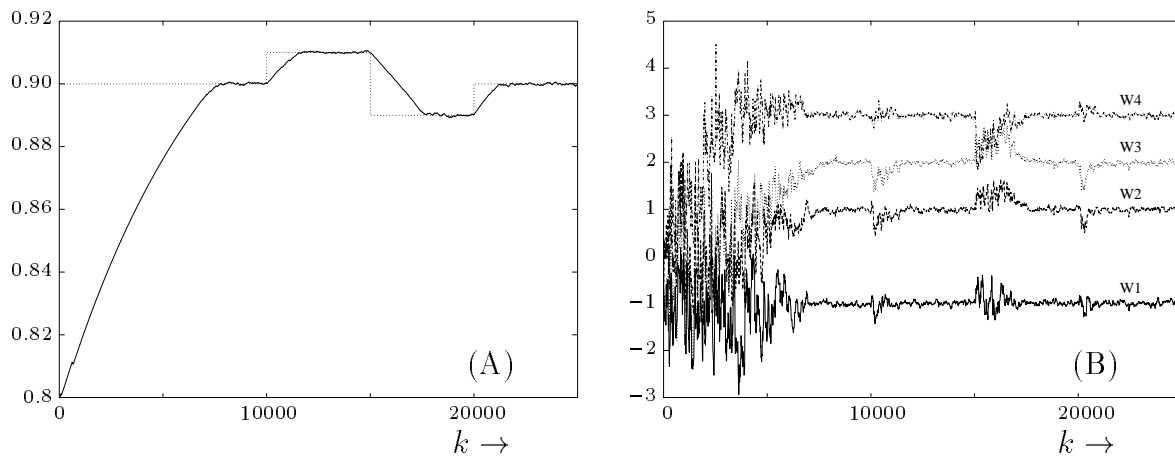


Figure 7.5: (A) Convergence and tracking behaviour of the adaptive Laguerre pole. The dotted line indicates the variations of the pole of the reference filter; (B) The behaviour of the weights.

7.5 Discussion

In this chapter we have presented an adaptive optimization method for the Laguerre pole in an adaptive Laguerre filter. The gradient required for the pole adaptation can easily be obtained, which makes the method simple and easy to implement. We have used a sign algorithm to update the Laguerre pole to have control of the step-sizes with which the pole is varied. These step-sizes have been designed in such a way that the cumulative transient signal caused by the continual tuning of the pole remains negligibly small in power.

The analysis in this chapter is done assuming that the excitation signal $x(k)$ is white noise. However, $x(k)$ may also have a low-pass character, as long as the power spectral density function of the output of the first Laguerre section (i.e. a first-order low-pass section) is not noticeably affected.

Bibliography

- Abramowitz, M. and I. A. Stegun (1970). *Handbook of Mathematical Functions*. New York (NY), U.S.A.: Dover Publications.
- Belt, H. J. W. and H. J. Butterweck (1996). Cascaded all-pass sections for LMS adaptive filtering. In *Signal Processing VIII: Theories and Applications, Proc. EUSIPCO-96, Eighth European Signal Processing Conference*, Trieste, Italy, pp. 1219–1222.
- Belt, H. J. W. and A. C. den Brinker (1996). Laguerre filters with adaptive pole optimization. In *Proc. IEEE International Symposium on Circuits and Systems (ISCAS)*, Atlanta (GA), U.S.A., pp. 37–40.

- Broome, P. W. (1965). Discrete orthonormal sequences. *Journal of the Association for Computing Machinery* 12, 151–168.
- den Brinker, A. C. (1993). Adaptive orthonormal filters. In *Preprints Proc. 12th World Congress of the International Federation of Automatic Control (IFAC)*, Volume 5, Sydney, Australia, pp. 287–292.
- den Brinker, A. C. (1994). Laguerre-domain adaptive filters. *IEEE Trans. Signal Process.* 42, 953–956.
- Gottlieb, M. J. (1938). Concerning some polynomials orthogonal on a finite or enumerable set of points. *Am. J. Math.* 60, 453–458.
- Haykin, S. (1996). *Adaptive Filter Theory, Third Edition*. London, U.K.: Prentice-Hall Int.
- King, R. E. and P. N. Paraskevopoulos (1977). Digital Laguerre filters. *Int. J. Circuit Theory Appl.* 5, 81–91.
- Levinson, N. (1947). The Wiener RMS error criterion in filter design and prediction. *J. Math. Phys.* 25, 261–278.
- Oliveira e Silva, T. (1994). Optimality conditions for truncated Laguerre networks. *IEEE Trans. Signal Process.* 42, 2528–2530.
- Oliveira e Silva, T. (1995). On the determination of the optimal pole position of Laguerre filters. *IEEE Trans. Signal Process.* 43, 2079–2087.

Chapter 8

A Second-Order IIR Adaptive Line Enhancer*

Abstract

A new Adaptive Line Enhancer (ALE) is proposed for the separation of a low-level sinusoid or narrow-band signal from broad-band noise. A specific second-order IIR filter is considered as the basic component of the (ALE). A new feature is that both the radius and the angle of a complex pole are adapted. To this end a sign algorithm is used. The step-size in the sign algorithm is pole dependent such that transients resulting from this adaptation remain sufficiently small. Also, with this step-size the poles are guaranteed to remain within the unit circle. Depending on the radius, we have either a fast adaptation (or tracking) or a high signal-to-noise improvement ratio. As an additional feature, a frequency estimate can be obtained by a simple procedure. Simulation results demonstrate the good performance of the proposed ALE with respect to convergence and tracking behaviour.

8.1 Introduction

Separation of a low-level sinusoid or narrow-band random signal from broad-band noise is a classical problem in the field of signal processing, see e.g. the introductory chapter in (Haykin 1996). If the frequency of the sinusoid is known, then the matched filter approach provides the best solution. If, however, the frequency of the sinusoid is unknown or time-varying, one could resort to adaptive filtering techniques. An *Adaptive Line Enhancer* (ALE) is widely used for this purpose. The ALE was first proposed by Widrow *et al.* (1975). The general scheme of the ALE is depicted in Fig. 8.1.

The ALE input $d(k)$ is assumed to be the sum of a narrow-band random signal $s(k)$

*This chapter is based on a paper presented in cooperation with A.C. den Brinker and F.P.A. Benders at the IEEE International Conference on Acoustics, Speech and Signal Processing (ICASSP), Detroit, MI, USA, 9-12 May 1995. See reference (Belt, den Brinker, and Benders 1995).

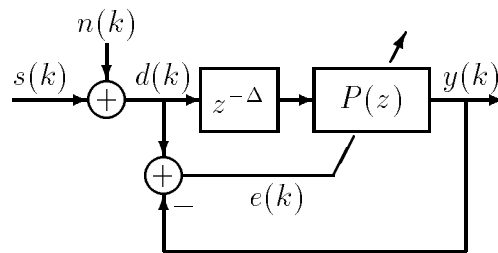


Figure 8.1: The general scheme of the adaptive line enhancer.

and a noisy broad-band random signal $n(k)$. The signal $d(k)$ is delayed by $z^{-\Delta}$, where z^{-1} represents a unit delay and Δ is a fixed positive integer. The prediction filter $P(z)$ operates on $d(k - \Delta)$, yielding the ALE output $y(k)$. The error signal $e(k)$ is obtained by subtracting $y(k)$ from $d(k)$. This error signal is used to adapt the prediction filter in such a way that the Mean-Squared Error (MSE), given by

$$\mathcal{J} = E \{ e^2(k) \}, \quad (8.1)$$

is minimized. The ALE operates by virtue of the difference between the correlation lengths of $s(k)$ and $n(k)$. The delay parameter Δ should be chosen larger than the correlation length of the noise, but smaller than the correlation length of $s(k)$. Then, it is possible for $P(z)$ to make a Δ -step ahead prediction of $s(k)$ based upon the present and past samples of $d(k - \Delta)$. However, $P(z)$ will not be able to predict $n(k)$ from knowledge about present and past samples of $n(k - \Delta)$. As a result, the noise is suppressed at the output $y(k)$ after adaptation of $P(z)$.

Ideally, when the parameters of $P(z)$ are optimal in MSE sense, $y(k)$ is approximately equal to $s(k)$ and $e(k)$ is approximately equal to $n(k)$. Thus, ideally $P(z)$ is a band-pass filter with center frequency corresponding to the frequency of $s(k)$. As a result, $H(z) = 1 - z^{-\Delta}P(z)$ is a notch filter. When $e(k)$ is taken as the output we speak of an *adaptive notch filter*.

Often a transversal filter or Tapped-Delay-Line (TDL) is used for the prediction filter $P(z)$, see e.g. (Widrow *et al.* 1975; Griffiths 1975; Treichler 1979; Zeidler 1990). The major drawback of the TDL is the large number of required weights to obtain the desired sharp band-pass characteristics. Recently, much attention has been paid to ALEs based on second-order IIR filters. An IIR filter with (only a few) appropriately chosen parameters has sharp band-pass characteristics, see (Friedlander 1984; Rao and Kung 1984; Nehorai 1985; David, Stearns, and Elliot 1983; Hush, Ahmed, David, and Stearns 1986; Cho, Choi, and Lee 1989). In most of these contributions the filter center frequency is optimized, whereas the filter bandwidth is fixed at a predetermined value based upon assumed *a priori* knowledge of the bandwidth of $s(k)$. In (Nehorai 1985) the bandwidth is varied by letting the radius of the poles grow exponentially in time towards its final predetermined value in order to get faster convergence. In none of the studies we know of, the filter bandwidth is optimized simultaneously with the peak frequency.

In this chapter an ALE based on a second-order IIR filter is proposed that includes adaptation of the filter bandwidth. In contrast to previous studies on IIR based ALEs, no *a priori* knowledge about the bandwidth of $s(k)$ is required. Also, it is shown that including adaptation of the filter bandwidth yields the possibility to combine fast adaptation with accuracy. Stability monitoring needs special attention when varying the filter bandwidth; in the proposed adaptation algorithm the filter $P(z)$ is guaranteed to be stable. This algorithm also guarantees that transients caused by the tuning of the filter remain much smaller than the response to the input signal.

In Section 8.2 the IIR filter is introduced, together with its properties. Sections 8.3 and 8.4 describe the update rules for the various parameters of the filter. In Section 8.5 it is explained how an estimate of the frequency parameter of a single sinusoid can be obtained. The experimental results in Section 8.6 show that the proposed ALE performs well. Finally, Section 8.7 contains a brief discussion.

8.2 The Second-Order IIR Prediction Filter

The proposed second-order IIR prediction filter is shown in Fig. 8.2. The second-order section $\Lambda(z)$ is given by

$$\Lambda(z) = \frac{z^2}{(z-p)(z-p^*)},$$

where p is the pole and $*$ denotes a complex conjugate. For the pole we write

$$p = re^{j\phi}.$$

Here, r is the pole radius ($0 < r < 1$) and ϕ is the pole angle ($0 < \phi < \pi$).

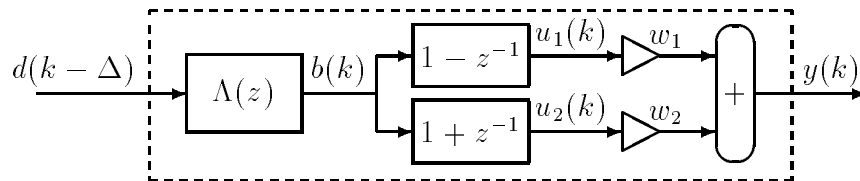


Figure 8.2: The second-order IIR prediction filter, with $\Lambda(z) = z^2/(z-p)(z-p^*)$.

As is shown in Fig. 8.2, $P(z)$ has two internal signals $u_1(k)$ and $u_2(k)$ composing the vector $\underline{u}(k) = [u_1(k), u_2(k)]^T$. Under the assumption that $b(k)$ is a stationary stochastic process, it can easily be verified that $u_1(k)$ and $u_2(k)$ are mutually orthogonal, meaning that their cross-power $E\{u_1(k)u_2(k)\}$ vanishes. As will be shown in Section 8.3, this property gives rise to a very easy-to-implement optimization algorithm for the weights. The weights w_1 and w_2 compose the weight vector $\underline{w} = [w_1, w_2]^T$. The inner product of $\underline{u}(k)$ and \underline{w} yields the ALE output signal $y(k)$. For the error signal shown in Fig. 8.1 we may write

$$e(k) = d(k) - \underline{w}^T \underline{u}(k). \quad (8.2)$$

The transfer function $P(z)$ is given by

$$P(z) = G \frac{z(z - z_0)}{(z - p)(z - p^*)},$$

where $G = (w_1 + w_2)$ is the gain and $z_0 = (w_1 - w_2)/G$ is a real zero of $P(z)$.

The bandwidth B of $P(z)$ is defined by the two half-power (-3dB) frequencies. To guarantee band-pass characteristics for both the transfers from $d(k)$ to $u_1(k)$ and from $d(k)$ to $u_2(k)$, we assume that ϕ is not too near the values 0 and π . In that case a good approximation of the bandwidth is given by

$$B \approx 2(1 - r), \quad (8.3)$$

and thus B is linearly related to the pole radius only. This approximation is a lower bound for the real bandwidth and is increasingly accurate for $r \rightarrow 1$.

The signal to noise ratios at the ALE input $d(k)$ and the ALE output $y(k)$ are denoted by SNR_d and SNR_y , respectively. When the weights and the pole angle are optimal in MSE sense (see Section 8.3) and again assuming that ϕ is not too near the values 0 and π , then the *Signal to Noise Improvement Ratio* (SNIR) of the ALE can be approximated by (Nehorai 1985)

$$\text{SNIR} = \frac{\text{SNR}_y}{\text{SNR}_d} \approx \frac{1}{1 - r}. \quad (8.4)$$

This approximation is increasingly accurate for $r \rightarrow 1$.

In the next two sections we consider the optimization of the four free parameters of $P(z)$, namely w_1 , w_2 , r , and ϕ . To analyze the adaptation of the weights and the poles separately, different time scales are introduced. This is possible because the weights are adapted much faster than the poles.

8.3 Adapting the Weights

During the time interval in which the weights \underline{w} are adapted, the poles are assumed to be fixed. This assumption is justified by the different time scales on which the weights and pole adaptations take place. For this case the optimal weights \underline{w}_o with respect to the MSE (8.1) are given by the Wiener-Hopf equations, which read in matrix form

$$\underline{w}_o = \mathbf{R}^{-1} \underline{p}.$$

The matrix \mathbf{R} is referred to as the (2×2) power matrix, since it contains the powers $E\{u_1^2(k)\}$ and $E\{u_2^2(k)\}$ on the diagonal. Because $u_1(k)$ and $u_2(k)$ are orthogonal (assuming $b(k)$ is a stationary, stochastic process), the off-diagonal elements of \mathbf{R} , i.e. $E\{u_1(k)u_2(k)\}$ and $E\{u_2(k)u_1(k)\}$, vanish. Thus, \mathbf{R} is given by

$$\mathbf{R} = \begin{pmatrix} E\{u_1^2(k)\} & E\{u_1(k)u_2(k)\} \\ E\{u_2(k)u_1(k)\} & E\{u_2^2(k)\} \end{pmatrix} = \begin{pmatrix} R_{11} & 0 \\ 0 & R_{22} \end{pmatrix}.$$

This simple structure of \mathbf{R} leads to an easy-to-implement RLS algorithm for the weights, as will be shown hereafter. The vector \underline{p} is referred to as the cross-power vector, with

$$\underline{p} = \begin{pmatrix} E\{u_1(k)d(k)\} \\ E\{u_2(k)d(k)\} \end{pmatrix} = \begin{pmatrix} p_1 \\ p_2 \end{pmatrix}.$$

Evidently, \mathbf{R} and \underline{p} are functions of the poles. Solving the Wiener-Hopf equations may generally lead to numerical problems. In our case however, the matrix inversion is not expected to pose numerical problems since \mathbf{R} is just a 2×2 diagonal matrix. Obviously, we have to choose a method to estimate the ensemble averages occurring in \mathbf{R} and \underline{p} and preferably an easily implementable procedure.

It is assumed that the stochastic processes $n(k)$ and $s(k)$ are ergodic. Then, time averaging can replace ensemble averaging of \mathbf{R} and \underline{p} . These estimates are denoted by $\hat{\mathbf{R}}$ and $\hat{\underline{p}}$, respectively. An exponential window is used for efficient implementation leading to an RLS algorithm:

$$\hat{R}_{ii}(k) = \theta \hat{R}_{ii}(k-1) + (1-\theta)u_i^2(k), \quad (8.5)$$

$$\hat{p}_i(k) = \theta \hat{p}_i(k-1) + (1-\theta)u_i(k)d(k), \quad (8.6)$$

$$\underline{w}(k) = \begin{pmatrix} \frac{\hat{p}_1(k)}{\hat{R}_{11}(k)} \\ \frac{\hat{p}_2(k)}{\hat{R}_{22}(k)} \end{pmatrix}^T, \quad (8.7)$$

where $i = 1, 2$ and $0 < \theta < 1$. The constant θ is a measure of *memory* of the updating algorithm. It determines the effective time interval over which time averaging is performed. In this context we define the center of energy k_c of a causal discrete time signal $h(k)$ as

$$k_c = \frac{\sum_{k=0}^{k=\infty} k|h(k)|^2}{\sum_{k=0}^{k=\infty} |h(k)|^2}.$$

In our case the exponential window in (8.5) and (8.6) is given by $h(k) = \theta^k$, and thus

$$k_c = \frac{\theta^2}{1-\theta^2}.$$

The parameter θ should be chosen sufficiently large to obtain accurate estimates of \mathbf{R} and \underline{p} . A large θ yields a large suppression of the noise and the second harmonics caused by the multiplications in (8.5) and (8.6). However, θ must be sufficiently small to ensure that the poles have not made any relevant changes in the effective time interval over which \mathbf{R} and \underline{p} are estimated. For example, with $\theta = 0.99$ we obtain $k_c \approx 50$. This implies that the poles are not allowed to make relevant changes within 50 samples.

Consider the special case that $s(k)$ is a sinusoid with amplitude A_0 and frequency Ω_0 according to

$$s(k) = A_0 \sin(\Omega_0 k + \psi). \quad (8.8)$$

Here the phase ψ is a random variable uniformly distributed on the interval $[0, 2\pi)$. Now the MSE as a function of the weights can be expressed as

$$\mathcal{J} = \mathcal{J}(\underline{w}) = E[n^2(k)] + \frac{A_0^2}{2} - 2\underline{w}^T \underline{p} + \underline{w}^T \mathbf{R} \underline{w}. \quad (8.9)$$

We require Ω_0 to approximately satisfy the bounds $0.2 \leq \Omega_0 \leq \pi - 0.2$. At these boundary frequencies the suppression of second harmonics at $2\Omega_0$ approximately equals -30dB with $\theta = 0.99$. For frequencies closer to 0 or π , a larger value for θ should be taken for the same suppression of second harmonics, resulting in a lower adaptation speed.

8.4 Adapting the Poles

The poles determine the filter bandwidth and the center frequency. The filter bandwidth should match the bandwidth of $s(k)$ and the filter center frequency should be adjusted to the center frequency of $s(k)$.

Consider the special case that $s(k)$ is a single sinusoid according to (8.8) with $A_0 = 1$ and $\Omega_0 = 0.5$, and $n(k)$ is zero-mean white noise (thus $\Delta = 1$ will be large enough) with variance $\sigma_n^2 = 1$. For each pair of complex conjugate filter poles inside the unit circle we can calculate the optimal weights \underline{w}_o . From (8.9) the MSE is known. The function $\mathcal{J}(r; \phi)|_{\underline{w}=\underline{w}_o}$ is shown in Fig. 8.3 as a function of the pole angle ϕ for different fixed values of the pole radius r . This function clearly is unimodal, meaning that only one optimum exists.

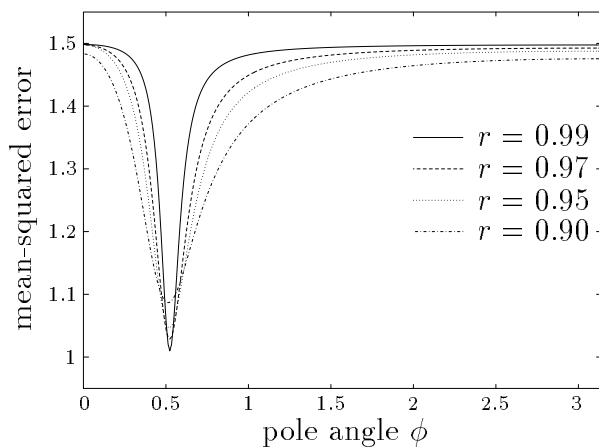


Figure 8.3: The MSE as a functions of ϕ for various values of r .

The minimal MSE that can be reached equals the noise power $\sigma_n^2 = 1$. The maximal MSE evidently equals the noise power plus the power of $s(k)$, here equal to 1.5. When the poles are close to the unit circle the transition in the MSE becomes very sharp. This fact will give serious convergence problems when using a gradient-based optimization algorithm such as LMS. In the flat area of Fig. 8.3 the gradient is small, therefore a large step-size is desirable for fast adaptation. However, near the optimum the gradient is large, so a small step-size should be chosen here to obtain an accurate final solution. With the choice for the step-size a trade-off must be made between adaptation speed and accuracy of the final solution. When the poles move closer to the unit circle, then at a certain point a useful

trade-off cannot be made anymore. In order to circumvent this problem a sign-algorithm is proposed.

The proposed algorithm adapts r and $\gamma = \cos \phi$. We prefer to adapt γ instead of ϕ since this simplifies calculating a gradient as will become clear later on in this section. In the remainder of this section the general symbol χ represents r or γ . The sign-algorithm is given by

$$\chi(k+1) = \chi(k) - \mu_\chi(k) \operatorname{sign} \left(\epsilon(k) \frac{\partial \epsilon(k)}{\partial \chi} \right). \quad (8.10)$$

The sign-function returns the value 1 when its argument is larger than 0, the value -1 when its argument is smaller than 0, and the value 0 when its argument equals 0. The sign-function controls the direction of adaptation and the step-sizes of the pole angle and radius are equal to $\mu_\gamma(k)$ and $\mu_r(k)$, respectively.

A change in the poles will cause a transient at the output of $P(z)$ due to errors introduced in the internal states. Since the poles are changed at each iteration step, a cumulation of transients is obtained. In order to prevent the filter from tracking its own transients it is required that this cumulated transient signal is much smaller than the filter response of $s(k)$. The choices for $\mu_\chi(k)$ that satisfy this requirement are given by

$$\begin{aligned} \mu_r(k) &= c_r(1-r(k))^2, \\ \mu_\gamma(k) &= c_\gamma(1-r(k))^2 \sin \phi(k), \end{aligned} \quad (8.11)$$

where c_r and c_γ are constants satisfying $c_r = c_\gamma \ll \frac{1}{2}\sqrt{2}$. These choices are motivated by the analysis in the Appendix. For a small radius the sign-algorithm can quickly move the poles to the correct angle since the step-sizes are large. Then the pole radius will increase, hereby enlarging the SNIR. Subsequently, the step-sizes become smaller yielding a more accurate final solution. Thus by variation of the bandwidth, adaptation speed is combined with accuracy. As an extra advantage it is noted that (8.11) ensures that the poles never move outside the unit circle, therefore $P(z)$ is guaranteed to remain stable.

In Section 8.2 the concept of different time scales between the adaptation process of the weights and the poles has been motivated. This concept allows us to assume that the weights have reached their optimal values \underline{w}_o (for the current pole position) when optimizing the poles. Using (8.2), the gradients of the instantaneous value of $\epsilon(k)$ with respect to the pole parameters r and γ are given by

$$\frac{\partial \epsilon(k)}{\partial \chi} = -\underline{w}_o^T \frac{\partial \underline{u}(k)}{\partial \chi} - \underline{u}^T(k) \frac{\partial \underline{w}_o}{\partial \chi}.$$

With reference to Fig. 8.2, we define $U_1(z)$, $U_2(z)$ and $B(z)$ as the z -transforms of $u_1(k)$, $u_2(k)$, and $b(k)$, respectively. The gradients $\partial \underline{u}(k)/\partial \chi$ can be obtained by filtering $b(k)$ with certain sensitivity filters. In the remainder of this section we take $i = 1, 2$. The z -transforms of the outputs of the above-mentioned sensitivity filters are given by

$$\begin{aligned} \frac{\partial U_i(z)}{\partial \gamma} &= 2rz^{-1}\Lambda(z) (1 + (-1)^i z^{-1}) B(z), \\ \frac{\partial U_i(z)}{\partial r} &= 2z^{-1}\Lambda(z) (1 + (-1)^i z^{-1}) (\gamma - rz^{-1}) B(z). \end{aligned}$$

Using (8.7) we obtain for the derivatives of the optimal weights with respect to the pole parameters ($i = 1, 2$):

$$\frac{\partial w_{\text{opt},i}}{\partial \chi} = \frac{\partial}{\partial \chi} \left\{ \frac{p_i}{R_{ii}} \right\} = \frac{1}{R_{ii}} \left\{ \frac{\partial p_i}{\partial \chi} - w_{\text{opt},i} \frac{\partial R_{ii}}{\partial \chi} \right\}.$$

The derivatives $\partial p_i/\partial \chi$ and $\partial R_{ii}/\partial \chi$ at sample moment k can be estimated recursively as follows

$$\frac{\partial \hat{p}_i(k)}{\partial \chi} = \theta \frac{\partial \hat{p}_i(k-1)}{\partial \chi} + (1-\theta)d(k) \frac{\partial u_i(k)}{\partial \chi}, \quad (8.12)$$

$$\frac{\partial \hat{R}_{ii}(k)}{\partial \chi} = \theta \frac{\partial \hat{R}_{ii}(k-1)}{\partial \chi} + 2(1-\theta)u_i(k) \frac{\partial u_i(k)}{\partial \chi}. \quad (8.13)$$

The complete adaptation algorithm for the pole radius and angle is now given by (8.10)-(8.13).

The adaptation algorithm describes the update of the poles; an initial value for the poles remains to be chosen. When *a priori* information about $s(k)$ is available (such as an idea of its center frequency or its bandwidth) the initial poles can be chosen accordingly. When no *a priori* information is available, then the initial poles are put on the imaginary axis ($\phi(0) = \frac{\pi}{2}$) for reasons of symmetry. The initial pole radius is chosen equal to 0.42. For this pole radius the bandwidth has numerically been shown to approximately equal 2.7 (equation (8.3) does not hold for such a small r), thus the whole frequency span $0.2 < \Omega_0 < \pi - 0.2$ is covered. Also, for such a small value of r the incorrect initial conditions of the IIR filter are soon 'forgotten'.

For reasons of robustness we also included a lower bound for $r(k)$. In the initial adaptation phase of the ALE we thus prevent $r(k)$ from accidentally becoming smaller than its initial choice. In view of previous remarks a value of $r(k)$ smaller than the initial value 0.42 is meaningless.

8.5 The Zero of the Notch Transfer

In this section we present a method to obtain an estimate of the dominant frequency of the signal $s(k)$ from the weights and poles. Consider the notch transfer $H(z)$ from $d(k)$ to $e(k)$ given by

$$H(z) = \frac{N_H(z)}{z^{\Delta-1}(z-p)(z-p^*)},$$

where the numerator polynomial $N_H(z)$ is given by

$$N_H(z) = z^{\Delta+1} - 2r \cos \phi z^{\Delta} + r^2 z^{\Delta-1} - (w_1 + w_2)z + (w_1 - w_2). \quad (8.14)$$

When $s(k)$ is a sinusoid according to (8.8), $H(z)$ ideally has a complex conjugate zero pair on the unit circle at an angle near Ω_0 . Therefore, instead of ϕ , the positive angle of this zero pair should be used as an approximation of Ω_0 . Also, the zeros of $N_H(z)$ (the zeros of

$H(z)$) are partly determined by the weights. From Section 8.3 we know that the weights converge much faster than the poles. It is therefore expected that during the adaptation process, the roots of $N_H(z)$ will yield an accurate estimate of Ω_0 at a much earlier instant than ϕ .

For $\Delta = 1$, $N_H(z)$ is a second-order polynomial and its two zeros can explicitly be calculated. However, for larger values of Δ an iterative procedure has to be used. In Fig. 8.4 the typical zeros of $H(z)$ after convergence are shown together with the two complex poles. Here we took $\Delta = 10$ and thus $H(z)$ has 11 zeros.

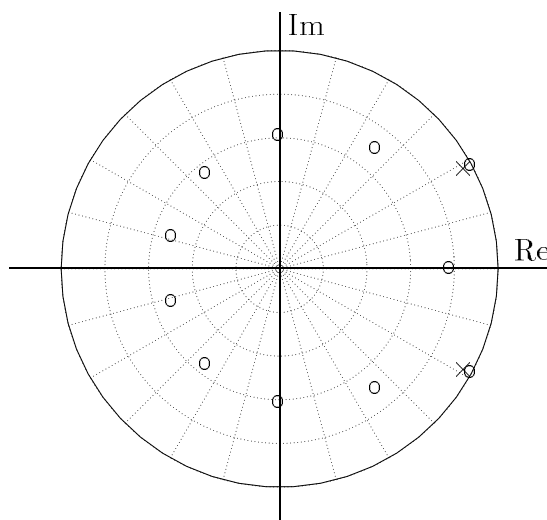


Figure 8.4: The zeros (o) and the two dominant poles (\times) of the notch filter $H(z)$. The 9 poles of $H(z)$ in the origin are not shown.

We notice that the zeros are approximately equally distributed on a circle with a radius that is clearly smaller than 1, except for the two complex conjugate zeros that have a radius near the value 1. The angles of these zeros correspond to Ω_0 . The complex poles lie at approximately the same angles as the two zeros near the unit circle, only at a slightly smaller radius. This produces the desired sharp band-pass characteristics.

Using a Newton-Raphson iteration procedure it is possible to calculate a complex zero of $N_H(z)$. For the result of such a procedure it must be checked whether it has the proper radius (e.g. larger than $r(k)$) and the proper angle (e.g. within the bandwidth of $P(z)$). Unfortunately, this method involves a lot of time-consuming calculations and therefore it will not be used. Instead, we use as an estimate of Ω_0 the frequency ω at which $|N_H(e^{j\omega})|^2$ is minimal. The minimum of $|N_H(e^{j\omega})|^2$ occurs when its derivative with respect to ω equals zero. The following notation will be used:

$$\left. \frac{\partial |N_H(e^{j\omega})|^2}{\partial \omega} \right|_{\omega=\omega(k)} = N_H^{(1)}(k),$$

$$\left. \frac{\partial^2 |N_H(e^{j\omega})|^2}{\partial \omega^2} \right|_{\omega=\omega(k)} = N_H^{(2)}(k).$$

These derivatives can easily be determined explicitly from the squared modulus of (8.14) with $z = e^{j\omega}$. Using a first-order Taylor series approximation around $\omega(k-1)$ we obtain

$$N_H^{(1)}(k) \approx N_H^{(1)}(k-1) + \{\omega(k) - \omega(k-1)\} N_H^{(2)}(k-1) = 0.$$

As an estimate for Ω_0 at sample moment k , we may thus use

$$\omega(k) = \omega(k-1) - \frac{N_H^{(1)}(k-1)}{N_H^{(2)}(k-1)}.$$

Initially, we take $\omega(0) = \phi(0)$. To avoid problems with local minima, the calculated frequency estimate is restricted to lie within the prediction filter bandwidth (8.3). For $|\omega(k) - \phi(k)| > 1 - r(k)$ we take $\omega(k) = \phi(k)$.

8.6 Computer Experiments

We consider the case that $s(k)$ is a sinusoid according to (8.8) with $A_0 = 1$, and that $n(k)$ is white, zero-mean Gaussian noise with variance $\sigma_n^2 = 1$. Consequently, we have $\text{SNR}_d = -3\text{dB}$. We take $\Delta = 10$ and $\theta = 0.99$ so that $k_c \approx 50$. With $c_r = c_\gamma = 0.01$ the pole parameters $r(k)$ and $\phi(k)$ will vary more slowly than $\underline{w}(k)$.

To test the convergence behaviour of the algorithm we perform the following experiment. As motivated in Section 8.4, the initial poles are put on the imaginary axis (thus $\phi(0) = \frac{\pi}{2}$) with $r(0) = 0.42$. For the initial weights we take $\underline{w}(0) = \underline{0}$. In Fig. 8.5 the results of a single run are shown. In Fig. 8.5A the pole angle $\phi(k)$ is plotted together with the frequency estimate $\omega(k)$. We notice that $\omega(k)$ is tracking a local minimum twice. This is corrected near the sampling instants $k = 1500$ and $k = 2800$ when $|\omega(k) - \phi(k)| > r(k)$ by making $\omega(k) = \phi(k)$. After approximately 3000 samples $\omega(k)$ has converged towards the proper end value 0.5. In Fig. 8.5B the pole radius $r(k)$ is plotted. We observe an initial adaptation phase where the radius remains virtually constant with a lower bound as discussed in Section 8.4. Thereafter $r(k)$ increases, in this way enlarging the SNIR. The mean value of $\phi(k)$ measured over the last 5000 samples is 0.513, the mean value of $\omega(k)$ measured over the last 5000 samples is 0.501. Apparently $\phi(k)$ is a biased estimate of Ω_0 , and therefore $\omega(k)$ is preferred. The variance of $\omega(k)$ is somewhat larger than the variance of $\phi(k)$, but this can easily be solved by filtering, e.g. with a low-pass or median filter.

In a second experiment we test the tracking behaviour of the algorithm. The frequency Ω_0 is changed abruptly from 0.5 to 0.55 or vice versa at samples 3000, 6000, 9000, 12000, and 15000. Again we take $A_0 = 1$, $\sigma_n^2 = 1$, $\Delta = 10$, $\theta = 0.99$, and $c_r = c_\gamma = 0.01$. Initially we choose $r(0) = 0.92$, $\phi(0) = 0.5$, and $w_1 = w_2 = 0$. In Fig. 8.6A the behaviour of $\phi(k)$ and $\omega(k)$ in a single run is shown. We see that $\phi(k)$ is not able to track the rapid changes

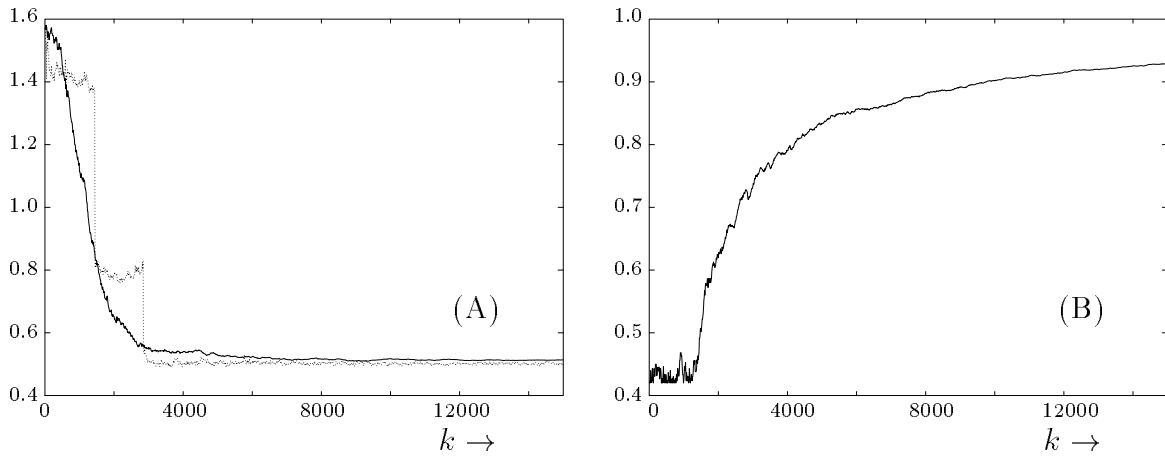


Figure 8.5: The convergence behaviour of the ALE parameters. (A) The pole angle $\phi(k)$ (solid) and frequency estimate $\omega(k)$ (dotted). (B) The pole radius $r(k)$.

in Ω_0 . Therefore, $\phi(k)$ moves towards the mean of Ω_0 . However, with $\theta = 0.99$, and thus $k_c \approx 50$, the weights $\underline{w}(k)$ can quickly converge towards their new optimal values when Ω_0 changes. This fast adaptability of the weights makes it possible for $\omega(k)$ to track Ω_0 . The pole radius plotted in Fig. 8.6B, converges towards a value determined by the degree of stationarity of Ω_0 .

We observe that using identical adaptation parameters the filter is able to obtain sharp band-pass characteristics when Ω_0 is constant (experiment 1) and the adaptation algorithm is suited for frequency tracking when Ω_0 is varied as well (experiment 2).

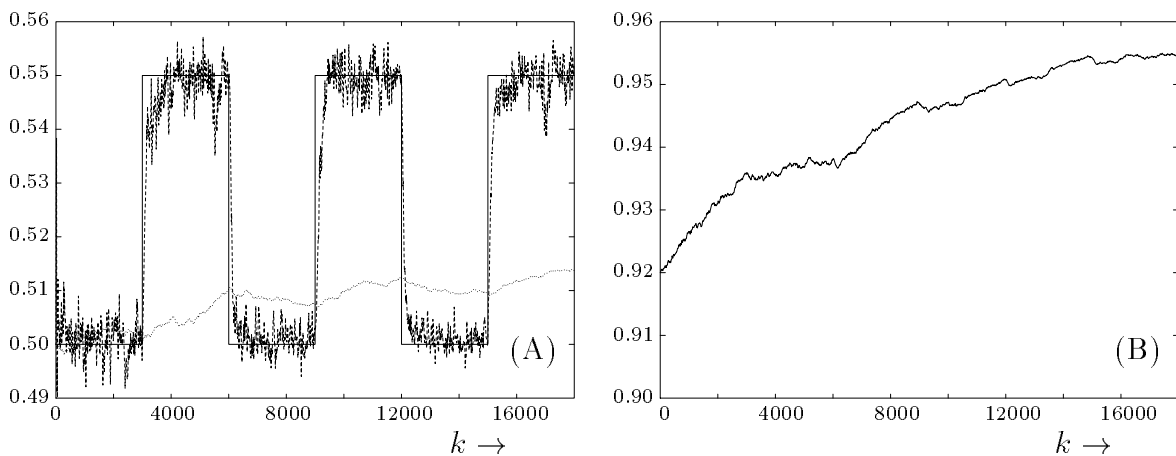


Figure 8.6: The tracking behaviour of the ALE parameters. (A) The pole angle $\phi(k)$ (dotted), the frequency estimate $\omega(k)$ (dashed), and the true frequency (solid). (B) The pole radius $r(k)$.

Finally, we consider the case that $s(k)$ is a narrow-band signal, i.e. $s(k)$ is white Gaussian noise filtered by a 16-th order Butterworth band-pass filter. The center frequency of the band-pass filter is taken $\pi/2$. Further, $n(k)$ is white Gaussian noise. Given a certain bandwidth of $s(k)$ we may numerically search for the optimal parameters of the prediction filter $P(z)$, where we keep the pole angle fixed at $\pi/2$. In Fig. 8.7 the -3dB bandwidth of the optimal prediction filter $P(z)$ is plotted as a function of the bandwidth of $s(k)$ for various input SNRs¹. Note that a larger bandwidth of $s(k)$ leads to a larger bandwidth of $P(z)$, which was to be expected, and that the relation between these two bandwidths is approximately linear. Note that also a larger input SNR leads to a larger bandwidth of $P(z)$. This is a consequence of the fact that $P(z)$ is of second order only and must therefore find a compromise between a good suppression of the unwanted noise $n(k)$ and a good enhancement of $s(k)$: for a large input SNR this compromise favours a good enhancement of $s(k)$, for a small input SNR this compromise favours a good suppression of $n(k)$.

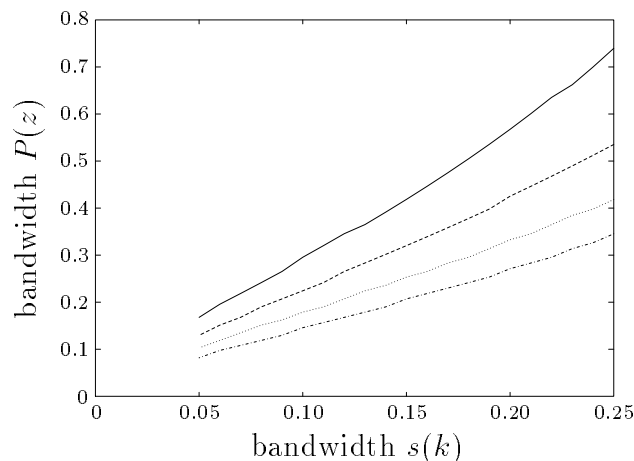


Figure 8.7: The bandwidth of the optimal prediction filter $P(z)$ as a function of the bandwidth of $s(k)$ for various input signal-to-noise levels. The solid, dashed, dotted and dash-dotted lines correspond to input SNRs of 0dB , -3dB , -6dB , and -9dB , respectively.

In Fig. 8.8 the SNIR for the optimal prediction filter is plotted as a function of the bandwidth of $s(k)$ for various input SNRs. We notice that a larger input SNR and a larger bandwidth of $s(k)$ both lead to a smaller SNIR. For a large bandwidth of $s(k)$ the SNIR becomes so small that at a certain point the ALE can no longer achieve a sensible separation of $s(k)$ and $n(k)$. Thus, Fig. 8.8 gives us a quantitative impression of how large the difference in bandwidths of $s(k)$ and $n(k)$ should at least be to expect a usable separation of the two signal components.

¹With thanks to the student Pedro Ignacio Gracia Latorre of the university of Zaragoza in Spain, who prepared Figures 8.7 and 8.8.

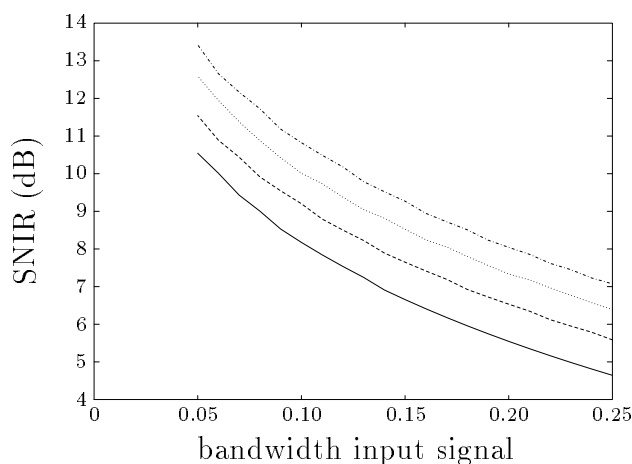


Figure 8.8: The signal-to-noise improvement ratio of the optimal ALE as a function of the bandwidth of $s(k)$ for various input signal-to-noise levels. The solid, dashed, dotted and dash-dotted lines correspond to input SNRs of 0dB, -3dB, -6dB, and -9dB, respectively.

8.7 Discussion

In this chapter a second-order IIR filter has been considered as the basic component of an ALE. Two separate optimization algorithms have been derived, namely a sign-algorithm for the poles and an RLS algorithm for the weights. The algorithms were analyzed separately though performed simultaneously. This can be justified by the fact that the adaptation processes operate at completely different time scales.

The step-size for the sign-algorithm is chosen such that the ALE remains stable and that the cumulative transient signal caused by the continual retuning of the poles remains much smaller in amplitude than the filter response to its input signal. The results of two experiments have been shown, illustrating the convergence behaviour and the frequency tracking behaviour of the ALE. It has been shown that fast frequency tracking is possible due to the capability of the weights to rapidly adjust the notch frequency. Finally, it was demonstrated that the ALE can also separate from broad-band noise a narrow-band signal (instead of a sinusoid). The ALE automatically adjusts its bandwidth according to the bandwidth of the narrow-band signal. Plots of the bandwidth of the optimal ALE and the signal-to-noise improvement ratio as functions of the bandwidth of the narrow-band signal for various input SNRs were presented.

Initial experiments have proved that extension of the proposed scheme towards a realization capable of tracking multiple sinusoids is feasible using the scheme proposed in (Soderstrand, Rangarao, and Loomis 1991). In that case a total number of $2N - 1$ sections of the type proposed in this chapter are required for an input signal $s(k)$ consisting of N sinusoids.

Appendix

The recursive nature of the prediction filter makes a pole change cause a transient at the output. In Fig. 8.9, $\Lambda(z)$ is shown implemented in the direct form 2. A similar analysis as the following can be applied to any other implementation of $\Lambda(z)$, yielding the same final result. We write $d'(k) = d(k - \Delta)$ for reasons of simplicity. The signals $x_1(k)$ and $x_2(k)$ are the internal state variables of $\Lambda(z)$.

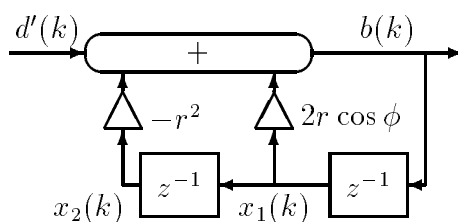


Figure 8.9: The second-order section $\Lambda(z)$ implemented in the direct form 2.

We define the transfer function from $d'(k)$ to $x_1(k)$ and $x_2(k)$ as $\Lambda_1(z)$ and $\Lambda_2(z)$, respectively. These transfers are given by

$$\Lambda_1(z) = \frac{z}{(z-p)(z-p^*)}, \quad \text{and}$$

$$\Lambda_2(z) = \frac{1}{(z-p)(z-p^*)}.$$

A change of the poles results in a change of $\Lambda_1(z)$ and $\Lambda_2(z)$. This change evaluated at the unit circle is defined by the derivatives

$$\left. \frac{\partial \Lambda_1(z)}{\partial r} \right|_{z=e^{j\phi}} \approx \frac{2 \sin \phi}{(1-r)^2} \frac{j e^{-2j\phi}}{(1-r e^{-2j\phi})^2}, \quad (8.15)$$

$$\left. \frac{\partial \Lambda_2(z)}{\partial \phi} \right|_{z=e^{j\phi}} = \frac{-2r \sin \phi}{(1-r^2)} \frac{e^{-2j\phi}}{(1-r e^{-2j\phi})^2}.$$

The approximation in (8.15) is valid for r close to but smaller than 1. With $i = 1, 2$ and using the notation

$$\left. \frac{\partial \Lambda_i(z)}{\partial r} \right|_{z=e^{j\phi}} = N_{ir} e^{j\psi_{ir}},$$

$$\left. \frac{\partial \Lambda_i(z)}{\partial \phi} \right|_{z=e^{j\phi}} = N_{i\phi} e^{j\psi_{i\phi}},$$

we obtain

$$N_{1\phi} = \frac{2r \sin \phi}{(1-r)^2(1+r^2-2r \cos(2\phi))} \approx r N_{1r},$$

$$\psi_{1\phi} \approx \psi_{1r} + \frac{\pi}{2},$$

and

$$\begin{aligned} N_{2\phi} &= N_{1\phi} \approx rN_{1r} = rN_{2r}, \\ \psi_{2\phi} &= \psi_{1\phi} - \phi \approx \psi_{1r} - \phi + \frac{\pi}{2} = \psi_{2r} + \frac{\pi}{2}. \end{aligned}$$

We take

$$d'(k) = A_0 \operatorname{Re}\{e^{j(\phi k + \psi)}\},$$

with $A_0 \in \mathbb{R}_+$ and ψ a random variable uniformly distributed on the interval $[0, 2\pi)$. Suppose that the pole radius and angle are changed at $k = 0$ with Δr and $\Delta\phi$, respectively. As a consequence of these changes, the state errors Δx_1 and Δx_2 are given by (with $i = 1, 2$)

$$\Delta x_i = -\operatorname{Re}\left\{\left[\Delta\phi \frac{\partial\Lambda_i(z)}{\partial\phi}\Big|_{z=e^{j\phi}} + \Delta r \frac{\partial\Lambda_i(z)}{\partial r}\Big|_{z=e^{j\phi}}\right] A_0 e^{j\psi}\right\},$$

or equivalently

$$\begin{aligned} \Delta x_1 &\approx -A_0 N_{1r} \sqrt{(r\Delta\phi)^2 + (\Delta r)^2} \operatorname{Re}\{e^{j(\psi_{1r} + \psi + \Delta\psi)}\}, \\ \Delta x_2 &\approx -A_0 N_{1r} \sqrt{(r\Delta\phi)^2 + (\Delta r)^2} \operatorname{Re}\{e^{j(\psi_{1r} + \psi + \Delta\psi)} e^{-j\phi}\}, \end{aligned}$$

with $\Delta\psi = \arg\{\Delta r + jr\Delta\phi\}$. By letting Δx_1 and Δx_2 be complex-valued, yielding a complex valued transient $t_c(k)$, and taking the real part afterwards, we obtain for the transient

$$\begin{aligned} t(k) = \operatorname{Re}\{t_c(k)\} &= \operatorname{Re}\{Cp^k + Dp^{*k}\} \\ &= Ap^k + (Ap^k)^*, \end{aligned}$$

with $A = \frac{1}{2}(C + D^*)$ and C and D are determined by

$$\begin{aligned} \Delta x_1 &= t(-1) = C/p + D/p^*, \\ \Delta x_2 &= t(-2) = C/p^2 + D/p^{*2}. \end{aligned}$$

It can readily be shown that

$$|A| = \frac{r}{4 \sin \phi} \left\{ A_0 N_{1r} \sqrt{(r\Delta\phi)^2 + (\Delta r)^2} \right\} \sqrt{(2-r)^2 + r^2 - 2r(2-r) \cos(2\phi)}.$$

During the adaptation process of the poles a pole change is made at each iteration step. Therefore, the total disturbance will be the sum of all the separate transients. In the worst case we obtain for the disturbance

$$\sum_{k=0}^{\infty} |t(k)| = \sum_{k=0}^{\infty} |Ap^k + (Ap^k)^*| \leq \frac{2|A|}{(1-r)}. \quad (8.16)$$

Remark: in the more restricted case that ϕ is not too near the value 0 or π , a good approximation of the left hand side of the inequality (8.16) can be shown to be given by $4|A|/\pi(1-r)$.

We require that this disturbance is relatively small compared to the response of the sinusoid, thus

$$\frac{\sum_{k=0}^{\infty} |t(k)|}{A_0 |\Lambda(e^{j\phi})|} \ll 1.$$

This leads to

$$\begin{aligned} \frac{\sum_{k=0}^{\infty} |t(k)|}{A_0 |\Lambda(e^{j\phi})|} &\leq \frac{r \sqrt{(2-r)^2 + r^2 - 2r(2-r) \cos(2\phi)}}{(1-r)^2 \sqrt{1+r^2 - 2r \cos(2\phi)}} \sqrt{(\Delta r)^2 + (r\Delta\phi)^2} \\ &\approx \frac{1}{(1-r)^2} \sqrt{(\Delta r)^2 + (\Delta\phi)^2} \ll 1. \end{aligned}$$

Again, the approximation is valid for r close to but smaller than 1. Therefore, we choose Δr and $\Delta\phi$ to be equal to $c_r(1-r)^2$ and $c_\phi(1-r)^2$, respectively, with $c_r = c_\phi \ll \frac{1}{2}\sqrt{2}$. In Section 8.4, $\gamma = \cos \phi$ is updated, instead of ϕ . This yields as a first-order approximation that $\Delta\gamma = c_\gamma(1-r)^2 \sin \phi(k)$, where $c_\gamma = c_\phi$.

Bibliography

- Belt, H. J. W., A. C. den Brinker, and F. P. A. Benders (1995). Adaptive line enhancement using a second-order IIR filter. In *Proc. IEEE International Conference on Acoustics, Speech and Signal Processing (ICASSP)*, Detroit (MI), U.S.A., pp. 1444–1447.
- Cho, N. I., C. Choi, and S. U. Lee (1989). Adaptive line enhancement by using an IIR lattice notch filter. *IEEE Trans. Acoust. Speech Signal Process.* *37*, 585–589.
- David, R. A., S. D. Stearns, and G. R. Elliot (1983). IIR algorithms for adaptive line enhancement. In *Proc. IEEE International Conference on Acoustics, Speech and Signal Processing (ICASSP)*, pp. 17–20.
- Friedlander, B. (1984). Analysis and performance evaluation of an adaptive notch filter. *IEEE Trans. I.T.* *30*, 283–295.
- Griffiths, L. J. (1975). Rapid measurement of digital instantaneous frequency. *IEEE Trans. Acoust. Speech Signal Process.* *23*, 207–222.
- Haykin, S. (1996). *Adaptive Filter Theory, Third Edition*. London, U.K.: Prentice-Hall Int.
- Hush, D. R., N. Ahmed, R. David, and S. D. Stearns (1986). An adaptive IIR structure for sinusoidal enhancement, frequency estimation, and detection. *IEEE Trans. Acoust. Speech Signal Process.* *34*, 1380–1390.
- Nehorai, A. (1985). A minimal parameter adaptive notch filter with constrained poles and zeros. *IEEE Trans. Acoust. Speech Signal Process.* *33*, 983–996.
- Rao, D. V. B. and S. Y. Kung (1984). Adaptive notch filtering for the retrieval of sinusoids in noise. *IEEE Trans. Acoust. Speech Signal Process.* *32*, 791–802.

-
- Soderstrand, M. A., K. V. Rangarao, and H. H. Loomis (1991). Improved real-time adaptive detection, enhancement, or elimination of multiple sinusoids. In *Proc. 34th Midwest Symp. Circuits and Systems*, pp. 1085–1089.
- Treichler, J. R. (1979). Transient and convergent behavior of the adaptive line enhancer. *IEEE Trans. Acoust. Speech Signal Process.* 27, 53–62.
- Widrow *et al.*, B. (1975). Adaptive noise cancelling: principles and applications. *Proc. IEEE* 63, 1692–1716.
- Zeidler, J. R. (1990). Performance analysis of LMS adaptive prediction filters. *Proc. IEEE* 78, 1781–1806.

Appendix A

Optimal Orthonormal Approximations

This appendix is concerned with the approximation of one-dimensional signals by truncated series of orthonormal basis functions. The considered basis functions satisfy a certain differential or difference equation. Also, they contain certain free parameters that need to be chosen beforehand. This can be done with the method proposed by Tanguy, Vilbé, and Calvez (1995), which yields an upper bound for the (quadratic) truncation error. This upper bound is a function of the free parameters in the basis functions and some simple signal measurements (moments). It is also demonstrated that this upper bound is identical to a certain enforced convergence rate error criterion that was first introduced by Fu and Dumont (1993) for approximations with truncated Laguerre series. Minimization of either the above-mentioned upper bound or the enforced convergence rate error criterion as a function of the free parameters yields the same optimal parameters.

We consider orthonormal series expansions of the Hilbert space $L_2(\mathbb{R}^+)$ of real, square-integrable functions on \mathbb{R}^+ and of the Hilbert space $\ell_2(\mathbb{N}_0)$ of real, square-summable functions on \mathbb{N}_0 . We start with the set of real basis functions $\phi_m(\theta; x)$ that satisfy

$$\langle \phi_m(\theta; x), \phi_n(\theta; x) \rangle \triangleq \int_0^{\infty} \phi_m(\theta; x) \phi_n(\theta; x) dx = \delta_{mn},$$

where θ denotes one or more free parameters that need to be selected optimally. It is required that the parameters θ are continuous real variables and that the $\phi_m(\theta; x)$ are continuous functions of these parameters. A parameter could for example be the scale factor σ as in the (generalized) Laguerre functions (see Chapter 4). It could be the Laguerre pole in the discrete Laguerre functions or in the Meixner-like functions (see Chapter 4). Also, it could be the order of generalization α of the generalized Laguerre functions (see Chapter 4). Another example is the center of time t_0 and the scale λ for the Hermite functions¹ in Chapter 5.

¹The Hermite functions are defined on $(-\infty, \infty)$, so for the Hermite functions the domain of the inner product should be altered.

A square-summable or square-integrable function $f(x)$ can be expanded as

$$f(x) = \sum_{m=0}^{\infty} c_m(\theta) \phi_m(\theta; x), \quad (\text{A.1})$$

where the generalized Fourier coefficients $c_m(\theta)$ depend on the free parameters θ and are given by

$$c_m(\theta) = \langle f(x), \phi_m(\theta; x) \rangle. \quad (\text{A.2})$$

In an M -term truncated expansion the following approximation is obtained:

$$f(x) \approx f_M(x) = \sum_{m=0}^{M-1} c_m(\theta) \phi_m(\theta; x). \quad (\text{A.3})$$

For a given θ , (A.3) is the best M -term approximation of $f(x)$ in the sense that the truncation error, given by

$$\zeta_M(\theta) = \sum_{m=M}^{\infty} c_m^2(\theta), \quad (\text{A.4})$$

is minimal. The truncation error can be reduced by optimization of the free parameter θ . In most cases, the truncation error depends on θ in a nonlinear way. In the following, the use of (iterative) nonlinear optimization techniques, afflicted with problems such as local minima, is avoided.

The key observation is that orthonormal functions related to the classical orthogonal polynomials satisfy the noteworthy relation

$$\mathcal{S} \{ \phi_m(\theta; x) \} = \lambda(m) \phi_m(\theta; x), \quad (\text{A.5})$$

where \mathcal{S} is a linear operator defined by

$$\mathcal{S} \{ \phi_m(\theta; x) \} = A(\theta; x) \mathcal{D}^2 \phi_m(\theta; x) + B(\theta; x) \mathcal{D}^1 \phi_m(\theta; x) + C(\theta; x) \mathcal{D}^0 \phi_m(\theta; x). \quad (\text{A.6})$$

The $\lambda(m)$ in (A.5) are independent of x and they form a sequence of increasing numbers:

$$\lambda(0) < \lambda(1) < \lambda(2) < \lambda(3) < \dots$$

Without loss of generality we can take $\lambda(0) = 0$ since if $\lambda(0) \neq 0$ this term can be absorbed in the linear operator \mathcal{S} . The coefficients $A(\theta; x)$, $B(\theta; x)$ and $C(\theta; x)$ are characteristic for the chosen basis and are independent of m . In the context of CT signals, \mathcal{D}^i stands for $\partial^i / \partial t^i$ and (A.5) becomes a differential equation. In the context of DT signals, we have that $\mathcal{D}^i f(k) = f(k + i - 1)$ and (A.5) becomes a difference equation. We require that the coefficients $A(\theta; x)$, $B(\theta; x)$, and $C(\theta; x)$ are all a finite sum of separable functions in x and the free parameters θ , i.e. they can be written as

$$\sum_{k=0}^K g_1(\theta) g_2(x).$$

In Table A.1 the coefficients A , B and C in (A.6) and the corresponding $\lambda(m)$ are given for some orthonormal basis functions used in this thesis. These functions are the continuous Laguerre functions, denoted by $\lambda_m(\sigma; t)$, the generalized Laguerre functions, denoted by $\lambda_m^{(\alpha)}(\sigma; t)$, the Hermite functions, denoted by $\mathcal{H}_m(\lambda, t_0; t)$, and the discrete Laguerre functions, denoted by $g_m(\xi; k)$.

$\phi_m(x)$	A	B	C	$\lambda(m)$
$\lambda_m(\sigma; t)$	$-\frac{t}{\sigma}$	$-\frac{1}{\sigma}$	$\frac{\sigma t - 2}{4}$	m
$\lambda_m^{(\alpha)}(\sigma; t)$	$-\frac{t}{\sigma}$	$-\frac{1}{\sigma}$	$\frac{\sigma t - 2(\alpha + 1)}{4} + \frac{\alpha^2}{4\sigma t}$	m
$\mathcal{H}_m(\lambda, t_0; t)$	$-\frac{\lambda^2}{2}$	0	$\frac{t^2 - 2t_0 t + t_0^2 - \lambda^2}{2\lambda^2}$	m
$g_m(\xi; k)$	$-\frac{(k+1)\xi}{1-\xi^2}$	$\frac{k(1+\xi^2) + \xi^2}{1-\xi^2}$	$-\frac{k\xi}{1-\xi^2}$	m

Table A.1: Some orthonormal basis functions on $L_2(\mathbb{R}^+)$ and $\ell_2(\mathbb{N}_0)$ with the coefficients of their differential or difference equations of the form $AD^2\phi_m(x) + BD^1\phi_m(x) + CD^0\phi_m(x) = \lambda(m)\phi_m(x)$.

Applying the linear operator \mathcal{S} to both sides of (A.1) results in

$$\mathcal{S}\{f(x)\} = \sum_{m=0}^{\infty} \lambda(m) c_m(\theta) \phi_m(\theta; x).$$

Then,

$$F(\theta) \triangleq \langle f(x), \mathcal{S}\{f(x)\} \rangle = \sum_{m=0}^{\infty} \lambda(m) c_m^2(\theta) \geq \lambda(M) \sum_{m=M}^{\infty} c_m^2(\theta).$$

Thus, the truncation error given in (A.4) is upper-bounded:

$$\zeta_M(\theta) \leq \frac{F(\theta)}{\lambda(M)}. \quad (\text{A.7})$$

Note that to get a useful bound in (A.7), M must be sufficiently large to guarantee that $\lambda(M) > F(\theta) \|f(x)\|^{-2}$.

It is easy to prove the existence of signals $f(x)$ for which the bound in (A.7) is attained. To this end, $f(x)$ must satisfy

$$\lambda(M) \sum_{m=M}^{\infty} \langle f(x), \phi_m(x) \rangle^2 = \sum_{m=0}^{\infty} \lambda(m) \langle f(x), \phi_m(x) \rangle^2.$$

Remembering that $\lambda(0) = 0$, and that $\lambda(m+1) > \lambda(m)$ for $m \in \mathbb{N}_0$, we find that in order to attain the bound in (A.7) $f(x)$ must be of the form

$$f(x) = a\phi_0(x) + b\phi_M(x),$$

where a and b may take on any real value.

The best value of θ is given by that value which minimizes $F(\theta)$. Let this value of θ be θ_0 . From (A.7) we now see that the maximum truncation error over the class of all functions with the same $F(\theta_0)$ is given by $F(\theta_0)/\lambda(M)$.

The method will now be illustrated with an example. Suppose we wish to approximate the function $f(t) \in L_2(\mathbb{R}^+)$ by a linear combination of Laguerre functions, according to

$$f(t) \approx \sum_{m=0}^{M-1} c_m(\sigma) \lambda_m(\sigma; t).$$

With Table A.1 the linear operator \mathcal{S} applied to a Laguerre function yields:

$$\begin{aligned} \mathcal{S} \{ \lambda_m(\sigma; t) \} &= A(\sigma; t) \lambda_m''(\sigma; t) + B(\sigma; t) \lambda_m'(\sigma; t) + C(\sigma; t) \lambda_m(\sigma; t), \\ &= -\frac{t}{\sigma} \lambda_m''(\sigma; t) - \frac{1}{\sigma} \lambda_m'(\sigma; t) + \frac{\sigma t - 2}{4} \lambda_m(\sigma; t), \end{aligned}$$

and since $f(t)$ can be represented by a Laguerre series:

$$\mathcal{S} \{ f(t) \} = -\frac{t}{\sigma} f''(t) - \frac{1}{\sigma} f'(t) + \frac{\sigma t - 2}{4} f(t).$$

We now obtain that $F(\sigma)$ is dependent on some limited number of moments² of $f(t)$, namely

$$F(\sigma) = \langle f(t), \mathcal{S} \{ f(t) \} \rangle = -\frac{1}{2} m_0 + \frac{\sigma}{4} m_1 + \frac{1}{\sigma} m_2.$$

The moments m_0 , m_1 and m_2 , are given by

$$m_0 = \langle f(t), f(t) \rangle, \quad m_1 = \langle f(t), t f(t) \rangle, \quad m_2 = \langle f'(t), t f'(t) \rangle.$$

We now have at our disposal an upper bound for the truncation error associated with the approximation of $f(t)$ by a linear combination of Laguerre functions:

$$\zeta_M(\sigma) = \sum_{m=M}^{\infty} c_m^2(\sigma) \leq \frac{F(\sigma)}{M}.$$

Setting the derivative of $F(\sigma)$ with respect to σ equal to zero yields the best σ for Laguerre approximations of the set of functions with the same moments m_0 , m_1 and m_2 . This optimal σ , denoted by $\hat{\sigma}$, is obtained as

$$\hat{\sigma} = 2\sqrt{\frac{m_2}{m_1}}. \tag{A.8}$$

²Note that this is a consequence of the fact that the coefficients $A(\sigma; t)$, $B(\sigma; t)$, and $C(\sigma; t)$ are separable in σ and t .

This result was obtained earlier by Parks (1971), where the notation $\sigma = p/2$ was used. It is noted here that in (Belt and den Brinker 1997) the method above is applied to approximations of functions $f(t) \in L_2(\mathbb{R}^+)$ by a linear combination of generalized Laguerre functions $\lambda_m^{(\alpha)}(\sigma; t)$ to obtain a good σ and α .

In (Fu and Dumont 1993), the authors also consider approximations of functions $f(t) \in L_2(\mathbb{R}^+)$ by a linear combination of Laguerre functions. Only, a different error criterion is used. Instead of using the truncation error defined in (A.4) they minimize the enforced rate error criterion

$$\tilde{\zeta}(\theta) = \sum_{m=0}^{\infty} \lambda(m) c_m^2(\theta), \quad (\text{A.9})$$

where in the Laguerre case $\lambda(m) = m$ and $\theta = \sigma$. Intuitively, from (A.9) one may expect an enforced convergence rate of the series expansion of $f(t)$. Note that the criterion $\tilde{\zeta}(\theta)$ in (A.9) is identical to the upper bound $F(\theta)$. As a consequence, it is found by Fu and Dumont (1993) that the σ that minimizes $\tilde{\zeta}(\sigma)$ is also given by (A.8).

We thus have two criteria to obtain optimal parameters in the considered series expansions, namely $F(\theta)$ and $\tilde{\zeta}(\theta)$. Both criteria yield the same parameters. However, the starting point in both cases is different. In the first case the optimality is defined over a class of functions satisfying the same moments. In the second case, the optimality is defined by a criterion over an individual function. From a practical point of view the second interpretation is more interesting since one usually has to deal with the approximation of a single function instead of a whole class of functions.

Bibliography

- Belt, H. J. W. and A. C. den Brinker (1997). Optimal parametrization of truncated generalized Laguerre series. In *Proc. IEEE International Conference on Acoustics, Speech and Signal Processing (ICASSP)*, Munich, Germany. To appear in April 1997.
- Fu, Y. and G. A. Dumont (1993). An optimum time scale for discrete Laguerre network. *IEEE Trans. Automat. Contr.* 38, 934–938.
- Parks, T. W. (1971). Choice of time scale in Laguerre approximations using signal measurements. *IEEE Trans. Automat. Contr.* 16, 511–513.
- Tanguy, N., P. Vilbé, and L. C. Calvez (1995). Optimum choice of free parameter in orthonormal approximations. *IEEE Trans. Automat. Contr.* 40, 1811–1813.

Samenvatting

In de praktijk wordt voor adaptieve filters meestal gebruik gemaakt van de zogeheten *tapped-delay line* (TDL). De TDL is opgebouwd uit een cascade van vertragers. Ieder vertragingselement bevat aldus een sample-waarde van een vertraagde versie van het ingangssignaal. Al deze vertraagde versies van het ingangssignaal worden gewogen en opgeteld. Dientengevolge wordt de uitgang van de TDL gevormd door een lineaire combinatie van verschillend vertraagde versies van zijn ingang. Het aantal vertragingselementen, dus ook het aantal gewichten, bepaalt de duur van de impulsresponsie van de TDL. In een algemeen adaptief filterschema probeert het adaptieve filter een bepaalde maat van een fout tussen zijn uitgangssignaal en een gewenst signaal te minimaliseren. Meestal wordt voor deze maat een kwadratisch criterium genomen, de zogeheten *mean-squared error*. Er is een uitgebreide literatuur over de adaptieve optimalisatie van de gewichten.

Een problematisch aspect van de TDL is dat zijn geassocieerde basisfuncties, vertraagde versies van de eenheidspulsfunctie, extreem gelokaliseerd zijn in de tijd. Dientengevolge is een groot aantal vertragingselementen benodigd om het gedrag van dynamische systemen met een groot geheugen na te bootsen. Een groot aantal gewichten kan om verschillende redenen problematisch zijn voor een adaptief filter. Ten eerste omdat veel (duur) geheugen vereist is om de gewichten en oude waarden van het ingangssignaal op te slaan. Daarnaast leidt een groot aantal gewichten tot een groot aantal rekenkundige bewerkingen om de convolutie met het ingangssignaal uit te voeren. Bovendien fluctueert ieder gewicht in de stationaire toestand rond zijn eindwaarde en levert hierdoor een bijdrage aan een ruissignaal op de uitgang. Het cumulatieve effect van de ruisbijdragen van een groot aantal gewichten is een beperkende factor met betrekking tot de prestaties van het adaptieve filter.

In dit proefschrift wordt een aantal alternatieve structuren voor adaptieve filters bestudeerd. In het bijzonder worden lineaire regressiemodellen onderzocht, waarvan de uitgang een gewogen sommatie is van gefilterde versies van het ingangssignaal. De filters in de beschouwde lineaire regressiemodellen hebben impulsresponsies van oneindige lengte, hetgeen goed past bij systemen met een lang geheugen. Door de overeenkomsten tussen de TDL en een lineair regressiemodel kunnen adaptatie-algoritmen zoals het *Least-Mean-Square* (LMS) algoritme en het *Recursive Least-Squares* (RLS) algoritme, die oorspronkelijk waren ontwikkeld voor de TDL, worden gebruikt. Een goede keuze van de filterset in het regressiemodel bij een bepaalde applicatie leidt ertoe dat men met minder adaptieve gewichten kan volstaan dan met een TDL. In dit proefschrift worden verschillende mogelijke sets van filters voor een adaptief lineair regressiemodel onderzocht. Voor adaptieve filters

zijn met name die sets van filters interessant, waarvan de impulsresponsies complete systemen van orthonormale functies vormen. We beschouwen (generaliseerde) Laguerre, Kautz, Jacobi, Legendre en Meixner-like filters en behandelen hun relevante eigenschappen. Deze filters bevatten parameters (bijvoorbeeld polen) die vantevoren gekozen dienen te worden. We beschouwen enige methoden om goede waarden voor deze parameters te vinden. Als bijproduct van de behandelde methoden stellen we een manier voor om goede waarden te vinden voor de vrije parameters in afgekapte Hermiet-expansies van signalen met een eindige *support*. Het gedrag van het LMS algoritme ten behoeve van de optimalisatie van de gewichten in lineaire regressiemodellen wordt bestudeerd. Hierbij wordt gekeken naar convergentiesnelheid en naar de *misadjustment*. Vervolgens stellen we een adaptief algoritme voor om de vrije parameter (een meervoudige pool) van een Laguerre filter te optimaliseren. Tenslotte beschouwen we de adaptieve optimalisatie van een complex poolpaar voor een specifiek tweede orde IIR adaptief filter, te weten een zogeheten *adaptive line enhancer*.

List of Scientific Publications

1. H.J.W. Belt and A.C. den Brinker, "Optimal Truncated Meixner-Like Networks", in: *Proc. ProRISC/IEEE Benelux Workshop on Circuits, Systems and Signal Processing*, pages 25–32, Mierlo, Netherlands, 1995.
2. H.J.W. Belt, A.C. den Brinker, and F.P.A. Benders, "Adaptive Line Enhancement using a Second-Order IIR Filter", in: *Proc. IEEE International Conference on Acoustics, Speech and Signal Processing (ICASSP)*, pages 1444–1447, Detroit (MI), U.S.A., 1995.
3. H.J.W. Belt and A.C. den Brinker. "Optimality Condition for Truncated Generalized Laguerre Networks", *Int. J. Circuit Theory Appl.*, 23:227–235, 1995.
4. H.J.W. Belt and A.C. den Brinker, "Filter Synthesis by Discrete-Time Generalized Laguerre Networks", in: *Proc. 12th European Conference on Circuit Theory & Design (ECCTD)*, pages 971–974, Istanbul, Turkey, 1995.
5. H.J.W. Belt and A.C. den Brinker, "Laguerre Filters with Adaptive Pole Optimization", in: *Proc. IEEE International Symposium on Circuits and Systems (ISCAS)*, pages 37–40, Atlanta (GA), U.S.A., 1996.
6. H.J.W. Belt and H.J. Butterweck, "Cascaded All-Pass Sections for LMS Adaptive Filtering", in: *Signal Processing VIII: Theories and Applications, Proc. EUSIPCO-96, Eighth European Signal Processing Conference*, pages 1219–1222, Trieste, Italy, 1996.
7. H.J.W. Belt and A.C. den Brinker, "Optimal Parametrization of Truncated Generalized Laguerre Series", to appear in: *Proc. IEEE International Conference on Acoustics, Speech and Signal Processing (ICASSP)*, pages 3805–3808, Munich, Germany, 1997.
8. A.C. den Brinker, H.J.W. Belt, and F.P.A. Benders, "An Adaptive Line Enhancer based on a Second-Order IIR Filter", in: *Proc. ProRISC/IEEE Benelux Workshop on Circuits, Systems and Signal Processing*, pages 59–65, Arnhem, Netherlands, 1994.
9. A.C. den Brinker and H.J.W. Belt, "Model Reduction by Orthogonalized Exponential Sequences", in: *Proc. ProRISC/IEEE Benelux Workshop on Circuits, Systems and Signal Processing*, pages 77–82, Mierlo, Netherlands, 1996.
10. A.C. den Brinker and H.J.W. Belt, "Model Reduction by Orthogonalized Exponential Sequences", to appear in: *Proc. European Conference on Signal Analysis and Prediction (ECSAP)*, Prague, Czech Republic, 1997.

11. T. Oliveira e Silva and H.J.W. Belt, "On the Determination of the Optimal Center and Scale Factor for Truncated Hermite Series", in *Signal Processing VIII: Theories and Applications, Proc. EUSIPCO-96, Eighth European Signal Processing Conference*, pages 1563–1566, Trieste, Italy, 1996.
12. A.C. den Brinker and H.J.W. Belt "Optimal Free Parameters in Orthonormal Approximations", *in preparation*, 1997.

Curriculum Vitae

Harm J.W. Belt was born in 's Hertogenbosch, the Netherlands, on July 4, 1968. In 1986 he finished secondary school (Atheneum) at the Radulphus College, Curaçao, the Netherlands Antilles. He received the M.Sc. degree in Electrical Engineering in February 1993 from the Eindhoven University of Technology, Eindhoven, the Netherlands. His graduation work on adaptive control was performed at the Measurement and Control group. In the spring of 1992 he was for a period of three months with the Cordless Communications group of the Philips Research Laboratories, Redhill, U.K., in the framework of a practical traineeship. In May 1993 he joined the Signal Processing group at the Eindhoven University of Technology, where he carried out the research on adaptive filtering and orthonormal series representations reported in this thesis. From Januari 1997 he is engaged as a researcher with the Digital Signal Processing group of the Philips Research Laboratories in Eindhoven, The Netherlands.